EXTRACELLULAR MATRIX FOR CARDIOVASCULAR RECONSTRUCTION

EDITED BY: Steve Bibevski, Sharan Ramaswamy and Joshua D. Hutcheson
PUBLISHED IN: Frontiers in Cardiovascular Medicine

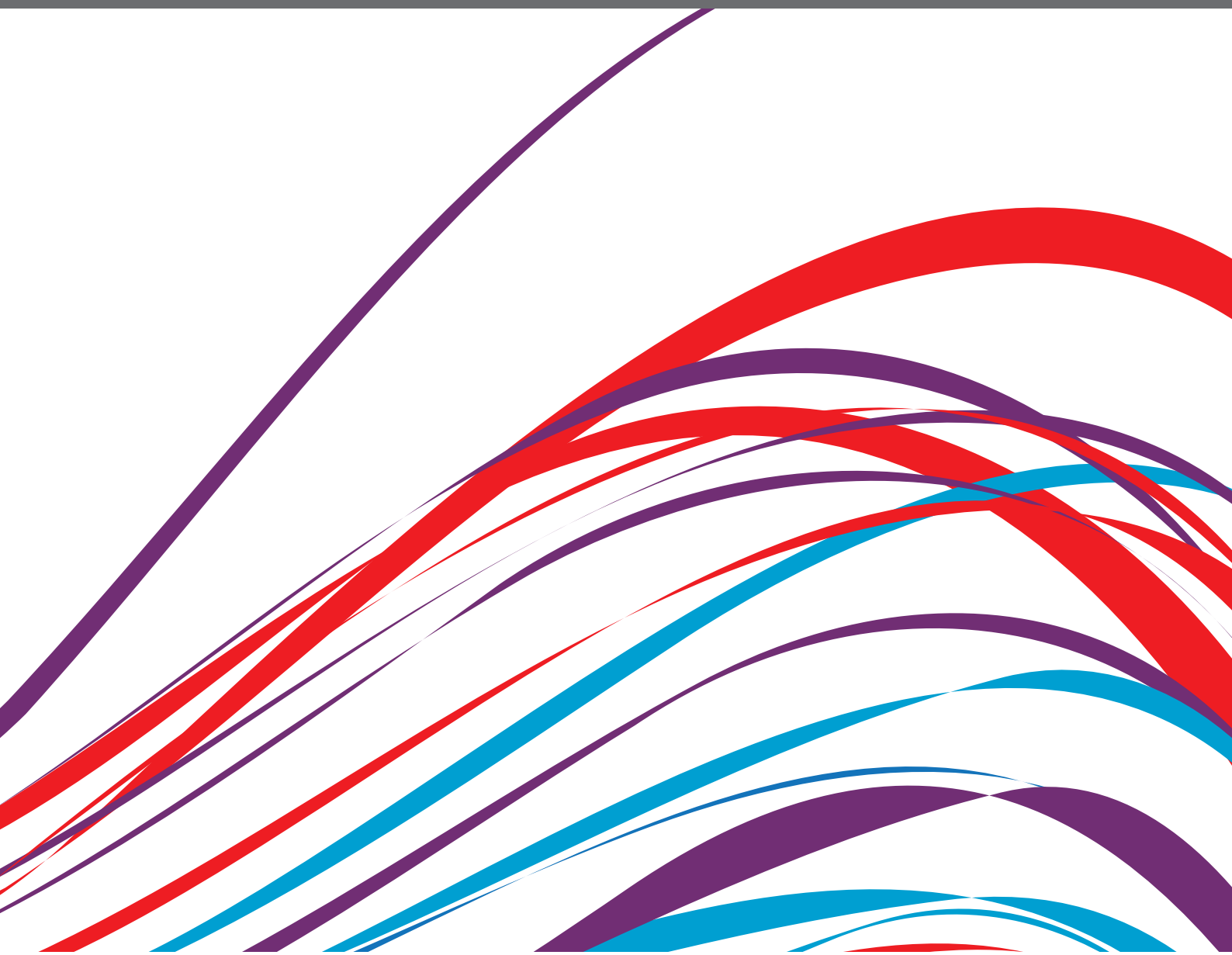

frontiers Research Topics

ISSN 1664-8714
ISBN 978-2-88966-838-0
DOI 10.3389/978-2-88966-838-0

About Frontiers

Frontiers is more than just an open-access publisher of scholarly articles: it is a pioneering approach to the world of academia, radically improving the way scholarly research is managed. The grand vision of Frontiers is a world where all people have an equal opportunity to seek, share and generate knowledge. Frontiers provides immediate and permanent online open access to all its publications, but this alone is not enough to realize our grand goals.

Frontiers Journal Series

The Frontiers Journal Series is a multi-tier and interdisciplinary set of open-access, online journals, promising a paradigm shift from the current review, selection and dissemination processes in academic publishing. All Frontiers journals are driven by researchers for researchers; therefore, they constitute a service to the scholarly community. At the same time, the Frontiers Journal Series operates on a revolutionary invention, the tiered publishing system, initially addressing specific communities of scholars, and gradually climbing up to broader public understanding, thus serving the interests of the lay society, too.

Dedication to Quality

Each Frontiers article is a landmark of the highest quality, thanks to genuinely collaborative interactions between authors and review editors, who include some of the world's best academicians. Research must be certified by peers before entering a stream of knowledge that may eventually reach the public - and shape society; therefore, Frontiers only applies the most rigorous and unbiased reviews.
Frontiers revolutionizes research publishing by freely delivering the most outstanding research, evaluated with no bias from both the academic and social point of view. By applying the most advanced information technologies, Frontiers is catapulting scholarly publishing into a new generation.

What are Frontiers Research Topics?

Frontiers Research Topics are very popular trademarks of the Frontiers Journals Series: they are collections of at least ten articles, all centered on a particular subject. With their unique mix of varied contributions from Original Research to Review Articles, Frontiers Research Topics unify the most influential researchers, the latest key findings and historical advances in a hot research area! Find out more on how to host your own Frontiers Research Topic or contribute to one as an author by contacting the Frontiers Editorial Office: frontiersin.org/about/contact

EXTRACELLULAR MATRIX FOR CARDIOVASCULAR RECONSTRUCTION

Topic Editors:
Steve Bibevski, Joe DiMaggio Children's Hospital, United States
Sharan Ramaswamy, Florida International University, United States
Joshua D. Hutcheson, Florida International University, United States

Topic editor Robert G. Matheny is employed by company CorMatrix Inc.. All other topic editors declare no competing interests with regards to the Research Topic subject.

Citation: Bibevski, S., Ramaswamy, S., Hutcheson, J. D., eds. (2021). Extracellular Matrix for Cardiovascular Reconstruction. Lausanne: Frontiers Media SA.
doi: 10.3389/978-2-88966-838-0

Table of Contents

frontiers in Cardiovascular Medicine

EDITORIAL
published: 08 April 2021
doi: 10.3389/fcvm.2021.664803

Editorial: Extracellular Matrix for Cardiovascular Reconstruction

Steven Bibevski[1,2]*, *Sharan Ramaswamy*[2] *and Joshua Hutcheson*[2]

[1] *Memorial Regional Hospital, Joe DiMaggio Children's Hospital, Hollywood, FL, United States,* [2] *Department of Biomedical Engineering, Florida International University, Miami, FL, United States*

Keywords: ECM, repair, regeneration, cardiovascular, scaffolds

Editorial on the Research Topic

Extracellular Matrix for Cardiovascular Reconstruction

The native extracellular matrix (ECM) is an active material which engages in multi-faceted and complex interactions with cells. Directed cell to ECM communications are known to be essential for functional tissue regeneration such that stem cells, whether native or therapeutically introduced, require an ECM for sensical structural development. Current technologies available for therapeutic interventions in cardiovascular disease have relied largely on mechanical products, xenografts, or some form of composite structure (Bioprosthetics). These products unlike native, biologically living tissues such as heart valves and blood vessels have a shortened life span because of a lack of self-repair and immune mediated destruction. These materials also do not grow with younger patients. Extracellular matrix as a medical therapeutic product involves decellularization of a tissue such that all that remains is the ECM framework, devoid of cellular structures or biological markers. Such scaffolds have enormous potential as a therapeutic option. A breakthrough in regenerative medicine would revolutionize the field of cardiovascular medicine and surgery, where a large sub-set of patients currently face limited treatment options. The advent of regenerative therapies could yield needed, life-saving treatment of congenital cardiovascular defects (e.g., valvular malformations) by supporting somatic growth in the young patient, aid in induction of neovascularization at sites of cardiac damage, and provide hemodynamically resilient, living vascular grafts to replace large arteries that have limited patency due to disease. This Research Topic, aptly named, "Extracellular Matrix for Cardiovascular Reconstruction," is being presented at this specific time because of the recent explosion of exciting *in vitro*, *in vivo* and *clinical* findings in regenerative medicine. A total of 8 contributions which includes two mini-reviews, two reviews and four original research articles are summarized here:

In a mini-review article, Delfín et al. remind us of the critical roles that selected ECM proteins play in both cardiovascular homeostasis and in pathologies. Specifically, they focus on a recently identified protein, ABI3BP, that is present in the cardiovascular tissues and whose concentrations are decreased in diseased conditions such as dilated cardiomyopathy. The article further emphasizes the multi-faceted and complex role that a single ECM protein, i.e., ABI3BP, has in both augmenting and reducing cardiac repair/regeneration. The other mini-review by Ramaswamy et al. sheds light on several matricellular proteins such as Decorin, Fibulin-1 and Lumican in the context of vascular tissue engineering. The article describes matricellular protein activity that could positively influence important properties in functional *de novo* blood vessels, such as mechanical integrity, anti-thrombogenicity, endothelialization, and measured recruitment of vascular smooth muscle cells.

Hostile vs. healing macrophage responses in tissue remodeling has long been an aggressively pursued area among cardiovascular researchers. O'Rourke et al. provide a comprehensive review of not only traditional understanding of macrophages in cardiovascular tissues but infuse the

OPEN ACCESS

Edited by:
Paolo Madeddu,
University of Bristol, United Kingdom

Reviewed by:
Zamaneh Kassiri,
University of Alberta, Canada
Nikolaos Frangogiannis,
Albert Einstein College of Medicine, United States

***Correspondence:**
Steven Bibevski
sbibevski@mhs.net

Specialty section:
This article was submitted to Cardiovascular Biologics and Regenerative Medicine, a section of the journal Frontiers in Cardiovascular Medicine

Received: *06 February 2021*
Accepted: *11 March 2021*
Published: *08 April 2021*

Citation:
Bibevski S, Ramaswamy S and Hutcheson J (2021) Editorial: Extracellular Matrix for Cardiovascular Reconstruction. Front. Cardiovasc. Med. 8:664803. doi: 10.3389/fcvm.2021.664803

article with a report of contemporary findings regarding the restriction of inflammatory responses by macrophages that lead to abnormal ECM remodeling and subsequent heart failure following myocardial infarction. Meanwhile, the other review article by Pattar et al. also targets the critical problem of poor ECM remodeling following myocardial infarction, and discusses the surgical repair of the disease-induced, damaged cardiac muscle, using decellularized ECM bioscaffolds. Of primary interest is the bio-active molecules that are contained within these bioscaffold materials and that can enhance healthy, cardiac regenerative processes while minimizing abnormal tissue remodeling.

Finally, four original research articles by Bax et al.; Gonzalez et al.; Bibevski et al.; Allen et al. round-up the list of contributions in this Research Topic, with all four having a materials and/or mechanobiological framework but in different settings. Following *in vivo* observations, Bax et al. developed an *in vitro* engineered tissue model system to study the individual and combined effects of TGFβ growth factor and cyclic strain on human epicardium-derived cells. Through TGFβ/ALK5-dependent signaling, these cells promoted remodeling of the cardiac ECM via the production of type I collagen. Gonzalez et al. utilized a bioreactor platform to identify how physiologically-relevant, fluid-induced oscillatory shear stresses can differentiate human bone-marrow derived mesenchymal stem cells seeded on a 3-dimensional substrate. The experiments led to ECM formation that exhibited a healthy valve phenotype, which could potentially accelerate heart valve regeneration *in vivo*. Such an approach may serve useful for a heart valve replacement strategy that supports somatic tissue growth in the treatment of critical congenital valve diseases in the young. In the case report with histologic study, Bibevski et al. showed that ECM implanted in the pulmonary artery to fill a defect remodels to mimic the surrounding tissue and the intended biologic function. Clinical reports such as this give us guidance as to what works with bare ECM and what doesn't. Equally relevant is the insightful article by Allen et al. that follows the clinical remodeling of small intestine submucosa (SIS)-ECM after endarterectomy, thereby demonstrating the utility of biological materials in cardiovascular repair procedures.

In summary, understanding the cellular mechanisms of pathological and healthy cardiovascular ECM remodeling under biochemical and/or biomechanical environments of pertinence, as well as the advancement of ECM-mimicking biomaterials for use in cardiovascular surgical repair hold promise for a breakthrough in overcoming current treatment limitations. The 8 articles presented herein have addressed this subject matter, with an appreciation of the state-of-the-field and the current challenges that await us. The topic editors are sincerely appreciative to the 47 authors who contributed to these 8 articles, which will help orient the research community on the ECM, to its properties/responses, and with the overall goal of improving existing treatments for cardiovascular disease. For now, the holy grail of replacing cardiovascular structures with ECM scaffold guided, biologically remodeling tissues that can grow with the patient although within sight, remains elusive.

AUTHOR CONTRIBUTIONS

SB, SR, and JH topic editors for this Research Topic, entitled "Extracellular Matrix for Cardiovascular Reconstruction" were responsible for the writing of this editorial. All authors contributed to the article and approved the submitted version.

Conflict of Interest: The authors declare that the research was conducted in the absence of any commercial or financial relationships that could be construed as a potential conflict of interest.

frontiers in Cardiovascular Medicine

MINI REVIEW
published: 14 March 2019
doi: 10.3389/fcvm.2019.00023

The Extracellular Matrix Protein ABI3BP in Cardiovascular Health and Disease

Dawn A. Delfín, Joshua L. DeAguero and Elizabeth N. McKown*

Department of Pharmaceutical Sciences, College of Pharmacy, University of New Mexico, Albuquerque, NM, United States

ABI3BP is a relatively newly identified protein whose general biological functions are not yet fully defined. It is implicated in promoting cellular senescence and cell-extracellular matrix interactions, both of which are of vital importance in the cardiovascular system. ABI3BP has been shown in multiple studies to be expressed in the heart and vasculature, and to have a role in normal cardiovascular function and disease. However, its precise role in the cardiovascular system is not known. Because ABI3BP is present in the cardiovascular system and is altered in cardiovascular disease states, further investigation into ABI3BP's biological and biochemical importance in cardiovascular health and disease is warranted.

Keywords: ABI3BP, extracellular matrix, heart, vasculature, cardiovascular

OPEN ACCESS

Edited by:
Steve Bibevski,
Joe DiMaggio Children's Hospital,
United States

Reviewed by:
Gabriela Kania,
University Hospital Zürich, Switzerland
Elisa Avolio,
University of Bristol, United Kingdom

****Correspondence:***
Dawn A. Delfín
ddelfin@salud.unm.edu

Specialty section:
This article was submitted to Cardiovascular Biologics and Regenerative Medicine, a section of the journal Frontiers in Cardiovascular Medicine

Received: *05 November 2018*
Accepted: *20 February 2019*
Published: *14 March 2019*

Citation:
Delfín DA, DeAguero JL and McKown EN (2019) The Extracellular Matrix Protein ABI3BP in Cardiovascular Health and Disease. Front. Cardiovasc. Med. 6:23. doi: 10.3389/fcvm.2019.00023

ABI3BP: AN OVERVIEW

ABI3BP is an extracellular matrix protein whose function is not well-known. However, previous and ongoing studies have demonstrated that ABI3BP is of emerging importance in both health and disease. The *ABI3BP* gene is expressed in multiple organs, including the heart, kidney, lung, pancreas, and placenta, with low-level or variable expression in the spleen, liver, brain, bone, and skeletal muscle (1–4). ABI3BP is best known for is its role in multiple forms of cancer, acting as a tumor suppressor via promotion of cellular senescence (2, 3, 5–18). Although it is expressed in the heart and vasculature, its role in the cardiovascular system is not yet defined. Still, there are a limited number of studies highlighting that its presence, upregulation, or downregulation plays a role in cardiovascular health and disease states. This minireview will present the research published to date on ABI3BP in the cardiovascular system.

The first study on ABI3BP was published in 2001 (1), after Matsuda et al., performed a yeast two-hybrid screen for binding partners of the SH3 binding domain of Nesh-SH3, also known as Abelson (Abl) interacting protein family member 3 (ABI3). Originally, the group named the newly identified gene, *Tarsh* because it was the target of Nesh-SH3. Today, it is known as Abl-interacting protein family member 3 binding protein, or ABI3BP.

At present, ABI3BP's general biological functions are largely unknown. Although it was identified in a yeast two-hybrid screen as a binding partner of the isolated SH3 domain of ABI3, it has not been empirically demonstrated that ABI3BP and the full ABI3 protein interact. However, both ABI3BP and ABI3 are downregulated in cancers with supporting evidence that they are both important in promoting cellular senescence (1, 14, 19–21). ABI3BP is also known as an extracellular/interstitial matrix protein and plays a role in cell-substrate adhesion (4, 22–26).

As a promotor of cellular senescence and cell-extracellular matrix binding interactions, it is possible that ABI3BP regulates these processes in the cardiovascular system. The adult heart has almost negligible cardiomyocyte turnover (27, 28), and the mature cardiomyocyte is considered a terminal cell. Additionally, cardiac fibroblasts are present in a non-activated state in the healthy myocardium (29, 30). Thus, ABI3BP may help maintain the non-proliferative state of the normal myocardium. Further, cell-extracellular matrix interactions are key in the heart and vasculature to organize the organ structure; provide biological, biochemical, and biophysical signals between the intracellular and extracellular environments; and provide mechanical strength against blood flow (31–35). ABI3BP may be an important component of the cell-extracellular matrix interactome in the cardiovascular system. Moreover, pathological extracellular matrix remodeling is a key feature of many cardiovascular diseases (35, 36). This pathological remodeling may affect or be affected by ABI3BP.

THE CARDIOVASCULAR ROLE OF ABI3BP

Research published to date shows that ABI3BP is expressed in the vasculature and the heart, but almost no more than that is currently known. A thorough and systematic study on the localization of ABI3BP in the cardiovascular system is lacking. We and others have shown that ABI3BP is present in the myocardium, the aorta, and in cardiac progenitor cells. Specific localization of ABI3BP in cardiovascular tissues and within cells has not yet been determined, but it is a research goal of our laboratory. Specific localization of ABI3BP will help clarify its potential role in cardiovascular health and disease.

The cardiovascular localization and roles of ABI3BP as published to date is detailed below, and summarized in **Table 1**.

TABLE 1 | The cardiovascular localization and/or role of ABI3BP.

ABI3BP cardiovascular localization and/or role	Changes in cardiovascular disease	References
Myocardial extracellular matrix (right and left atria, left ventricle)	Reduced from left ventricle in failing hearts	(24, 37)
Aorta, vascular endothelial cells, vascular smooth muscle cells	Upregulated in stressed vascular endothelial and smooth muscle cells	(22, 38, 39)
Cardiac progenitor cells (CPCs)	Reduces CPC proliferation, promotes CPC transdifferentiation toward cardiomyocytes, protects against myocardial infarction, acts through integrin-β1 binding and signaling	(40)
Link between cardiovascular disease and psychological stress	Single nucleotide polymorphism (SNP) associated with high blood pressure in response to unfair discrimination	(41)
Early-onset preeclampsia	Upregulated in early-onset preeclampsia	(42)
Protection against cigarette smoke-induced emphysema	Downregulated in a strain of mice resistant to cigarette smoke-induced emphysema	(43)

ABI3BP in the Myocardial Extracellular Matrix

ABI3BP is expressed in the decellularized extracellular matrix of the human heart's right and left atria (24) and the left ventricle (37), as identified in separate proteomics studies. In both studies, the heart tissue was decellularized, and the isolated extracellular matrix was subjected to mass spectrometry to identify global protein and glycoprotein alterations. ABI3BP (listed as "target of Nesh-SH3") was one of 12 extracellular matrix or matricellular proteins identified in our study of the extracellular matrix of the left ventricle (37), and one of 75 glycoproteins identified in the Barallobre-Barreiro atrial extracellular matrix study (24). We further showed that ABI3BP levels are reduced by approximately half from the left ventricular extracellular matrix in failing human hearts with dilated cardiomyopathy (37). These studies support that ABI3BP is present specifically in the extracellular matrix of the heart, where it can potentially perform its putative role in promoting cell-extracellular matrix interactions.

ABI3BP in the Vasculature and Vascular Cells

ABI3BP (listed as "target of Nesh-SH3") was identified in a proteomics study of the isolated extracellular matrix of the human aorta (22), out of 103 total proteins identified. This was the first report of ABI3BP in the vasculature, and its function there is still unknown. Endothelial cells, which line blood vessels, are sensitive to cardiovascular stress. In a proteomic analysis of the vesicular "secretome" of human umbilical vein endothelial cells (HUVECs), Yin et al., demonstrated that ABI3BP protein was found in serum-starved (stressed), phorbol-12-myristate-13-acetate (PMA)-stimulated HUVECs (38). Scherer et al., knocked down the transcription factor nuclear factor of activated T-cells 5 (NFAT5) in vascular smooth muscle cells obtained from human umbilical cords. NFAT5 is known to control vascular smooth muscle cell phenotypes. After NFAT5 was knocked down in umbilical vascular smooth muscle cells, the cells were subjected to stretching stress. *ABI3BP* mRNA levels were upregulated 2.7-fold in NFAT5 knockdown cells compared to cells expressing NFAT5, indicating that NFAT5 normally suppresses *ABI3BP* expression in umbilical vascular smooth muscle cells (39). These studies demonstrate that ABI3BP is expressed in the vasculature, including under starvation or stretching stress, and may play a role in blood vessels.

ABI3BP in Cardiac Progenitor Cells

Following a study of *ABI3BP* in pluripotent stem cells, Hodgkinson et al., studied the effects of *ABI3BP* knockout and knockdown in a cardiac stem cell, or c-Kit$^+$ cardiac progenitor

cells. They isolated cardiac progenitor cells from ABI3BP-knockout and wild-type mice. They found that *ABI3BP* mRNA and protein levels increased during the transdifferentiation process toward cardiomyocytes in wild-type cardiac progenitor cells, along with increases in markers of cardiomyocyte transdifferentiation, including *Gata4*, *Gata6*, *Mef2C*, and *TNNI3* mRNA and protein. In contrast, ABI3BP-knockout cardiac progenitor cells showed significantly reduced levels of cardiomyocyte transdifferentiation markers. Reinstating *ABI3BP* expression in knockout cardiac progenitor cells using an expression plasmid led to expression of differentiation markers. Wild-type and *ABI3BP*-knockout mice were subjected to myocardial infarction via coronary artery restriction, or a sham operation. Myocardial infarction induced c-Kit$^+$ cardiac progenitor cells in both wild-type and *ABI3BP*-knockout mice, but more so in knockout mice. There was a higher abundance of double positive c-Kit$^+$ and Gata4$^+$ cells in wild-type infarcted mice compared to wild-type shams, indicating early-stage cardiac progenitor cell-to-cardiomyocyte transdifferentiation activity. However, this transdifferentiation was impaired in knockout mice. Wild-type mice showed a reduction in cardiac fibrosis and improved cardiac function 1 month post-myocardial infarction compared to *ABI3BP* knockout mice. Blocking integrin-β_1 binding using antibodies inhibited cardiac progenitor cell transdifferentiation, indicating that the activity of ABI3BP is mediated through integrin-β_1. Knockout cardiac progenitor cells showed reduced levels of phospho-protein kinase c and phospho-Akt, which are downstream signaling factors of integrin-β_1. Thus, while cardiac progenitor cells were induced to a higher level in the ABI3BP knockout mice, they were blocked from commitment to the cardiomyocyte lineage (40). This implies that ABI3BP suppresses cardiac progenitor cell activation toward cardiac repair, but its suppression improves functional outcomes post-myocardial infarction.

ABI3BP in Cardiovascular Disease

In African Americans living in Tallahassee, Florida, USA, an *ABI3BP* gene single nucleotide polymorphism was associated with patients having high blood pressure and experiencing unfair treatment (discrimination), implying that individuals possessing this single nucleotide polymorphism may be prone to enough distress during unfair treatment that it contributes to their high blood pressure (41). Of note, a single nucleotide polymorphism in the *ABI3BP* gene was shown to be strongly associated with suicide attempts (44, 45). Thus, ABI3BP may contribute to neuropsychological distress alongside cardiovascular disease. Preeclampsia is a cardiovascular condition in pregnancy defined by pregnancy-induced hypertension and proteinuria. ABI3BP mRNA was upregulated in early-onset preeclampsia compared to late-onset preeclampsia and gestational age-matched controls (42). This study supports that ABI3BP is a potential contributor to severe cardiovascular disease.

In a survey of mouse models either susceptible to cigarette smoke-induced emphysema or not, they found that the genetic variation most significantly associated with susceptibility (i.e., comparing susceptible A/J mice and in resistant CBA/J mice) is in the *ABI3BP* gene, with two mutations that are predicted to be deleterious. Susceptible A/J mice, lacking the key mutations, express *ABI3BP* mRNA at 100-fold higher levels than the resistant CBA/J mice. Thus, a decrease in expression of ABI3BP appears to be protective to cigarette smoke-induced emphysema. Perhaps, the authors speculate, this occurs by promoting regrowth and survival of the lung epithelium when ABI3BP is absent (43). Recalling that ABI3BP is suspected to promote cellular senescence, it follows that its presence at higher levels in the lung inhibits lung epithelium regeneration.

IMPLICATIONS OF ABI3BP IN CARDIOVASCULAR RESEARCH

ABI3BP is generally known as a component of the extracellular matrix. Studies of the isolated extracellular matrix from the heart and aorta show that it is a component of the extracellular matrix of the cardiovascular system specifically (22, 24, 37). Furthermore, our study showed that ABI3BP levels were significantly reduced in failing human hearts with dilated cardiomyopathy (37). Pathological remodeling of the extracellular matrix of the heart and vasculature during the progression of cardiovascular disease plays an important role in disease pathology (35, 36). Thus, alteration of ABI3BP expression in the extracellular matrix during cardiovascular disease can be a cause and/or consequence of pathological remodeling. This possibility must be further explored to show whether ABI3BP plays a role in pathological remodeling of the cardiovascular extracellular matrix, and whether inhibiting alterations in ABI3BP expression can be a viable therapeutic target. Our laboratory is currently investigating the role of ABI3BP in cell-extracellular matrix adhesion in heart failure.

ABI3BP also affects cell cycle progression, promoting cellular senescence (1, 4, 14). ABI3BP's presence in the heart and blood vessels may promote a normal homeostatic condition of low cell proliferation. However, reductions in ABI3BP in cardiovascular disease may increase proliferation of key cells involved repair, such as activated fibroblasts (myofibroblasts) and cardiac progenitor cells (40). However, ABI3BP reductions may also inhibit healing by blocking cardiac progenitor cell transdifferentiation toward cardiomyocytes (40), or its presence at high levels can inhibit healing due to attenuation of epithelial regeneration (43). *ABI3BP* genetic mutations may also be responsible for early-onset preeclampsia (42). The potential role of ABI3BP in senescence in cells of the cardiovascular system needs to be fully explored.

At the cutting edge of pre-clinical investigation and clinical trials for cardiac repair and regeneration are solid patches or injectable hydrogels comprised of isolated extracellular matrix. The extracellular matrix of the patches and hydrogels may be derived from mammalian tissues (including the heart), generated synthetically, or even a mixture of the two (46, 47). In many studies, the extracellular matrix is pre-seeded with a source of stem cells for implantation onto/into the heart. The expectation is that the patch/hydrogel will engraft with the native myocardial tissue, and the embedded stem cells would differentiate into cardiomyocytes, vascular endothelial cells, or other cardiac

cells to promote myocardial repair and regeneration. Various sources of stem cells and extracellular matrix products have been tested. The ability of stem cells to engraft into the matrix material and differentiate into the desired cardiac cells is quite variable. It is possible that a uniform application of ABI3BP into the patch could improve stem cell adhesion, engraftment and cardiomyocyte differentiation, since current evidence supports that may ABI3BP play a role in cell-ECM adhesion and stem cell transdifferentiation (4, 24, 37, 40).

The possible roles for ABI3BP in cardiovascular health maintenance and disease progression appear variable. It is difficult to ascertain whether it is a helpful or harmful protein in cardiovascular health and disease. However, the confusion in ABI3BP's role is likely due to the scarcity of studies published on this protein to date. These discrepancies might be resolved with an increase in active investigation into this intriguing new protein. With further investigation, ABI3BP may prove to be a novel therapeutic target for cardiovascular disease.

AUTHOR CONTRIBUTIONS

DD, JD, and EM researched the articles cited in the review, and wrote and edited the manuscript in whole or in part, read and revised the final manuscript before submission, and approved the submitted version.

FUNDING

This work was supported by the American Heart Association (to DD, grant numbers 15BGIA22840012, 18AIREA33900010), the CTSC KL2 program (to DD, NIH grant number UL1TR001448), the NIH National Human Genome Research Institute FlyBase Postbaccalaureate Fellowship (to JD, grant number R25HG007630), and the University of New Mexico College of Pharmacy, and Cardiovascular and Metabolic Disease Signature Program (to DD).

REFERENCES

1. Matsuda S, Iriyama C, Yokozaki S, Ichigotani Y, Shirafuji N, Yamaki K, et al. Cloning and sequencing of a novel human gene that encodes a putative target protein of Nesh-SH3. *J Hum Genet.* (2001) 46:483–6. doi: 10.1007/s100380170049
2. Terauchi K, Shimada J, Uekawa N, Yaoi T, Maruyama M, Fushiki S. Cancer-associated loss of TARSH gene expression in human primary lung cancer. *J Cancer Res Clin Oncol.* (2006) 132:28–34. doi: 10.1007/s00432-005-0032-1
3. Uekawa N, Terauchi K, Nishikimi A, Shimada J, Maruyama M. Expression of TARSH gene in MEFs senescence and its potential implication in human lung cancer. *Biochem Biophys Res Commun.* (2005) 329:1031–8. doi: 10.1016/j.bbrc.2005.02.068
4. Hodgkinson CP, Naidoo V, Patti KG, Gomez JA, Schmeckpeper J, Zhang Z, et al. Abi3bp is a multifunctional autocrine/paracrine factor that regulates mesenchymal stem cell biology. *Stem Cells.* (2013) 31:1669–82. doi: 10.1002/stem.1416
5. Schulten H-J, Hussein D, Al-Adwani F, Karim S, Al-Maghrabi J, Al-Sharif M, et al. Microarray expression data identify DCC as a candidate gene for early meningioma progression. *PLoS ONE.* (2016) 11:e0153681. doi: 10.1371/journal.pone.0153681
6. Berghauser Pont LM, Spoor JK, Venkatesan S, Swagemakers S, Kloezeman JJ, Dirven CM, et al. The Bcl-2 inhibitor obatoclax overcomes resistance to histone deacetylase inhibitors SAHA and LBH589 as radiosensitizers in patient-derived glioblastoma stem-like cells. *Genes Cancer.* (2014) 5:445–59. doi: 10.18632/genesandcancer.42
7. Kafetzopoulou LE, Boocock DJ, Dhondalay GKR, Powe DG, Ball GR. Biomarker identification in breast cancer: beta-adrenergic receptor signaling and pathways to therapeutic response. *Comput Struct Biotechnol.* (2013) 6:e201303003. doi: 10.5936/csbj.201303003
8. Kim JC, Kim SY, Roh SA, Cho DH, Kim DD, Kim JH, et al. Gene expression profiling: canonical molecular changes and clinicopathological features in sporadic colorectal cancers. *World J Gastroenterol.* (2008) 14:6662–72. doi: 10.3748/wjg.14.6662
9. Britze A, Birkler RID, Gregersen N, Ovesen T, Palmfeldt J. Large-scale proteomics differentiates cholesteatoma from surrounding tissues and identifies novel proteins related to the pathogenesis. *PLoS ONE.* (2014) 9:e104103. doi: 10.1371/journal.pone.0104103
10. Kristjansdottir B, Levan K, Partheen K, Carlsohn E, Sundfeldt K. Potential tumor biomarkers identified in ovarian cyst fluid by quantitative proteomic analysis, ITRAQ. *Clin Proteomics.* (2013) 10:4. doi: 10.1186/1559-0275-10-4
11. Nishikawa R, Goto Y, Sakamoto S, Chiyomaru T, Enokida H, Kojima S, et al. Tumor-suppressive microRNA-218 inhibits cancer cell migration and invasion via targeting of LASP1 in prostate cancer. *Cancer Sci.* (2014) 105:802–11. doi: 10.1111/cas.12441
12. Cerutti JM, Delcelo R, Amadei MJ, Nakabashi C, Maciel RM, Peterson B, et al. A preoperative diagnostic test that distinguishes benign from malignant thyroid carcinoma based on gene expression. *J Clin Invest.* (2004) 113:1234–42. doi: 10.1172/JCI19617
13. Guimarães GS, Latini FR, Camacho CP, Maciel RM, Dias-Neto E, Cerutti JM. Identification of candidates for tumor-specific alternative splicing in the thyroid. *Genes Chromosomes Cancer.* (2006) 45:540–53. doi: 10.1002/gcc.20316
14. Latini FR, Hemerly JP, Oler G, Riggins GJ, Cerutti JM. Re-Expression of ABI3-binding protein suppresses thyroid tumor growth by promoting senescence and inhibiting invasion. *Endocrine-Related Cancer.* (2008) 15:787–99. doi: 10.1677/ERC-08-0079
15. Salo S, Bitu C, Merkku K, Nyberg P, Bello IO, Vuoristo J, et al. Human bone marrow mesenchymal stem cells induce collagen production and tongue cancer invasion. *PLoS ONE.* (2013) 8:e77692. doi: 10.1371/journal.pone.0077692
16. Horpaopan S, Kirfel J, Peters S, Kloth M, Hüneburg R, Altmüller J, et al. Exome sequencing characterizes the somatic mutation spectrum of early serrated lesions in a patient with serrated polyposis syndrome (SPS). *Hereditary Cancer Clin Pract.* (2017) 15:22. doi: 10.1186/s13053-017-0082-9
17. Wakoh T, Uekawa N, Terauchi K, Sugimoto M, Ishigami A, Shimada J, et al. Implication of P53-dependent cellular senescence related gene, TARSH in tumor suppression. *Biochem Biophys Res Commun.* (2009) 380:807–12. doi: 10.1016/j.bbrc.2009.01.171
18. Wakoh T, Sugimoto M, Terauchi K, Shimada J, Maruyama M. A novel P53-dependent apoptosis function of TARSH in tumor development. *Nagoya J Med Sci.* (2009) 71:109–14.
19. Ichigotani Y, Fujii K, Hamaguchi M, Matsuda S. In search of a function for the E3B1/Abi2/Argbp1/NESH family (review). *Int J Mol Med.* (2002) 9:591–5. doi: 10.3892/ijmm.9.6.591
20. Ichigotani Y, Yokozaki S, Fukuda Y, Hamaguchi M, Matsuda S. Forced expression of NESH suppresses motility and metastatic dissemination of malignant cells. *Cancer Res.* (2002) 62:2215–9.
21. Latini FR, Hemerly JP, Freitas BC, Oler G, Riggins GJ, Cerutti JM. ABI3 ectopic expression reduces *in vitro* and *in vivo* cell growth properties while inducing senescence. *BMC Cancer.* (2011) 11:11. doi: 10.1186/1471-2407-11-11
22. Didangelos A, Yin X, Mandal K, Baumert M, Jahangiri M, Mayr M. Proteomics characterization of extracellular space components in the human aorta. *Mol Cell Proteomics.* (2010) 9:2048–62. doi: 10.1074/mcp.M110.001693

23. Naba A, Pearce OMT, Del Rosario A, Ma D, Ding H, Rajeeve V, et al. Characterization of the extracellular matrix of normal and diseased tissues using proteomics. *J Proteome Res.* (2017) 16:3083–91. doi: 10.1021/acs.jproteome.7b00191
24. Barallobre-Barreiro J, Gupta SK, Zoccarato A, Kitazume-Taneike R, Fava M, Yin X, et al. Glycoproteomics reveals decorin peptides with anti-myostatin activity in human atrial fibrillation. *Circulation.* (2016) 134:817–32. doi: 10.1161/CIRCULATIONAHA.115.016423
25. ABI3BP. *Target of Nesh-SH3 Precursor—Homo Sapiens (Human)—ABI3BP Gene & Protein.* (2003). Available online at: https://www.uniprot.org/uniprot/Q7Z7G0 (Accessed October 23, 2018).
26. ABI3BP. *ABI Family Member 3 Binding Protein [Homo Sapiens (Human)]—Gene—NCBI.* (2005). Available online at: https://www.ncbi.nlm.nih.gov/gene/?term=25890 (Accessed October 23, 2018).
27. Piek A, de Boer RA, Silljé HH. The fibrosis-cell death axis in heart failure. *Heart Fail Rev.* (2016) 21:199–211. doi: 10.1007/s10741-016-9536-9
28. Bergmann O, Bhardwaj RD, Bernard S, Zdunek S, Barnabé-Heider F, Walsh S, et al. Evidence for cardiomyocyte renewal in humans. *Science.* (2009) 324:98–102. doi: 10.1126/science.1164680
29. Elson EL, Qian H, Fee JA, Wakatsuki T. A model for positive feedback control of the transformation of fibroblasts to myofibroblasts. *Prog Biophys Mol Biol.* (2018). doi: 10.1016/j.pbiomolbio.2018.08.004 [Epub ahead of print]
30. Frangogiannis NG. Cardiac fibrosis: cell biological mechanisms, molecular pathways and therapeutic opportunities. *Mol Aspects Med.* (2018) 65:70–99. doi: 10.1016/j.mam.2018.07.001
31. Takawale A, Sakamuri SS, Kassiri Z. Extracellular matrix communication and turnover in cardiac physiology and pathology. *Comprehens Physiol.* (2015) 5:687–719. doi: 10.1002/cphy.c140045
32. Valiente-Alandi I, Schafer AE, Blaxall BC. Extracellular matrix-mediated cellular communication in the heart. *J Mol Cell Cardiol.* (2016) 91:228–37. doi: 10.1016/j.yjmcc.2016.01.011
33. Bang C, Antoniades C, Antonopoulos AS, Eriksson U, Franssen C, Hamdani N, et al. Intercellular communication lessons in heart failure. *Eur J Heart Fail.* (2015) 17:1091–103. doi: 10.1002/ejhf.399
34. Marchand M, Monnot C, Muller L, Germain S. Extracellular matrix scaffolding in angiogenesis and capillary homeostasis. *Semin Cell Dev Biol.* (2018). doi: 10.1016/j.semcdb.2018.08.007 [Epub ahead of print]
35. Imanaka-Yoshida K. Extracellular matrix remodeling in vascular development and disease. In: Nakanishi T, Markwald RR, Baldwin HS, Keller BB, Srivastava D, Yamagishi H, editors. *Etiology and Morphogenesis of Congenital Heart Disease: From Gene Function and Cellular Interaction to Morphology*. Tokyo: Springer (2016). Available online at: http://www.ncbi.nlm.nih.gov/books/NBK500279/
36. Li L, Zhao Q, Kong W. Extracellular matrix remodeling and cardiac fibrosis. *Matrix Biol.* (2018) 68–69, 490–506. doi: 10.1016/j.matbio.2018.01.013
37. DeAguero JL, McKown EN, Zhang L, Keirsey J, Fischer EG, Samedi VG, et al. Altered protein levels in the isolated extracellular matrix of failing human hearts with dilated cardiomyopathy. *Cardiovasc Pathol.* (2017) 26:12–20. doi: 10.1016/j.carpath.2016.10.001
38. Yin X, Bern M, Xing Q, Ho J, Viner R, Mayr M. Glycoproteomic analysis of the secretome of human endothelial cells. *Mol Cell Proteomics.* (2013) 12:956–78. doi: 10.1074/mcp.M112.024018
39. Scherer C, Pfisterer L, Wagner AH, Hödebeck M, Cattaruzza M, Hecker M, et al. Arterial wall stress controls NFAT5 activity in vascular smooth muscle cells. *J Am Heart Assoc.* (2014) 3:e000626. doi: 10.1161/JAHA.113.000626
40. Hodgkinson CP, Gomez JA, Payne AJ, Zhang L, Wang X, Dal-Pra S, et al. Abi3bp regulates cardiac progenitor cell proliferation and differentiation. *Circ Res.* (2014) 115:1007–16. doi: 10.1161/CIRCRESAHA.115.304216
41. Quinlan J, Pearson LN, Clukay CJ, Mitchell MM, Boston Q, Gravlee CC, et al. Genetic loci and novel discrimination measures associated with blood pressure variation in African Americans living in Tallahassee. *PLoS ONE.* (2016) 11:e0167700. doi: 10.1371/journal.pone.0167700
42. Nevalainen J, Skarp S, Savolainen ER, Ryynänen M, Järvenpää J. Intrauterine growth restriction and placental gene expression in severe preeclampsia, comparing early-onset and late-onset forms. *J Perinatal Med.* (2017) 45:869–77. doi: 10.1515/jpm-2016-0406
43. Radder JE, Gregory AD, Leme AS, Cho MH, Chu Y, Kelly NJ, et al. Variable susceptibility to cigarette smoke-induced emphysema in 34 inbred strains of mice implicates abi3bp in emphysema susceptibility. *Am J Respir Cell Mol Biol.* (2017) 57:367–75. doi: 10.1165/rcmb.2016-0220OC
44. Perlis RH, Huang J, Purcell S, Fava M, Rush AJ, Sullivan PF, et al. Genome-wide association study of suicide attempts in mood disorder patients. *Am J Psychiatry.* (2010) 167:1499–507. doi: 10.1176/appi.ajp.2010.10040541
45. Kimbrel NA, Garrett ME, Dennis MF, Clinical Center Workgroup, Hauser MA, Ashley-Koch AE, et al. A genome-wide association study of suicide attempts and suicidal ideation in U.S. *Military Veterans. Psychiatry Res.* (2018) 269:64–9. doi: 10.1016/j.psychres.2018.07.017
46. Bejleri D, Davis ME. Decellularized extracellular matrix materials for cardiac repair and regeneration. *Adv Healthcare Mater.* (2019) 2019:1801217. doi: 10.1002/adhm.201801217
47. Spang MT, Christman KL. Extracellular matrix hydrogel therapies: *in vivo* applications and development. *Acta Biomater.* (2018) 68:1–14. doi: 10.1016/j.actbio.2017.12.019

Conflict of Interest Statement: The authors declare that the research was conducted in the absence of any commercial or financial relationships that could be construed as a potential conflict of interest.

frontiers in Cardiovascular Medicine

MINI REVIEW
published: 31 May 2019
doi: 10.3389/fcvm.2019.00074

Functional Vascular Tissue Engineering Inspired by Matricellular Proteins

Aneesh K. Ramaswamy[1,2], *David A. Vorp*[1,2,3,4,5] *and Justin S. Weinbaum*[1,2,6]*

[1] Department of Bioengineering, University of Pittsburgh, Pittsburgh, PA, United States, [2] McGowan Institute for Regenerative Medicine, University of Pittsburgh, Pittsburgh, PA, United States, [3] Department of Surgery, University of Pittsburgh, Pittsburgh, PA, United States, [4] Department of Cardiothoracic Surgery, University of Pittsburgh, Pittsburgh, PA, United States, [5] Department of Chemical and Petroleum Engineering, University of Pittsburgh, Pittsburgh, PA, United States, [6] Department of Pathology, University of Pittsburgh, Pittsburgh, PA, United States

Modern regenerative medicine, and tissue engineering specifically, has benefited from a greater appreciation of the native extracellular matrix (ECM). Fibronectin, collagen, and elastin have entered the tissue engineer's toolkit; however, as fully decellularized biomaterials have come to the forefront in vascular engineering it has become apparent that the ECM is comprised of more than just fibronectin, collagen, and elastin, and that cell-instructive molecules known as matricellular proteins are critical for desired outcomes. In brief, matricellular proteins are ECM constituents that contrast with the canonical structural proteins of the ECM in that their primary role is to interact with the cell. Of late, matricellular genes have been linked to diseases including connective tissue disorders, cardiovascular disease, and cancer. Despite the range of biological activities, this class of biomolecules has not been actively used in the field of regenerative medicine. The intent of this review is to bring matricellular proteins into wider use in the context of vascular tissue engineering. Matricellular proteins orchestrate the formation of new collagen and elastin fibers that have proper mechanical properties—these will be essential components for a fully biological small diameter tissue engineered vascular graft (TEVG). Matricellular proteins also regulate the initiation of thrombosis via fibrin deposition and platelet activation, and the clearance of thrombus when it is no longer needed—proper regulation of thrombosis will be critical for maintaining patency of a TEVG after implantation. Matricellular proteins regulate the adhesion, migration, and proliferation of endothelial cells—all are biological functions that will be critical for formation of a thrombus-resistant endothelium within a TEVG. Lastly, matricellular proteins regulate the adhesion, migration, proliferation, and activation of smooth muscle cells—proper control of these biological activities will be critical for a TEVG that recellularizes and resists neointimal formation/stenosis. We review all of these functions for matricellular proteins here, in addition to reviewing the few studies that have been performed at the intersection of matricellular protein biology and vascular tissue engineering.

Keywords: collagen, elastin, extracellular matrix, endothelial cells, smooth muscle cells, thrombosis

OPEN ACCESS

Edited by:
Steve Bibevski,
Joe DiMaggio Children's Hospital,
United States

Reviewed by:
Axel Haverich,
Hannover Medical School, Germany
Xuechong Hong,
Boston Children's Hospital, Harvard Medical School, United States

***Correspondence:**
Justin S. Weinbaum
juw51@pitt.edu

Specialty section:
This article was submitted to Cardiovascular Biologics and Regenerative Medicine, a section of the journal Frontiers in Cardiovascular Medicine

Received: *28 February 2019*
Accepted: *15 May 2019*
Published: *31 May 2019*

Citation:
Ramaswamy AK, Vorp DA and Weinbaum JS (2019) Functional Vascular Tissue Engineering Inspired by Matricellular Proteins. Front. Cardiovasc. Med. 6:74. doi: 10.3389/fcvm.2019.00074

INTRODUCTION

Modern regenerative medicine, and tissue engineering specifically, has benefited from a greater appreciation of the native extracellular matrix (ECM). Fibronectin, collagen, and elastin have entered the tissue engineer's toolkit: peptides derived from fibronectin are routinely added to synthetic scaffolds to promote adhesion of seeded cells, high collagen content has been desirable for mechanically strong engineered tissues, and elastin has been an agreed-upon target for tissues that rely on recoil such as engineered blood vessels, skin, and lungs. It has become apparent that ECM-based biomaterials obtained by decellularization of native intestine, bladder, and heart tissues have a strong positive influence on *in vivo* regeneration. This cell-instructive potential includes the recruitment of host stem cells, modulation of the immune system, and promotion of cell differentiation to a beneficial phenotype for repair and later homeostasis. Notably, the ECM molecules present in these decellularized biomaterials go beyond just fibronectin, collagen, and elastin and include cell-instructive molecules known as matricellular proteins.

The term "matricellular" was coined by Paul Bornstein and members of his group in 1995. Of note, a special issue of Matrix Biology was published in the summer of 2014 to celebrate Paul Bornstein's legacy, and is recommended reading for more details on the evolution of this field. In brief, matricellular proteins are ECM constituents that contrast with the canonical structural proteins of the ECM in that their primary role is to interact with the cell. General observations of matricellular activity have included a modulatory effect on cell adhesion (hence their alternate name, "modulatory adhesion proteins") and mouse phenotypes characterized by an altered response to injury. Of late, matricellular genes have been linked to diseases including connective tissue disorders, cardiovascular disease, and cancer. Despite the range of biological activities, this class of biomolecules has not been actively used in the field of regenerative medicine. The intent of this review is to bring these proteins (and their constitutive active peptides) into wider use in the context of vascular tissue engineering. A list of the proteins reviewed here can be found in **Table 1**.

In the realm of vascular engineering, there are four key design parameters that must be met for a successful tissue engineered vascular graft (TEVG). First, the graft must have mechanical strength compatible with hemodynamics and local tissue deformation. Second, the implanted graft must present a non-thrombogenic luminal surface; that is, it will not induce activation of the host extrinsic or intrinsic clotting pathways or promote platelet adhesion and activation. Third, the luminal surface of the graft must support the formation and maintenance of an endothelial lining, with the endothelial cell source either an implanted graft or the host. Finally, the interior of the graft wall should be, or become, populated by cells; the most important cell type to populate the new media will be vascular smooth muscle cells. Of note, the smooth muscle cells that repopulate the graft must be restricted from over-proliferation, which could lead to graft blood flow restrictions by neointimal formation and eventual stenosis. In this review, we will examine how the biological activity of matricellular proteins could help vascular engineers achieve each of these four parameters for graft design.

TABLE 1 | Matricellular proteins discussed in this review.

Protein name	Col/Eln	Thr.	EC	SMC
Aggrecan	X			
CCN1 (also Cyr61)	X		X	
CCN2 (also CTGF)	X		X	X
CCN3 (also Nov)			X	X
CCN4 (also Wisp-1)				X
CCN5 (also COMP)				X
Decorin	X		X	
Emilin-1	X	X		
Emilin-2		X		
Fibrillin-1	X		X	
Fibrillin-2	X			
Fibromodulin				X
Fibulin-1	X	X		X
Fibulin-2	X			
Fibulin-5	X			X
Galectin-1				X
Latent TGF-binding protein-1 (LTBP-1)	X			
Lumican	X		X	
Microfibril-associated glycoprotein-1 (MAGP-1)	X	X		X
Microfibril-associated glycoprotein-2 (MAGP-2)			X	X
Osteopontin (OPN, also bone sialoprotein I, BSP-1)				X
SPARC (also osteonectin)	X		X	
Syndecan-4	X			
Tenascin-C (TNC)				X
Tenascin-X (TNX)	X		X	
Thrombospondin-1 (TSP-1)		X	X	X
Thrombospondin-2 (TSP-2)		X	X	
Versican	X			
Vitronectin		X	X	

MATRICELLULAR PROTEINS REGULATE THE PRODUCTION OF COLLAGEN AND ELASTIN, THE KEY MOLECULAR DETERMINANTS OF VASCULAR BIOMECHANICS

The compliance, elastic modulus, and burst strength of grafts have been primary criteria for success. In native vessels, the primary load-bearing proteins in the ECM are collagen and elastin, which combine to give the vessel a biphasic passive response to mechanical stretch (1). To mimic the native vessel, the presence of collagen, elastin, or synthetic substitutes for these molecules has been desirable in engineered grafts. In this section, we will focus on how matricellular proteins regulate the production of collagen and elastin in the context of biological grafts.

Collagen Overview

In the vasculature, the primary collagens which contribute to mechanical strength are the fibrillar collagens, Type I and Type III. Two human genes, COL1A1 and COL1A2, encode the protein components of Type I collagen. In contrast, Type III collagen is produced from a single gene, COL3A1. After transcription and translation, the collagen chains are then post-translationally modified (by proteins such as members of the prolyl hydroxylase and lysyl oxidase (LOX) families) and wound into a collagen triple-helix, comprised of three protein chains per collagen fiber. Collagen fibers are then combined with a staggered overlap into a larger bundle, resulting in fiber cooperativity and a high overall tensile strength of the higher order structure.

Collagen Transcription

Research into the transcriptional control of fibrillar collagens has benefited from the study of scarring in skin. Of note, one hallmark of scarring is the secretion of pro-inflammatory cytokines by immune cells during the wound healing response. The canonical signaling pathway for fibrosis involves transforming growth factor (TGF)-β1. After binding of TGF-β1 to its cellular receptor, the SMAD 2/3 signaling pathway is activated, leading to translocation of SMAD3/4 to the cell's nucleus. SMAD-binding enhancer sequences are found in the promoters for COL1A1 (2), COL1A2 (3), and COL3A1 (4). TGF-β1 functionality is primarily regulated in the vasculature by its binding to the matricellular proteins latent TGF-β binding protein (LTBP)-1 and−4 (5). A molecule with many overlapping functions to TGF-β1 in fibrosis, connective tissue growth factor (CTGF or CCN2) directly promotes collagen synthesis to support either new or healing vascular beds (6), and parallels collagen I expression in pericytes (7).

Collagen Post-translational Modification

In Ehlers-Danlos Syndrome, defects in the vascular wall, particularly in collagen fibers, lead to vascular fragility. One key player in this process is the matricellular protein tenascin-X (TNX). TNX absence results in the loss of structural integrity of the vascular collagenous matrix and a reduction of collagen-processing enzyme efficacy (8). Proteoglycan syndecan-4 promotes post-translational collagen LOX modification directly via its extracellular domain ECsyn4, and indirectly via osteopontin (9). Additionally, stimulation of cardiac fibroblasts with recombinant lumican, a collagen-binding proteoglycan, increased LOX and matrix metalloproteinase-9 (10), leading to hypotheses about the role of lumican in myocardial fibrosis (11) and as a biomarker for acute aortic dissection (12).

Collagen Fiber Assembly

Perhaps the greatest effect of matricellular proteins is on the assembly of collagen fibers, where they act as quality control regulators of collagen fiber size and stability. CCN family member 1 (CCN1), otherwise known as cysteine-rich angiogenic inducer 61 (CYR61), modulates collagen I stability through surface integrins in response to serum concentration levels of basic fibroblast growth factor (bFGF) and vascular endothelial growth factor (VEGF) (6). Secreted protein acidic and rich in cysteine (SPARC), or osteonectin, plays a vital role in binding and organizing collagen (13). SPARC primarily aggregates in vascular basement membranes, modulating procollagen processing and collagen interactions with cardiac fibroblasts (14) producing a series of smaller and more tightly organized collagen I fibrils (15).

Decorin is a member of the small leucine-rich proteoglycan family of matricellular proteins that sequesters TGF-(beta) activity, with glycoproteomic analysis showing decorin-derived peptide fragments present throughout the cardiac ECM (16). Decorin has been shown to influence collagen matrix organization and gel contraction, binding to collagens I-III, VI, and XIV (17) resulting in increased collagen fibril density and decreased diameter (18). The effects of decorin-derived peptides have been studied as a potential way of modulating collagen fibrillogenesis (19) and neointimal hyperplasia following balloon angioplasty (20, 21). Decorin in the context of aortic aneurysm has a complex role: decorin associates with a lowered risk of rupture in murine abdominal aortic aneurysm (22), but while decorin serves a protective role in early in murine aneurysm formation it also correlates strongly with macrophage matrix metalloproteinase (MMP)-9 expression and lesion location (23).

Elastin Overview

In the vasculature, the property of passive recoil in response to pulsatile blood flow is provided by the elastic fiber. While other proteins are responsible for the assembly and biological activity of the elastic fiber, the primary protein component is elastin. A single elastin gene is present in the mammalian genome, and mutation or heterozygosity of the gene is linked to several human diseases including Williams Syndrome (24), cutis laxa (25), and supravalvular aortic stenosis (26). After transcription and translation, elastin is trafficked to the surface of the cell, where it is chaperoned to fibrillin microfibrils and assembled. Intra and inter-molecular crosslinking of elastin is then performed by members of the lysyl oxidase family, producing a resilient, and elastic macrostructure.

Elastin Transcription

Like collagen, elastin can be upregulated by TGF-β signaling. Uniquely, TGF-β regulation of elastin message level occurs post-transcriptionally through stabilization of the messenger RNA (27).

One component of the elastic fiber, the matricellular protein microfibril-associated glycoprotein-1 (MAGP-1), activates latent TGF-β signaling directly (28), potentially presenting an opportunity for molecular engineers looking to encourage elastogenesis. MAGP-1 inhibits binding of LTBP-1 to fibrillin-1 and could fine tune concentration and deposition of the large latent TGF-β (LLC) complex (29). MAGP-1 null mice showed a lack of competition for LLC-microfibril binding, resulting in a reduced concentration of active TGF-β (28).

An additional potential regulator of TGF-β activity upstream of elastin transcription is the matricellular protein emilin-1, which associates with elastic fiber components (30) and inhibits activation of all three pro-TGF-β molecules as a regulatory mechanism for blood pressure (31, 32).

Elastin Post-translational Modification

Elastic recoil is essential during aortic development and physiological blood flow. A murine vSMC lysyl oxidase (LOX) overexpression model resulted in more organized elastic fibers, stronger collagen assembly, and enhanced fibulin-5 production (33); however, an accompanying local H_2O_2 concentration increase was seen, suggesting LOX is a source of oxidative vascular wall stress. LOX knockout mice are prone to thoracic aortic aneurysm and dissection and die soon after birth, with a 60% reduction in elastin crosslinks observed in aortic tissue (34), underscoring LOX inactivation as a key prognostic indicator for aneurysm and dissection prognosis. MAGP-1 and fibronectin both repress endothelial cell LOX deposition (35), which is a secondary but significant LOX source within the vascular wall.

Elastic Fiber Assembly

Fibrillin-1 and fibrillin-2 are both important for elastic fiber development and maintenance of a healthy vasculature. Fibrillin-2 displays preferential accumulation in elastin rich areas (36) while fibrillin-1 is more widely expressed, making it unsurprising that Marfan Syndrome patients have a wide spectrum of pathologies (37). Fibrillin-1 (38) and fibrillin-2 (39) deficient mice both die soon after birth due to aortic rupture, although qualitative differences were observed in the medial wall between the two forms of fibrillin deficiency. One theory for the different modes of action of the fibrillin isoforms is that initial fibrillin-2 involvement aids aortic matrix stability, but continued fibrillin-1 expression is essential for maturation and post-neonatal vascular function (39). This suggests that vascular engineers concerned with repair modulation must give equal attention to the initial embryonic role of fibrillins as well as adult phenotypes in order to achieve a stable engineered vessel.

Fibulin-2, a protein that binds extracellular ligands, is thought to provide redundancy with fibulin-1 (which interacts with elastin precursor tropoelastin), since fibulin-1 knockout mice produce vessels with viable elastic fibers (40). Fibulin-2 interacts with virtually all elastin precursors [though it is not associated with tropoelastin deposition by fibroblasts (41)] and is expressed in basement membrane of heart, with an enhanced role during development (42). Fibulin-2 has the highest elastin-binding affinity of the fibulins and interacts with fibulin-5 to form the elastic lamina by directing elastic fiber microassembly during development and after injury (43). Fibulin-5 is itself an elastin binding protein involved in primary organization and assembly of elastic fibers (44). In a mouse fibrosis model, loss of fibulin-5 resulted in a reduction in aortic stiffness, possibly halting the stiffness-induced local inflammatory response and deposition of ECM (45). Based on the importance of the fibulins, a calcium-dependent elastin binding protein structure domain mimicking aspects of the fibulin family could be replicated to develop a therapeutic to aid in elastin assembly (46) or interrupt the pro-fibrotic feedback loop.

Fibulin-1 and aggrecan content within the aortic wall have recently shown key roles in age-related aortic stiffening (47), with significant deposits of aggrecan and versican accumulation found during proteomic analysis of human thoracic aortic aneurysm and dissection samples (48) due to either increased synthesis or decreased proteolytic turnover. Given high stiffening conditions and predisposition toward dissection and aneurysm, fibulin-1, aggrecan, and versican present as a potential biomarker combination for aneurysmal risk evaluation.

MATRICELLULAR PROTEINS THAT LIMIT THROMBOSIS

In large diameter vascular grafts, such as those used to repair the thoracic aorta, synthetic materials have shown great success. However, when the same synthetic materials (e.g., PTFE) have been used to make small diameter grafts (< 5 mm), thrombosis has been a major failure mechanism (49). Indeed, chemical incorporation of non-thrombogenic coatings (50) and seeding of cells that secrete pro-fibrinolytic factors (51) have been used by engineers to reduce thrombotic failure. The size of the vessel has a clear inverse relationship with the tendency to occlude, which results from the activation of thrombin and platelets (52). Upon activation of thrombin, fibrinogen in serum is converted to fibrin, which forms an insoluble fibrous mesh. Activated platelets adhere to the vascular wall and fibrin, and signal to circulating cells. The net effect of these two activation events is the formation of a thrombus loaded with fibrin and platelets that eventually occludes the small vessel. In this section we will examine how matricellular proteins regulate thrombin activation, ensuing fibrin homeostasis, as well as platelet activation in order to assess new anti-thrombotic engineering strategies.

Thrombin Activation

Thrombosis occurs when prothrombin in the blood is cleaved and thereby gains enzymatic activity. Thrombin activation can occur through one of two distinct pathways. The extrinsic pathway is initiated by trauma and is the primary initiator of the thrombosis cascade, while the intrinsic pathway is initiated through complex formation on collagen and functions as an amplification method for homeostasis. Both pathways result in downstream activation of Factor X and subsequent thrombin activation, but the intrinsic pathway is often associated with inflammatory responses following biomedical material implantation. In either case, activated thrombin cleaves its substrate, fibrinogen, which releases fibrinogen degradation products and initiates fibril formation.

The matricellular protein vitronectin binds to plasminogen activator inhibitor 1 (PAI-1), inhibiting downregulation of PAI-1 via its receptor, LRP (53). Vitronectin is co-released with PAI-1 as a counterbalance mechanism during platelet activation and incorporates into the clot where it can modulate PAI-1 activity (54).

Fibulin-1, a fibrinogen binding blood-borne matricellular protein, displays a characteristic overlapping pattern with fibrinogen within atheromatous regions displaying fresh thrombi. This suggests that fibulin-1 correlates with thrombotic aspects of atherosclerosis and on-site thrombus formation, which serve as the leading side-effect of vascular therapies (55).

Platelet Activation

Platelet activation is a key companion of thrombosis. Platelets interact with the vessel wall by first "rolling" along the surface, then attaching and spreading through integrin-mediated interactions. In order to activate, platelets must bind to exposed extracellular matrix, generally via the interaction of integrin on the cell surface with type I collagen.

Matricellular proteins in the thrombospondin (TSP) family (of which there are five known members) have key regulatory roles for both platelet recruitment and platelet aggregation. TSP-1 regulates platelet recruitment and anti-ADAMTS13 antibodies within stimulated endothelium (56). TSP-1 also stimulates platelet aggregation by blocking the antithrombotic activity of nitric oxide (NO)/cGMP signaling, resulting in vessel occlusion if it occurs in vascular engineered settings like balloon angioplasty, stent expansion, or therapeutic delivery (57). TSP-1 and CD36 have a co-dependent effect on platelet adhesion and collagen-dependent thrombus stabilization, with CD36 serving in an anchoring role in a TSP-1 knockout model (58). Emilin-2 regulates platelet activation/contractility and aggregation via adenosine diphosphate, collagen, and thrombin; emilin-1 also promotes platelet aggregation but in contrast reduces clot retraction (59). Both members of the emilin family therefore represent key molecules for platelet regulation.

Many alterations of vascular hemostasis have been identified in mouse models of matricellular protein deficiency. Notably, phenotypes of altered hemostasis have been difficult to identify because they are only revealed in response to injury. Mice deficient for either TSP-2 or MAGP-1 exhibit bleeding diathesis; in the case of the latter, this phenotype can be rescued with intravenous injection of recombinant protein (60). Lack of MAGP-1 alters the morphology of the thrombus, which is slow to permanently establish itself in the site of vessel damage (60, 61). The phenotype of TSP-2 deficient mice is inherent to the extracellular matrix. When fibroblasts from TSP-2 deficient mice are used as the source of a cell derived matrix, this matrix resists thrombosis compared to matrix synthesized by wild-type fibroblasts (62). Current vascular engineering strategies are exploiting this cell-derived matrix as an anti-thrombotic coating (63).

MATRICELLULAR PROTEINS THAT SUPPORT ENDOTHELIAL FORMATION AND MAINTENANCE

Physiological control of thrombosis is primarily performed by the endothelium lining the luminal surface of a blood vessel. To mimic the native state, an implanted vascular graft should ideally be "pre-coated" with a permanent, antithrombotic lining; unfortunately, this is rarely a feasible strategy. In contrast, a vascular graft that encourages recellularization by endothelial cells (ECs) from the host, and treatment with anticoagulants during this recellularization period, is more often used. The design parameters responsible for proper formation of a new endothelial lining are endothelial cell adhesion, migration, proliferation, and survival. In this section, we will illustrate how these functions are modulated by matricellular proteins *in vitro* and *in vivo*.

Endothelial Cell Adhesion and Migration

CCN1 binding with $\alpha_v\beta_3$ and $\alpha_{II}\beta_3$ integrins promotes both adhesion and migration of ECs (64). A dose-dependent adhesion enhancement of ECs was also shown using CCN2 within a 2D *in vitro* model (65). CCN1 also enhances VEGF signaling by promoting VEGF production (66) and enhancing VEGF-R2 phosphorylation (67). Together, enhanced EC tubule formation (68, 69) and nitric oxide production (70) are observed with CCN1 treatment. Additionally, CCN3 has been shown to stimulate EC adhesion and migration in an $\alpha_v\beta_3$ / $\alpha_5\beta_1$ dependent manner (71). MAGP-2 antagonizes Notch signaling to promote cell sprouting and EC migration (72, 73). Initial formation of endothelial tubes is also promoted by SPARC, enabled primarily through TGF-β1 inhibition and preceded by pericyte migration (74).

Vitronectin, a serum glycoprotein, is found at high concentrations to promote differentiation of EC/SMC phenotypes (75). ECs bind to vitronectin via heparin sulfate proteoglycans (76), leading to EC spreading (77). $\alpha_v\beta_3$ integrin binding has shown to decrease cellular motility *in vitro* on HUVECs in vitronectin coated flasks (78), and can be a target for vitronectin-focused vascular engineering. Thrombogenic PAI-1, co-released with binding target vitronectin, induces HUVEC dysfunction and procoagulant states through mast cell exosome signaling (79), underscoring vitronectin and PAI-1 as EC-linked antithrombogenic vascular engineering targets.

The proteoglycan decorin regulates EC migration and adhesion indirectly, by binding to the receptors for EGF (80, 81) and IGF (82), thereby attenuating downstream Akt and MAPK signaling. An engineered decorin mimic has also been shown to directly promote both endothelial migration and proliferation (83). Lumican, another proteoglycan, inhibits EC migration by interfering with p38 MAPK signaling (84).

TSP-1 has a generally anti-angiogenic effect on ECs (85), mediated by CD36 (86). Similarly, TSP-2 is anti-angiogenic as TSP-2 knockout mice have shown increased angiogenesis (87) and impaired von Willebrand Factor accumulation on secreted ECM (62). In double TSP-1/TSP-2 knockout animals, neoangiogenesis is mediated by MMP9 activation (88). In contrast to the anti-angiogenic activities of TSP-1 and TSP-2, TSP-4 is required for proper increased adhesion, migration, and proliferation of ECs (89, 90). CD47, an essential TSP-1 receptor (91), can mediate TSP-1 function and is therefore another useful target for controlling angiogenesis. CD47 function is altered by a lipid environment (92), so angiogenesis can be manipulated by controlling the VLDL receptor in endothelial cells and thus decrease Akt and MAPK phosphorylation (93).

From an engineering perspective, TSP-2 knockout mouse dermal fibroblast secreted ECM was used to coat decellularized rat aorta, resulting in an anti-thrombotic and pro-migratory vascular graft that improved EC recruitment and decreased failure rate following interpositional rat abdominal aortic implantation (63).

Endothelial Cell Proliferation and Survival

CCN1 enhances proliferation of endothelial cells by augmenting bFGF signaling (94), and also promotes endothelial cell survival (64). CCN2's effect is somewhat more complex, as it contains modules that can either enhance (95) or decrease (96) proliferative signaling. CCN3 overexpression suppressed VCAM-1 (which supports adhesion) and normal CCN3 expression reduced monocyte adhesion. TNX increases EC proliferation through interactions with VEGF (97). Fibrillin-1 RGD-containing sequences have the ability to stimulate EC proliferation *in vitro* (98). TSP-2 alone inhibits growth-factor induced microvascular EC proliferation in a caspase-independent manner (99). SPARC reduces VEGFR-1 after injury, resulting in anti-angiogenic activities early in the development cascade and opening the door for VEGF-A targeted therapeutics that route through VEGFR-1 pathway (100).

MATRICELLULAR PROTEINS THAT RECRUIT AND REGULATE VASCULAR SMOOTH MUSCLE CELLS

As described above, a native vessel must possess the mechanical strength and resilience to survive the dynamic forces it will encounter over the course of a human life. In turn, an engineered vessel must be able to outlast the patient; in the case of pediatric patients, grafts must also grow with them. Vascular smooth muscle cells (vSMCs) are essential in the maintenance of vascular walls *in vivo*, and thus are prime targets for vascular engineers.

For the purposes of this review, we will highlight two main functions of vSMC in small vessels. First, vSMC are responsible for the synthesis, alignment, and maintenance of elastin during development to provide effective passive recoil in response to hemodynamics and local tissue deformation. vSMC also can potentially synthesize new elastin in response to damage; however, it appears that adult vSMC are limited in their elastin expression at the transcriptional level. Second, vSMC cooperate with EC to regulate vascular tone. EC receive signals from the circulation that stimulate production of the second messenger nitric oxide (NO), inducing vSMC relaxation and vessel dilation. In contrast, agents such as angiotensin II act directly on vSMC, causing the cell to contract and the vessel to constrict.

It is clear, then, that the presence of functional vSMC in a mature vascular graft would be ideal. As was the case for ECs, implanting a graft which already contains vSMC is rarely feasible, and more often recellularization by host cells is used. Therefore, in this section we will examine how matricellular proteins modulate vSMC adhesion, migration, proliferation, and survival, as well as vSMC function in the context of neointima formation.

Smooth Muscle Cell Adhesion and Migration

Angiotensin II promotes atherosclerosis by inducing the adhesion and migration of vSMCs, and is mediated by osteopontin using putative binding site miR181a in its inhibition (101). MAGP-1 is dependent on MAGP-2 in binding/activating Notch 1, which activates Notch signaling and modulates homeostasis during aortic SMC spreading (72).

Fibulin-5, in addition to its well-documented role on elastogenesis, is the primary mediator of uPA-driven migration of vSMCs (102). The mechanism for this appears to be that fibulin-5 binding facilitates activation of uPA, which then activates plasmin to cleave the portion of fibulin-5 that binds β_1 integrin, driving cell migration. This action increases vSMC remodeling and vascularization after injury and antagonizes angiogenesis by inducing TSP-1 and antagonizing fibronectin receptors (102, 103). Galectin-1, a glycan-binding protein primarily involved within the anti-inflammatory cardiac tissue response to acute myocardial infarction, has been shown to restrict vSMC motility and modulates focal adhesion turnover on fibronectin, via *in vitro* assays using galectin-1 knockout mouse SMCs (104).

Smooth Muscle Cell Survival, Proliferation, and Neointimal Formation

In post-injury vasculature, galectin-1 is upregulated within proliferating SMCs, and in confirmatory studies an engineered galectin-1/GST fusion protein is able to drive SMC proliferation (105). Taken with its effects on increasing SMC proliferation and restricting SMC motility (105), galectin-1 presents as a potential supplement for cardiac therapeutics post-myocardial infarction and a serum biomarker for cardiac stress (106) with a well-characterized mouse model for *in vivo* evaluations.

The CCN family of matricellular proteins have significant, yet indirect, effects aiding vascularization and angiogenesis that might be considered in engineering microenvironment applications. Full length CCN2 utilizes integrin $\alpha_6\beta_1$ to promote adhesion and spreading of vSMCs (65). CCN5 also inhibits vSMC proliferation and motility without affecting apoptosis and adhesion (107, 108), and has potential to be used as an delivered therapeutic CCN2 antagonist to control vSMC migration, adhesion, and phenotype (109). CCN5's effects are modulated in a dose-dependent fashion by PDGF and TGF-β, with some possible quiescence-related SMC properties (107). A reduction in CCN2 expression was observed in Notch1 haploinsufficiency murine abdominal aortic aneurysm models, leading to a maintenance of contractile vSMC phenotype and a reduction in aortic dilation (110). CCN2 presents with a key target for SMC phenotype maintenance in vasculopathy.

CCN4 (also known as Wisp-1), is upregulated in migrating vSMC in a Wnt2-dependent manner; loss of CCN4 leads to inhibited vSMC integrin mediated migration (111). Wnt5a, which induces β-catenin signaling in mouse via vSMCs, saw CCN4 rescue VSMCs from H_2O_2 induced apoptosis within atherosclerotic plaque (112, 113). CCN4 was expressed within advanced human coronary artery lesions (111) but absent in Wnt5a positive intimal SMCs, indicating that CCN4 deficiency

may provoke vSMC apoptosis in coronary plaques, ultimately resulting in instability. Loss of CCN4 leads to reduced intimal thickening, related to CCN4's aforementioned positive effect on vSMC migration (111).

Tenascin-C (TNC) within the context of atherosclerotic plaques promotes SMC proliferation and migration via PDGF signaling (114). Areas of human abdominal aortic aneurysm with high TNC expression by medial SMCs correlate strongly with inflammation and tissue ECM destruction (115). TNC overexpression can also result in pulmonary hypertension, and it is expressed in adventitia and media of saphenous vein grafts under above average arterial stress pressure (116). Taken together, TNC presents with a SMC-linked biomarker target to assess atherosclerosis or aneurysm pathological state.

Neointimal hyperplasia is a common complication of vascular disease intervention (117). The main target for anti-neointimal formation is SMC phenotype, given the predisposition of unregulated hyperplastic vSMC proliferation to accelerate neointimal formation. Many matricellular proteins have shown efficacy in controlling vSMC phenotype and adhesion, and therapeutics often target at upregulation of these factors. TSP-1 targets NO-mediated vSMC relaxation to increase tissue survival and facilitate tissue perfusion to preserve tissues under ischemic stress (118). vSMC are also induced to proliferate by TSP-1 (119). Fibromodulin adenovirus-mediated gene transfer inhibits restenosis in an organ culture saphenous vein graft disease model of neointimal hyperplasia, at a much greater level than decorin or beta-galactosidase gene transfer (120). Fibromodulin could be a key SLRP for study within ECM-based vein grafts.

Another ECM-related inducer of neointimal formation is fibulin-1, where expression is closely overlapped with fibrinogen. Fibulin-1 and fibrinogen bind tightly within atherosclerotic legions, but this does not hold true in ECM associated with SMC surrounding the identified lesion. Fibulin-1 is associated with atherogenesis in diabetic patients, and at high levels fibulin-1 becomes an accurate indicator of cardiovascular risk in patients prior to acute cardiovascular events, obesity, or diabetes risk markers (121). vSMCs display increased SMC contractile differentiation markers with fibulin-5 overexpression (44), and vSMC phenotype has also been regulated through fibulin-4 expression in murine models (122). Overexpression of fibulin-5 has been shown post-injury to increase SMC motility in a step to aid in vascular remodeling (102).

CCN3 exhibited a protective role within the progression of murine abdominal aortic aneurysm model (123), and inhibited neointimal hyperplasia by inhibiting vSMC migration and proliferation (124). With this background, novel CCN3-based peptides have recently been developed, aiding in the modulation of pro-fibrotic factors CCN2, PAI-1, and post-translational fibrotic collagen modification (125).

Osteopontin (OPN, also known as bone sialoprotein I, abbr. BSP-1), a matricellular protein first identified within osteoblasts, is expressed by vSMC derived foam cells after immune response, and plays a large role in the calcification of atherosclerotic lesions (126). Increased OPN expression during neointimal hyperplasia formation was seen as a major microenvironment component of human atherosclerotic plaque progression. OPN downregulates vSMC differentiation markers αSMA and calponin, transitioning from quiescent status into an unregulated proliferative phenotype (127). Galectin-1 binds to lipoprotein(a), which binds tightly to LDL and are both co-implicated in atherogenesis. Lipoprotein(a) binds poorly to tissue with galectin-1 inhibition, suggesting that lipoprotein(a) accumulation changes have an effect on atherogenesis, possibly mediated through t-antigens on lipoprotein(a) and LDL (128). A novel engineering approach modulating OPN protein expression or galectin-1 binding within atherogenic arterial walls could present as a key mediating factor for downstream neointimal hyperplasia.

MATRICELLULAR PROTEINS IN VASCULAR TISSUE ENGINEERING

To date, only a few of the matricellular proteins reviewed here have been pursued in the context of vascular tissue engineering, hence the need for future tissue engineering strategies harnessing these proteins. What follows is a brief summary of the findings from this small library of published work—note that by far the most predominant area of study has been how to encourage endothelial adhesion to biomaterials in the vascular context.

Production of New Vascular Matrix

Mature elastic fibers that are mechanically competent are a highly sought-after component of a TEVG. Several groups have investigated methods to improve elastin content, or production, within grafts and unsurprisingly a few of these studies have harnessed matricellular proteins to do so. Versican, as explored by the Wight group, has a complex relationship with elastogenesis. Full length glycosylated versican, known as V0, negatively impacts new elastin fiber formation. However, a splice variant of versican that cannot be glycosylated, known as V3, drives new elastin formation and cross linking by SMCs (129). With this background, the Wight group collaborated with a vascular tissue engineering company, Cytograft, to explore the potential for a TEVG with enhanced elastin content. Cell sheets of SMCs retrovirally expressing V3, or control cells, were cultured for 12 weeks to form a rich cell-derived matrix, rolled on a mandrel, and allowed to fuse for 18 more weeks. During the initial cell culture period (4 weeks), not only was expression of elastin elevated at the gene level, as expected, but also fibulin-5 (130). Mature crosslinking was also elevated by V3, as well as higher mechanical strength as judged by burst strength. It should be noted that in the cell-sheet TEVG strategy, the cells are generally removed before further TEVG processing, so the initial transduction of the cells should not serve as a hurdle to final FDA approval.

An alternate method for exploring improved elastin production was published by the Suzuki group. As reported by others (131), collagen is generally a poor 3D matrix for cellular elastic fiber production. The Suzuki group had previously discovered a beneficial effect of LTBP-4 on elastic fiber assembly (132) and reasoned that it could also then encourage elastic fiber formation in collagen gels. Here, human skin fibroblasts were

seeded on top of porous collagen sponges, allowing the cells to infiltrate the sponge during culture. Recombinant LTBP-4 was added to experimental cultures at a concentration of 5 μg/ml, and replaced along with media changes every week for 3 weeks. Increased LTBP-4 immunostaining was observed in the LTBP-4 treated cultures (both recombinant and native human protein), as well as improved fibrillin-1 and elastin (133). Interestingly, the benefit on elastin was also observed with a single dose of LTBP-4 at 1 week, as opposed to the 3 week treatment described above—although immunostaining for fibrillin-1 was not explored. This work was limited by lacking more rigorous analysis of the elastic fibers (such as desmosine assay) but the simple addition of recombinant LTBP-4 to culture media is more amenable to the typical tissue engineer than retroviral work, and therefore of note.

Limiting Thrombosis

Because thrombosis can be initiated upon contact of blood with ECM such as the vascular basement membrane and internal elastic lamella, most groups have focused on endothelialization (see next section). However, in work by the Kyriakides lab analyzing a mouse model for TSP-2 deficiency, it became clear that TSP-2 deficient arteries are resistant to thrombosis for reasons linked to the ECM of the vessel wall (not just inherent to thrombus formation) (62). In a similar situation to the Wight group collaboration with Cytograft explored in the previous section, Kyriakides teamed up with Laura Niklason from the vascular tissue engineering company Humacyte to explore if a TSP-2 deficient matrix could serve as a thrombosis-resistant lumenal coating for the Humacyte graft. Modification with the TSP-2 deficient matrix had no effect on the mechanical properties of the graft, but both inhibited platelet activation *in vitro* and improved endothelialization of interpositional abdominal aortic implants after 4 weeks *in vivo* (63). They do not report an effect on patency as seen by our group when evaluating TEVGs in a similar model (51), but it could be expected that as they move to a larger animal model a patency effect could be revealed.

Endothelial Formation and Maintenance

As discussed above, CCN1 has a pro-adhesive and pro-migratory effect on ECs. Hilfiker, Haverich, Wilhelmi, and Boer have performed collaborative work for nearly a decade using recombinant CCN1 to promote re-endothelialization of decellularized small intestine with preserved artery and vein pedicles (134), heart valves (135), and decellularized arteries (136, 137). Introduction of recombinant CCN1 (100 ng/ml overnight for the intestine and arteries, 400 μg/ml 6 h for the heart valves) was performed either by perfusion of cannulated tissue (intestines) or end-over-end incubation of the tissue and CCN1 solution (heart valves and arteries). In either case, introduction of matricellular protein to engineered tissues appears to be both simple and effective using these methods, and could be extended to other molecules.

The Chaikof group has investigated the use of elastin-like peptides (ELPs) as the basis of a new biocompatible and tunable hydrogel scaffold for vascular tissue engineering. Since the ELPs self-assemble, coacervating at a tunable transition temperature, it is relatively simple to incorporate other cargo into the gelation mixture. Two matricellular proteins have been investigated in this context—fibronectin (138) and CCN1 (139). Two methods were used for incorporation of fibronectin into ELPs. In one method, ELPs were coacervated into hydrogels, which were then incubated in a 1 mg/ml solution of fibronectin for 4 h of adsorption before genipin crosslinking of the ELPs. In the second method, ELPs and fibronectin were blended at 4°C before coacervation into hydrogels at 37°C and subsequent genipin cross-linking. While improved pro-adhesive activity toward ECs was observed with the adsorption method, both fibronectin-loaded hydrogel strategies outperformed ELPs alone. Other beneficial outcomes included improved spreading and migration of ECs (138). A distinct strategy was used to incorporate beneficial CCN1 activities into ELP hydrogels—instead of adding recombinant protein to the gelation mixture the peptides themselves were engineered to contain a biologically active sequence derived from CCN1. Specifically, this 20-residue sequence, known as the V2 domain, is critical for integrin $\alpha_v\beta_3$-dependent binding of ECs to CCN1 (140) and therefore represents a new cell-interaction site for engineered biomaterials. Ten repeats of the V2 sequence were introduced into the standard triblock structure of the ELP; hydrogels containing V2 had improved EC adhesion that could be blocked by soluble V2 peptide or an antibody that interferes with $\alpha_v\beta_3$ function (139). As was the case with fibronectin-functionalized ELPs, beneficial outcomes included improved migration and spreading of ECs.

In a similar vein to the Chaikof CCN1 experiments, the Heath lab has recently published work exploring the synergistic EC-adhesive effect of traditional integrin-binding RGD peptide along with peptides used for binding to syndecans −1, −2, and −4 (141). In this case, the hydrogel system used was polyethylene glycol (PEG), a common biomaterial explored in tissue engineering; within the PEG network, RGD peptide and/or one of two different syndecan-binding peptides were conjugated. While RGD and syndecan-binding peptides did promote EC adhesion beyond their respective controls (RGE and a scrambled syndecan-binding peptide) the combination of RGD and syndecan peptide at ratios of 1:1 or 3:1 promoted superior adhesion. Interestingly, this worked whether the two peptides were in separate PEG chains (nanoclusters) or in the same PEG chain (heteroclusters). Beyond adhesion, proliferation was also accelerated with the peptide mixture, vs. single peptides. Perhaps the most astonishing finding of this work was revealed with flow. ECs adherent to single peptides stayed adherent under 10 h of flow (3.1 dyn/cm^2) but did not form proper focal adhesions or align to flow—in contrast ECs adherent to the peptide mixture formed prominent focal adhesions, stress fibers, and re-aligned with flow (141). A recent review on syndecans has explored their role in the context of regeneration and their potential to regulate stem cell function, though not specifically in the context of vascular tissue engineering (142).

As discussed earlier, small diameter PTFE grafts typically undergo thrombotic failure. While seeding of ECs has been explored, they are generally unable to remain within the graft long term and ultimately the graft continues to fail. The Flugelman group has explored the use of fibulin-5, in addition

to VEGF, as a method to retain ECs (143). Specifically, ECs were retrovirally transduced to express both fibulin-5 and VEGF, and then dually transduced, GFP transduced, or naïve ECs were seeded into PTFE scaffolds for *in vivo* testing. Both short term (2 weeks, interpositional) and middle term (3 or 6 months, end-to-side) carotid artery implantations were performed in sheep. A substantial benefit was observed using the fibulin-5/VEGF ECs with respect to patency, vs. GFP transduced and naïve EC controls. While there are some limitations to the study concerning a lack of evaluation of fibulin-5/elastin deposition in explants or a fibulin-5 only control, it is an exciting foray in the context of matricellular proteins in vascular tissue engineering.

An alternate method for inducing endothelialization of vascular scaffolds is to recruit circulating endothelial progenitor cells (EPCs). Work by the Schenke-Layland has explored the use of decorin as a ligand to attract EPCs from the circulation and thereby quickly coat an implanted scaffold with a "pre-endothelium." An electrospun PEGdma-PLA scaffold, meant to serve as a heart valve equivalent, was coated with recombinantly expressed decorin, stromal-derived factor 1, or were left uncoated. Using a dynamic *in vitro* cell capture system, human and mouse EPCs were exposed to the scaffolds for 24 or 48 h, respectively. Decorin and stromal-derived factor 1 both led to higher capture of EPCs compared to bare scaffolds, in addition the captured cells proceeded to form focal adhesions at the conclusion of the incubation period (144). While it should be noted that this has not yet been tested with whole blood, or under flow, the system described here could be a novel method for endothelializing an a cellular implanted scaffold.

Smooth Muscle Cell Recruitment

Aside from the above studies regarding new elastin production by SMCs, little has been published regarding the role of matricellular proteins in SMC recruitment for vascular tissue engineering. One study of note, however, investigated the chemical conjugation of whole fibronectin, not just the RGD peptide, to porous poly(carbonate) urethane scaffolds (145). Considering that fibronectin is a 500 kD protein, this conjugation was not trivial. In this work, scaffolds functionalized with full-length fibronectin encouraged SMC recruitment to a depth of up to 300 μm within the material; non-functionalized scaffolds only supported SMC growth on the surface. Therefore, fibronectin incorporation into porous scaffolds for vascular tissue engineering may promote host cell SMC recruitment.

SUMMARY

Much of the groundwork for matricellular protein-based protein engineering has been laid by the two decades of biological studies reviewed here. The goal of this review is to get the results of these studies into the hands of bioengineers developing new cardiovascular technologies, and to spark interdisciplinary discussions that can lead to novel solutions for cardiovascular disease. A summary of the biological effects of each individual matricellular protein is shown in **Table 2**. Admittedly, the knowledge base reviewed here is constantly evolving, but the intent is that established collaborations will then stay informed about their protein(s) of interest. Another caveat is that regeneration of the vasculature likely involves the cooperation of several of these factors in concert, which may not have a simple summative effect compared to the individual activities.

Matricellular proteins can be used to enhance production of new collagen and elastin, the primary contributors to vascular strength and resilience. Much of the literature on

TABLE 2 | Summary of biological effects for each matricellular protein discussed in this review (see respective sections for details and references).

Protein name	Summary of effects
Aggrecan	Potential biomarker for aneurysm risk
CCN1	Stabilizes collagen fibers, promotes adhesion and migration of ECs
CCN2	Promotes collagen transcription, EC adhesion, and SMC adhesion/spreading
CCN3	Reduces EC adhesion and inhibits SMC proliferation
CCN4	Promotes SMC migration, inhibits SMC apoptosis in atherosclerotic plaque
CCN5	Antagonizes CCN2, inhibits SMC proliferation and motility
Decorin	Increases density of collagen bundles, associated with aneurysm risk
Emilin-1	Inhibits TGF-β activation, binds to elastic fiber microfibrils, promotes platelet aggregation and inhibits clot retraction
Emilin-2	Binds to elastic fiber microfibrils, promotes platelet aggregation and clot retraction
Fibrillin-1	Regulates TGF-β activation, scaffold for elastic fibers, promote EC proliferation
Fibrillin-2	Regulates TGF-β activation, scaffold for elastic fibers
Fibromodulin	Inhibits SMC proliferation/restenosis
Fibulin-1	Associated with thrombosis, aneurysm, and cardiovascular disease risk
Fibulin-2	Directs elastic fiber assembly
Fibulin-5	Directs elastic fiber assembly, promotes SMC migration and contractility
Galectin-1	Promotes SMC spreading and adhesion, reduces motility, mediates atherogenesis
LTBP-1 and−4	Inhibit TGF-β activation, binds to elastic fiber microfibrils
Lumican	Promotes LOX activity, inhibits EC migration
MAGP-1	Modulates sequestration of TGF-β, integral to elastic fiber microfibrils, required for proper thrombosis
MAGP-2	Integral to elastic fiber microfibrils, inhibits EC Notch signal to promote migration
OPN	Promotes proliferation of SMCs and calcification of atherosclerotic lesions
SPARC	Promotes collagen bundling, EC migration
Syndecan-4	Promotes collagen post-translational processing
TNC	Promotes SMC proliferation and migration
TNX	Promotes collagen post-translational modidication, EC proliferation
TSP-1	Promotes platelet aggregation, inhibits EC angiogenesis, promotes SMC proliferation
TSP-2	Required for proper thrombosis, inhibits EC proliferation and angiogenesis
Versican	Associated with aneurysm risk, inhibits elastic fiber formation
Vitronectin	Via PAI-1 reduces thrombus removal, promotes EC adhesion, and spreading

collagen transcriptional regulation can be informative for future engineering of collagen-rich tissues, and reciprocally informative for strategies to reduce graft fibrosis or the foreign body response to cardiovascular devices. Understanding how matricellular proteins guide collagen bundling can be used to inform future collagen-based biomaterials. Notably, new elastin production by adult cells has been something of a holy grail in the field of vascular regenerative medicine, with several recent studies in the field of aneurysm therapeutics focused on production of this important molecule (146, 147). Including matricellular proteins such as members of the fibulin family in future cardiovascular tissue engineering strategies will be critical for achieving fully mature, mechanically sound, elastic fibers. Understanding how these elastin chaperones work will also be important for designing devices to help patients with deficiency in these important proteins.

A key limitation of synthetic small diameter grafts is the occurrence of thrombotic occlusion; as explored here it has become clear that matricellular proteins such as members of the TSP family can have a significant effect on how thrombosis occurs. The work by Kyriakides et al. demonstrating thrombosis resistance in the absence of TSP-2 is particularly striking in this regard (62, 63). Regulation of thrombosis by matricellular proteins can be due to inhibition of thrombin activation, platelet activation, or both. While the focus in this review has been on thrombotic failure in vascular grafts, these findings also have implications for the design of cardiovascular devices with lower risk of embolism and stroke.

In a tissue-engineered graft, formation of an intact, thromboresistant endothelium is critical to enable prolonged function. In development and maintenance of the endothelium, matricellular proteins found in both the circulation and the underlying basement membrane have critical roles. Not only are these proteins important to support endothelial adhesion, they also are important for promoting survival of adherent ECs, which will be critical for a small-diameter engineered graft. Maintenance of ECs in a non-pathologic phenotype is also an area of interest in vascular engineering, so understanding the role of matricellular proteins on EC differentiation state will also be critical for future device design.

Finally, an understanding of the effects of matricellular proteins on vascular SMCs will be beneficial for future vascular engineering, since SMCs not only are critical for production (and turnover) of new vascular matrix in the graft context but also perform multiple roles in normal vascular physiology. Implanted cell-free grafts must support survival and ingrowth of host SMCs to better mimic the native artery. Matricellular proteins have the ability to promote both of these outcomes. In addition, a common failure method for the most used graft in coronary bypass operations—an autologous saphenous vein graft—is neointimal formation and occlusion due to excessive proliferation of SMCs. Control of SMC overproliferation by peptides derived from matricellular proteins could replace conventional drug-eluting stent technologies, and also be used to augment current vascular graft strategies.

In summary, we would propose that the use of matricellular proteins and matricellular-derived peptides could serve as a paradigm shift in the field of vascular tissue engineering.

AUTHOR CONTRIBUTIONS

Conception of this article was primarily by JW. Literature research was performed by AR and JW. Writing and critical revision were performed by AR, DV, and JW.

FUNDING

This work was supported by the Leonard H. Berenfield Graduate Fellowship in Cardiovascular Bioengineering and NIH T32 HL094295 (AR), the NIH grants HL129066, HL130784, and HL13077 as well as McCune Foundation Pediatric Device Initiative (DV), and the NIH grant HL104768 and University of Pittsburgh Competitive Medical Research Fund (JW).

REFERENCES

1. Wagenseil JE, Mecham RP. Vascular extracellular matrix and arterial mechanics. *Physiol Rev.* (2009) 89:957–89. doi: 10.1152/physrev.00041.2008
2. Lok CN, Ehrlich HP, White SL, Buttolph TR, Cutroneo KR, Chiu JF. Oligodeoxynucleotide decoy therapy blocks type 1 procollagen transcription and the prolyl hydroxylase beta subunit translation. *J Cell Biochem.* (2008) 103:1066–75. doi: 10.1002/jcb.21477
3. Bagchi RA, Czubryt MP. Synergistic roles of scleraxis and Smads in the regulation of collagen 1alpha2 gene expression. *Biochim Biophys Acta.* (2012) 1823:1936–44. doi: 10.1016/j.bbamcr.2012.07.002
4. Kim HJ, Kim MY, Jin H, Kim HJ, Kang SS, Kim HJ, et al. Peroxisome proliferator-activated receptor {delta} regulates extracellular matrix and apoptosis of vascular smooth muscle cells through the activation of transforming growth factor-β1/Smad3. *Circ Res.* (2009) 105:16–24. doi: 10.1161/CIRCRESAHA.108.189159
5. Robertson IB, Horiguchi M, Zilberberg L, Dabovic B, Hadjiolova K, Rifkin DB. Latent TGF-beta-binding proteins. *Matrix Biol.* (2015) 47:44–53. doi: 10.1016/j.matbio.2015.05.005
6. Brigstock DR. Regulation of angiogenesis and endothelial cell function by connective tissue growth factor (CTGF) and cysteine-rich 61 (CYR61). *Angiogenesis.* (2002) 5:153–65. doi: 10.1023/A:1023823803510
7. Shiwen X, Rajkumar V, Denton CP, Leask A, Abraham DJ. Pericytes display increased CCN2 expression upon culturing. *J Cell Commun Signal.* (2009) 3:61–4. doi: 10.1007/s12079-009-0053-7
8. Schalkwijk J, Zweers MC, Steijlen PM, Dean WB, Taylor G, van Vlijmen IM, et al. A recessive form of the Ehlers-Danlos syndrome caused by tenascin-X deficiency. *N Engl J Med.* (2001) 345:1167–75. doi: 10.1056/NEJMoa002939
9. Herum KM, Lunde IG, Skrbic B, Louch WE, Hasic A, Boye S, et al. Syndecan-4 is a key determinant of collagen cross-linking and passive myocardial stiffness in the pressure-overloaded heart. *Cardiovasc Res.* (2015) 106:217–26. doi: 10.1093/cvr/cvv002
10. Engebretsen KVT, Lunde IG, Strand ME, Waehre A, Sjaastad I, Marstein HS, et al. Lumican is increased in experimental and clinical heart failure, and its production by cardiac fibroblasts is induced by mechanical and proinflammatory stimuli. *Febs J.* (2013) 280:2382–98. doi: 10.1111/febs.12235

11. Christensen G, Herum KM, Lunde IG. Sweet, yet underappreciated: proteoglycans and extracellular matrix remodeling in heart disease. *Matrix Biol.* (2018) 75–6:286–99. doi: 10.1016/j.matbio.2018.01.001
12. Gu G, Wan F, Xue Y, Cheng W, Zheng H, Zhao Y, et al. Lumican as a novel potential clinical indicator for acute aortic dissection: a comparative study, based on multi-slice computed tomography angiography. *Experi Therap Med.* (2016) 11:923–8. doi: 10.3892/etm.2016.3020
13. Bradshaw AD, Sage EH. SPARC, a matricellular protein that functions in cellular differentiation and tissue response to injury. *J Clin Invest.* (2001) 107:1049–54. doi: 10.1172/JCI12939
14. Harris BS, Zhang Y, Card L, Rivera LB, Brekken RA, Bradshaw AD. SPARC regulates collagen interaction with cardiac fibroblast cell surfaces. *Am J Physiol Heart Circ Physiol.* (2011) 301:H841–847. doi: 10.1152/ajpheart.01247.2010
15. Puolakkainen P, Bradshaw AD, Kyriakides TR, Reed M, Brekken R, Wight T, et al. Compromised production of extracellular matrix in mice lacking secreted protein, acidic and rich in cysteine (SPARC) leads to a reduced foreign body reaction to implanted biomaterials. *Am J Pathol.* (2003) 162:627–35. doi: 10.1016/S0002-9440(10)63856-4
16. Barallobre-Barreiro J, Gupta SK, Zoccarato A, Kitazume-Taneike R, Fava M, Yin X, et al. Glycoproteomics reveals decorin peptides with anti-myostatin activity in human atrial fibrillation. *Circulation.* (2016) 134:817–32. doi: 10.1161/CIRCULATIONAHA.115.016423
17. Ferdous Z, Wei VM, Iozzo R, Hook M, Grande-Allen KJ. Decorin-transforming growth factor- interaction regulates matrix organization and mechanical characteristics of three-dimensional collagen matrices. *J Biol Chem.* (2007) 282:35887–98. doi: 10.1074/jbc.M705180200
18. Ferdous Z, Lazaro LD, Iozzo RV, Hook M, Grande-Allen KJ. Influence of cyclic strain and decorin deficiency on 3D cellularized collagen matrices. *Biomaterials.* (2008) 29:2740–8. doi: 10.1016/j.biomaterials.2008.03.018
19. Paderi JE, Panitch A. Design of a synthetic collagen-binding peptidoglycan that modulates collagen fibrillogenesis. *Biomacromolecules.* (2008) 9:2562–6. doi: 10.1021/bm8006852
20. Paderi JE, Stuart K, Sturek M, Park K, Panitch A. The inhibition of platelet adhesion and activation on collagen during balloon angioplasty by collagen-binding peptidoglycans. *Biomaterials.* (2011) 32:2516–23. doi: 10.1016/j.biomaterials.2010.12.025
21. Scott RA, Paderi JE, Sturek M, Panitch A. Decorin mimic inhibits vascular smooth muscle proliferation and migration. *PLoS ONE.* (2013) 8:e82456. doi: 10.1371/journal.pone.0082456
22. Ang LS, Boivin WA, Williams SJ, Zhao H, Abraham T, Carmine-Simmen K, et al. Serpina3n attenuates granzyme B-mediated decorin cleavage and rupture in a murine model of aortic aneurysm. *Cell Death Dis.* (2011) 2:e209. doi: 10.1038/cddis.2011.88
23. Ueda K, Yoshimura K, Yamashita O, Harada T, Morikage N, Hamano K. Possible dual role of decorin in abdominal aortic aneurysm. *PLoS ONE.* (2015) 10:e0120689. doi: 10.1371/journal.pone.0120689
24. Kozel BA, Danback JR, Waxler JL, Knutsen RH, de Las Fuentes L, Reusz GS, et al. Williams syndrome predisposes to vascular stiffness modified by antihypertensive use and copy number changes in NCF1. *Hypertension.* (2014) 63:74–9. doi: 10.1161/HYPERTENSIONAHA.113.02087
25. Callewaert B, Renard M, Hucthagowder V, Albrecht B, Hausser I, Blair E, et al. New insights into the pathogenesis of autosomal-dominant cutis laxa with report of five ELN mutations. *Hum Mutat.* (2011) 32:445–55. doi: 10.1002/humu.21462
26. Li DY, Faury G, Taylor DG, Davis EC, Boyle WA, Mecham RP, et al. Novel arterial pathology in mice and humans hemizygous for elastin. *J Clin Invest.* (1998) 102:1783–7. doi: 10.1172/JCI4487
27. Zhang M, Pierce RA, Wachi H, Mecham RP, Parks WC. An open reading frame element mediates posttranscriptional regulation of tropoelastin and responsiveness to transforming growth factor beta1. *Mol Cell Biol.* (1999) 19:7314–26. doi: 10.1128/MCB.19.11.7314
28. Weinbaum JS, Broekelmann TJ, Pierce RA, Werneck CC, Segade F, Craft CS, et al. Deficiency in microfibril-associated glycoprotein-1 leads to complex phenotypes in multiple organ systems. *J Biol Chem.* (2008) 283:25533–43. doi: 10.1074/jbc.M709962200
29. Massam-Wu T, Chiu M, Choudhury R, Chaudhry SS, Baldwin AK, McGovern A, et al. Assembly of fibrillin microfibrils governs extracellular deposition of latent TGF beta. *J Cell Sci.* (2010) 123:3006–18. doi: 10.1242/jcs.073437
30. Schiavinato A, Keene DR, Wohl AP, Corallo D, Colombatti A, Wagener R, et al. Targeting of EMILIN-1 and EMILIN-2 to fibrillin microfibrils facilitates their incorporation into the extracellular matrix. *J Invest Dermatol.* (2016) 136:1150–60. doi: 10.1016/j.jid.2016.02.021
31. Zacchigna L, Vecchione C, Notte A, Cordenonsi M, Dupont S, Maretto S, et al. Emilin1 links TGF-beta maturation to blood pressure homeostasis. *Cell.* (2006) 124:929–42. doi: 10.1016/j.cell.2005.12.035
32. Litteri G, Carnevale D, D'Urso A, Cifelli G, Braghetta P, Damato A, et al. Vascular smooth muscle Emilin-1 is a regulator of arteriolar myogenic response and blood pressure. *Arterioscl Thromb Vasc Biol.* (2012) 32:2178–84. doi: 10.1161/ATVBAHA.112.254664
33. Varona S, García-Redondo AB, Martínez-González J, Salaices M, Briones AM, Rodríguez C. La sobreexpresión vascular de la lisil oxidasa altera la estructura de la matriz extracelular e induce estrés oxidativo. *Clín Invest Arteriosc.* (2017) 29:157–65. doi: 10.1016/j.arteri.2017.01.004
34. Staiculescu MC, Kim J, Mecham RP, Wagenseil JE. Mechanical behavior and matrisome gene expression in the aneurysm-prone thoracic aorta of newborn lysyl oxidase knockout mice. *Am J Physiol-Heart Circul Physiol.* (2017) 313:H446–56. doi: 10.1152/ajpheart.00712.2016
35. Villain G, Lelievre E, Broekelmann T, Gayet O, Havet C, Werkmeister E, et al. MAGP-1 and fibronectin control EGFL7 functions by driving its deposition into distinct endothelial extracellular matrix locations. *FEBS J.* (2018) 285:4394–412. doi: 10.1111/febs.14680
36. Zhang H, Apfelroth SD, Hu W, Davis EC, Sanguineti C, Bonadio J, et al. Structure and expression of fibrillin-2, a novel microfibrillar component preferentially located in elastic matrices. *J Cell Biol.* (1994) 124:855–63. doi: 10.1083/jcb.124.5.855
37. Carta L, Smaldone S, Zilberberg L, Loch D, Dietz HC, Rifkin DB, et al. p38 MAPK is an early determinant of promiscuous Smad2/3 signaling in the aortas of fibrillin-1 (Fbn1)-null mice. *J Biol Chem.* (2009) 284:5630–6. doi: 10.1074/jbc.M806962200
38. Pereira L, Andrikopoulos K, Tian J, Lee SY, Keene DR, Ono R, et al. Targetting of the gene encoding fibrillin-1 recapitulates the vascular aspect of Marfan syndrome. *Nat Genet.* (1997) 17:218–22. doi: 10.1038/ng1097-218
39. Carta L, Pereira L, Arteaga-Solis E, Lee-Arteaga SY, Lenart B, Starcher B, et al. Fibrillins 1 and 2 perform partially overlapping functions during aortic development. *J Biol Chem.* (2006) 281:8016–23. doi: 10.1074/jbc.M511599200
40. Sicot FX, Tsuda T, Markova D, Klement JF, Arita M, Zhang RZ, et al. Fibulin-2 is dispensable for mouse development and elastic fiber formation. *Mol Cell Biol.* (2008) 28:1061–7. doi: 10.1128/MCB.01876-07
41. Yamauchi Y, Tsuruga E, Nakashima K, Sawa Y, Ishikawa H. Fibulin-4 and−5, but not Fibulin-2, are associated with tropoelastin deposition in elastin-producing cell culture. *Acta Histochem Cytochem.* (2010) 43:131–8. doi: 10.1267/ahc.10026
42. de Vega S, Iwamoto T, Yamada Y. Fibulins: multiple roles in matrix structures and tissue functions. *Cell Mol Life Sci.* (2009) 66:1890–902. doi: 10.1007/s00018-009-8632-6
43. Chapman SL, Sicot FX, Davis EC, Huang J, Sasaki T, Chu ML, et al. Fibulin-2 and fibulin-5 cooperatively function to form the internal elastic lamina and protect from vascular injury. *Arterioscler Thromb Vasc Biol.* (2010) 30:68–74. doi: 10.1161/ATVBAHA.109.196725
44. Spencer JA, Hacker SL, Davis EC, Mecham RP, Knutsen RH, Li DY, et al. Altered vascular remodeling in fibulin-5-deficient mice reveals a role of fibulin-5 in smooth muscle cell proliferation and migration. *Proc Natl Acad Sci USA.* (2005) 102:2946–51. doi: 10.1073/pnas.0500058102
45. Nakasaki M, Hwang Y, Xie Y, Kataria S, Gund R, Hajam EY, et al. The matrix protein Fibulin-5 is at the interface of tissue stiffness and inflammation in fibrosis. *Nat Commun.* (2015) 6:8574. doi: 10.1038/ncomms9574
46. Yanagisawa H, Davis EC, Starcher BC, Ouchi T, Yanagisawa M, Richardson JA, et al. Fibulin-5 is an elastin-binding protein essential for elastic fibre development *in vivo*. *Nature.* (2002) 415:168–71. doi: 10.1038/415168a

47. Yasmin MRA, McEniery CM, Cleary SE, Li Y, Siew K, Figg NL, et al. The matrix proteins aggrecan and fibulin-1 play a key role in determining aortic stiffness. *Sci Rep.* (2018) 8:8550. doi: 10.1038/s41598-018-25851-5
48. Cikach FS, Koch CD, Mead TJ, Galatioto J, Willard BB, Emerton KB, et al. Massive aggrecan and versican accumulation in thoracic aortic aneurysm and dissection. *JCI Insight.* (2018) 3:e97167. doi: 10.1172/jci.insight.97167
49. Kaufman JS, O'Connor TZ, Zhang JH, Cronin RE, Fiore LD, Ganz MB, et al. Randomized controlled trial of clopidogrel plus aspirin to prevent hemodialysis access graft thrombosis. *J Am Soc Nephrol.* (2003) 14:2313–21. doi: 10.1097/01.ASN.0000081661.10246.33
50. Soletti L, Nieponice A, Hong Y, Ye SH, Stankus JJ, Wagner WR, et al. *In vivo* performance of a phospholipid-coated bioerodable elastomeric graft for small-diameter vascular applications. *J Biomed Mater Res A.* (2011) 96:436–48. doi: 10.1002/jbm.a.32997
51. Krawiec JT, Weinbaum JS, Liao HT, Ramaswamy AK, Pezzone DJ, Josowitz AD, et al. *In vivo* functional evaluation of tissue-engineered vascular grafts fabricated using human adipose-derived stem cells from high cardiovascular risk populations. *Tissue Eng Part A.* (2016) 22:765–75. doi: 10.1089/ten.tea.2015.0379
52. Wootton DM, Ku DN. Fluid mechanics of vascular systems, diseases, and thrombosis. *Annu Rev Biomed Eng.* (1999) 1:299–329. doi: 10.1146/annurev.bioeng.1.1.299
53. Kamikubo Y, Neels JG, Degryse B. Vitronectin inhibits plasminogen activator inhibitor-1-induced signalling and chemotaxis by blocking plasminogen activator inhibitor-1 binding to the low-density lipoprotein receptor-related protein. *Int J Biochem Cell Biol.* (2009) 41:578–85. doi: 10.1016/j.biocel.2008.07.006
54. Podor TJ, Campbell S, Chindemi P, Foulon DM, Farrell DH, Walton PD, et al. Incorporation of vitronectin into fibrin clots. Evidence for a binding interaction between vitronectin and gamma A/gamma' fibrinogen. *J Biol Chem.* (2002) 277:7520–8. doi: 10.1074/jbc.M109677200
55. Argraves WS, Tanaka A, Smith EP, Twal WO, Argraves KM, Fan D, et al. Fibulin-1 and fibrinogen in human atherosclerotic lesions. *Histochem Cell Biol.* (2009) 132:559–65. doi: 10.1007/s00418-009-0628-7
56. Bonnefoy A, Daenens K, Feys HB, De Vos R, Vandervoort P, Vermylen J, et al. Thrombospondin-1 controls vascular platelet recruitment and thrombus adherence in mice by protecting (sub)endothelial VWF from cleavage by ADAMTS13. *Blood.* (2006) 107:955–64. doi: 10.1182/blood-2004-12-4856
57. Isenberg JS, Hyodo F, Ridnour LA, Shannon CS, Wink DA, Krishna MC, et al. Thrombospondin 1 and vasoactive agents indirectly alter tumor blood flow. *Neoplasia.* (2008) 10:886–96. doi: 10.1593/neo.08264
58. Kuijpers MJ, de Witt S, Nergiz-Unal R, van Kruchten R, Korporaal SJ, Verhamme P, et al. Supporting roles of platelet thrombospondin-1 and CD36 in thrombus formation on collagen. *Arteriosc Thromb Vasc Biol.* (2014) 34:1187–92. doi: 10.1161/ATVBAHA.113.302917
59. Huang M, Sannaningaiah D, Zhao N, Gong Y, Grondolsky J, Hoover-Plow J. EMILIN2 regulates platelet activation, thrombus formation, and clot retraction. *PLoS ONE.* (2015) 10:e0115284. doi: 10.1371/journal.pone.0115284
60. Werneck CC, Vicente CP, Weinberg JS, Shifren A, Pierce RA, Broekelmann TJ, et al. Mice lacking the extracellular matrix protein MAGP1 display delayed thrombotic occlusion following vessel injury. *Blood.* (2008) 111:4137–44. doi: 10.1182/blood-2007-07-101733
61. Vassequi-Silva T, Pereira DS, Nery Diez ACC, Braga GG, Godoy JA, Mendes CB, et al. Losartan and captopril treatment rescue normal thrombus formation in microfibril associated glycoprotein-1 (MAGP1) deficient mice. *Thromb Res.* (2016) 138:7–15. doi: 10.1016/j.thromres.2015.12.004
62. Kristofik N, Calabro NE, Tian W, Meng A, MacLauchlan S, Wang Y, et al. Impaired von Willebrand factor adhesion and platelet response in thrombospondin-2 knockout mice. *Blood.* (2016) 128:1642–50. doi: 10.1182/blood-2016-03-702845
63. Kristofik NJ, Qin L, Calabro NE, Dimitrievska S, Li G, Tellides G, et al. Improving *in vivo* outcomes of decellularized vascular grafts via incorporation of a novel extracellular matrix. *Biomaterials.* (2017) 141:63–73. doi: 10.1016/j.biomaterials.2017.06.025
64. Leu SJ, Lam SC, Lau LF. Pro-angiogenic activities of CYR61 (CCN1) mediated through integrins alphavbeta3 and alpha6beta1 in human umbilical vein endothelial cells. *J Biol Chem.* (2002) 277:46248–55. doi: 10.1074/jbc.M209288200
65. Ball DK, Rachfal AW, Kemper SA, Brigstock DR. The heparin-binding 10 kDa fragment of connective tissue growth factor (CTGF) containing module 4 alone stimulates cell adhesion. *J Endocrinol.* (2003) 176:R1–7. doi: 10.1677/joe.0.176r001
66. Chen CY, Su CM, Hsu CJ, Huang CC, Wang SW, Liu SC, et al. CCN1 Promotes VEGF production in osteoblasts and induces endothelial progenitor cell angiogenesis by inhibiting miR-126 expression in rheumatoid arthritis. *J Bone Miner Res.* (2017) 32:34–45. doi: 10.1002/jbmr.2926
67. Chintala H, Krupska I, Yan L, Lau L, Grant M, Chaqour B. The matricellular protein CCN1 controls retinal angiogenesis by targeting VEGF, Src homology 2 domain phosphatase-1 and Notch signaling. *Development.* (2015) 142:2364–74. doi: 10.1242/dev.121913
68. Di Y, Zhang Y, Nie Q, Chen X. CCN1/Cyr61-PI3K/AKT signaling promotes retinal neovascularization in oxygen-induced retinopathy. *Int J Mol Med.* (2015) 36:1507–18. doi: 10.3892/ijmm.2015.2371
69. Di Y, Zhang Y, Yang H, Wang A, Chen X. The mechanism of CCN1-enhanced retinal neovascularization in oxygen-induced retinopathy through PI3K/Akt-VEGF signaling pathway. *Drug Des Dev Ther.* (2015) 9:2463–73. doi: 10.2147/DDDT.S79782
70. Hwang S, Lee HJ, Kim G, Won KJ, Park YS, Jo I. CCN1 acutely increases nitric oxide production via integrin alphavbeta3-Akt-S6K-phosphorylation of endothelial nitric oxide synthase at the serine 1177 signaling axis. *Free Radic Biol Med.* (2015) 89:229–40. doi: 10.1016/j.freeradbiomed.2015.08.005
71. Lin CG, Leu SJ, Chen N, Tebeau CM, Lin SX, Yeung CY, et al. CCN3 (NOV) is a novel angiogenic regulator of the CCN protein family. *J Biol Chem.* (2003) 278:24200–8. doi: 10.1074/jbc.M302028200
72. Miyamoto A, Lau R, Hein PW, Shipley JM, Weinmaster G. Microfibrillar proteins MAGP-1 and MAGP-2 induce Notch1 extracellular domain dissociation and receptor activation. *J Biol Chem.* (2006) 281:10089–97. doi: 10.1074/jbc.M600298200
73. Albig AR, Becenti DJ, Roy TG, Schiemann WP. Microfibril-associate glycoprotein-2 (MAGP-2) promotes angiogenic cell sprouting by blocking notch signaling in endothelial cells. *Microvasc Res.* (2008) 76:7–14. doi: 10.1016/j.mvr.2008.01.001
74. Rivera LB, Brekken RA. SPARC promotes pericyte recruitment via inhibition of endoglin-dependent TGF-beta1 activity. *J Cell Biol.* (2011) 193:1305–19. doi: 10.1083/jcb.201011143
75. Heydarkhan-Hagvall S, Gluck JM, Delman C, Jung M, Ehsani N, Full S, et al. The effect of vitronectin on the differentiation of embryonic stem cells in a 3D culture system. *Biomaterials.* (2012) 33:2032–40. doi: 10.1016/j.biomaterials.2011.11.065
76. Preissner KT, Seiffert D. Role of vitronectin and its receptors in haemostasis and vascular remodeling. *Thromb Res.* (1998) 89:1–21. doi: 10.1016/S0049-3848(97)00298-3
77. Re F, Zanetti A, Sironi M, Polentarutti N, Lanfrancone L, Dejana E, et al. Inhibition of anchorage-dependent cell spreading triggers apoptosis in cultured human endothelial cells. *J Cell Biol.* (1994) 127:537–46. doi: 10.1083/jcb.127.2.537
78. Reinmuth N, Liu W, Ahmad SA, Fan F, Stoeltzing O, Parikh AA, et al. $\alpha_v\beta_3$ integrin antagonist S247 decreases colon cancer metastasis and angiogenesis and improves survival in mice. *Cancer Res.* (2003) 63:2079–87. Available online at: http://cancerres.aacrjournals.org/content/63/9/2079.long
79. Al-Nedawi K, Szemraj J, Cierniewski CS. Mast Cell-Derived derived exosomes activate endothelial cells to secrete plasminogen activator inhibitor type 1. *Arterioscler Thromb Vasc Biol.* (2005) 25:1744–9. doi: 10.1161/01.ATV.0000172007.86541.76
80. Iozzo RV, Moscatello DK, McQuillan DJ, Eichstetter I. Decorin is a biological ligand for the epidermal growth factor receptor. *J Biol Chem.* (1999) 274:4489–92. doi: 10.1074/jbc.274.8.4489
81. Seidler DG, Goldoni S, Agnew C, Cardi C, Thakur ML, Owens RT, et al. Decorin protein core inhibits *in vivo* cancer growth and metabolism by hindering epidermal growth factor receptor function and triggering apoptosis via caspase-3 activation. *J Biol Chem.* (2006) 281:26408–18. doi: 10.1074/jbc.M602853200

82. Iozzo RV, Buraschi S, Genua M, Xu SQ, Solomides CC, Peiper SC, et al. Decorin antagonizes IGF receptor I (IGF-IR) function by interfering with IGF-IR activity and attenuating downstream signaling. *J Biol Chem*. (2011) 286:34712–21. doi: 10.1074/jbc.M111.262766
83. Scott RA, Ramaswamy AK, Park K, Panitch A. Decorin mimic promotes endothelial cell health in endothelial monolayers and endothelial-smooth muscle co-cultures. *J Tissue Eng Regen Med*. (2017) 11:1365–76. doi: 10.1002/term.2035
84. Albig AR, Roy TG, Becenti DJ, Schiemann WP. Transcriptome analysis of endothelial cell gene expression induced by growth on matrigel matrices: identification and characterization of MAGP-2 and lumican as novel regulators of angiogenesis. *Angiogenesis*. (2007) 10:197–216. doi: 10.1007/s10456-007-9075-z
85. Iruela-Arispe ML, Bornstein P, Sage H. Thrombospondin exerts an antiangiogenic effect on cord formation by endothelial cells *in vitro*. *Proc Natl Acad Sci USA*. (1991) 88:5026–30. doi: 10.1073/pnas.88.11.5026
86. Dawson DW, Pearce SF, Zhong R, Silverstein RL, Frazier WA, Bouck NP. CD36 mediates the *in vitro* inhibitory effects of thrombospondin-1 on endothelial cells. *J Cell Biol*. (1997) 138:707–17. doi: 10.1083/jcb.138.3.707
87. Yang Z, Kyriakides TR, Bornstein P. Matricellular proteins as modulators of cell-matrix interactions: adhesive defect in thrombospondin 2-null fibroblasts is a consequence of increased levels of matrix metalloproteinase-2. *Mol Biol Cell*. (2000) 11:3353–64. doi: 10.1091/mbc.11.10.3353
88. Kopp HG, Hooper AT, Broekman MJ, Avecilla ST, Petit I, Luo M, et al. Thrombospondins deployed by thrombopoietic cells determine angiogenic switch and extent of revascularization. *J Clin Invest*. (2006) 116:3277–91. doi: 10.1172/JCI29314
89. Muppala S, Frolova E, Xiao R, Krukovets I, Yoon S, Hoppe G, et al. Proangiogenic properties of thrombospondin-4. *Arterioscler Thromb Vasc Biol*. (2015) 35:1975–86. doi: 10.1161/ATVBAHA.115.305912
90. Muppala S, Xiao R, Krukovets I, Verbovetsky D, Yendamuri R, Habib N, et al. Thrombospondin-4 mediates TGF-beta-induced angiogenesis. *Oncogene*. (2017) 36:5189–98. doi: 10.1038/onc.2017.140
91. Isenberg JS, Ridnour LA, Dimitry J, Frazier WA, Wink DA, Roberts DD. CD47 is necessary for inhibition of nitric oxide-stimulated vascular cell responses by thrombospondin-1. *J Biol Chem*. (2006) 281:26069–80. doi: 10.1074/jbc.M605040200
92. McDonald JF, Zheleznyak A, Frazier WA. Cholesterol-independent interactions with CD47 enhance alphavbeta3 avidity. *J Biol Chem*. (2004) 279:17301–11. doi: 10.1074/jbc.M312782200
93. Oganesian A, Armstrong LC, Migliorini MM, Strickland DK, Bornstein P. Thrombospondins use the VLDL receptor and a nonapoptotic pathway to inhibit cell division in microvascular endothelial cells. *Mol Biol Cell*. (2008) 19:563–71. doi: 10.1091/mbc.e07-07-0649
94. Kolesnikova TV, Lau LF. Human CYR61-mediated enhancement of bFGF-induced DNA synthesis in human umbilical vein endothelial cells. *Oncogene*. (1998) 16:747–54. doi: 10.1038/sj.onc.1201572
95. Kubota S, Kawaki H, Kondo S, Yosimichi G, Minato M, Nishida T, et al. Multiple activation of mitogen-activated protein kinases by purified independent CCN2 modules in vascular endothelial cells and chondrocytes in culture. *Biochimie*. (2006) 88:1973–81. doi: 10.1016/j.biochi.2006.07.007
96. Karagiannis ED, Popel AS. Peptides derived from type I thrombospondin repeat-containing proteins of the CCN family inhibit proliferation and migration of endothelial cells. *Int J Biochem Cell Biol*. (2007) 39:2314–23. doi: 10.1016/j.biocel.2007.06.018
97. Ishitsuka T, Ikuta T, Ariga H, Matsumoto K. Serum tenascin-X strongly binds to vascular endothelial growth factor. *Biol Pharm Bull*. (2009) 32:1004–11. doi: 10.1248/bpb.32.1004
98. Mariko B, Ghandour Z, Raveaud S, Quentin M, Usson Y, Verdetti J, et al. Microfibrils and fibrillin-1 induce integrin-mediated signaling, proliferation and migration in human endothelial cells. *Am J Physiol Cell Physiol*. (2010) 299:C977–87. doi: 10.1152/ajpcell.00377.2009
99. Armstrong LC, Bjorkblom B, Hankenson KD, Siadak AW, Stiles CE, Bornstein P. Thrombospondin 2 inhibits microvascular endothelial cell proliferation by a caspase-independent mechanism. *Mol Biol Cell*. (2002) 13:1893–905. doi: 10.1091/mbc.e01-09-0066
100. Nozaki M, Sakurai E, Raisler BJ, Baffi JZ, Witta J, Ogura Y, et al. Loss of SPARC-mediated VEGFR-1 suppression after injury reveals a novel antiangiogenic activity of VEGF-A. *J Clin Invest*. (2006) 116:422–9. doi: 10.1172/JCI26316
101. Remus EW, Lyle AN, Weiss D, Landazuri N, Weber M, Searles C, et al. miR181a protects against angiotensin II-induced osteopontin expression in vascular smooth muscle cells. *Atherosclerosis*. (2013) 228:168–74. doi: 10.1016/j.atherosclerosis.2013.01.037
102. Kapustin A, Stepanova V, Aniol N, Cines DB, Poliakov A, Yarovoi S, et al. Fibulin-5 binds urokinase-type plasminogen activator and mediates urokinase-stimulated beta1-integrin-dependent cell migration. *Biochem J*. (2012) 443:491–503. doi: 10.1042/BJ20110348
103. Albig AR, Schiemann WP. Fibulin-5 Antagonizes Vascular Endothelial Growth Factor (VEGF) signaling and angiogenic sprouting by endothelial cells. *DNA Cell Biol*. (2004) 23:367–79. doi: 10.1089/104454904323145254
104. Tsai M-S, Chiang M-T, Tsai D-L, Yang C-W, Hou H-S, Li Y-R, et al. Galectin-1 restricts vascular smooth muscle cell motility via modulating adhesion force and focal adhesion dynamics. *Scient Rep*. (2018) 8:11497. doi: 10.1038/s41598-018-29843-3
105. Moiseeva EP, Javed Q, Spring EL, de Bono DP. Galectin 1 is involved in vascular smooth muscle cell proliferation. *Cardiovasc Res*. (2000) 45:493–502. doi: 10.1016/S0008-6363(99)00276-X
106. Hashmi S, Al-Salam S. Galectin-1: a biomarker of surgical stress in murine model of cardiac surgery. *Int J Clini Exp Pathol*. (2015) 8:7157–64. Available online at: http://www.ijcep.com/files/ijcep0008555.pdf
107. Lake AC, Bialik A, Walsh K, Castellot JJ Jr. CCN5 is a growth arrest-specific gene that regulates smooth muscle cell proliferation and motility. *Am J Pathol*. (2003) 162:219–31. doi: 10.1016/S0002-9440(10)63813-8
108. Lake AC, Castellot JJ Jr. CCN5 modulates the antiproliferative effect of heparin and regulates cell motility in vascular smooth muscle cells. *Cell Commun Signal*. (2003) 1:5. doi: 10.1186/1478-811X-1-5
109. Castellot J, Gray MR, Simon AR. Use of CCN5 for Treatment Of Smooth Muscle Proliferation Disorders. *USA patent application US*20080207489A1 (2007).
110. Sachdeva J, Mahajan A, Cheng J, Baeten JT, Lilly B, Kuivaniemi H, et al. Smooth muscle cell-specific Notch1 haploinsufficiency restricts the progression of abdominal aortic aneurysm by modulating CTGF expression. *PLoS ONE*. (2017) 12:e0178538. doi: 10.1371/journal.pone.0178538
111. Williams H, Mill CA, Monk BA, Hulin-Curtis S, Johnson JL, George SJ. Wnt2 and WISP-1/CCN4 induce intimal thickening via promotion of smooth muscle cell migration. *Arterioscler Thromb Vasc Biol*. (2016) 36:1417–24. doi: 10.1161/ATVBAHA.116.307626
112. Mill C, Jeremy JY, George SJ. WNT5A signalling promotes vsmc survival via WISP-1: consequences for vsmc viability in atherosclerotic plaques. *Heart*. (2011) 97:1–2. doi: 10.1136/heartjnl-2011-300920a.4
113. Mill C, Monk BA, Williams H, Simmonds SJ, Jeremy JY, Johnson JL, et al. Wnt5a-induced Wnt1-inducible secreted protein-1 suppresses vascular smooth muscle cell apoptosis induced by oxidative stress. *Arterioscler Thromb Vasc Biol*. (2014) 34:2449–56. doi: 10.1161/ATVBAHA.114.303922
114. Ishigaki T, Imanaka-Yoshida K, Shimojo N, Matsushima S, Taki W, Yoshida T. Tenascin-C enhances crosstalk signaling of integrin αvβ3/PDGFR-β complex by SRC recruitment promoting PDGF-induced proliferation and migration in smooth muscle cells. *J Cell Physiol*. (2011) 226:2617–24. doi: 10.1002/jcp.22614
115. Kimura T, Yoshimura K, Aoki H, Imanaka-Yoshida K, Yoshida T, Ikeda Y, et al. Tenascin-C is expressed in abdominal aortic aneurysm tissue with an active degradation process. *Pathol Int*. (2011) 61:559–64. doi: 10.1111/j.1440-1827.2011.02699.x
116. Wallner K, Li C, Fishbein MC, Shah PK, Sharifi BG. Arterialization of human vein grafts is associated with tenascin-C expression. *J Am Coll Cardiol*. (1999) 34:871–5. doi: 10.1016/S0735-1097(99)00272-7
117. Isaji T, Hashimoto T, Yamamoto K, Santana JM, Yatsula B, Hu H, et al. Improving the outcome of vein grafts: should vascular surgeons turn veins into arteries? *Ann Vasc Dis*. (2017) 10:8–16. doi: 10.3400/avd.ra.17-00008
118. Isenberg JS, Hyodo F, Matsumoto K, Romeo MJ, Abu-Asab M, Tsokos M, et al. Thrombospondin-1 limits ischemic tissue survival by inhibiting nitric oxide-mediated vascular smooth muscle relaxation. *Blood*. (2007) 109:1945–52. doi: 10.1182/blood-2006-08-041368

119. Majack RA, Cook SC, Bornstein P. Control of smooth muscle cell growth by components of the extracellular matrix: autocrine role for thrombospondin. *Proc Natl Acad Sci USA*. (1986) 83:9050–4. doi: 10.1073/pnas.83.23.9050
120. Ranjzad P, Salem HK, Kingston PA. Adenovirus-mediated gene transfer of fibromodulin inhibits neointimal hyperplasia in an organ culture model of human saphenous vein graft disease. *Gene Ther*. (2009) 16:1154–62. doi: 10.1038/gt.2009.63
121. Bergmann K, Mankowska-Cyl A, Kretowicz M, Manitius J, Sypniewska G. Fibulin-1 is associated with cardiovascular risk in non-obese, non-diabetic individuals. *Folia Medica Copernicana*. (2013) 1:18–22. Available online at: https://journals.viamedica.pl/medical_research_journal/article/view/35429
122. Huang J, Davis EC, Chapman SL, Budatha M, Marmorstein LY, Word RA, et al. Fibulin-4 deficiency results in ascending aortic aneurysms: a potential link between abnormal smooth muscle cell phenotype and aneurysm progression. *Circul Res*. (2010) 106:583–92. doi: 10.1161/CIRCRESAHA.109.207852
123. Zhang C, van der Voort D, Shi H, Zhang R, Qing Y, Hiraoka S, et al. Matricellular protein CCN3 mitigates abdominal aortic aneurysm. *J Clini Invest*. (2016) 126:1282–99. doi: 10.1172/JCI82337
124. Shimoyama T, Hiraoka S, Takemoto M, Koshizaka M, Tokuyama H, Tokuyama T, et al. CCN3 inhibits neointimal hyperplasia through modulation of smooth muscle cell growth and migration. *Arterioscler Thromb Vasc Biol*. (2010) 30:675–U680. doi: 10.1161/ATVBAHA.110.203356
125. Riser BL, Barnes JL, Varani J. Balanced regulation of the CCN family of matricellular proteins: a novel approach to the prevention and treatment of fibrosis and cancer. *J Cell Comm Signal*. (2015) 9:327–39. doi: 10.1007/s12079-015-0309-3
126. Ikeda T, Shirasawa T, Esaki Y, Yoshiki S, Hirokawa K. Osteopontin messenger-rna is expressed by smooth muscle-derived foam cells in human atherosclerotic lesions of the aorta. *J Clini Invest*. (1993) 92:2814–20. doi: 10.1172/JCI116901
127. Gao H, Steffen MC, Ramos KS. Osteopontin regulates alpha-smooth muscle actin and calponin in vascular smooth muscle cells. *Cell Biol Int*. (2012) 36:155–61. doi: 10.1042/CBI20100240
128. Chellan B, Narayani J, Appukuttan PS. Galectin-1, an endogenous lectin produced by arterial cells, binds lipoprotein(a) [Lp(a)] in situ: relevance to atherogenesis. *Exp Mol Pathol*. (2007) 83:399–404. doi: 10.1016/j.yexmp.2007.04.004
129. Merrilees MJ, Lemire JM, Fischer JW, Kinsella MG, Braun KR, Clowes AW, et al. Retrovirally mediated overexpression of versican v3 by arterial smooth muscle cells induces tropoelastin synthesis and elastic fiber formation *in vitro* and in neointima after vascular injury. *Circ Res*. (2002) 90:481–7. doi: 10.1161/hh0402.105791
130. Keire PA, L'Heureux N, Vernon RB, Merrilees MJ, Starcher B, Okon E, et al. Expression of versican isoform V3 in the absence of ascorbate improves elastogenesis in engineered vascular constructs. *Tissue Eng Part A*. (2010) 16:501–12. doi: 10.1089/ten.tea.2009.0129
131. Long JL, Tranquillo RT. Elastic fiber production in cardiovascular tissue-equivalents. *Matrix Biol*. (2003) 22:339–50. doi: 10.1016/S0945-053X(03)00052-0
132. Noda K, Dabovic B, Takagi K, Inoue T, Horiguchi M, Hirai M, et al. Latent TGF-beta binding protein 4 promotes elastic fiber assembly by interacting with fibulin-5. *Proc Natl Acad Sci USA*. (2013) 110:2852–7. doi: 10.1073/pnas.1215779110
133. Aya R, Ishiko T, Noda K, Yamawaki S, Sakamoto Y, Tomihata K, et al. Regeneration of elastic fibers by three-dimensional culture on a collagen scaffold and the addition of latent TGF-beta binding protein 4 to improve elastic matrix deposition. *Biomaterials*. (2015) 72:29–37. doi: 10.1016/j.biomaterials.2015.08.036
134. Bar A, Dorfman SE, Fischer P, Hilfiker-Kleiner D, Cebotari S, Tudorache I, et al. The pro-angiogenic factor CCN1 enhances the re-endothelialization of biological vascularized matrices *in vitro*. *Cardiovasc Res*. (2010) 85:806–13. doi: 10.1093/cvr/cvp370
135. Theodoridis K, Tudorache I, Calistru A, Cebotari S, Meyer T, Sarikouch S, et al. Successful matrix guided tissue regeneration of decellularized pulmonary heart valve allografts in elderly sheep. *Biomaterials*. (2015) 52:221–8. doi: 10.1016/j.biomaterials.2015.02.023
136. Boer U, Spengler C, Jonigk D, Klingenberg M, Schrimpf C, Lutzner S, et al. Coating decellularized equine carotid arteries with CCN1 improves cellular repopulation, local biocompatibility, and immune response in sheep. *Tissue Eng Part A*. (2013) 19:1829–42. doi: 10.1089/ten.tea.2012.0558
137. Jeinsen N, Magel L, Jonigk D, Klingenberg M, Haverich A, Wilhelmi M, et al. Biocompatibility of intensified decellularized equine carotid arteries in a rat subcutaneous implantation model and in a human *in vitro* model. *Tissue Eng Part A*. (2018) 24:310–21. doi: 10.1089/ten.tea.2016.0542
138. Ravi S, Caves JM, Martinez AW, Haller CA, Chaikof EL. Incorporation of fibronectin to enhance cytocompatibility in multilayer elastin-like protein scaffolds for tissue engineering. *J Biomed Mater Res A*. (2013) 101:1915–25. doi: 10.1002/jbm.a.34484
139. Ravi S, Haller CA, Sallach RE, Chaikof EL. Cell behavior on a CCN1 functionalized elastin-mimetic protein polymer. *Biomaterials*. (2012) 33:2431–8. doi: 10.1016/j.biomaterials.2011.11.055
140. Chen N, Leu SJ, Todorovic V, Lam SC, Lau LF. Identification of a novel integrin alphavbeta3 binding site in CCN1 (CYR61) critical for pro-angiogenic activities in vascular endothelial cells. *J Biol Chem*. (2004) 279:44166–76. doi: 10.1074/jbc.M406813200
141. Karimi F, Thombare VJ, Hutton CA, O'Connor AJ, Qiao GG, Heath DE. Beyond RGD; nanoclusters of syndecan- and integrin-binding ligands synergistically enhance cell/material interactions. *Biomaterials*. (2018) 187:81–92. doi: 10.1016/j.biomaterials.2018.10.002
142. Chung H, Multhaupt HA, Oh ES, Couchman JR. Minireview: Syndecans and their crucial roles during tissue regeneration. *FEBS Lett*. (2016) 590:2408–17. doi: 10.1002/1873-3468.12280
143. Preis M, Schneiderman J, Koren B, Ben-Yosef Y, Levin-Ashkenazi D, Shapiro S, et al. Co-expression of fibulin-5 and VEGF165 increases long-term patency of synthetic vascular grafts seeded with autologous endothelial cells. *Gene Ther*. (2016) 23:237–46. doi: 10.1038/gt.2015.104
144. Hinderer S, Sudrow K, Schneider M, Holeiter M, Layland SL, Seifert M, et al. Surface functionalization of electrospun scaffolds using recombinant human decorin attracts circulating endothelial progenitor cells. *Sci Rep*. (2018) 8:110. doi: 10.1038/s41598-017-18382-y
145. Dubey G, Mequanint K. Conjugation of fibronectin onto three-dimensional porous scaffolds for vascular tissue engineering applications. *Acta Biomater*. (2011) 7:1114–25. doi: 10.1016/j.actbio.2010.11.010
146. Blose KJ, Ennis TL, Arif B, Weinbaum JS, Curci JA, Vorp DA. Periadventitial adipose-derived stem cell treatment halts elastase-induced abdominal aortic aneurysm progression. *Regen Med*. (2014) 9:733–41. doi: 10.2217/rme.14.61
147. Swaminathan G, Gadepalli VS, Stoilov I, Mecham RP, Rao RR, Ramamurthi A. Pro-elastogenic effects of bone marrow mesenchymal stem cell-derived smooth muscle cells on cultured aneurysmal smooth muscle cells. *J Tissue Eng Regen Med*. (2017) 11:679–93. doi: 10.1002/term.1964

Conflict of Interest Statement: The authors declare that the research was conducted in the absence of any commercial or financial relationships that could be construed as a potential conflict of interest.

frontiers in Cardiovascular Medicine

ORIGINAL RESEARCH
published: 19 June 2019
doi: 10.3389/fcvm.2019.00081

OPEN ACCESS

Edited by:
Sharan Ramaswamy, Florida International University, United States

Reviewed by:
Elisa Avolio, Bristol Medical School, Faculty of Health Sciences, University of Bristol, United Kingdom
Manuel M. Mazo, University of Navarra, Spain

***Correspondence:**
Marie José Goumans
m.j.goumans@lumc.nl

†*These authors have contributed equally to this work as first authors*
§*These authors have contributed equally to this work as last authors*

‡***Present Address:***
Noortje A. M. Bax, Department of Biomedical Engineering, Eindhoven University of Technology, Eindhoven, Netherlands
Sjoerd N. Duim, Medical Center Haaglanden, Clinical Chemistry, Den Haag, Netherlands
Boudewijn P. T. Kruithof, Laboratory for CardioVascular Cell Biology, Department of Cell and Chemical Biology, Leiden University Medical Center, Leiden, Netherlands
Anke M. Smits, Laboratory for CardioVascular Cell Biology, Department of Cell and Chemical Biology, Leiden University Medical Center, Leiden, Netherlands
Carlijn V. C. Bouten, Department of Biomedical Engineering, Eindhoven University of Technology, Eindhoven, Netherlands
Marie José Goumans, Laboratory for CardioVascular Cell Biology, Department of Cell and Chemical Biology, Leiden University Medical Center, Leiden, Netherlands

Specialty section:
This article was submitted to Cardiovascular Biologics and Regenerative Medicine, a section of the journal Frontiers in Cardiovascular Medicine

Received: *22 January 2019*
Accepted: *03 June 2019*
Published: *19 June 2019*

In vivo and *in vitro* Approaches Reveal Novel Insight Into the Ability of Epicardium-Derived Cells to Create Their Own Extracellular Environment

Noortje A. M. Bax[1,2,3†‡], Sjoerd N. Duim[1,2†‡], Boudewijn P. T. Kruithof[1‡], Anke M. Smits[1‡], Carlijn V. C. Bouten[2,3‡§] and Marie José Goumans[1‡§]*

[1] *Department of Cell and Chemical Biology, Leiden University Medical Center, Leiden, Netherlands,* [2] *Department of Biomedical Engineering, Eindhoven University of Technology, Eindhoven, Netherlands,* [3] *Institute for Complex Molecular Systems, Eindhoven University of Technology, Eindhoven, Netherlands*

Human epicardium-derived cells (hEPDCs) transplanted in the NOD-SCID mouse heart after myocardial infarction (MI) are known to improve cardiac function, most likely orchestrated by paracrine mechanisms that limit adverse remodeling. It is not yet known, however, if hEPDCs contribute to preservation of cardiac function via the secretion of matrix proteins and/or matrix proteases to reduce scar formation. This study describes the ability of hEPDCs to produce human collagen type I after transplantation into the infarct border zone, thereby creating their own extracellular environment. As the *in vivo* environment is too complex to investigate the mechanisms involved, we use an *in vitro* set-up, mimicking biophysical and biochemical cues from the myocardial tissue to unravel hEPDC-induced matrix remodeling. The *in vivo* contribution of hEPDCs to the cardiac extracellular matrix (ECM) was assessed in a historical dataset of the NOD-SCID murine model of experimentally induced MI and cell transplantation. Analysis showed that within 48 h after transplantation, hEPDCs produce human collagen type I. The build-up of the human collagen microenvironment was reversed within 6 weeks. To understand the hEPDCs response to the pathologic cardiac microenvironment, we studied the influence of cyclic straining and/or transforming growth beta (TGFβ) signaling *in vitro*. We revealed that 48 h of cyclic straining induced collagen type I production via the TGFβ/ALK5 signaling pathway. The *in vitro* approach enables further unraveling of the hEPDCs ability to secrete matrix proteins and matrix proteases and the potential to create and remodel the cardiac matrix in response to injury.

Keywords: epicardium-derived cells, extracellular matrix (ECM), mechanosensitivity, cardiac fibrosis, cardiac remodeling, cardiac repair

INTRODUCTION

Cell-based therapies for the heart aim to recover cardiac function by restoring or preserving contractility of and blood supply in the myocardium. Next to delivery of functional cardiomyocytes as contractile units and restoration of blood vessels for oxygen supply, reconstruction of the cardiac extracellular matrix (ECM) is crucial to eventually rebuild the complex architecture

of the myocardium. The cardiac ECM plays a key role in cardiac function, since it provides the structural and functional integrity of the myocardial wall (1). Moreover, the ECM is involved in the presentation of biochemical and biomechanical cues that orchestrate tissue development, differentiation, and homeostasis (2). After a myocardial infarction (MI), the damaged cardiomyocytes are replaced by non-contractile fibrotic scar tissue to prevent rupture of the weakened cardiac wall. Unfortunately, over time, the imbalance between deposition and degradation of the ECM and the disturbance in organization of the ECM will impair cardiac function and ultimately result in heart failure (1, 3, 4). For cardiac regeneration, proper deposition, composition, and organization of the ECM is therefore essential to restore the integrity of the cardiac wall and to improve cardiac function. How cells after transplantation influence the matrix remodeling process in cardiac repair is far from clear.

Recent studies positioned the epicardium, the outer layer of the heart, as a potential source of cardiac stem or progenitor cells for cardiac repair (5–8). The epicardium is essential during cardiac development as it plays a role in the establishment of the myocardium (9, 10). From the epicardial layer, a subset of activated cells undergo epithelial-to-mesenchymal transformation (EMT), and are thereafter defined as epicardium-derived cells (EPDCs) (5, 11). EPDCs migrate into the subepicardium and contribute to the formation of cardiac fibroblasts and smooth muscle cells (11–14). The potential differentiation of EPDCs into endothelial cells and cardiomyocytes is still topic of debate (15). However, besides their cellular contribution, EPDCs play an important role in enhancing proliferation, maturation, and alignment of cardiomyocytes and as such contribute to the synchronized beating of the heart (16–18). Animal studies in which human adult EPDCs (hEPDCs) were injected after experimentally induced MI showed attenuation of cardiac function which could not be explained by renewal of murine cardiomyocytes, nor by the differentiation of hEPDCs into cardiomyocytes. Other studies showed that transplantation of hEPDCs in the murine heart resulted in increased vascular density and limited post-MI adverse remodeling (6), suggesting that the contribution of hEPDCs was mainly the result of a paracrine effect on the host tissue (6, 19). If hEPDCs improve cardiac function by reducing scar formation via secretion of matrix proteins and participation in structural remodeling of the ECM after MI and which mechanisms are involved is still unclear.

Therefore, the objective of the present study was to investigate the matrix remodeling behavior of hEPDCs both *in vivo* and *in vitro*. The matrix remodeling process involves changes in the ECM driven by both protein synthesis as well as specific enzymes that are responsible for ECM degradation, such as metalloproteinases. Since physical degradation is difficult to determine, we in this study define remodeling as the ability of cells to synthesize ECM protein in the presence of MMPs and TIMPS. It is likely that presence of these enzymes will contribute to degradation. In the *in vivo* approach, we aimed to assess the contribution of hEPDCs to scar remodeling in a non-paracrine fashion. Here, we investigated the presence of human collagen type I, the most abundant fibrillar collagen of the heart, in NOD-SCID mouse hearts after experimentally induced MI and hEPDC injection. To interrogate the mechanisms involved in matrix remodeling, the *in vivo* environment is too complex. Therefore, an *in vitro* modeling approach was chosen. Since, the heart is a continuously beating organ and thereby exposes cyclic strain to its resident cells, the effect of cyclic stain on the matrix remodeling behavior capacity of hEPDCs was investigated. Next, we investigated the contribution of transforming growth factor beta (TGFβ), as one of the key growth factors involved in cardiac repair and fibrosis (20, 21), to the matrix remodeling behavior of hEPDCs.

Our *in vivo* data demonstrate that hEPDCs produce and deposit human collagen in the injured mouse myocardium within the first days after transplantation and are thus able to start the creation of their own matrix environment. Our *in vitro* data further reveal that the expression of collagen type I in hEPDCs is significantly induced by cyclic straining—such as occurring in the native beating heart—and regulated via TGFβ signaling, thereby providing the first insight in hEPDC activation during early stages of matrix remodeling.

MATERIALS AND METHODS

Animal Studies

The *in vivo* contribution of hEPDCs to cardiac ECM remodeling after MI was assessed in a historical dataset of the NOD-SCID murine model of MI and cell transplantation (6, 19). For details on the creation of the MI and the cell transplantation, details can be found in the original manuscripts and the online data supplements (6, 19). In short, to create the MI a permanent ligation using 7.0 suture (Prolene, Johnson and Johnson, New Brunswick, NJ, USA) was created in the left anterior descending coronary artery (LAD). For short term (up till 2 weeks) follow-up, the ligation was located 1 mm caudally from the tip of the left auricle. For long term (6 weeks) experiments, only the frontal branch of the LAD was ligated, since extended survival until 6 weeks is impossible with total LAD ligation. In total 4×10^5 spindle-shaped hEPDCs (passage (P) 2–4) in 20 μl M199 medium were transplanted over 5 injections using a beveled meddle into the ischemic myocardium of the left ventricle and borderzone. To trace the injected hEPDCs, cells were transduced with enhanced green fluorescent protein (eGFP) gene 72 h before transplantation. For the short term experiments cells are transduced with adenoviral vector (hAd/F50.CMV.eGFP, 50 infectious units (IU) per cell. Since adenoviral expression is lost within a few weeks, for long term follow-up hEPDCs were transduced with the lentiviral vector Lv.hPgk.eGFP (12.5 HeLa transducing units/ml per cell) instead of the adenoviral vector.

Cell Culture

Cultures of hEPDCs were prepared from anonymous human adult right atrial appendages excised during cardiac surgery, as previously described (22, 23). The layer of epicardium was stripped from the auricle, after which the tissue was placed in a gelatin coated culture disk and capped with a

round coverslip to prevent the tissue from floating. Cells were cultured in a 1:1 mixture of Dulbecco's modified Eagle's medium (DMEM) (Invitrogen) and Medium 199 (M199) (Invitrogen) 0.5% penicillin (Invitrogen), 0.5% streptomycin (Invitrogen), and 10% heat inactivated fetal calf serum (Invitrogen). Seven days after culturing, when outgrowths of epithelium-like cells were visible the coverslips and remaining tissue were removed. When outgrowth was confluent, the cells were passaged (1:3) to induce spontaneous EMT to create spindle-shaped EPDCs and medium was refreshed every 3 days. Phenotypical profiling of cultured hEPDCs was performed previously to support their epicardial origin (22–24). Biophysical and biochemical stimulation experiments were performed with spindle-shaped hEPDCs from P 4–8 of five different patients. Purity of the hEPDC culture was determined with staining for Wilms tumor-1 (WT1) (**Table 1**).

In vitro Experimental Conditions

For the *in vitro* experiments, cells were plated at a density of 10.000 cells/cm^2. Cells were allowed to attach for 24 h prior to the onset of the experiments. To elucidate the role of mechanical cues on the remodeling behavior of hEPDCs, cells were cultured under static conditions or exposed to cyclic strain (8%−1 Hz) with the use of the Flexcell system as described below. For biochemical stimulation the culture medium was supplemented with TGFβ3 (0.5 ng/ml) or small molecular inhibitor of the ALK5 pathway, SB-431542 (iALK5, 10 μM) (23). After 48 h of biophysical and/or biochemical stimulators, cells were conducted for further analysis as described below.

Cyclic Straining of hEPDCs

Cells were seeded on UniFlex® Culture Plates, coated with collagen I (Dunnlab). After 24 h, the cells were subjected to uniaxial cyclic strain (8%) for 48 h by using a Flexcell FX-4,000 Tension straining device (Flexcell, Dunnlab) and compared to static culture (0%). A strain magnitude of 8% and a frequency of 1 Hz were chosen as a suitable strain condition based on the physiological mechanical loads on cells in the myocardial wall (25). Strain experiments were performed with cells derived from five individual human atrial appendages in two independent experiments per subject.

Immunofluorescent Staining

In vivo Material

Paraffin sections were immunofluorescently labeled as described previously (26). Briefly, slides were deparaffinized, rehydrated and subjected to heat-induced epitope retrieval with Vector® Antigen Unmasking Solution (Vector). Sections were incubated overnight at 4°C with primary antibodies directed against GFP (Abcam), human collagen I (Abcam), and collagen I (Sigma Aldrich) and were visualized with Alexa-conjugated fluorescent secondary antibodies (Invitrogen) (**Table 1**). Sections were mounted with ProLong® Gold antifade reagent (Invitrogen) containing 4′,6-diamidino-2-phenylinodol (DAPI).

In vitro Material

EPDCs cultured on UniFlex® Culture Plates were fixated in 4% paraformaldehyde (Merck) in PBS at RT for 15 min, permeabilized with 0.5% Triton X-100 (Merck) in PBS for 10 min and blocked with 5% BSA in PBS for 30 min. Subsequently, incubation with primary antibodies was performed overnight at 4°C in NET-gel (50 mM Tris, pH 7.4, 150 mM NaCl, 5 mM EDTA, 0.05% NP40, 0.25% gelatin) with 0.5% BSA. The antibodies and their suitable dilutions are listed in **Table 1**. Incubation for 2 h with Alexa-conjugated fluorescent secondary antibodies (Invitrogen) were used to visualize the primary antibody binding. Nuclear counterstain was achieved by DAPI (1:500) in NET-gel incubation for 5 min. Finally, cover glasses were mounted on microscopic slides with Mowiol.

mRNA Isolation and Quantitative PCR Analysis

Total RNA was isolated using TriPure and treated with DNAse-I (Qiagen) according to the manufacturer's protocol. Subsequently 250 ng RNA per sample was reverse transcribed into cDNA using the MMLV based cDNA synthesis kit (Bio-Rad). Primers for quantitative PCR (qPCR) were designed with Beacon Designer 7.0 (Premier Biosoft International). Primer sequences and annealing temperatures are presented in **Table 2**. cDNA samples were subjected to qPCR using IQ^{TM}5 SYBR@ Green Supermix (Bio-Rad) and the Bio-Rad IQ^{TM}5 detection system (Version 2.0). The average acquired expression cycle threshold (CT) for matrix proteins and modulators and differentiation markers of hEPDCs in different experimental conditions are presented in **Table 3.**

Gelatin Zymography

Gelatin zymography was performed to semi-quantitatively determine the proteolytic activity of metalloproteinases (MMP)-2 and−9 in media samples, as described previously (27, 28). Total protein concentrations were determined by BCA Protein Assay (Pierce), before 5 mg protein was separated on a 10% sodium dodecyl sulfate-polyacrylamide gel (SDS-page). Gels were rinsed in 2.5% Triton X-100 to remove the SDS and incubated overnight in zymography substrate buffer (50 mM Tris/HCL, 0.05% (w/v), calcium chloride ($CaCl_2$); pH8.5) to activate the MMPs. Gelatinolytic activity was visualized with Coomassie Blue solution, followed by destaining in destainer solution. The amount of active or latent MMP-2 (resp. 66 and 72 kDa) and active or latent MMP-9 (resp. 86 and 92 kDa) was visualized using Proxima C16 Phi+ (Isogen). Intensity of the bands (INT*mm^2 with global background correction) was determined using Quantity One image analysis software ($n = 4$).

Statistical Analysis

All data is presented as mean ± SD. Quantification of qPCR data was performed with comparative threshold cycle (Ct) method (ΔΔCt) of Livak et al. (29), using GAPDH as internal control gene and the average of the unstrained samples as calibrator. Data is presented as fold change in scatter-plots and each dot on the scatter-plot represents the observation of cells derived from one patient (total $n = 5$ patients). Statistical analysis of the results

TABLE 1 | Antibodies used for Immunofluorescent stainings.

Antigen	Source	Cat.no	Clone	Isotype	Label	Species	Dilution
Antibodies used for immunofluorescent staining of *in vivo* material							
GFP	AB	ab13970		IgG		Chicken	1/1,000
Collagen I	AB	ab138492	–	IgG	–	Rabbit	1/200
Collagen I	SA	C-2456	COL-1	IgG1	–	Mouse	1/100
Antibodies used for immunofluorescent staining of *in vitro* material							
WT1	CA	CA1026	–	IgG	–	Rabbit	1/50
αSMA	SA	a2547	1A4	IgG2a	–	Mouse	1/500
Vinculin	SA	V9264	hVIN-1	IgG1	–	Mouse	1/400
pFAK (Y397)	BD	bd-611723	14/FAKY397	IgG1	–	Mouse	1/1,000
Phalloidin	SA	49409	–	–	Atto 488	Rabbit	1/200
Collagen I	SA	C2456	COL-1	IgG1	–	Mouse	1/100
Collagen III	SA	ab7778	–	IgG	–	Rabbit	1/200
Elastin	AB	ab23747	–	IgG	–	Rabbit	1/100
Fibronectin	SA	F3648	–	IgG	–	Rabbit	1/200
β1-Integrin	SC	sc-53711	TS2/16	IgG1	–	Mouse	1/50
CD44	AB	ab24504		IgG	–	Rabbit	1/100
Mouse IgG1	IG	A21121		IgG1	Alexa Fluor 488	Goat	1/300
Rabbit IgG	IG	A31572		IgG (H+L)	Alexa Fluor 555	Donkey	1/300
Rabbit IgG	MP	A11008		IgG (H+L)	Alexa Fluor 555	Goat	1/200
Mouse IgG1	MP	A21127		IgG1	Alexa Fluor 555	Donkey	1/300
Mouse IgG1	MP	A21240		IgG1	Alexa Fluor 647	Donkey	1/250

AB, Abcam; SA, Sigma Aldrich; CA, Calbiochem, BD, BD Biosciences; SC, Santa Cruz; IG, Invitrogen; MP, Millipore.

was accomplished by the non-parametric Mann-Whitney test to compare the grouped samples. For statistical analysis for multiple comparisons a one-way ANOVA with Bonferoni correction for multiple comparisons was used when equal variances were assumed or a Kruskall-Wallis assuming non-equal variances, with Dunn's *post-hoc* test. Zymographic results were quantified by comparing Density (INT) of the MMP bands. Statistical analysis of zymography data was performed using a Kruskall-Wallis test, assuming non-equal variances, with Dunn's *post-hoc* test for multiple comparisons. Statistical significance was considered when $P < 0.05$. Graphics and statistical analysis were performed using the Graphpad Prism 6 software package (Graphpad Software).

RESULTS

In vivo Evaluation of the Production of Collagen I by hEPDCs After MI

It was previously reported that in NOD-SCID mice after experimentally induced MI and transplanted with GFP-labeled hEPDCs show preservation of the left ventricular function accompanied with increased wall thickness and vascular density (6). To investigate the ability of transplanted hEPDCs to contribute to matrix synthesis in a non-paracrine fashion, we determined the presence of human collagen type I, the predominant cardiac ECM component, by immunofluorescent staining at several time points in the first week after injection and at 6 weeks post-MI. Already 2 days after cell injection, the presence of human collagen I was observed in the NOD-SCID murine heart (**Figures 1A–A"**). The collagen type I protein was found both intra- and extracellular, indicating both production and deposition of human collagen within the mouse heart by injected hEPDCs. During the first 7 days post MI, the protein was stably expressed (**Figures 1B–B",C–C"**).

Six weeks after injection, hEPDCs still resided within the injured mouse myocardium, as shown by the presence of eGFP positive cells (**Figures 1D',D"**). The total amount of collagen type I present in the myocardium was more intense and prominent compared to earlier time points, while the expression of human collagen type I was strongly reduced (**Figure 1D**). These *in vivo* data suggest that hEPDCs have an early response to the infarcted mouse heart by creating their own collagen type I niche.

Cyclic Strain Induces Collagen I Expression by hEPDCs

The first signs of collagen I synthesis and thereby contribution to matrix deposition by hEPDCs, were already visible 48 h after transplantation into the NOD-SCID mouse heart. Therefore, this early time point in matrix remodeling was chosen for the duration of application of cyclic strain *in vitro*. To secure that hEPDCs are sensitive for mechanical cues, the presence of the F-actin and the mechanosome proteins pFAK and vinculin were investigated (**Figure S1**).

To gain more insight into the contribution of hEPDCs to matrix production, next to collagen type I, other cardiac matrix components were investigated. Analysis of ECM proteins at the mRNA level showed that under static conditions, hEPDCs express collagen I, collagen III, and fibronectin with Ct values

TABLE 2 | Primer sequences.

Primer		Sequence	Temp
ECM Genes			
Collagen I	fw	AAT CAC CTG CGT ACA GAA CGG	60
	rv	TCG TCA CAG ATC ACG TCA TCG	
Collagen III	fw	ATC TTG GTC AGT CCT ATG C	60
	rv	TGG AAT TTC TGG GTT GGG	
Elastin	fw	CTG GAA TTG GAG GCA TCG	60
	rv	TCC TGG GAC ACC AAC TAC	
Fibronectin	fw	AAG ACC AGC AGA GGC ATA AGG	60
	rv	CAC TCA TCT CCA ACG GCA TAA TG	
Matrix Remodelers			
MMP-1	fw	CGC ACA AAT CCC TTC TAC CC	55
	rv	CTG TCG GCA AAT TCG TAA GC	
MMP-2	fw	ATG ACA GCT GCA CCA CTG AG	60
	rv	ATT TGT TGC CCA GGA AAG TG	
MMP-9	fw	TGG GGG GCA ACT CGG C	60
	rv	GGA ATG ATC TAA GCC CAG	
TIMP-1	fw	TGA CAT CCG GTT CGT CTA CA	49
	rv	TGC AGT TTT CCA GCA ATG AG	
TIMP-2	fw	GGA GGA ATC GGT GAG GTC	60
	rv	AAC AGG CAA GAA CAA TGG	
TIMP-4	fw	GAA TCA TCA CTA CCA TCT	55
	rv	TGC TTC ATA CAG ACA TAA	
TGFβ Pathway			
Pai	fw	TCT TTG GTG AAG GGT CTG CT	60
	rv	GTG GGT TTC TCC TCC TGT TG	
Differentiation Markers			
WT1-isoA	fw	TAT TCT GTA TTG GGC TCC GC	60
	rv	CAG CTT GAA TGC ATG ACC TG	
αSMA	fw	CGT GTT GCC CCT GAA GAG CAT	60
	rv	ACC GCC TGG ATA GCC ACA TAC A	

of approximately 20, 23, and 22 (**Figures 2A–C**; **Table 3**), respectively, while expression of elastin was nearly absent (Ct value of 37).

Double immunofluorescent staining with either the cell-surface marker CD44 or β1 integrin to visualize the cell boundaries confirmed presence of collagen I, collagen III, and fibronectin inside the unstrained cells (**Figures 2D–F**). Although elastin was hardly expressed on mRNA level, staining was present in close proximity to the nuclei in the unstrained samples (**Figure 2G**). Exposure of the cells to cyclic strain for 48 h increased the expression of collagen I mRNA significantly ($p = 0.0079$), while application of cyclic strain only showed a trend toward up-regulation for the other ECM genes. On protein level this strain induced gene expression resulted in re-localization of collagen I and -III protein from near the nucleus to more divided throughout the cell (**Figures 2D',E'**). Fibronectin expression was clear at the border of the cell in unstrained samples, but after exposure to cyclic strain the protein was distributed throughout the cytoplasm (**Figure 2F'**). The expression pattern of elastin was not changed by application of strain (**Figure 2G'**). Altogether, these data show that hEPDCs are able to synthesize ECM proteins and that exposure to biomechanical cues *in vitro* induces relocalization of the protein, which might be indicative for new synthesis.

ECM Remodeling Capacity of hEPDCs Is Not Affected by Cyclic Strain

In later stages after MI, the ability of cells to remodel the ECM is of great importance for cardiac repair and the maintenance of cardiac function. Since matrix metalloproteinases (MMPs) play an important role in matrix degradation and remodeling we analyzed their presence. Interestingly, MMP-1 and−2 were expressed by unstrained hEPDCs (**Figure S2**; **Table 3**), while MMP-9 was hardly present (mean Ct-value around 34 in unstrained hEPDCs). Exposure to cyclic strain for 48 h revealed no clear changes in expression of MMPs probably due to large variation between patients (**Figure S2**; **Table 3**).

Since not only the expression of MMPs, but also their enzymatic activity plays a role in matrix remodeling, we determined MMP-2 and−9 activity in culture media. Zymography on plain media samples showed already expression of latent MMP-2 and−9 and active MMP-2 (**Figure S2D**), which is caused by the presence of serum in the culture media which contains MMPs. Analysis of the zymography data showed that the levels of both inactive and active MMP-9 and MMP-2 were increased in hEPDC-derived media samples compared to culture media alone (**Figure S2D**). Semi-quantitative analysis was performed and corrected per experiment for the INT of the unstrained samples, due to high variance between experiments probably caused by the amount of MMPs already present in the plain media. Analysis revealed stable levels of latent and active MMP-9 between unstrained and strained media samples (**Figures S2E,F**). In all hEPDC conditioned media samples all three forms of MMP-2, latent, active intermediate MMP-2 form (64 kDa) and active MMP-2 (66 kDa) were present. In the time span of 48 h application of cyclic strain did not induce any change in activity of MMP2 (**Figure S2**).

MMP activation is regulated by the tissue inhibitors of metalloproteinases (TIMPs). TIMP-1 and−2 were moderately expressed by hEPDCs, while the expression of TIMP-4 was low (mean Ct-value of 33.0 in unstrained hEPDCs (**Figure S2**; **Table 3**). The application of strain for 48 h did not influence the expression of any of the TIMPs (**Figure S2**).

Cyclic Strain Induces the TGFβ Signaling Pathway

Cytokines and growth factors are excessively produced by the injured heart and mechanical cues can modify and activate cytokines and growth factors from their reservoirs within the ECM (30). Although, several signaling pathways are involved in tissue repair, pathogenesis and matrix remodeling, TGFβ is the key factor in matrix production for tissue repair and is rapidly induced and activated in the injured heart (24, 31–33). Furthermore, the TGFβ-pathway plays an important role in the activation and the differentiation of hEPDCs (23, 24). Therefore,

TABLE 3 | Expression cycle threshold Ct) for matrix proteins and modulators and differentiation markers of hEPDCs in different experimental conditions.

Gene	Experimental conditions				
	Unstrained	**Unstrained + TGFβ**	**Strained**	**Strained + iALK5**	**Strained + TGFβ**
Collagen I	20.06 ± 1.02	19.35 ± 1.32	19.28 ± 0.77	21.47 ± 0.68	20.25 ± 1.16
Collagen III	22.91 ± 1.15	23.14 ± 1.20	22.77 ± 0.78	23.42 ± 1.51	24.25 ± 1.25
Fibronectin	22.00 ± 0.68	21.85 ± 0.93	21.90 ± 0.68	23.08 ± 0.90	22.98 ± 1.41
Elastin	36.97 ± 2.98	37.84 ± 2.49	38.66 ± 2.25	38.48 ± 2.27	35.90 ± 1.35
MMP-1	22.74 ± 1.87	23.96 ± 2.00	23.82 ± 1.45	23.39 ± 1.71	22.43 ± 1.33
MMP-2	23.00 ± 0.93	22.80 ± 1.95	22.89 ± 1.83	23.93 ± 1.16	23.69 ± 1.87
MMP-9	34.20 ± 3.74	35.41 ± 1.71	35.42 ± 1.60	35.22 ± 1.78	34.53 ± 1.11
TIMP-1	21.65 ± 0.94	21.87 ± 0.83	21.67 ± 0.74	21.84 ± 0.92	–
TIMP-2	23.31 ± 0.38	23.60 ± 0.84	23.28 ± 0.55	23.99 ± 0.75	23.66 ± 0.35
TIMP-4	33.03 ± 0.69	31.94 ± 0.56	32.72 ± 0.68	33.71 ± 0.72	–
Pai-1	22.73 ± 1.30	22.08 ± 1.30	21.76 ± 1.01	23.75 ± 1.30	22.92 ± 1.81
WT1-isoA	29.28 ± 2.35	30.38 ± 2.58	30.43 ± 2.46	29.63 ± 3.43	32.07 ± 2.42
αSMA	24.93 ± 1.16	24.24 ± 1.70	24.46 ± 1.25	26.71 ± 0.59	25.58 ± 1.56

The cycle threshold Ct) for each gene varied over the different experimental conditions and between patients. Not applicable Ct values were set at a value of 40. The table represents mean Ct values + SD. Genes that are highly expressed gave a Ct value <20, moderate expression was shown by Ct values of 20–26. Low and hardly expressed genes gave a high Ct value of 26–34 and 34–40, respectively.

the role of TGFβ as a biochemical cue on the contribution of hEPDCs on matrix production and remodeling was investigated.

To determine whether the TGFβ signaling pathway is involved in the strain induced collagen I production, the effect of cyclic strain on one of the major downstream TGFβ targets and important modulator of matrix/tissue remodeling, gene platelet activator inhibitor-1 (Pai-1) was investigated. The expression of Pai-1 increased almost 2-fold after application of cyclic strain ($p < 0.05$) and reduced 1.3-fold compared to the unstrained sample when TGFβ signaling was blocked by addition of the ALK5 kinase inhibitor (SB-431542) to the media of the strained samples ($p < 0.01$) (**Figure 3A**). To gain more insight in the involvement of the TGFβ signaling pathway in strain induced collagen production, the effect of cyclic strain in combination with SB-431542 on mRNA level was investigated. Analysis showed that under strained conditions combined with blocking of the TGFβ signaling pathway, the expression of collagen I decreased with 65% ($p < 0.05$) (**Figure 3B**), while the expression of collagen III was unaffected (**Figure 3C**). Double immunofluorescent staining with either the cell-surface marker CD44 or β1 integrin to visualize the cell boundaries confirmed this change of collagen I and the stability of collagen III inside the strained cells treated with ALK5 kinase inhibitor (**Figures 3D,D',E,E'**). These data suggest that strain induces signaling via the TGFβ/ALK5 pathway.

In addition, the influence of TGFβ signaling on presence of MMPs and TIMPs was analyzed. Zymography revealed no significant effect of TGFβ addition on the activity of MMP2 or MMP9 nor does the inhibition of the TGFβ/ALK5 signaling pathway (**Figure S3**). On gene level the same trend for MMP mRNA expression was shown in unstrained samples supplemented with TGFβ and strained samples (**Figure S3**).

TGFβ signaling is known for its role in the differentiation of hEPDCs toward fibroblasts and/or smooth muscle cells. Fibroblasts have a role in the matrix biosynthesis as major collagen producers (34, 35), therefore the differentiation status of hEPDCs was evaluated. Although the epicardial marker WT1 was present both at mRNA and protein level in unstrained as well as strained hEPDCs, application of uniaxial cyclic strain reduced the expression of WT1 by 38% (n.s.) (**Figure 4A**). Most of the hEPDCs showed nuclear expression of WT1 protein (**Figure 4C**), while under strain conditions WT1 was also present in the cytoplasm (**Figure 4D**). The expression of this epicardial marker increased significantly when strain was applied in the presence of iALK5 (**Figure 4A**) and was accompanied with translocation of WT1 from the cytoplasm to the nucleus (**Figure 4E**). When differentiating into fibroblast and/or smooth muscle cell, hEPDCs start to form actin filaments which is accompanied by an increase in alpha smooth muscle actin (αSMA) mRNA (**Figure 4D**). Although qPCR revealed a slight increase in αSMA expression under strain conditions (n.s.), on protein levels hEPDCs display more clear actin fibers compared to unstrained cells (**Figures 4C',D'**). The expression of αSMA, was significantly downregulated in cells exposed to both strain and iALK5 (**Figure 4B**). This down regulation was confirmed by fluorescent staining, revealing absence of actin fibers (**Figure 4E'**). These data suggest that the ALK5 dependent TGFβ signaling induces hEPDC differentiation into a matrix producing mesenchymal cell phenotype.

To elucidate whether mechanical cues, the excessive presence of TGFβ in the injured heart, or the combination of both is the trigger for matrix production and remodeling ability by hEPDCs, all three conditions were compared. Data revealed that addition of an excess of TGFβ to unstrained cells or combining the application of strain simultaneously with addition of TGFβ for 48 h had no significant effect on the expression of matrix proteins (**Figure S4**) or on the differentiation potential of hEPDCs compared to cells only exposed to strain (**Figure S4**). This

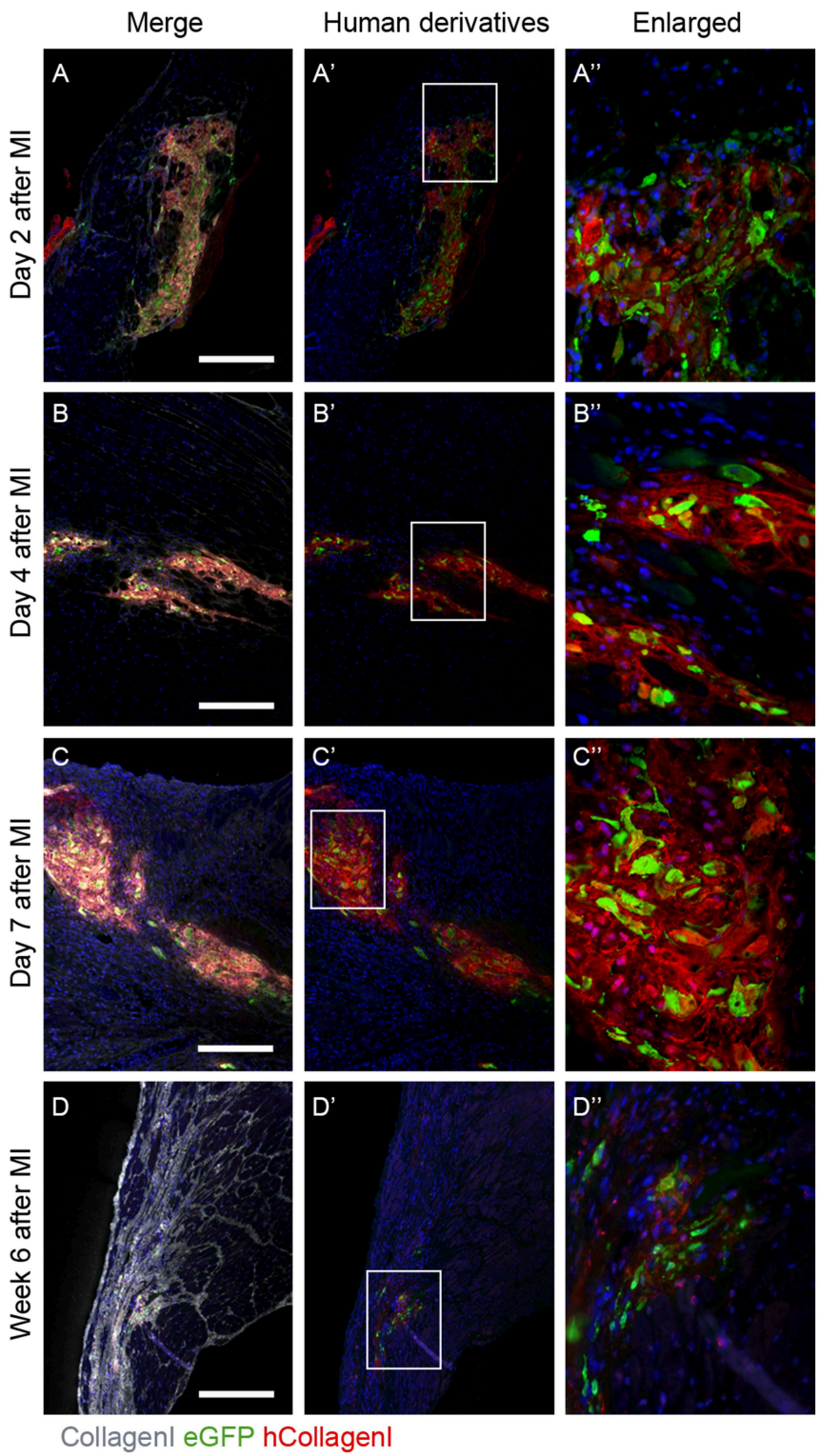

FIGURE 1 | Human collagen type I is present in the infarcted NOD-SCID mouse heart after hEPDC injection. **(A)** Two days after injection of hEPDCs (green) in the mouse infarcted heart, human collagen I (red) is present. The expression of human collagen I (red) increased at day 4 **(B)** and 7 **(C)** after MI. **(D)**. After 6 weeks, hEPDCs (green) were still present in the infarcted mouse heart. At this time point, the total amount of collagen I (white) was prominent, while the amount of human collagen type I (red) was markedly reduced. Images **(A'–D')** represent location of hEPDCs (green) and human collagen I (red) and images **(A"–D")** represent enlargements of images **(A'–D')**. Scale bar 250 μm.

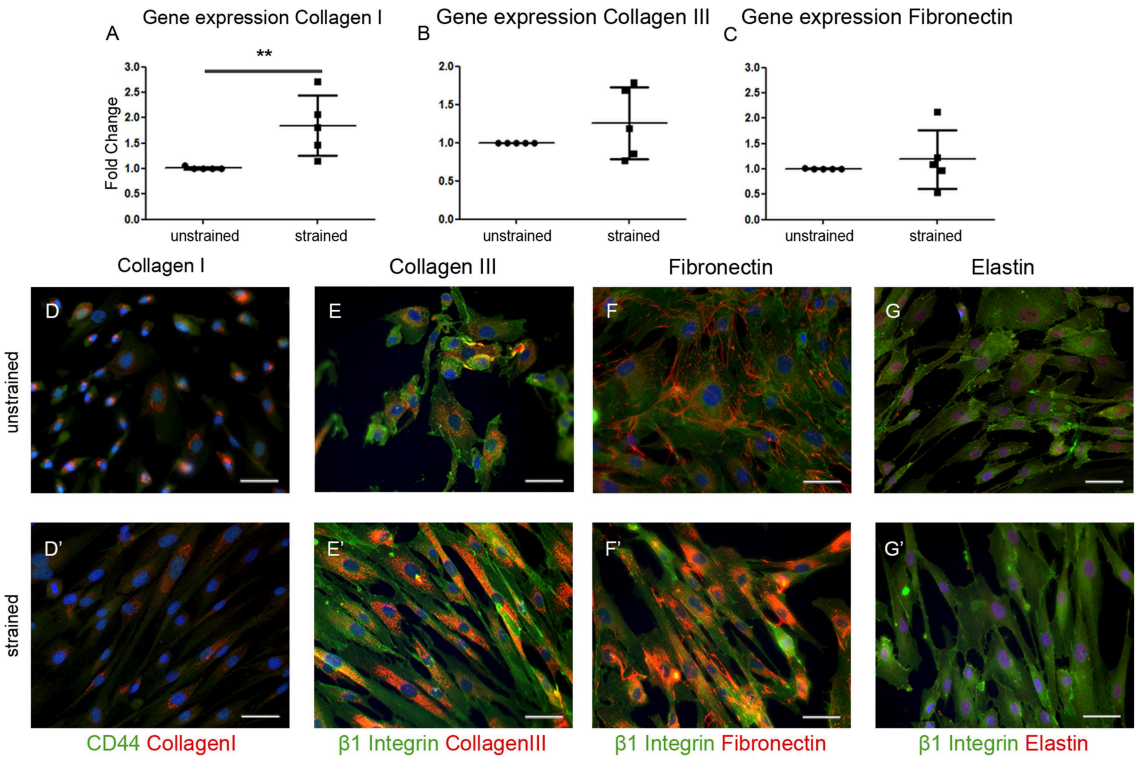

FIGURE 2 | Extracellular matrix (ECM) proteins are synthesized by hEPDCs. Validation of qPCR data on the expression of ECM genes collagen I **(A)** collagen III **(B)**, and fibronectin **(C)** revealed induction of these genes under exposure to uniaxial cyclic strain. These data are represented as mean fold increase ± SD. Since the average ΔCt of the unstrained samples was used as calibrator, the fold change ($2^{\Delta\Delta Ct}$) of the unstrained group is close to 1.0. Representative fluorescent images confirm the biosynthesis of these ECM proteins collagen I **(D)**, collagen III **(E)**, fibronectin **(F),** and elastin **(G)** in red, co-stained by cell surface markers CD44 **(D'),** and β1 Integrin **(E'-G')** both in green. $^{**}P < 0.01$. Scale bar 50 μm.

lack of synergistic effect on ECM production with combining cyclic stretching and TGFβ was previously shown in dermal fibroblasts (36).

DISCUSSION

Cardiac reparative therapies for the diseased heart aim at functional repair of myocardial contractibility to prevent heart failure. The challenge is to not only create new contractile units and vessels, but to also strive for favorable remodeling or even replacement of the fibrotic matrix, thereby fulfilling the basic requirements for long term improvement of heart function. In this study, we investigated the ability of hEPDCs to secrete human collagen I in the myocardial infarction microenvironment as first step in understanding the contribution of hEPDCs to scar composition in a non-paracrine manner. Additionally, an *in vitro* approach was used in which cells were exposed to cyclic strain and exogenous stimulation or inhibition of TGFβ signaling to start unraveling the mechanisms involved in the matrix remodeling capacity of hEPDCs. Our key findings reveal that (1) hEPDCs are able to produce collagen I in the acute phase after MI, (2) cyclic straining induces collagen type I by hEPDCs, (3) TGFβ/ALK5 signaling is an important driver in hEPDC induced matrix synthesis.

Human Collagen I Is Synthesized in the Injured Mouse Heart

As previous shown, transplantation of hEPDCs into the ischemic myocardium of NOD-SCID mice was able to attenuated ventricular remodeling via a paracrine stimulatory effect (6). Characterization of these transplanted hEPDCs *in vivo* revealed expression of αSMA, von Willebrand factor (vWF), sarcoplasmic or endoplasmic reticulum Ca^{2+}-ATPase (SERCA2a) and voltage-gated sodium channel (α-subunit; SCN5a), suggesting a myoendothelial phenotype (6). Our data indicate that hEPDCs not only contribute to ventricular remodeling via secretion of growth factors and cytokines, but are also able to create their own matrix environment when transplanted in the acute phase after MI. The creation of this human microenvironment is only temporary, since human collagen is almost absent in the infarcted area 6 weeks after transplantation suggesting active remodeling of the human matrix during myocardial wound healing. This remodeling could be induced by the hEPDCs themselves or by the high expression levels of remodeling proteins in the injured mouse heart (37). This is, to the best of our knowledge, the first study describing that adult hEPDCs directly contribute to matrix production in the early response phase after MI, although indirect paracrine effects of hEPDCs on matrix remodeling have been speculated (10, 38) and matrix

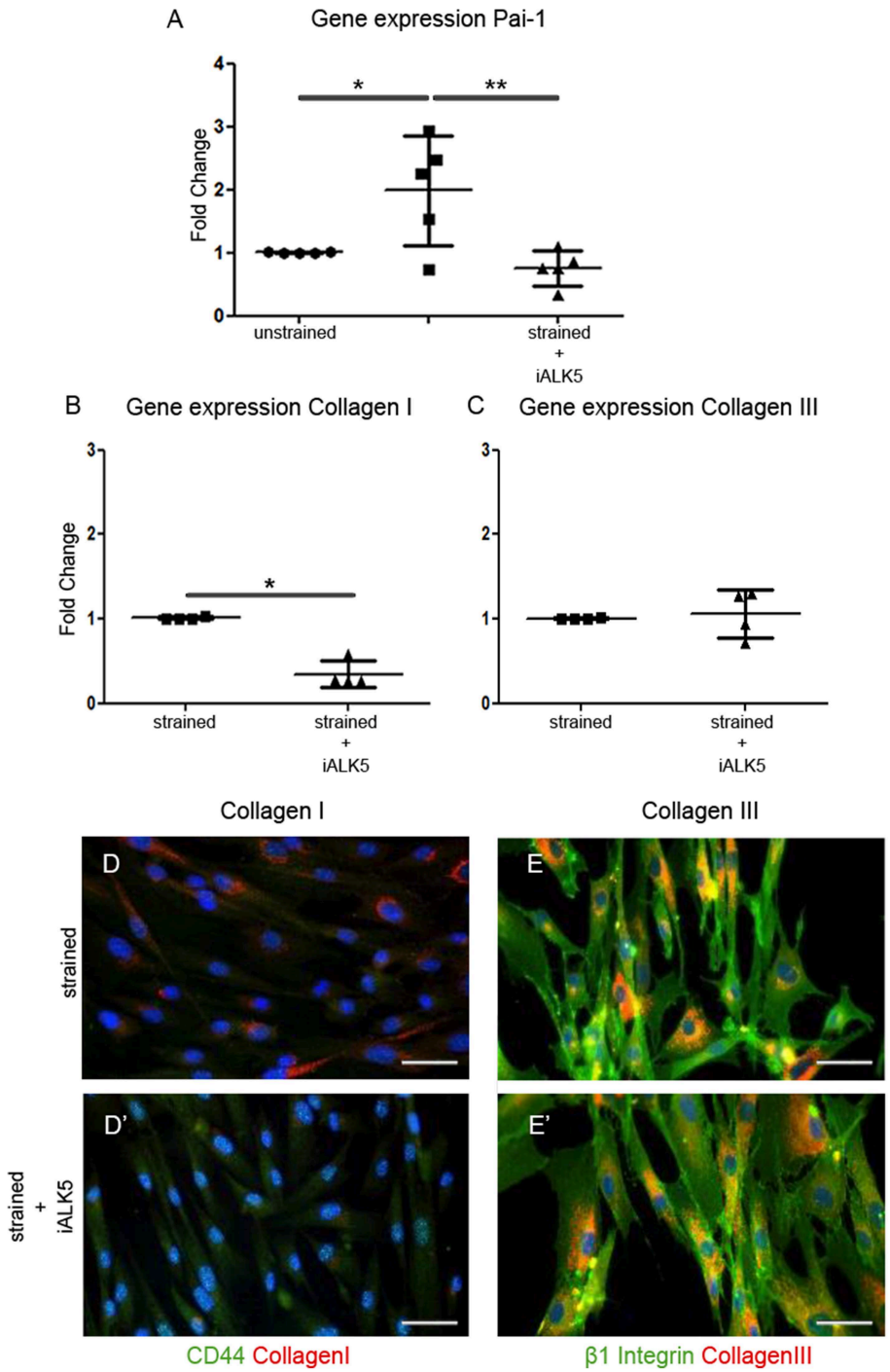

FIGURE 3 | TGFβ signaling is induced in hEPDCs exposed to uniaxial cyclic strain. Gene expression of unstrained and strained hEPDCs showed that the expression of *Pai-1* was increased by application of strain **(A)**. Gene expression of hEPDCs exposed to strain in the presence of iALK5 showed a significant decrease in *Pai-1*. Inhibition of TGFβ signaling also resulted in a significant downregulation of collagen I **(B,D,D')**, while no significant change was found in the expression of collagen III **(C,E,E')**. The data are represented as mean fold change ± SD. $^{*}P < 0.05$, $^{**}P < 0.01$.

production by EPDCs is described in the embryonic mammalian heart or by endogenous EPDCs in mouse models (8, 39). The production of collagen type I by hEPDCs can positively regulate cardiac function and repair. By producing human collagen I, hEPDCs create their own local supportive environment to maintain cellular structure and function, thereby favoring cell

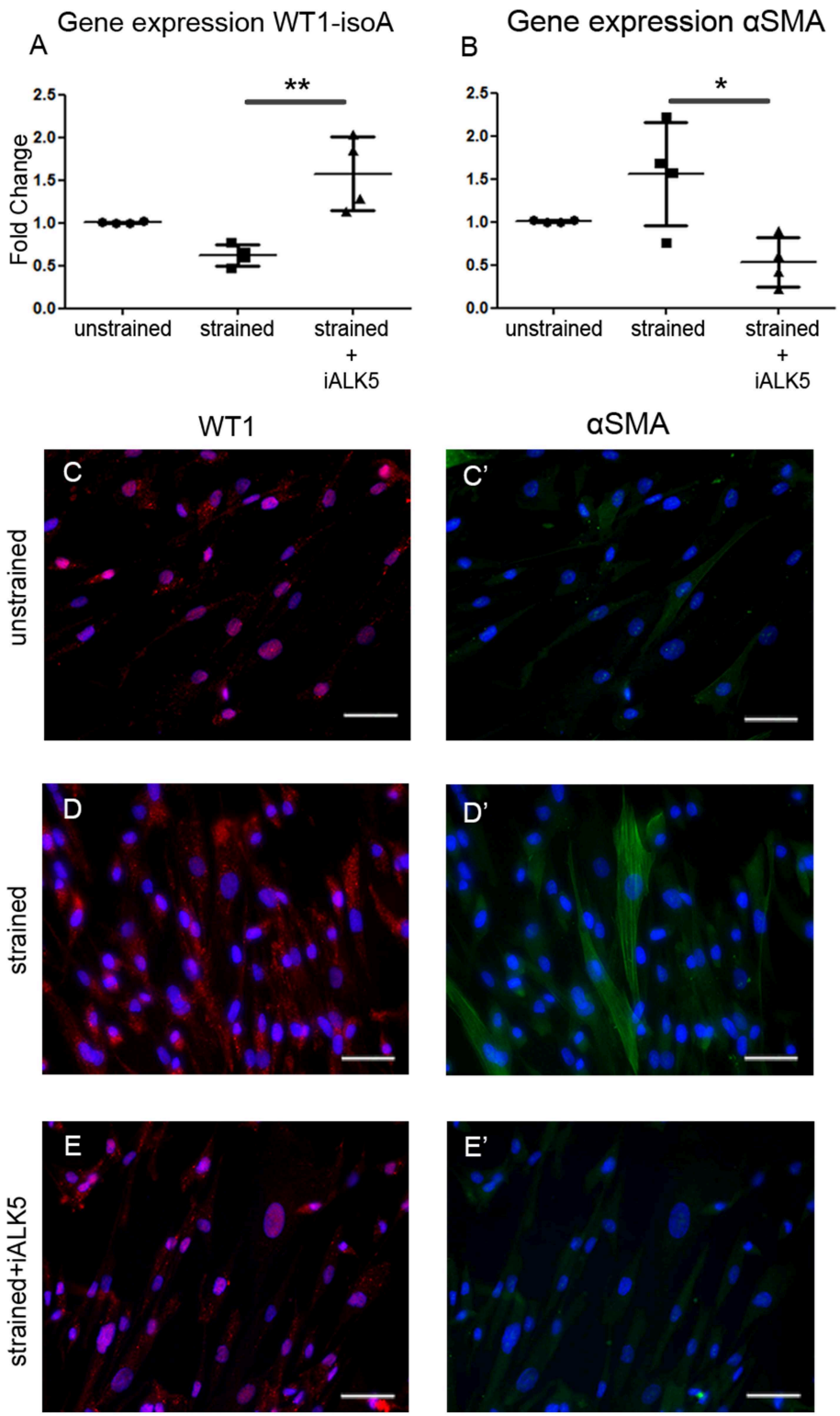

FIGURE 4 | Application of cyclic strain induces changes in differentiation markers in hEPDCs and ALK5 is required for this effect. Quantification of *WT1* isoform A mRNA expression decreased after application to strain and increased again by simultaneous exposure to strain and iALK5 **(A)**. The onset of differentiation was also shown by the increase in αSMA mRNA in strained hEPDCs, which was inhibited in the presence of iALK5 **(B)**. **(C–E)** The process of differentiation was confirmed by staining for WT1 and αSMA **(C'–E')** as shown by translocation of the WT1 expression from the nuclei to the cytoplasm and the presence of αSMA after exposure to cyclic strain. The data is represented as represented as mean fold change ± SD. $^{*}P < 0.05$, $^{**}P < 0.01$. Scale bar 50 μm.

survival which will enhance repair. Furthermore, collagen I provides tensile strength and structural integrity, which creates resistance to stretch and deformation during each contraction. In the injured heart this prevents the myocardial wall from rupture and contributes to preservation of contractility (40). Moreover, the deposition of epicardial-derived ECM could promote wound healing and thereby might direct cardiac regeneration (41). The negative impact of human collagen I production by EPDCs on cardiac regeneration may arise by the fact that collagen type I is the major fibrillar collagen present in the mature scar, and therefore might have negative consequences for repair, remodeling and functional competence of the heart on the long term (3, 38). The production of human collagen type I by the hEPDCs could be a response to the inflammatory cytokines or other remodeling factors present after MI. However, we have shown that hEPDCs are mechanosensitive, and our *in vitro* data suggest that mechanical stress contributes to the increase in collagen type I deposition. Therefore, we think that the *in vivo* response of these cells, especially during the early phase post MI when a definitive scar is not yet formed, is a combination of mechanical stress and inflammatory cytokines. Further research is needed to unravel if collagen production by hEPDCs in the early response phase after MI may trigger the transition from reparative fibrosis to malignant scaring at late remodeling phases.

EPDCs Respond to Environmental Mechanical Stimuli *in vitro*

Given the complexity of the environment in the injured heart, we used an *in vitro* approach to elucidate how the different environmental stimuli interplay and guide cellular responses. This systematic and reductionist approach *in vitro* was followed to gain understanding in the contribution of cyclic strain and biochemical stimulation. Our data reveal that adult hEPDCs are able to sense and respond to mechanical cues from their environment. Indeed, when exposed to uniaxial cyclic strain, EPDCs reorient perpendicular to the stretch direction, a behavior also observed in several mesenchymal cell types, known as "strain avoidance" (42, 43) (**Figure S1**). In response to cyclic strain the TGFβ signaling pathway in hEPDCs is induced and cells thereby change matrix synthesis and their differentiation profile. These findings confirm the suggestion of mechanosensitivity of epicardial cells by Andrés-Delgado et al. who reported that during cardiac development the heart beat drives the epicardium formation from the pro-epicardial organ (44).

To date, little is known about matrix modulation by adult mammalian EPDCs and the influence of mechanical stimulation on this process. EPDCs display stromal cell properties and they are progenitors of cardiac fibroblasts (9, 10). Cardiac fibroblasts are key players in matrix remodeling in the developing, adult and diseased heart (34, 35) and application of cyclic mechanical strain increase the synthesis of collagens and fibronectin by cardiac fibroblasts (45–48). In this research we investigated the early matrix remodeling response, after 48 h and therefore it is difficult to draw definitive conclusions regarding the effect of mechanical stimuli on differentiation outcome. After 48 h of exposure to cyclic strain, hEPDCs still express WT1 and they lack expression of elastin, which suggest that these hEPDCs are different from cardiac fibroblasts. A recent study using cardiac fibroblasts, suggested that strain-induced matrix production could precede differentiation toward myofibroblasts, since cardiac fibroblasts are adapted to the physiological cyclic strains or have a memory that reminds them how to coop with mechanical stimuli, which prevents them from myofibroblast activation (46). This hypothesis is also plausible for hEPDCs, suggesting that cyclic strain causes the onset of transformation toward a matrix producing mesenchymal cell (35, 48, 49).

TGFβ-Signaling Is Part of Strain-Induced Matrix Reorganization Ability of hEPDCs

As also shown in this study, mechanical stimulation has an important impact on the activity of TGFβ (30). Next to mechanical stimulation, proteases like MMP-2 and MMP-9 are able to activate TGFβ (31). Interestingly, TGFβ also suppresses protease activity by inhibiting MMP expression and the induction of synthesis of protease inhibitors like Pai-1 and TIMPs (32, 33) and Pai-1 induction is shown in our study.

We found no additional effect when combining mechanical cyclic stimuli and addition of exogenous TGFβ on matrix synthesis and remodeling by hEPDCs. The ability of cells to respond to experimental conditions is dependent on the activation status of the cells prior to start of the experiment (49). The lack of response of hEPDCs to exogenous TGFβ could be due to already elevated TGFβ levels as inhibiting the pathway did influence the ability of hEPDCs to respond (35, 48). Elevation in TGFβ levels could be induced by cell passaging, which in cardiac fibroblasts leads to differentiation into myofibroblasts after the third passage (50). In addition, presence of TGFβ will influence the activation and differentiation profile of the cells at the start of the experiments, which might also explain the large inter-patient variation we observe. Therefore, it is important to determine the heterogeneity in activation status and differentiation profile prior to start of the experiment. For translation to clinical application it is important to gain more insight in the link between the activation and differentiation profile of hEPDCs and the contribution of these cells to matrix synthesis and remodeling both *in vivo* and *in vitro*.

Implications for Cardiac Repair Therapy

Given its developmental contribution in cardiomyogenesis (15), the epicardium is a highly interesting cell layer in the context of cardiac repair after ischemic injury. Therefore, EPDCs offer promising outlooks for cell-based cardiac therapy; either via exogenous application, or via endogenous reactivation (6, 9, 10, 15, 18, 19, 38). EPDCs can contribute to cardiac repair by (1) providing new cells via differentiation into cardiac fibroblasts and smooth muscle cells and (2) paracrine signaling. The latter process leads to production of essential proteins and influences myocardial growth, which can further guide cardiac repair after injury and maintain the beating rate of cardiomyocytes (15, 32).

The production of collagen I by hEPDCs directly after MI is crucial for preserving myocardial function, since inhibition of collagen deposition leads to worsening of cardiac dilation and heart dysfunction (37). ECM production by EPDCs during MI healing can both be positive or negative for cardiac repair, and the right balance in the production and remodeling of the cardiac ECM is of great importance. Therefore, it is important to explore how pathological myocardial conditions contribute to physical and paracrine properties of hEPDCs in more detail. This future research will provide new insights, which might lead to new treatment modalities for cardiac repair.

CONCLUSION

In summary, we show that hEPDCs are able to synthesize and excrete collagen I after MI and thereby create their own extracellular environment. To elucidate the role of the pathological environment in the hEPDC response to cardiac injury, we proposed an *in vitro* set-up to elucidate the role of mechanical stimuli and/or TGFβ signaling as biochemical cue. We revealed that mechanical stimulation is able to trigger matrix reorganization, mainly through collagen I production, via the TGFβ/ALK5 signaling pathway. The *in vitro* approach enables unraveling the ability of hEPDCs to create and remodel the cardiac matrix in response to injury. These insights have impact on future studies on the contribution of hEPDCs to reverse or adverse remodeling and better understanding of this process might tailor new treatment modalities.

ETHICAL STATEMENT

All animal procedures to achieve this dataset were approved by the Animal Ethics Committee of the Leiden University and conformed the Guide for the Care and Use of Laboratory Animals (National Institutes of Health publications No. 85-23, Revised 1996).

AUTHOR CONTRIBUTIONS

NB, SD, CB, and MG contributed substantially to the conception and design of the work. While NB, SD, BK, AS, CB, and MG contributed to the acquisition, analysis, and interpretation of data. NB and SD drafted the work and CB and MG revised it critically for intellectual content. All authors approved of the final version to be published and agreed to be accountable for all aspects of the work in ensuring that questions related to the accuracy or integrity of any part of the work are appropriately investigated and resolved.

FUNDING

This study is supported by the Dutch Heart Foundation, projects DHF-2009B063 (MG) and project DHF-2014T013 (NB), the Netherlands Institute for Regenerative Medicine (NIRM), and Smartcare, part of the research program of the BioMedical Materials institute is co-funded by the Dutch Ministry of Economic Affairs, Agriculture and Innovation (MG and CB).

ACKNOWLEDGMENTS

We thank Samantha de Witte and Duy Nguyen for preliminary work and Tessa van Herwaarden for expert technical assistance.

SUPPLEMENTARY MATERIAL

The Supplementary Material for this article can be found online at: https://www.frontiersin.org/articles/10.3389/fcvm.2019.00081/full#supplementary-material

REFERENCES

1. Lindsey ML, Mann DL, Entman ML, Spinale FG. Extracellular matrix remodeling following myocardial injury. *Ann Med.* (2003) 35:316–26. doi: 10.1080/07853890310001285
2. Frantz C, Stewart KM, Weaver VM. The extracellular matrix at a glance. *J Cell Sci*. (2010) 123:4195–200. doi: 10.1242/jcs.023820
3. Cleutjens JP, Blankesteijn WM, Daemen MJ, Smits JF. The infarcted myocardium: simply dead tissue, or a lively target for therapeutic interventions. *Cardiovasc Res.* (1999) 44:232–41. doi: 10.1016/S0008-6363(99)00212-6
4. Sun Y, Weber KT. Infarct scar: a dynamic tissue. *Cardiovasc Res*. (2000) 46:250–6. doi: 10.1016/S0008-6363(00)00032-8
5. Wessels A, Perez-Pomares JM. The epicardium and epicardially derived cells EPDCs. as cardiac stem cells. *Anat Rec A Discov Mol Cell Evol Biol*. (2004) 276:43–57. doi: 10.1002/ar.a.10129
6. Winter EM, Grauss RW, Hogers B, van Tuyn J, van der Geest R, Lie-Venema H, et al. Preservation of left ventricular function and attenuation of remodeling after transplantation of human epicardium-derived cells into the infarcted mouse heart. *Circulation*. (2007) 116:917–27. doi: 10.1161/CIRCULATIONAHA.106.668178
7. Smits A, Riley P. Epicardium-derived heart repair. *J Dev Biol*. (2014) 2:84–100. doi: 10.3390/jdb2020084
8. van Wijk B, Gunst QD, Moorman AF, van den Hoff MJ. Cardiac regeneration from activated epicardium. *PloS ONE.* (2012) 7:e44692. doi: 10.1371/journal.pone.0044692
9. Lie-Venema H, van den Akker NM, Bax NA, Winter EM, Maas S, Kekarainen T, et al. Origin, fate and function of epicardium-derived cells EPDCs. in normal and abnormal cardiac development. *Sci World J*. (2007) 7:1777–98. doi: 10.1100/tsw.2007.294
10. Gittenberger-de Groot AC, Winter EM, Bartelings MM, Goumans MJ, deRuiter MC, Poelmann RE. The arterial and cardiac epicardium in development, disease and repair. *Differentiation*. (2012) 84:41–53. doi: 10.1016/j.diff.2012.05.002
11. Gittenberger-de Groot AC, Vrancken Peeters MP, Mentink MM, Gourdie RG, Poelmann RE. Epicardium-derived cells contribute a novel population to the myocardial wall and the atrioventricular cushions. *Circ Res*. (1998) 82:1043–52. doi: 10.1161/01.RES.82.10.1043
12. Cai CL, Martin JC, Sun Y, Cui L, Wang L, Ouyang K, et al. A myocardial lineage derives from Tbx18 epicardial cells. *Nature*. (2008) 454:104–8. doi: 10.1038/nature06969

13. Wessels A, van den Hoff MJ, Adamo RF, Phelps AL, Lockhart MM, Sauls K, et al. Epicardially derived fibroblasts preferentially contribute to the parietal leaflets of the atrioventricular valves in the murine heart. *Dev Biol*. (2012) 366:111–24. doi: 10.1016/j.ydbio.2012.04.020
14. Cano E, Carmona R, Ruiz-Villalba A, Rojas A, Chau YY, Wagner KD, et al. Extracardiac septum transversum/proepicardial endothelial cells pattern embryonic coronary arterio-venous connections. *Proc Natl Acad Sci USA*. (2016) 113:656–61. doi: 10.1073/pnas.1509834113
15. Smits AM, Dronkers E, Goumans MJ. The epicardium as a source of multipotent adult cardiac progenitor cells: their origin, role and fate. *Pharmacol Res*. (2018) 127:129–40. doi: 10.1016/j.phrs.2017.07.020
16. Stuckmann I, Evans S, Lassar AB. Erythropoietin and retinoic acid, secreted from the epicardium, are required for cardiac myocyte proliferation. *Dev Biol*. (2003) 255:334–49. doi: 10.1016/S0012-1606(02)00078-7
17. Chen T, Chang TC, Kang JO, Choudhary B, Makita T, Tran CM, et al. Epicardial induction of fetal cardiomyocyte proliferation via a retinoic acid-inducible trophic factor. *Dev Biol*. (2002) 250:198–207. doi: 10.1006/dbio.2002.0796
18. Weeke-Klimp A, Bax NA, Bellu AR, Winter EM, Vrolijk J, Plantinga J, et al. Epicardium-derived cells enhance proliferation, cellular maturation and alignment of cardiomyocytes. *J Mol Cell Cardiol*. (2010) 49:606–16. doi: 10.1016/j.yjmcc.2010.07.007
19. Winter EM, van Oorschot AA, Hogers B, van der Graaf LM, Doevendans PA, Poelmann RE, et al. A new direction for cardiac regeneration therapy: application of synergistically acting epicardium-derived cells and cardiomyocyte progenitor cells. *Circ Heart Fail*. (2009) 2:643–53. doi: 10.1161/CIRCHEARTFAILURE.108.843722
20. Frantz S, Hu K, Adamek A, Wolf J, Sallam A, Maier SK, et al. Transforming growth factor beta inhibition increases mortality and left ventricular dilation after myocardial infarction. *Basic Res Cardiol*. (2008) 103:485–92. doi: 10.1007/s00395-008-0739-7
21. Goumans MJ, Ten Dijke P. TGF-β signaling in control of cardiovascular function. *Cold Spring Harb Perspect Biol*. (2018) 10:a0022210. doi: 10.1101/cshperspect.a022210
22. van Tuyn J, Atsma DE, Winter EM, van der Velde-van Dijke I, Pijnappels DA, Bax NA, et al. Epicardial cells of human adults can undergo an epithelial-to-mesenchymal transition and obtain characteristics of smooth muscle cells *in vitro*. *Stem Cells*. (2007) 25:271–8. doi: 10.1634/stemcells.2006-0366
23. Bax NA, van Oorschot AA, Maas S, Braun J, van Tuyn J, de Vries AA, et al. *In vitro* epithelial-to-mesenchymal transformation in human adult epicardial cells is regulated by TGFβ-signaling and WT. *Basic Res Cardiol*. (2011) 105:829–47. doi: 10.1007/s00395-011-0181-0
24. Moerkamp AT, Lodder K, van Herwaarden T, Dronkers E, Dingenouts CK, Tengström FC, et al. Human fetal and adult epicardial-derived cells: a novel model to study their activation. *Stem Cell Res Ther*. (2016) 7:174. doi: 10.1186/s13287-016-0434-9
25. Gupta V, Grande-Allen KJ. Effects of static and cyclic loading in regulating extracellular matrix synthesis by cardiovascular cells. *Cardiovasc Res*. (2006) 72:375–83. doi: 10.1016/j.cardiores.2006.08.017
26. Duim SN, Kurakula K, Gouman MJ, Kruithof BP. Cardiac endothelial cells express Wilm's tumor-1: Wt1 expression in the developing, adult and infarcted heart. *J Mol Cell Cardiol*. (2015) 81:127–35. doi: 10.1016/j.yjmcc.2015.02.007
27. Bax NA, van Marion MH, Shah B, Goumans MJ, Bouten CV, van der Schaft DW. Matrix production and remodeling capacity of cardiomyocyte progenitor cells during *in vitro* differentiation. *J Mol Cell Cardiol*. (2012) 53:497–508. doi: 10.1016/j.yjmcc.2012.07.003
28. Boonen KJ, Langelaan ML, Polak RB, van de Schaft DW, Baaijens FP, Post MJ. Effect of a combined mechanical stimulation protocol: value for skeletal muscle tissue engineering. *J Biomech*. (2010) 43:1514–21. doi: 10.1016/j.jbiomech.2010.01.039
29. Livak KJ, Schmittgen TD. Analysis of relative gene expression data using real-time quantitative PCR and the 2-Delta.Delta. CT method. *Methods*. (2001) 25:402–8. doi: 10.1006/meth.2001.1262
30. Hinz B. The extracellular matrix and transforming growth factor-β1: tale of a strained relationship. *Matrix Biol*. (2015) 47:54–65. doi: 10.1016/j.matbio.2015.05.006
31. Chuva de Sousa Lopes SM, Feijen A, Korving J, Korchynskyi O, Larsson J, Karlsson S, et al. Connective tissue growth factor expression and Smad signaling during mouse heart development and myocardial infraction. *Dev Dyn*. (2004) 231:542–50. doi: 10.1002/dvdy.20162
32. Bujak M, Frangogiannis NG. The role of TGF-beta signaling in myocardial infarction and cardiac remodeling. *Cardiovasc Res*. (2007) 74:184–95. doi: 10.1016/j.cardiores.2006.10.002
33. Dobaczewski M, Chen W, Frangiogiannis NG. Transforming growth factor TGF.-β signaling in cardiac remodeling. *J Mol Cell Cardiol*. (2011) 51:600–6. doi: 10.1016/j.yjmcc.2010.10.033
34. Leask A. TGFbeta, cardiac fibroblasts, and the fibrotic response. *Cardiovasc Res*. (2007) 74:207–12. doi: 10.1016/j.cardiores.2006.07.012
35. Fan D, Takawale A, Lee J, Kassiri Z. Cardiac fibroblasts, fibrosis and extracellular matrix remodeling in heart disease. *Fibrogenesis Tissue Repair*. (2007) 5:15. doi: 10.1186/1755-1536-5-15
36. Syedain ZH, Tranquillo RT. TGF-β1 diminishes collagen production during long-term cyclic stretching of engineered connective tissue: implication of decreased ERK signaling. *J Biomech*. (2011) 44:848–55. doi: 10.1016/j.jbiomech.2010.12.007
37. Vanhoutte D, Schellings M, Pinot Y, Heymans S. Relevance of matrix metalloproteinases and their inhibitors after myocardial infarction: a temporal and spatial window. *Cardiovasc Res*. (2006) 69:604–13. doi: 10.1016/j.cardiores.2005.10.002
38. Masters M, Riley PR. The epicardium signals the way towards heart regeneration. *Stem Cell Res*. (2014) 13:683–92. doi: 10.1016/j.scr.2014.04.007
39. Muñoz-Chápuli R, Macías D, González-Iriarte M, Carmona R, Atencia G, Pérez-Pomares JM. The epicardium and epicardial-derived cells: multiple functions in cardiac development. *Rev Esp Cardiol*. (2002) 55:1070–82. doi: 10.1016/S0300-8932(02)76758-4
40. Talman V, Ruskoaho H. Cardiac fibrosis in myocardial infarction-from repair and remodeling to regeneration. *Cell Tissue Res*. (2016) 365:363–581. doi: 10.1007/s00441-016-2431-9
41. Mercer SE, Odelberg SJ, Simon HG. A dynamic spatiotemporal extracellular matrix facilitates epicardial-mediated vertebrate heart regeneration. *Dev Biol*. (2013) 382:457–69. doi: 10.1016/j.ydbio.2013.08.002
42. Livne A, Bouchbinder E, Geiger B. Cell reorientation under cyclic stretching. *Nat Commun*. (2014) 5:3938. doi: 10.1038/ncomms4938
43. Mauretti A, Bax NA, van Marion MH, Goumans MJ, Sahlgren C, Bouten CV. Cardiomyocyte progenitor cell mechanoresponse unrevealed: strain avoidance and mechanosome development. *Integr Biol Camb*. (2016) 8:991–1001. doi: 10.1039/C6IB00117C
44. Andrés-Delgado L, Mercader N. Interplay between cardiac function and heart development. *Biochim Biophys Acta*. (2016) 1863:1707–16. doi: 10.1016/j.bbamcr.2016.03.004
45. Carver W, Naqpal ML, Nachtigal M, Borg TK, Terracio L. Collagen expression in mechanically stimulated cardiac fibroblasts. *Circ Res*. (1991) 69:116–22. doi: 10.1161/01.RES.69.1.116
46. Ugolini GS, Pavesi A, Rasponi M, Fiore GB, Kamm R, Soncini M. Human cardiac fibroblasts adaptive response to controlled

combined mechanical strain and oxygen changes *in vitro*. *Elife.* (2017) 6:e22847. doi: 10.7554/eLife.22847
47. van Putten S, Shafieyan Y, Hinz B. Mechanical control of cardiac myofibroblasts. *J Mol Cell Cardiol.* (2016) 93:133–42. doi: 10.1016/j.yjmcc.2015.11.025
48. Watson CJ, Phelan D, Xu M, Collier P, Neary R, Smolenski A, et al. Mechanical stretch up-regulates the B-type natriuretic peptide system in human cardiac fibroblasts: a possible defense against transforming growth factor-β mediated fibrosis. *Fibrogensis Tissue Repair*. (2012) 5:9. doi: 10.1186/1755-1536-5-9
49. O'Callaghan CJ, Williams B. Mechanical strain-induced extracellular matrix production by human vascular smooth muscle cells: role of TGF-beta1. *Hypertension.* (2000) 36:319–24. doi: 10.1161/01.HYP.36.3.319
50. Petrov VV, Fagard RH, Lijnen PJ. Stimulation of collagen production by transforming growth factor-beta1 during differentiation of cardiac fibroblasts to myofibroblasts. *Hypertension*. (2002) 39:258–63. doi: 10.1161/hy0202.103268

Conflict of Interest Statement: The authors declare that the research was conducted in the absence of any commercial or financial relationships that could be construed as a potential conflict of interest.

Citation: Bax NAM, Duim SN, Kruithof BPT, Smits AM, Bouten CVC and Goumans MJ (2019) In vivo and in vitro Approaches Reveal Novel Insight Into the Ability of Epicardium-Derived Cells to Create Their Own Extracellular Environment. Front. Cardiovasc. Med. 6:81. doi: 10.3389/fcvm.2019.00081

frontiers in Cardiovascular Medicine

REVIEW
published: 31 July 2019
doi: 10.3389/fcvm.2019.00101

The Role of Macrophages in the Infarcted Myocardium: Orchestrators of ECM Remodeling

Sinead A. O'Rourke[1,2,3], *Aisling Dunne*[2] *and Michael G. Monaghan*[1,3,4*]

[1] *Department of Mechanical and Manufacturing Engineering, Trinity College Dublin, Dublin, Ireland,* [2] *School of Biochemistry & Immunology and School of Medicine, Trinity Biomedical Science Institute, Trinity College Dublin, Dublin, Ireland,* [3] *Trinity Centre for Bioengineering, Trinity Biomedical Science Institute, Trinity College Dublin, Dublin, Ireland,* [4] *Advanced Materials for BioEngineering Research (AMBER) Centre, Trinity College Dublin and Royal College of Surgeons in Ireland, Dublin, Ireland*

Myocardial infarction is the most common form of acute cardiac injury attributing to heart failure. While there have been significant advances in current therapies, mortality and morbidity remain high. Emphasis on inflammation and extracellular matrix remodeling as key pathological factors has brought to light new potential therapeutic targets including macrophages which are central players in the inflammatory response following myocardial infarction. Blood derived and tissue resident macrophages exhibit both a pro- and anti-inflammatory phenotype, essential for removing injured tissue and facilitating repair, respectively. Sustained activation of pro-inflammatory macrophages evokes extensive remodeling of cardiac tissue through secretion of matrix proteases and activation of myofibroblasts. As the heart continues to employ methods of remodeling and repair, a destructive cycle prevails ultimately leading to deterioration of cardiac function and heart failure. This review summarizes not only the traditionally accepted role of macrophages in the heart but also recent advances that have deepened our understanding and appreciation of this dynamic cell. We discuss the role of macrophages in normal and maladaptive matrix remodeling, as well as studies to date which have aimed to target the inflammatory response in combatting excessive matrix deposition and subsequent heart failure.

Keywords: macrophages, myocardial infarction, ECM, fibrosis, inflammation, wound healing, immunomodulation, macrophages (M1/M2)

OPEN ACCESS

Edited by:
Joshua D. Hutcheson, Florida International University, United States

Reviewed by:
Nikolaos G. Frangogiannis, Albert Einstein College of Medicine, United States
Alison Schroer, Stanford University, United States

***Correspondence:**
Michael G. Monaghan
monaghmi@tcd.ie

Specialty section:
This article was submitted to Cardiovascular Biologics and Regenerative Medicine, a section of the journal Frontiers in Cardiovascular Medicine

Received: *01 May 2019*
Accepted: *09 July 2019*
Published: *31 July 2019*

Citation:
O'Rourke SA, Dunne A and Monaghan MG (2019) The Role of Macrophages in the Infarcted Myocardium: Orchestrators of ECM Remodeling. Front. Cardiovasc. Med. 6:101. doi: 10.3389/fcvm.2019.00101

INTRODUCTION

Heart failure is a global pandemic, accounting for 31% of deaths worldwide (1). Health expenditures associated with heart failure are substantial, and expected to increase dramatically with an aging population (2). Myocardial infarction (MI) is the most common form of acute cardiac injury attributing to heart failure, and while there have been significant advances in therapies, mortality and morbidity remain high. Our understanding of MI has evolved in recent years with inflammation driven by macrophages now recognized as playing a key pathological role in the progression of tissue remodeling and fibrosis which, in turn, limits cardiac function. A greater appreciation of the role of the inflammatory response and the interaction between macrophages and the extracellular matrix (ECM) is required in order to provide greater insight into tissue remodeling and disease progression within the myocardium, as well as revealing therapeutic

targets for the treatment of heart failure. In this review we will discuss the importance and role of macrophages in the healthy and infarcted myocardium, and how these innate immune cells contribute toward ECM remodeling and fibrosis.

MULTICELLULARITY OF THE HEART

The myocardium is a multicellular complex tissue comprised of a range of distinct cell-types. Cardiomyocytes (CMs) constitute approximately one third of resident myocardial cells by number (3), with the remaining two thirds referred to as non-excitable cells (non-CMs), such as fibroblasts, smooth muscle cells, endothelial cells, autonomic motor neurons, and immune cells, such as mast cells and macrophages (4). While CMs possess inherent conduction capabilities which mediate the characteristic contractile forces of the heart, non-CMs are responsible for matrix deposition, vascularization and autonomic regulation (5). CMs and non-CMs communicate via biochemical signaling through cytokine and growth factor secretion (5, 6). Such signals arise, for example, during development and regulation and include the release of vascular endothelial growth factor (VEGF) which activates endothelial cells to initiate angiogenesis (7), or in response to trauma or injury, where signaling is mediated by pro-inflammatory cytokines such as tumor necrosis factor alpha (TNFα) (8, 9). Numerous networks also exist between non-CMs, such as fibroblasts and macrophages, working in tangent to maintain the structural integrity of the heart.

Fibroblasts are traditionally defined as cells of mesenchymal origin, arising from bone marrow derived cells known as fibrocytes (10, 11). Cardiac fibroblasts produce the necessary components for the construction of the ECM in order to maintain the integrity of the myocardium (10). As a result, fibroblasts have been highlighted as key mediators of both normal cardiac function and the remodeling response to injury (6, 10, 12). In addition to producing components of the ECM, fibroblasts are also observed to secrete regulatory proteins and matrix metalloproteinases as well as their corresponding inhibitors, tissue inhibitors of metalloproteinases, thus maintaining a well-controlled balance for ECM homeostasis (13).

MACROPHAGES—KEY DRIVERS OF THE INNATE IMMUNE RESPONSE

Macrophages (and their precursors, monocytes) are key mediators of the innate immune response involved in the recognition, phagocytosis and elimination of pathogens. They exist as both circulating and tissue resident cells within the body and have the ability to change their function and phenotype based on environmental cues (14). While they exist as a heterogenous population they can be broadly classified as M1 or M2 macrophages (15). M1 macrophages are traditionally associated with a pro-inflammatory response, and are referred to as classically activated macrophages, induced by IFNγ, LPS, and TNFα. When stimulated, M1 macrophages secrete high levels of pro-inflammatory cytokines IL-12, IL-23, IL-1, and IL-6 (16). M2 macrophages, or "alternatively activated" macrophages exhibit an anti-inflammatory, pro-regenerative phenotype largely due to their ability to secrete high levels of anti-inflammatory cytokines including IL-10 and growth factors, such as VEGF as well as matrix metalloproteinases (MMPs) (16). In murine models, M1 and M2 macrophages are distinguished from another through the expression of the inflammatory monocyte marker Ly6C. $Ly6C^{high}$ monocytes are preferentially recruited to sites of inflammation and exhibit an M1 pro-inflammatory phenotype while $Ly6C^{low}$ monocytes represent the non-classical population and differentiate into M2 macrophages to promote tissue healing and angiogenesis (17).

While the M1/M2 paradigm proves useful as a preliminary introduction to these innate immune cells, the full story is not as black and white. The macrophage phenotype exhibits more plasticity than historically assumed, and M1/M2 classification merely represents two extremes of a continuum of activated states. For example, macrophages treated with the pathogen associated molecule, lipopolysaccharide (LPS), exhibit a reduced phagocytic capacity compared to macrophages treated with the endogenous cytokine; IFNγ. While both produce pro-inflammatory mediators, LPS polarized macrophages are now referred to as M1b macrophages, whereas IFNγ polarized macrophages are referred to as M1a macrophages (16, 18).

Distinct M2 macrophage subsets also exist. For example, M2a macrophages are induced by IL-4 and IL-13 and have a pre-dominantly anti-inflammatory phenotype, secreting high levels of IL-10 and IL-1 receptor antagonist as a means of dampening the inflammatory response. M2b macrophages, on the other hand, exhibit both pro- and anti-inflammatory responses, producing IL-1β, TNFα, and IL-6 as well as IL-10 in response to LPS stimulation. M2c macrophages are induced by IL-10 and secrete high levels of transforming growth factor beta 1 (TGFβ1), and glucocorticoids. They assume a regenerative, pro-healing phenotype and play a major role in promoting tissue repair and silencing the inflammatory response. These cells also play a significant role in matrix deposition (15). More recently, M2d and M2f phenotypes have been characterized (19, 20). M2d macrophages are activated by Toll-like receptor agonists and adenosine A2a receptor agonists. In response, these cells secrete high levels of VEGF and IL-10, and in turn downregulate TNFα and IL-12 production (19). M2f cells are induced by efferocytosis which involves the removal of apoptotic cells by macrophages. This process is similar to phagocytosis, however, it involves distinct receptors and signaling pathways and results in the secretion of high levels of TGFβ1, prostaglandin E2 and platelet activating factor, all of which are known to inhibit LPS-induced pro-inflammatory cytokine production (21).

TISSUE RESIDENT MACROPHAGES

Tissue resident macrophages exist at various sites throughout the body and can include microglia in the brain and Kuppfer cells in the liver (22). The heart, being no exception; contains its own resident macrophages which possess a specific role in the regulation of cardiac function (23). The distinction between

tissue residing cardiac macrophages and circulating monocyte-derived macrophages has become a considerable area of focus in recent years (24). While long established tissue resident cells appear to facilitate coronary development and tissue homeostasis, it appears that monocyte-derived infiltrating cells have a predominant role in tissue injury and destruction. This highlights that macrophages, whether circulating or permanently residing, originate from diverse lineages, and as a result have different functions.

CCR2$^+$ AND CCR2$^-$ TISSUE RESIDENT MACROPHAGES

Gene mapping of cardiac resident macrophages reveals two distinct lineages arising at the embryonic stage and post-natal stage (25). Developmental studies of early cell migration in murine models affirms this, with the earliest cardiac resident macrophages derived from an erythromyeloid progenitor in the yolk sac (26). These progenitor macrophages migrate out of the yolk-sac either directly to the developing myocardium or else to the fetal liver, where they progress to hemopoietic stem cells and eventually cardiac tissue-resident macrophages (26). Post-natally, monocyte-derived macrophages can also migrate to the myocardium to become tissue resident macrophages (27). These embryonic and post-natal resident cells can be distinguished from one another based on expression of the chemokine receptor, Chemokine Receptor Type 2 (CCR2) (25). This receptor and its corresponding ligand, chemokine ligand 2 (CCL2), also known as monocyte chemoattractant protein 1 (MCP-1), play an important role in monocyte/macrophage migration. Studies have demonstrated that CCR2$^+$ cardiac resident macrophages are derived from monocytes while CCR2$^-$ macrophages originate from the embryonic developmental stage (25, 28). Furthermore, CCR2$^-$ macrophages undergo local proliferation in order to replenish their population whereas CCR2$^+$ macrophages are repopulated by monocyte-derived macrophages extravasating into the myocardium (25). Both CCR2$^+$ and CCR2$^-$ cell populations orchestrate diverse responses following traumatic events, such as MI. CCR2$^+$ cells facilitate monocyte recruitment into the heart following MI via CCR2-MCP1 mediated trafficking and secrete high levels of pro-inflammatory mediators including IL-1β, TNF, and IL-6 (28). Not surprisingly, depletion of this cell population has resulted in reduced infarct size in a murine model of MI (28).

Conversely, CCR2$^-$ macrophages appear to play an immune-modulatory, pro-regenerative role, expressing high levels of growth factors including Insulin-like growth factor 1 (IGF1) and Platelet derived growth factor C (PDGF-C) (28). Depletion of this CCR2$^-$ population has enhanced monocyte/macrophage infiltration to the heart and further implicates these cells as potential immune-modulators during MI (28, 29). In addition to immune modulatory functions, recent studies have also demonstrated that CCR2$^-$ macrophages express high levels of the sodium channel, SCN4, and sodium channel modulator, FGF13, suggesting that macrophages can modulate the electrical activity of cardiomyocytes (25, 30). Fracktalkine receptor (CX3CR1$^+$) expressing resident macrophages have also been reported to facilitate conductivity, further implicating their role in regular functioning of the heart and broadening the role of macrophages beyond local inflammation and immune-modulation (30). It is not yet clear if both CCR2$^+$ and CCR2$^-$ macrophages contribute to the electrical homeostasis of the heart and, given that both subsets express the CX3CR1 (31), delineation of the direct impact of these individual cell-types on cellular conductivity is a promising avenue of exploration.

THE EXTRACELLULAR MATRIX

The ECM is a complex and dynamic structure of hundreds of numerous proteins which provide a support system for cells. Within the myocardium, it acts as a mechanical scaffold to create cellular and acellular networks. Conceptually, the cardiac ECM can be divided into two segments, the interstitial matrix, comprised of primarily type I and type III collagen, and the basement membrane, comprised of collagen IV, V, VII, X as well as laminins (32). Proteins residing in the interstitial matrix and basement membrane of the ECM serve a specific function, either facilitating structural support of the matrix itself, or regulating local cell behavior and function (33). Type I and Type III collagens for example allow the myocardium to maintain structural integrity through tensile support. Cardiac tissue undergoes mechanical stress via shear and pressure forces of muscle contraction and the organization and continuity of the collagen networks within the ECM allows for appropriate distribution of this physical stress. Elastin in the interstitial matrix provides elasticity to the cardiac tissue, with reduced expression post-MI contributing to stiffer scar tissue (34). Proteoglycans along with glycoproteins play a key role in signaling and turnover of the ECM (35), highlighting the alternative function of ECM as a transducer of signals within the cardiac environment.

The ECM is not an inert structure, with matrix continuously responding to signals from the surrounding environment and exerting its own signaling through mechanical and chemical cues. In the context of MI and chronic inflammation, disruption to the ECM via adverse remodeling leads to disarray of physical stress, applying strain on the myocardium and leading to dysfunction. Key initiators of remodeling can include ischemia, pressure overload, and aging of the heart, all of which have significant association with systemic inflammation (36–38) Thus, it is established that remodeling of the ECM as a consequence of sustained inflammation, is a critical etiological factor of heart failure, making the study of ECM and the innate immune activity in the failing myocardium one of great importance (39, 40).

ROLE OF INFLAMMATION IN HEART FAILURE -MI AND ISCHEMIA

MI refers to mass cardiomyocyte death as a result of ischemia, which is often worsened by a subsequent reperfusion of oxygen supply, and the ensuing inflammatory response (41). This association between inflammation and adverse cardiac events

is well-acknowledged. Multiple studies have demonstrated that elevated pro-inflammatory cytokine production in the heart correlates with worsening outcome. Furthermore, inhibition of pro-inflammatory cytokines, such as TNFα, which is heavily implicated in cardiac disease, results in improved cardiac function in rat models of heart failure (8, 9). Two classifications of infarction are often presented, both which occur as a result of ischemia. Acute MI is caused by an atherosclerotic plaque rupture causing coronary artery occlusion and cardiac tissue damage due to ischemia. Chronic MI refers to continued loss of cardiomyocytes from gradual and prolonged ischemia, often >8 weeks. The vast amount of cell death following MI poses a detriment, as the heart itself possesses a limited regenerative capacity (42). Left untreated, cardiac tissue undergoes extensive remodeling to compensate for cell loss and to maintain structural integrity. The inflammatory response facilitates the removal of necrotic cells in addition to tissue remodeling (43). However, extensive remodeling imposes stress on the heart, instigating maladaptive mechanisms, such as chronic inflammation and cellular apoptosis. As the heart continues to employ methods of remodeling and repair to resolve this, a destructive cycle prevails, ultimately leading to deterioration of cardiac function and heart failure (44). These events are summarized in **Figure 1**.

Infiltration of monocyte-derived macrophages to the infarct is a key feature of MI, and can be characterized by stages of macrophage infiltration, and their subsequent actions within the myocardium. Immediately following infarction, resident cardiac macrophages begin to die in response to ischemia, with a complete loss of resident macrophages within the infarct observed in murine models 24 h post-infarction (45). The resident macrophage population lost in the ischemic region is rapidly replaced by infiltrating monocyte-derived macrophages within 24 h (45). Day 1–3 post-MI, infiltrating macrophages exhibit a pro-inflammatory M1-like phenotype, driving acute inflammation and facilitating clearance of dead cells. At approximately day 5–7 post-MI, these macrophages begin to adopt a reparative M2-like phenotype, working to resolve inflammation and rebuild cardiac tissue (46). Mouse models of MI have revealed distinct subsets of infiltrating monocyte-derived macrophages, with earlier recruitment of pro-inflammatory $Ly6C^{high}$ macrophages dependent on CCR2/CCL2 signaling, and the later pro-regenerative $Ly6C^{low}$ macrophages recruited via CX3CR1 signaling (47). One can, therefore, hypothesize that inflammation and resolution is achieved in the myocardium through differential recruitment of macrophages.

It has also recently been demonstrated that infiltrating macrophages in murine mouse models of MI undergo metabolic reprogramming to increase oxidative phosphorylation at approximately day 5 post-MI (48). Increased oxidative phosphorylation in addition to fatty acid synthesis and oxidation is a signature of the M2 phenotype (49) and implies that there is a phenotypic switch from the early pro-inflammatory state to a more pro-regenerative one. Thus, not only is there the possibility of recruitment of separate subsets of macrophages via CCR2 and CXC3R dependent signaling, but in addition, there is a switch from the M1 to the M2f phenotype subset based on fatty acid synthesis and oxidation. This switch is key in the appropriate resolution of inflammation and progression to a pro-healing state and is promoted through efferocytosis of cell debris at the site of injury (50). Engulfment of dead cells by macrophages has been observed to elevate fatty acid synthesis and triggers production of the anti-inflammatory, pro-reparative cytokine TGFβ1 (20, 51). However, in circumstances of chronic ischemia or severe infarction, continuous cardiomyocyte death leads to sustained activation of M1 macrophages, which have a diminished efferocytotic ability (52). This is heightened in patients suffering from diabetes and obesity whereby underlying chronic inflammation exacerbates the pro-inflammatory response to infarction. In this instance, elevated levels of the pro-inflammatory cytokines, TNFα and IL-6, as well as C Reactive Protein (CRP), are associated with worse patient outcome (53, 54).

Failure to clear dying cells also leads to the release of damage-associated molecular patterns (DAMPs) which contribute to a robust secretion of pro-inflammatory cytokines, prolonging activation of the inflammatory response and escalating damage in the myocardium. A timely switch from low efferocytotic M1 macrophages to highly efferocytotic anti-inflammatory M2 macrophages is therefore necessary to clear dead cells and promote tissue repair.

ALTERATIONS TO THE EXTRACELLULAR MATRIX

In any circumstances of injury within the body, ECM degradation is necessary to allow for repair and/or replacement of the damaged tissue. In the instance of MI, ECM degradation is triggered as early as 10 min following an ischemic event (55). MMPs, predominantly produced by macrophages and fibroblasts, are secreted as part of a programmed inflammatory response in order to deconstruct matrix architecture. As MI progresses, subsequent necrosis of cardiomyocytes accentuates matrix degradation. MMPs target various components of the ECM, for example, the collagenases MMP1, MMP8, and MMP13 cleave the α-chains of type I and type II collagens while MMP3 and MMP10 target proteoglycans, fibronectin, and laminins (33). Gelatinases, such as MMP2 along with MMP9 digest gelatin in addition to degrading type IV collagen, the most abundant component of the basement membrane (56).

As ECM breakdown persists, a provisional matrix enriched in fibrins forms in its place (57). This plasma-derived matrix does not serve a particularly structural role in the same manner as native ECM, but rather modulates cell phenotype and behavior, setting the stage for tissue repair. Components of this provisional plasma-derived matrix interact with migrating cells, such as macrophages via cell surface integrins. It has been hypothesized that the provisional matrix is capable of modulating gene expression and immune cell phenotype through these integrin-mediated interactions and, thus, progress the repair of cardiac tissue (58). Furthermore, the provisional matrix acts as a reservoir for numerous growth factors including PDGF, VEGF and members of the TGF family (59). These growth factors are secreted by pro-regenerative cells, such as M2 macrophages and

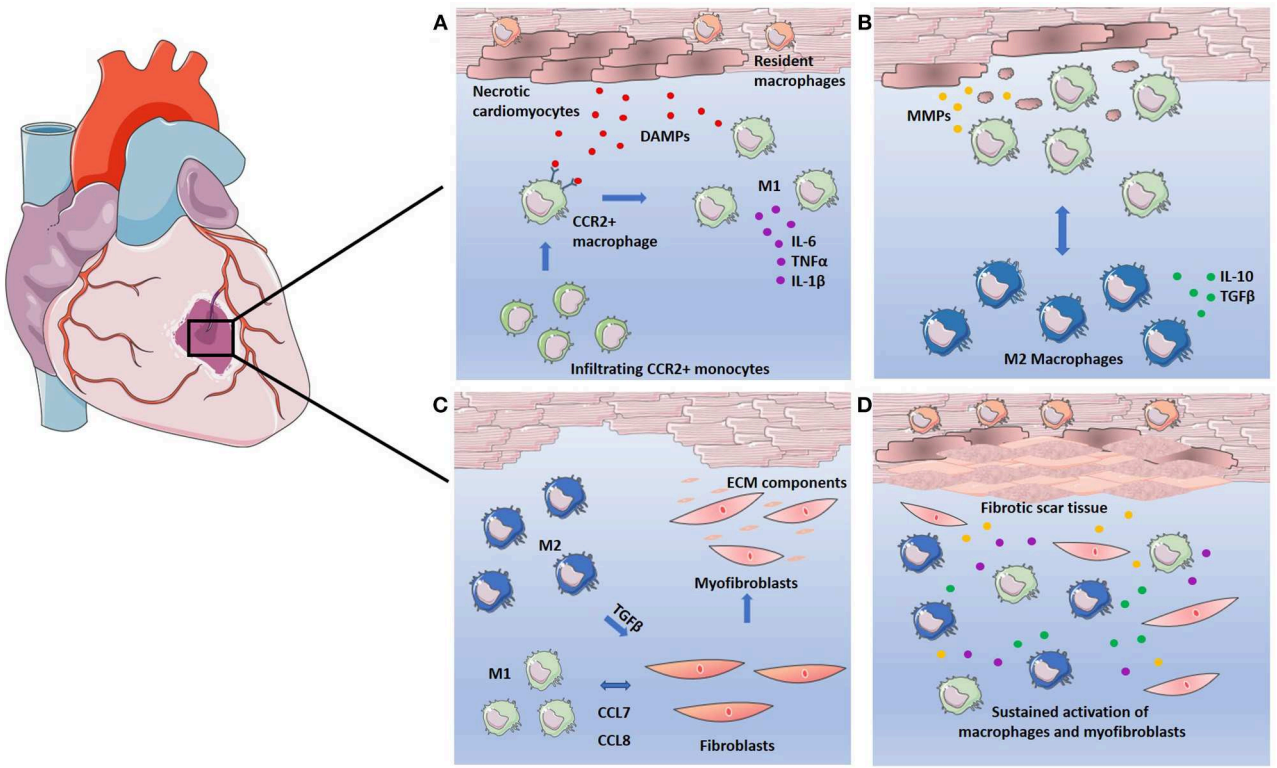

FIGURE 1 | Macrophages in the response to infarction. **(A)** Cardiomyocytes undergo necrosis, releasing DAMPs and attracting CCR2$^+$ circulating monocytes. CCR2$^+$ monocytes differentiate into pro-inflammatory M1 macrophages replacing resident macrophages and secreting high levels of pro-inflammatory cytokines IL-6, TNFα, and IL-1β. **(B)** M1 macrophages clear necrotic cell debris through phagocytosis and induce breakdown of the ECM through secretion of MMPs. Phagocytosis of the necrotic debris causes macrophage polarization to the M2 phenotype. M2 macrophages secrete high levels of anti-inflammatory cytokine IL-10 and growth factor TGFβ. **(C)** Both M1 and M2 macrophages facilitate the fibrotic response. M1 macrophages recruit fibroblasts via CCL7 and CCL8 mediated signaling. M2 macrophages induce fibroblast differentiation into myofibroblasts, which in turn secrete ECM components to facilitate tissue repair. **(D)** Sustained activation of macrophages leads to continuous secretion of growth factors, pro-inflammatory cytokines, and MMPs. Continued breakdown of ECM as well as overproduction of ECM components by myofibroblasts leads to adverse remodeling of ECM and results in fibrotic scar tissue.

subsequently deposited within the provisional matrix, bound via the heparin binding domain (59). Sequestering of growth factors in this fashion regulates their function and may influence the activation of fibroblasts and vascular cells. However, the full extent of these processes remains to be understood.

Healing of the infarct area greatly relies on clearance of this provisional matrix which has been clearly demonstrated in mouse models. In mice lacking the plasminogen/plasmin system responsible for this clearance, a lack of leukocyte infiltration into the infarct region is observed, and thus repair of the myocardium impeded (60). Fragments of the provisional matrix are endocytosed by CCR2$^+$ macrophages and postulated to induce a switch to an anti-inflammatory, reparative state within the infarct area (61). *In vitro*, interactions with a fibrin matrix lead bone marrow derived macrophages to adopt an M2 like anti-inflammatory state (62), therefore it has been suggested that the fibrin enriched matrix and its removal promote an anti-inflammatory phenotype in local macrophages. Removal of the provisional matrix is followed by secretion of cellular fibronectin to form a cell-derived matrix (33). This matrix is enriched with macromolecules, such as thrombospondins, which facilitate the recruitment and activation of fibroblasts and macrophages to a pro-regenerative phenotype in order to promote healing.

The dynamics of the ECM, from native, to plasma derived, and then a cell-derived remodeled matrix, is a highly ordered process to allow for efficient transition from the inflammatory response to wound healing. Any anomalies in this process can lead to sustained inflammation and fibrosis, i.e., the accumulation of interstitial matrix components, predominantly collagen type I. Newly synthesized ECM differs from that of the original native ECM, with turnover of cross-linked collagen being significantly faster than that of normal collagen (63). This leads much stiffer collagen fibers, and ultimately, a stiff scar tissue post-MI. High expression of lysyl oxidase (indicative of cross-linking) has been observed in murine models of infarction, and correlates with a stiffer myocardium (64). In rat models of infarction, a 5-fold increase of lysyl oxidase is observed at day 3, and remains elevated at day 7 post-infarction (65). While the formation of scar tissue post-MI is important for maintaining structural integrity while the myocardium is under reconstruction, extensive scarring or remodeling limits the functional capacity of the heart by impeding ventricular

contraction and relaxation (66). Furthermore, the detrimental effects of ECM remodeling extend beyond the infarct site as formation of scar peripheral to the site of infarction is also observed. This further limits myocardial function and heightens the progression of heart failure. To greater understand how these adverse effects arise, we look to the key mediators of ECM turnover.

MACROPHAGES AS MEDIATORS OF ECM REMODELING

The cascade of events which lead to tissue remodeling post-infarction may be attributed to chronic inflammation and sustained activity of pro-inflammatory macrophages within the infarcted myocardium. In the early stages of infarction (Day 0–3), the mass influx of pro-inflammatory macrophages promotes clearance of matrix and debris through phagocytosis of dying cells and secretion of matrix proteases. The secretion of pro-inflammatory cytokines including TNFα and IL-6 by macrophages activates resident fibroblasts, which further increases the production of MMPS, such as MMP2 and MMP9 (67). These "immune-activated" fibroblasts also secrete pro-inflammatory cytokines including IL-1β and IL-6 in response to the macrophage secretome (68), which serves as a positive feedback and augments the pro-inflammatory response. While MMP production is required for natural matrix turnover, sustained activation of pro-inflammatory macrophages, and therefore continuous production of MMPs, results in extensive matrix remodeling and impaired wound healing. High levels of MMP9 have been reported in patients, serving as a biomarker for adverse left ventricle remodeling and heart failure (69). Mice overexpressing MMP14 also show lower survival and ejection fraction following MI (70). TIMPs can also contribute to adverse remodeling if produced in abundance as this can lead to unrestricted matrix deposition, thus highlighting the need for a controlled balance between MMPs and their inhibitors (71).

While the influx of pro-inflammatory macrophages enhances matrix breakdown post-MI, it is the transition from acute inflammation to fibrosis, facilitated by the switch from M1 to M2 dominant macrophage subsets that further exacerbates ECM remodeling. M2 macrophages secrete high levels of TGFβ1, which drives transcription of alpha smooth muscle actin (α-SMA) in the resident fibroblasts (72). As a result, these fibroblasts undergo a dramatic phenotypic transformation to become myofibroblasts (73, 74). Myofibroblasts have superior mobility compared to the homeostatic fibroblast and possess a higher capacity to produce matrix components (75). Macrophages not only amplify activation of these cells, but also facilitate their recruitment to the site of injury via signaling mediated by chemokines, such as CCL7 and CCL8 (76). As a result, overproduction of ECM components is observed, with an increased deposition of collagen, which stabilizes and crosslinks to form scar tissue. M2 macrophages can further promote fibrogenesis through the production of arginase, which activates glutamate and proline, both of which are necessary for collagen synthesis (77).

Clearly, both pro- and anti-inflammatory macrophages play a distinct pathological role in ECM remodeling, yet both subsets also have necessary roles in natural healing and repair. Therefore, it is difficult to pinpoint precisely which subset is a therapeutic target without further delineation of their functions in the infarcted myocardium. Certain pro-inflammatory cytokines, such as IL-6, elicit cardio-protective effects in the short term, and only pose a danger when their presence is sustained long-term (78–80). Furthermore, without $CCR2^{+}$ pro-inflammatory macrophages, the clearance of fibrin-derived provisional matrix is impaired, thus limiting progression to the more permanent cell derived matrix (61). Moreover, a prolonged presence of fibrin fragments can prompt a pro-inflammatory response (58) and contribute to a state of chronic inflammation. Conversely, eliminating M2 macrophages can lead to a worsened outcome, as they are a potent source of IL-10. This anti-inflammatory cytokine exerts protection against cardiac fibrosis, with knockout murine models demonstrating that a lack of IL-10 leads to adverse tissue remodeling and more severe cardiac fibrosis when compared to wildtype counterparts (81). A more pragmatic approach, therefore, may be to harness the effects of the macrophages through immunomodulation rather than selective elimination.

IMMUNOMODULATION: TARGETED THERAPY OF HEART FAILURE

While clinical studies in MI patients are limited, strategies aimed at targeting dysregulated immune responses have been explored as treatment options for heart failure post-MI. Early trials involved the use of general immunosuppressants based on the hypothesis that non-specific inflammation following MI is unfavorable (82). Such trials included a broad range of candidates that are considered the gold standard of immunosuppression, such as corticosteroids, methotrexate and cyclosporin A to name but a few. However, their use in the context of cardiac treatment has yielded conflicting results. A review of clinical trials dating 1964 to 1989 reported that while corticosteroids appear to reduce mortality rates compared to placebo treatments, overall they do not provide a significant cardio-protective effect (82). Methotrexate, a well-established immunosuppressive routinely used for the treatment of rheumatoid arthritis, has also produced conflicting results with one trial reporting a reduction in TNFα and IL-6 together with an increase in IL-10 (83), while others reported no beneficial effects, instead worsening of left ventricle ejection fraction following treatment (84, 85). Cyclosporin A has also been considered for post-MI treatment given its ability to inhibit the mitochondrial permeability transition pore and therefore prevent necrotic cell death (86). However, no improvement of infarct size or mortality was observed in patients in a 3 day follow up (87).

While the lack of success for these drug trials may be attributed to short follow up periods and small sample numbers, it may also be that non-specific suppression of inflammation is insufficient to alleviate the adverse effects associated with infarction and more targeted approaches are required. IL-1β, for example, has

proved to be a promising candidate to target due to elevated levels of the cytokine associated with poor prognosis in MI patients. Numerous pre-clinical studies have reported that inhibition of this cytokine results in reduced inflammation and remodeling in mice post-infarction (88, 89). Anakinra, an established antagonist for the IL-1β receptor; has been assessed in multiple pilot studies for efficacy in reducing left ventricular remodeling in patients (90–92). Antagonizing IL-1β in the above studies appears to blunt the acute inflammatory response exhibited post-infarction with an increase in pro-inflammatory marker CRP, observed following discontinuation of treatment. While the results of the 2010 study demonstrated an overall improvement in left ventricular remodeling, the small sample size proved limiting in their results. A larger study conducted in 2015 failed to show any improvement in remodeling compared to placebo treatment (91). Targeting IL-1β also reduces the risk of new MI events in patients with previous history of infarction. The CANTOS trial involving 10,061 patients, reported a 15% reduction in major adverse cardiovascular events upon treatment with the IL-1β targeting drug, canakinumab. However, no significant reduction in risk of cardiovascular death or overall mortality was observed (93).

Clinical trials targeting TNFα have also been conducted. In patients with acute MI, treatment with etanercept, a high affinity TNF receptor antagonist, resulted in reduced levels of IL-6 and lower neutrophil counts, however, no improvements in ventricular dilation or cardiac function were observed (94). Furthermore, in patients with chronic heart failure, trials involving anti-TNFα treatment were terminated prematurely due to lack of benefit (95). Despite encouraging preclinical results from *in vivo* models, targeting single cytokines alone may not be enough to counteract the complex pathophysiology associated with heart failure, and instead, targeting the source of inflammation may represent a more viable approach.

Targeting Macrophages

Targeting macrophage infiltration to combat inflammation is not an entirely new concept, however many studies have failed to show a clear efficacy *in vivo*. Previous work using small molecule inhibitors to target the migration of $CCR2^{+}$ macrophages, while showing a promising *in vitro* result, have failed to overcome challenges *in vivo* due to lack of tissue selectivity for the CCR2 receptor as well as poor potency in administered treatments (96). Advances in short interfering RNA (siRNA) technology, including improved specificity of targeting sequences, as well as new methods of delivery, have opened the door to novel therapies to treat inflammation and heart failure. For example, siRNA targeting of the cell adhesion molecules ICAM 1/2, VCAM, and E and P selectins have been shown to reduce inflammation and infarct size in a murine model of MI; ultimately preserving left ventricle ejection fraction and improving recovery after infarction (97). While this study emphasizes that a multi-targeted strategy may be necessary, targeting the CCR2 receptor alone has also yielded promising results with two separate studies demonstrating that siRNA-mediated targeting of the CCR2 receptor significantly reduces infarct size in mouse models (98, 99). Specifically, siRNA targeting the CCR2 receptor 1-h post-infarction (induced by coronary ligation) resulted in a 34% reduction in infarct size/area-at-risk at 24 h post-siRNA delivery (98). A similar study resulted in a reduction in expression of pro-inflammatory cytokines, IL-6, IL-1β, and TNFα at day 4 post-infarction, while levels of IL-10 appeared to increase (99). At 3 weeks post-infarction; a significant reduction of ventricular remodeling was observed compared to untreated mice (99). These results not only strongly implicate macrophages in the etiology of heart failure, but also demonstrate the ability to diminish their effects through single molecule targeting, which if tissue specific, may represent a viable option for future therapy. Targeting the CCR2 receptor proves particularly advantageous compared to pre-existing immunosuppressive treatments as the strategy does not affect the resident homeostatic macrophages present within the myocardium, nor does it hinder clearance of necrotic matter in the infarct. To improve siRNA delivery, nanoparticles and scaffolds are being extensively explored. Scaffolds can also be placed directly at the intended location of therapy. In particular scaffolds can also enable a controlled rate of delivery through interactions with the siRNA and designated target, as well as timed degradation of the scaffold itself (100, 101). This proves optimal for MI treatment whereby timing of inflammatory resolution is critical. Premature intervention of the inflammatory response may hinder wound repair, whereas a delayed response could fail to prevent adverse cardiac remodeling and heart failure (102).

Targeting the ECM

Given that the ECM plays a pivotal role in driving macrophages activation, consideration for novel therapies should also be given to the interactions between cellular matrix and macrophage. For example, the role of the metalloproteinases is not limited to breakdown of ECM components; such enzymes also have a role in regulation of the inflammatory response through proteolytic cleavage of cytokines, chemokines, and growth factors (103). Protease mediated fragmentation of matrix proteins results in the generation of ECM-derived macromolecules known as matrikines which possess a distinct role in regulation of cell activity (104). Elastin fragments and collagen peptides are the most well-studied in this context and both have been implicated in numerous reports as activators of immune cells and fibroblasts during pro-inflammatory responses (105). Proline-glycine-proline, a tripeptide derived from collagen has been observed to act as a chemoattractant for neutrophil infiltration in models of pulmonary inflammation, in addition to promoting overall wound healing in mouse models. This peptide signals via the CCR2 chemokine receptor, which as mentioned previously, plays a prominent role in macrophage infiltration (106, 107). The dysregulated accumulation of these matrikines via continuous breakdown and remodeling of the ECM therefore may prove a detriment to the myocardium. Taking this into consideration, it is possible that the release of ECM fragments as well as their producers, the MMPs; hold promise as novel targets for the regulation of macrophage infiltration and subsequent inflammatory responses. Preliminary work to date has examined elastin and fibrillin-1 fragments which contain repeated Glycine proline motifs (GxxPG). In mice, neutralization of these GxxPG

fragments via antibody administration reduces macrophage infiltration into the aorta as well as production of MMP2 and MMP9 (108). However, there have been little if any translational studies concerning the targeting of ECM fragments for cardiovascular treatment. This may be due to a substantial lack of knowledge surrounding the interactions between matrix fragments and the adverse inflammatory response within the myocardium.

Over recent years a plethora of matrikines have been recognized for their behavior-modulating abilities (summarized in **Table 1**), yet their precise mechanisms of action in sustaining inflammation remain to be elucidated. A focus therefore on interactions with ECM and the immune response, specifically with macrophages within the myocardium is required in future research. Breakdown of matrix will always be a natural requirement of wound healing and repair, yet perhaps it is the presence of matrikines or their dysregulation which contributes to adverse remodeling post-infarction. Their presence may have to be considered in future targeted therapy by means of combined therapy, where both effectors and actuators of

TABLE 1 | ECM derived matrikines and their respective modulatory functions.

Identified cryptid	Function	Source	References
GETGPAGPAGPIGPVGARGPA, GPQGPRGDKGETGEQ	Facilitate wound healing via enhanced cell adhesion and antioxidative activities	Bovine collagen α-1(I) chain	(109)
RQVFQVAYIIIKA	Facilitate wound healing via enhanced cell migration	α-1 chain laminin	(110)
YGDEY	Antioxidant activity	Tilapia skin gelatin hydrolysates	(111)
KNVLVTLYERDEGNNLLTEK	Induces MMP9 production in monocytes	SPARC glycoprotein	(112)
VGVAPG	Induces MMP2 production in fibroblasts	Elastin	(113)
RGD	Cell adhesion via integrin binding	Fibronectin	(114)
DGGRYY	Activates polymorphonuclear neutrophils	A-1 chain type 1 collagen	(115)
GHK	Chemoattractant for macrophages and mast cells	A-2 chain type 1 collagen	(116)

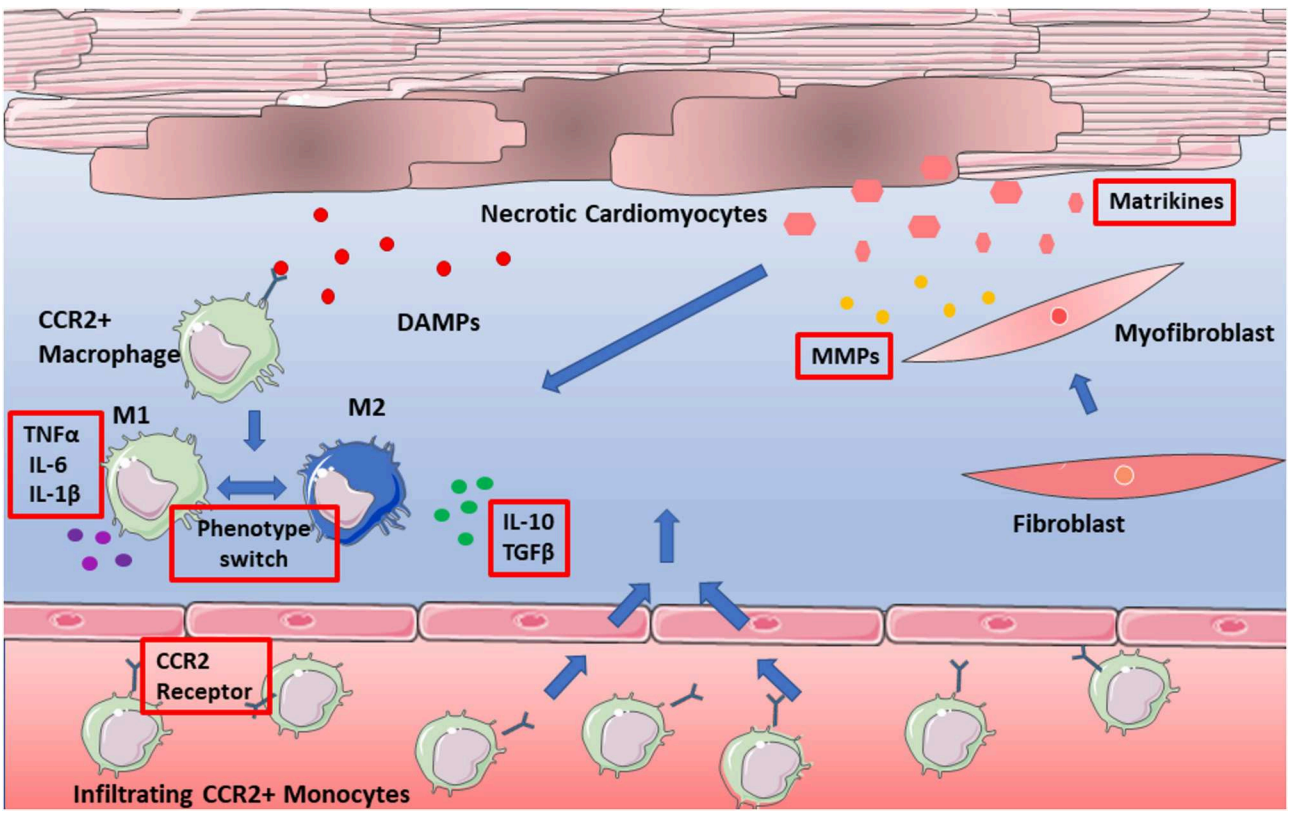

FIGURE 2 | Potential therapeutic targets of adverse remodeling. Targets depicted in red boxes and include pro-inflammatory cytokines, as well as the CCR2 receptor. Also, to be considered are matrikines, which have yet to be assessed in targeted therapy of adverse remodeling.

remodeling are targeted. This is an important consideration going forward, in both therapeutic design, and research models of heart failure. **Figure 2** depicts the numerous possible therapeutic targets of infarction and subsequent heart failure.

CONCLUDING REMARKS AND FUTURE PROSPECTS

Undoubtedly, inflammation driven by macrophages plays a key role in heart failure. Numerous studies have been discussed in this review which pinpoint macrophages as critical mediators of inflammation and adverse remodeling of ECM. Yet there still remains substantial gaps in our knowledge of the precise role of macrophages, particularly resident macrophages within the myocardium. It remains to be established which specific subsets of macrophages are precisely responsible for the adverse effects of the inflammatory response, and which are necessary for normal homestatic function. Knockout models which eliminate specific subsets may bring to light the exact function of resident macrophages, and aid future research in harnessing their protective nature. As discussed throughout this review, although macrophages are not an active producer of ECM, they are intimately linked throughout the myocardial milleau in orchestrating remodeling and deposition; a role that becomes highly prominent following myocardial infarction. Greater efforts must be made to elucidate the role of the ECM in sustaining activation of macrophages via matrikines. Further studies of matrix-macrophage communication may reveal not only the precise mechanisms by which infiltrating macrophages drive remodeling, but also possible novel targets for future therapies.

AUTHOR CONTRIBUTIONS

MM, SO'R, and AD contributed to the conception and writing of the article. MM and SO'R wrote the first draft of the manuscript. All authors contributed to manuscript revision, read, and approved the submitted version.

FUNDING

SO'R is supported by a Trinity College Dublin Faculty of Engineering Maths and Sciences Intrafaculty Ph.D. Award.

REFERENCES

1. Benjamin EJ, Blaha MJ, Chiuve SE, Cushman M, Das SR, Deo R, et al. Heart disease and stroke statistics-2017 update: a report from the american heart association. *Circulation*. (2017) 135:e146–603. doi: 10.1161/CIR.0000000000000491
2. Savarese G, Lund LH. Global public health burden of heart failure. *Card Fail Rev*. (2017) 3:7–11. doi: 10.15420/cfr.2016:25:2
3. Perbellini F, Watson SA, Bardi I, Terracciano CM. Heterocellularity and cellular cross-talk in the cardiovascular system. *Front Cardiovasc Med*. (2018) 5:143. doi: 10.3389/fcvm.2018.00143
4. Wang BX, Kit-Anan W, Terracciano CMN. Many cells make life work-multicellularity in stem cell-based cardiac disease modelling. *Int J Mol Sci*. (2018) 19:3361. doi: 10.3390/ijms19113361
5. Fountoulaki K, Dagres N, Iliodromitis EK. Cellular communications in the heart. *Card Fail Rev*. (2015) 1:64–8. doi: 10.15420/cfr.2015.1.2.64
6. Howard CM, Baudino TA. Dynamic cell-cell and cell-ECM interactions in the heart. *J Mol Cell Cardiol*. (2014) 70:19–26. doi: 10.1016/j.yjmcc.2013.10.006
7. Olsson AK, Dimberg A, Kreuger J, Claesson-Welsh L. VEGF receptor signalling–in control of vascular function. *Nat Rev Mol Cell Biol*. (2006) 7:359–71. doi: 10.1038/nrm1911
8. Bryant D, Becker L, Richardson J, Shelton J, Franco F, Peshock R, et al. Cardiac failure in transgenic mice with myocardial expression of tumor necrosis factor-alpha. *Circulation*. (1998) 97:1375–81. doi: 10.1161/01.CIR.97.14.1375
9. Jiang YR, Du JY, Wang DD, Yang X. miRNA-130a improves cardiac function by down-regulating TNF-alpha expression in a rat model of heart failure. *Eur Rev Med Pharmacol Sci*. (2018) 22:8454–61.
10. vey MJ, Tallquist MD. Defining the cardiac fibroblast. *Circ J*. (2016) 80:2269–76. doi: 10.1253/circj.CJ-16-1003
11. Kanekar S, Hirozanne T, Terracio L, Borg TK. Cardiac fibroblasts form and function. *Cardiovasc Pathol*. (1998) 7:127–33. doi: 10.1016/S1054-8807(97)00119-1
12. Daskalopoulos EP, Hermans KC, Blankesteijn WM. Cardiac (myo)fibroblast: novel strategies for its targeting following myocardial infarction. *Curr Pharm Des*. (2014) 20:1987–2002. doi: 10.2174/13816128113199990452
13. Fan D, Takawale A, Lee J, Kassiri Z. Cardiac fibroblasts, fibrosis and extracellular matrix remodeling in heart disease. *Fibrogenesis Tissue Repair*. (2012) 5:15. doi: 10.1186/1755-1536-5-15
14. Murray PJ, Wynn TA. Protective and pathogenic functions of macrophage subsets. Nat Rev Immunol. (2011) 11:723–37. doi: 10.1038/nri3073
15. Murray PJ, Allen JE, Biswas SK, Fisher EA, Gilroy DW, Goerdt S, et al. Macrophage activation and polarization: nomenclature and experimental guidelines. *Immunity*. (2014) 41:14–20. doi: 10.1016/j.immuni.2014.06.008
16. Martinez FO, Sica A, Mantovani A, Locati M. Macrophage activation and polarization. *Front Biosci*. (2008) 13:453–61. doi: 10.2741/2692
17. Yang J, Zhang L, Yu C, Yang X-F, Wang H. Monocyte and macrophage differentiation: circulation inflammatory monocyte as biomarker for inflammatory diseases. *Biomarker Res*. (2014) 2:1. doi: 10.1186/2050-7771-2-1
18. Mukhopadhyay S, Peiser L, Gordon S. Activation of murine macrophages by Neisseria meningitidis and IFN-gamma *in vitro*: distinct roles of class A scavenger and Toll-like pattern recognition receptors in selective modulation of surface phenotype. *J Leukoc Biol*. (2004) 76:577–84. doi: 10.1189/jlb.0104014
19. Ferrante CJ, Pinhal-Enfield G, Elson G, Cronstein BN, Hasko G, Outram S, et al. The adenosine-dependent angiogenic switch of macrophages to an M2-like phenotype is independent of interleukin-4 receptor alpha (IL-4Ralpha) signaling. *Inflammation*. (2013) 36:921–31. doi: 10.1007/s10753-013-9621-3
20. Fadok VA, Bratton DL, Konowal A, Freed PW, Westcott JY, Henson PM. Macrophages that have ingested apoptotic cells *in vitro* inhibit proinflammatory cytokine production through autocrine/paracrine mechanisms involving TGF-beta, PGE2, and PAF. *J Clin Invest*. (1998) 101:890–8. doi: 10.1172/JCI1112
21. Martin CJ, Peters KN, Behar SM. Macrophages clean up: efferocytosis and microbial control. *Curr Opin Microbiol*. (2014) 17:17–23. doi: 10.1016/j.mib.2013.10.007
22. Davies LC, Jenkins SJ, Allen JE, Taylor PR. Tissue-resident macrophages. *Nat Immunol*. (2013) 14:986–95. doi: 10.1038/ni.2705
23. Chen B, Brickshawana A, Frangogiannis NG. The functional heterogeneity of resident cardiac macrophages in myocardial injury CCR2(+) cells promote inflammation, whereas CCR2(-) cells protect. *Circ Res*. (2019) 124:183–5. doi: 10.1161/CIRCRESAHA.118.314357

24. Honold L, Nahrendorf M. Resident and monocyte-derived macrophages in cardiovascular disease. *Circ Res*. (2018) 122:113–27. doi: 10.1161/CIRCRESAHA.117.311071
25. Bajpai G, Schneider C, Wong N, Bredemeyer A, Hulsmans M, Nahrendorf M, et al. The human heart contains distinct macrophage subsets with divergent origins and functions. *Nat Med*. (2018) 24:1234–45. doi: 10.1038/s41591-018-0059-x
26. Epelman S, Lavine Kory J, Randolph Gwendalyn J. Origin and functions of tissue macrophages. *Immunity*. (2014) 41:21–35. doi: 10.1016/j.immuni.2014.06.013
27. Leid J, Carrelha J, Boukarabila H, Epelman S, Jacobsen SE, Lavine KJ. Primitive embryonic macrophages are required for coronary development and maturation. *Circ Res*. (2016) 118:1498–511. doi: 10.1161/CIRCRESAHA.115.308270
28. Bajpai G, Bredemeyer A, Li W, Zaitsev K, Koenig AL, Lokshina I, et al. Tissue resident CCR2- and CCR2+ cardiac macrophages differentially orchestrate monocyte recruitment and fate specification following myocardial injury. *Circ Res*. (2019) 124:263–78. doi: 10.1161/CIRCRESAHA.118.314028
29. Dick SA, Macklin JA, Nejat S, Momen A, Clemente-Casares X, Althagafi MG, et al. Self-renewing resident cardiac macrophages limit adverse remodeling following myocardial infarction. *Nat Immunol*. (2019) 20:29–39. doi: 10.1038/s41590-018-0272-2
30. Hulsmans M, Clauss S, Xiao L, Aguirre AD, King KR, Hanley A, et al. Macrophages facilitate electrical conduction in the heart. *Cell*. (2017) 169:510–22.e20. doi: 10.1016/j.cell.2017.03.050
31. Panek CA, Ramos MV, Mejias MP, Abrey-Recalde MJ, Fernandez-Brando RJ, Gori MS, et al. Differential expression of the fractalkine chemokine receptor (CX3CR1) in human monocytes during differentiation. *Cell Mol Immunol*. (2015) 12:669–80. doi: 10.1038/cmi.2014.116
32. Nielsen SH, Mouton AJ, DeLeon-Pennell KY, Genovese F, Karsdal M, Lindsey ML. Understanding cardiac extracellular matrix remodeling to develop biomarkers of myocardial infarction outcomes. *Matrix Biol*. (2019) 75–6:43–57. doi: 10.1016/j.matbio.2017.12.001
33. Frangogiannis NG. The extracellular matrix in myocardial injury, repair, and remodeling. *J Clin Invest*. (2017) 127:1600–12. doi: 10.1172/JCI87491
34. Mizuno T, Mickle DA, Kiani CG, Li RK. Overexpression of elastin fragments in infarcted myocardium attenuates scar expansion and heart dysfunction. *Am J Physiol Heart Circ Physiol*. (2005) 288:H2819–27. doi: 10.1152/ajpheart.00862.2004
35. Lockhart M, Wirrig E, Phelps A, Wessels A. Extracellular matrix and heart development. *Birth Defects Res A Clin Mol Teratol*. (2011) 91:535–50. doi: 10.1002/bdra.20810
36. Chen WY, Hong J, Gannon J, Kakkar R, Lee RT. Myocardial pressure overload induces systemic inflammation through endothelial cell IL-33. *Proc Natl Acad Sci USA*. (2015) 112:7249–54. doi: 10.1073/pnas.1424236112
37. Entman ML, Michael L, Rossen RD, Dreyer WJ, Anderson DC, Taylor AA, et al. Inflammation in the course of early myocardial ischemia. *FASEB J*. (1991) 5:2529–37. doi: 10.1096/fasebj.5.11.1868978
38. Ferrucci L, Fabbri E. Inflammageing: chronic inflammation in ageing, cardiovascular disease, and frailty. *Nat Rev Cardiol*. (2018) 15:505–22. doi: 10.1038/s41569-018-0064-2
39. Pagano F, Angelini F, Castaldo C, Picchio V, Messina E, Sciarretta S, et al. Normal versus pathological cardiac fibroblast-derived extracellular matrix differentially modulates cardiosphere-derived cell paracrine properties and commitment. *Stem Cells Int*. (2017) 2017:7396462. doi: 10.1155/2017/7396462
40. van Nieuwenhoven FA, Munts C, Op't Veld RC, Gonzalez A, Diez J, Heymans S, et al. Cartilage intermediate layer protein 1 (CILP1): a novel mediator of cardiac extracellular matrix remodelling. *Sci Rep*. (2017) 7:16042. doi: 10.1038/s41598-017-16201-y
41. Anversa P, Sonnenblick EH. Ischemic cardiomyopathy: pathophysiologic mechanisms. *Prog Cardiovasc Dis*. (1990) 33:49–70. doi: 10.1016/0033-0620(90)90039-5
42. Isomi M, Sadahiro T, Ieda M. Progress and challenge of cardiac regeneration to treat heart failure. *J Cardiol*. (2019) 73:97–101. doi: 10.1016/j.jjcc.2018.10.002
43. Frangogiannis NG. Inflammation in cardiac injury, repair and regeneration. *Curr Opin Cardiol*. (2015) 30:240–5. doi: 10.1097/HCO.0000000000000158
44. Cohn JN, Ferrari R, Sharpe N. Cardiac remodeling–concepts and clinical implications: a consensus paper from an international forum on cardiac remodeling. behalf of an international forum on cardiac remodeling. *J Am Coll Cardiol*. (2000) 35:569–82. doi: 10.1016/S0735-1097(99)00630-0
45. Heidt T, Courties G, Dutta P, Sager HB, Sebas M, Iwamoto Y, et al. Differential contribution of monocytes to heart macrophages in steady-state and after myocardial infarction. *Circ Res*. (2014) 115:284–95. doi: 10.1161/CIRCRESAHA.115.303567
46. Ma Y, Mouton AJ, Lindsey ML. Cardiac macrophage biology in the steady-state heart, the aging heart, and following myocardial infarction. *Transl Res*. (2018) 191:15–28. doi: 10.1016/j.trsl.2017.10.001
47. Nahrendorf M, Swirski FK, Aikawa E, Stangenberg L, Wurdinger T, Figueiredo JL, et al. The healing myocardium sequentially mobilizes two monocyte subsets with divergent and complementary functions. *J Exp Med*. (2007) 204:3037–47. doi: 10.1084/jem.20070885
48. Mouton AJ, DeLeon-Pennell KY, Rivera Gonzalez OJ, Flynn ER, Freeman TC, Saucerman JJ, et al. Mapping macrophage polarization over the myocardial infarction time continuum. *Basic Res Cardiol*. (2018) 113:26. doi: 10.1007/s00395-018-0686-x
49. Galvan-Pena S, O'Neill LA. Metabolic reprograming in macrophage polarization. *Front Immunol*. (2014) 5:420. doi: 10.3389/fimmu.2014.00420
50. Poon IKH, Lucas CD, Rossi AG, Ravichandran KS. Apoptotic cell clearance: basic biology and therapeutic potential. *Nat Rev Immunol*. (2014) 14:166. doi: 10.1038/nri3607
51. Zhang S, Weinberg S, DeBerge M, Gainullina A, Schipma M, Kinchen JM, et al. Efferocytosis fuels requirements of fatty acid oxidation and the electron transport chain to polarize macrophages for tissue repair. *Cell Metab*. (2019) 29:443–56.e5. doi: 10.1016/j.cmet.2018.12.004
52. Yurdagul A Jr, Doran AC, Cai B, Fredman G, Tabas IA. Mechanisms and consequences of defective efferocytosis in atherosclerosis. *Front Cardiovasc Med*. (2017) 4:86. doi: 10.3389/fcvm.2017.00086
53. Gruzdeva O, Uchasova E, Dyleva Y, Akbasheva O, Matveeva V, Karetnikova V, et al. Relationship key factor of inflammation and the development of complications in the late period of myocardial infarction in patients with visceral obesity. *BMC Cardiovasc Disord*. (2017) 17:36. doi: 10.1186/s12872-017-0473-x
54. Tilg H, Moschen AR. Inflammatory mechanisms in the regulation of insulin resistance. *Mol Med*. (2008) 14:222–31. doi: 10.2119/2007-00119.Tilg
55. Lu P, Takai K, Weaver VM, Werb Z. Extracellular matrix degradation and remodeling in development and disease. *Cold Spring Harb Perspect Biol*. (2011) 3:ea005058. doi: 10.1101/cshperspect.a005058
56. Aimes RT, Quigley JP. Matrix metalloproteinase-2 is an interstitial collagenase. Inhibitor-free enzyme catalyzes the cleavage of collagen fibrils and soluble native type I collagen generating the specific 3/4- and 1/4-length fragments. *J Biol Chem*. (1995) 270:5872–6. doi: 10.1074/jbc.270.11.5872
57. Barker TH, Engler AJ. The provisional matrix: setting the stage for tissue repair outcomes. *Matrix Biol*. (2017) 60–61:1–4. doi: 10.1016/j.matbio.2017.04.003
58. Flick MJ, Du X, Witte DP, Jirouskova M, Soloviev DA, Busuttil SJ, et al. Leukocyte engagement of fibrin(ogen) via the integrin receptor alphaMbeta2/Mac-1 is critical for host inflammatory response *in vivo*. *J Clin Invest*. (2004) 113:1596–606. doi: 10.1172/JCI20741
59. Martino MM, Briquez PS, Ranga A, Lutolf MP, Hubbell JA. Heparin-binding domain of fibrin(ogen) binds growth factors and promotes tissue repair when incorporated within a synthetic matrix. *Proc Natl Acad Sci USA*. (2013) 110:4563–8. doi: 10.1073/pnas.1221602110
60. Creemers E, Cleutjens J, Smits J, Heymans S, Moons L, Collen D, et al. Disruption of the plasminogen gene in mice abolishes wound healing after myocardial infarction. *Am J Pathol*. (2000) 156:1865–73. doi: 10.1016/S0002-9440(10)65060-2
61. Motley MP, Madsen DH, Jurgensen HJ, Spencer DE, Szabo R, Holmbeck K, et al. A CCR2 macrophage endocytic pathway mediates extravascular fibrin clearance *in vivo*. *Blood*. (2016) 127:1085–96. doi: 10.1182/blood-2015-05-644260
62. Hsieh JY, Smith TD, Meli VS, Tran TN, Botvinick EL, Liu WF. Differential regulation of macrophage inflammatory activation by fibrin and fibrinogen. *Acta Biomater*. (2017) 47:14–24. doi: 10.1016/j.actbio.2016.09.024

63. Rucklidge GJ, Milne G, McGaw BA, Milne E, Robins SP. Turnover rates of different collagen types measured by isotope ratio mass spectrometry. *Biochim Biophys Acta*. (1992) 1156:57–61. doi: 10.1016/0304-4165(92)90095-C
64. Gonzalez-Santamaria J, Villalba M, Busnadiego O, Lopez-Olaneta MM, Sandoval P, Snabel J, et al. Matrix cross-linking lysyl oxidases are induced in response to myocardial infarction and promote cardiac dysfunction. *Cardiovasc Res*. (2016) 109:67–78. doi: 10.1093/cvr/cvv214
65. Blackburn NJR, Vulesevic B, McNeill B, Cimenci CE, Ahmadi A, Gonzalez-Gomez M, et al. Methylglyoxal-derived advanced glycation end products contribute to negative cardiac remodeling and dysfunction post-myocardial infarction. *Basic Res Cardiol*. (2017) 112:57. doi: 10.1007/s00395-017-0646-x
66. Richardson WJ, Clarke SA, Quinn TA, Holmes JW. Physiological implications of myocardial scar structure. *Compr Physiol*. (2015) 5:1877–909. doi: 10.1002/cphy.c140067
67. Kaikita K, Hayasaki T, Okuma T, Kuziel WA, Ogawa H, Takeya M. Targeted deletion of CC chemokine receptor 2 attenuates left ventricular remodeling after experimental myocardial infarction. *Am J Pathol*. (2004) 165:439–47. doi: 10.1016/S0002-9440(10)63309-3
68. Huleihel M, Douvdevani A, Segal S, Apte RN. Regulation of interleukin 1 generation in immune-activated fibroblasts. European journal of immunology. (1990) 20:731–8. doi: 10.1002/eji.1830200404
69. Halade GV, Jin YF, Lindsey ML. Matrix metalloproteinase (MMP)-9: a proximal biomarker for cardiac remodeling and a distal biomarker for inflammation. *Pharmacol Ther*. (2013) 139:32–40. doi: 10.1016/j.pharmthera.2013.03.009
70. Zavadzkas JA, Mukherjee R, Rivers WT, Patel RK, Meyer EC, Black LE, et al. Direct regulation of membrane type 1 matrix metalloproteinase following myocardial infarction causes changes in survival, cardiac function, and remodeling. *Am J Physiol Heart Circ Physiol*. (2011) 301:H1656–66. doi: 10.1152/ajpheart.00141.2011
71. Leask A. Potential therapeutic targets for cardiac fibrosis: TGFbeta, angiotensin, endothelin, CCN2, and PDGF, partners in fibroblast activation. *Circ Res*. (2010) 106:1675–80. doi: 10.1161/CIRCRESAHA.110.217737
72. Dobaczewski M, Bujak M, Li N, Gonzalez-Quesada C, Mendoza LH, Wang XF, et al. Smad3 signaling critically regulates fibroblast phenotype and function in healing myocardial infarction. *Circ Res*. (2010) 107:418–28. doi: 10.1161/CIRCRESAHA.109.216101
73. Saxena A, Chen W, Su Y, Rai V, Uche OU, Li N, et al. IL-1 induces proinflammatory leukocyte infiltration and regulates fibroblast phenotype in the infarcted myocardium. *J Immunol*. (2013) 191:4838–48. doi: 10.4049/jimmunol.1300725
74. van Nieuwenhoven FA, Hemmings KE, Porter KE, Turner NA. Combined effects of interleukin-1alpha and transforming growth factor-beta1 on modulation of human cardiac fibroblast function. *Matrix Biol*. (2013) 32:399–406. doi: 10.1016/j.matbio.2013.03.008
75. Walker GA, Masters KS, Shah DN, Anseth KS, Leinwand LA. Valvular myofibroblast activation by transforming growth factor-beta: implications for pathological extracellular matrix remodeling in heart valve disease. *Circ Res*. (2004) 95:253–60. doi: 10.1161/01.RES.0000136520.07995.aa
76. Sahin H, Wasmuth HE. Chemokines in tissue fibrosis. *Biochim Biophys Acta*. (2013) 1832:1041–8. doi: 10.1016/j.bbadis.2012.11.004
77. Thompson RW, Pesce JT, Ramalingam T, Wilson MS, White S, Cheever AW, et al. Cationic amino acid transporter-2 regulates immunity by modulating arginase activity. *PLoS Pathogens*. (2008) 4:e1000023. doi: 10.1371/journal.ppat.1000023
78. Fontes JA, Rose NR, Cihákova D. The varying faces of IL-6: from cardiac protection to cardiac failure. *Cytokine*. (2015) 74:62–8. doi: 10.1016/j.cyto.2014.12.024
79. Mayfield AE, Kanda P, Nantsios A, Parent S, Mount S, Dixit S, et al. Interleukin-6 mediates post-infarct repair by cardiac explant-derived stem cells. *Theranostics*. (2017) 7:4850–61. doi: 10.7150/thno.19435
80. Müller J, Gorressen S, Grandoch M, Feldmann K, Kretschmer I, Lehr S, et al. Interleukin-6-dependent phenotypic modulation of cardiac fibroblasts after acute myocardial infarction. *Basic Res Cardiol*. (2014) 109:440. doi: 10.1007/s00395-014-0440-y
81. Verma Suresh K, Krishnamurthy P, Barefield D, Singh N, Gupta R, Lambers E, et al. Interleukin-10 treatment attenuates pressure overload–induced hypertrophic remodeling and improves heart function via signal transducers and activators of transcription 3–dependent inhibition of nuclear factor-κB. *Circulation*. (2012) 126:418–29. doi: 10.1161/CIRCULATIONAHA.112.112185
82. Giugliano GR, Giugliano RP, Gibson CM, Kuntz RE. Meta-analysis of corticosteroid treatment in acute myocardial infarction. *Am J Cardiol*. (2003) 91:1055–9. doi: 10.1016/S0002-9149(03)00148-6
83. Gong K, Zhang Z, Sun X, Zhang X, Li A, Yan J, et al. The nonspecific anti-inflammatory therapy with methotrexate for patients with chronic heart failure. *Am Heart J*. (2006) 151:62–8. doi: 10.1016/j.ahj.2005.02.040
84. Moreira DM, Lueneberg ME, da Silva RL, Fattah T, Gottschall CAM. MethotrexaTE THerapy in ST-Segment Elevation MYocardial InfarctionS: a randomized double-blind, placebo-controlled trial (TETHYS Trial). *J Cardiovasc Pharmacol Ther*. (2017) 22:538–45. doi: 10.1177/1074248417699884
85. Moreira DM, Vieira JL, Gottschall CA. The effects of METhotrexate therapy on the physical capacity of patients with ISchemic heart failure: a randomized double-blind, placebo-controlled trial (METIS trial). *J Card Fail*. (2009) 15:828–34. doi: 10.1016/j.cardfail.2009.06.439
86. Hausenloy DJ, Boston-Griffiths EA, Yellon DM. Cyclosporin A and cardioprotection: from investigative tool to therapeutic agent. *Br J Pharmacol Chemother*. (2012) 165:1235–45. doi: 10.1111/j.1476-5381.2011.01700.x
87. Yingzhong C, Lin C, Chunbin W. Clinical effects of cyclosporine A on reperfusion injury in myocardial infarction: a meta-analysis of randomized controlled trials. *SpringerPlus*. (2016) 5:1117. doi: 10.1186/s40064-016-2751-y
88. Sager HB, Heidt T, Hulsmans M, Dutta P, Courties G, Sebas M, et al. Targeting interleukin-1beta reduces leukocyte production after acute myocardial infarction. *Circulation*. (2015) 132:1880–90. doi: 10.1161/CIRCULATIONAHA.115.016160
89. Toldo S, Mezzaroma E, Van Tassell BW, Farkas D, Marchetti C, Voelkel NF, et al. Interleukin-1beta blockade improves cardiac remodelling after myocardial infarction without interrupting the inflammasome in the mouse. *Exp Physiol*. (2013) 98:734–45. doi: 10.1113/expphysiol.2012.069831
90. Abbate A, Kontos MC, Grizzard JD, Biondi-Zoccai GG, Van Tassell BW, Robati R, et al. Interleukin-1 blockade with anakinra to prevent adverse cardiac remodeling after acute myocardial infarction (Virginia Commonwealth University Anakinra Remodeling Trial [VCU-ART] pilot study). *Am J Cardiol*. (2010) 105:1371–7.e1. doi: 10.1016/j.amjcard.2009.12.059
91. Morton AC, Rothman AM, Greenwood JP, Gunn J, Chase A, Clarke B, et al. The effect of interleukin-1 receptor antagonist therapy on markers of inflammation in non-ST elevation acute coronary syndromes: the MRC-ILA Heart Study. *Eur Heart J*. (2015) 36:377–84. doi: 10.1093/eurheartj/ehu272
92. Abbate A, Van Tassell BW, Biondi-Zoccai G, Kontos MC, Grizzard JD, Spillman DW, et al. Effects of interleukin-1 blockade with anakinra on adverse cardiac remodeling and heart failure after acute myocardial infarction [from the Virginia Commonwealth University-Anakinra Remodeling Trial (2) (VCU-ART2) pilot study]. *Am J Cardiol*. (2013) 111:1394–400. doi: 10.1016/j.amjcard.2013.01.287
93. Ridker PM, MacFadyen JG, Everett BM, Libby P, Thuren T, Glynn RJ. Relationship of C-reactive protein reduction to cardiovascular event reduction following treatment with canakinumab: a secondary analysis from the CANTOS randomised controlled trial. *Lancet*. (2018) 391:319–28. doi: 10.1016/S0140-6736(17)32814-3
94. Padfield GJ, Din JN, Koushiappi E, Mills NL, Robinson SD, Cruden Nle M, et al. Cardiovascular effects of tumour necrosis factor alpha antagonism in patients with acute myocardial infarction: a first in human study. *Heart*. (2013) 99:1330–5. doi: 10.1136/heartjnl-2013-303648
95. Mann DL, McMurray JJ, Packer M, Swedberg K, Borer JS, Colucci WS, et al. Targeted anticytokine therapy in patients with chronic heart failure: results of the Randomized Etanercept Worldwide Evaluation (RENEWAL). *Circulation*. (2004) 109:1594–602. doi: 10.1161/01.CIR.0000124490.27666.B2
96. Struthers M, Pasternak A. CCR2 antagonists. *Curr Top Med Chem*. (2010) 10:1278–98. doi: 10.2174/156802610791561255

97. Sager HB, Dutta P, Dahlman JE, Hulsmans M, Courties G, Sun Y, et al. RNAi targeting multiple cell adhesion molecules reduces immune cell recruitment and vascular inflammation after myocardial infarction. *Sci Transl Med*. (2016) 8:342ra80. doi: 10.1126/scitranslmed.aaf1435
98. Leuschner F, Dutta P, Gorbatov R, Novobrantseva TI, Donahoe JS, Courties G, et al. Therapeutic siRNA silencing in inflammatory monocytes in mice. *Nat Biotechnol*. (2011) 29:1005. doi: 10.1038/nbt.1989
99. Majmudar MD, Keliher EJ, Heidt T, Leuschner F, Truelove J, Sena BF, et al. Monocyte-directed RNAi targeting CCR2 improves infarct healing in atherosclerosis-prone mice. *Circulation*. (2013) 127:2038–46. doi: 10.1161/CIRCULATIONAHA.112.000116
100. Monaghan M, Browne S, Schenke-Layland K, Pandit A. A Collagen-based scaffold delivering exogenous MicroRNA-29B to modulate extracellular matrix remodeling. *Mol Ther*. (2014) 22:786–96. doi: 10.1038/mt.2013.288
101. Monaghan MG, Holeiter M, Brauchle E, Layland SL, Lu Y, Deb A, et al. Exogenous miR-29B delivery through a hyaluronan-based injectable system yields functional maintenance of the infarcted myocardium. *Tissue Eng Part A*. (2017) 24:57–67. doi: 10.1089/ten.tea.2016.0527
102. Panahi M, Papanikolaou A, Torabi A, Zhang J-G, Khan H, Vazir A, et al. Immunomodulatory interventions in myocardial infarction and heart failure: a systematic review of clinical trials and meta-analysis of IL-1 inhibition. *Cardiovasc Res*. (2018) 114:1445–61. doi: 10.1093/cvr/cvy145
103. Parks WC, Wilson CL, Lopez-Boado YS. Matrix metalloproteinases as modulators of inflammation and innate immunity. *Nat Rev Immunol*. (2004) 4:617–29. doi: 10.1038/nri1418
104. Maquart FX, Bellon G, Pasco S, Monboisse JC. Matrikines in the regulation of extracellular matrix degradation. *Biochimie*. (2005) 87:353–60. doi: 10.1016/j.biochi.2004.10.006
105. Adair-Kirk TL, Senior RM. Fragments of extracellular matrix as mediators of inflammation. *Int J Biochem Cell Biol*. (2008) 40:1101–10. doi: 10.1016/j.biocel.2007.12.005
106. Kwon YW, Heo SC, Lee TW, Park GT, Yoon JW, Jang IH, et al. N-Acetylated proline-glycine-proline accelerates cutaneous wound healing and neovascularization by human endothelial progenitor cells. *Sci Rep*. (2017) 7:43057. doi: 10.1038/srep43057
107. Weathington NM, van Houwelingen AH, Noerager BD, Jackson PL, Kraneveld AD, Galin FS, et al. A novel peptide CXCR ligand derived from extracellular matrix degradation during airway inflammation. *Nat Med*. (2006) 12:317–23. doi: 10.1038/nm1361
108. Guo G, Munoz-Garcia B, Ott CE, Grunhagen J, Mousa SA, Pletschacher A, et al. Antagonism of GxxPG fragments ameliorates manifestations of aortic disease in Marfan syndrome mice. *Human Mol Genet*. (2013) 22:433–43. doi: 10.1093/hmg/dds439
109. Banerjee P, Suseela G, Shanthi C. Isolation and identification of cryptic bioactive regions in bovine achilles tendon collagen. *Protein J*. (2012) 31:374–86. doi: 10.1007/s10930-012-9415-8
110. Malinda KM, Wysocki AB, Koblinski JE, Kleinman HK, Ponce ML. Angiogenic laminin-derived peptides stimulate wound healing. *Int J Biochem Cell Biol*. (2008) 40:2771–80. doi: 10.1016/j.biocel.2008.05.025
111. Zhang Y, Duan X, Zhuang Y. Purification and characterization of novel antioxidant peptides from enzymatic hydrolysates of tilapia (*Oreochromis niloticus*) skin gelatin. *Peptides*. (2012) 38:13–21. doi: 10.1016/j.peptides.2012.08.014
112. Shankavaram UT, DeWitt DL, Funk SE, Sage EH, Wahl LM. Regulation of human monocyte matrix metalloproteinases by SPARC. *J Cell Physiol*. (1997) 173:327–34. doi: 10.1002/(SICI)1097-4652(199712)173:3<327::AID-JCP4>3.0.CO;2-P
113. Brassart B, Randoux A, Hornebeck W, Emonard H. Regulation of matrix metalloproteinase-2 (gelatinase A, MMP-2), membrane-type matrix metalloproteinase-1 (MT1-MMP) and tissue inhibitor of metalloproteinases-2 (TIMP-2) expression by elastin-derived peptides in human HT-1080 fibrosarcoma cell line. *Clin Exp Metastasis*. (1998) 16:489–500. doi: 10.1023/A:1006550503612
114. Mooradian DL, McCarthy JB, Skubitz AP, Cameron JD, Furcht LT. Characterization of FN-C/H-V, a novel synthetic peptide from fibronectin that promotes rabbit corneal epithelial cell adhesion, spreading, and motility. *Invest Ophthalmol Vis Sci*. (1993) 34:153–64.
115. Monboisse JC, Bellon G, Randoux A, Dufer J, Borel JP. Activation of human neutrophils by type I collagen. Requirement of two different sequences. *Biochem J*. (1990) 270:459–62. doi: 10.1042/bj2700459
116. Zetter BR, Rasmussen N, Brown L. An *in vivo* assay for chemoattractant activity. *Lab Invest*. (1985) 53:362–8.

Conflict of Interest Statement: The authors declare that the research was conducted in the absence of any commercial or financial relationships that could be construed as a potential conflict of interest.

frontiers in Cardiovascular Medicine

REVIEW
published: 20 August 2019
doi: 10.3389/fcvm.2019.00123

Application of Bioengineered Materials in the Surgical Management of Heart Failure

*Simranjit S. Pattar, Ali Fatehi Hassanabad and Paul W. M. Fedak**

Section of Cardiac Surgery, Department of Cardiac Sciences, Cumming School of Medicine, Libin Cardiovascular Institute of Alberta, University of Calgary, Calgary, AB, Canada

The epicardial surface of the heart is readily accessible during cardiac surgery and presents an opportunity for therapeutic intervention for cardiac repair and regeneration. As an important anatomic niche for endogenous mechanisms of repair, targeting the epicardium using decellularized extracellular matrix (ECM) bioscaffold therapy may provide the necessary environmental cues to promote functional recovery. Following ischemic injury to the heart caused by myocardial infarction (MI), epicardium derived progenitor cells (EPDCs) become activated and migrate to the site of injury. EPDC differentiation has been shown to contribute to endothelial cell, cardiac fibroblast, cardiomyocyte, and vascular smooth muscle cell populations. Post-MI, it is largely the activation of cardiac fibroblasts and the resultant dysregulation of ECM turnover which leads to maladaptive structural cardiac remodeling and loss of cardiac function. Decellularized ECM bioscaffolds not only provide structural support, but have also been shown to act as a bioactive reservoir for growth factors, cytokines, and matricellular proteins capable of attenuating maladaptive cardiac remodeling. Targeting the epicardium post-MI using decellularized ECM bioscaffold therapy may provide the necessary bioinductive cues to promote differentiation toward a pro-regenerative phenotype and attenuate cardiac fibroblast activation. There is an opportunity to leverage the clinical benefits of this innovative technology with an aim to improve the prognosis of patients suffering from progressive heart failure. An enhanced understanding of the utility of decellularized ECM bioscaffolds in epicardial repair will facilitate their growth and transition into clinical practice. This review will provide a summary of decellularized ECM bioscaffolds being developed for epicardial infarct repair in coronary artery bypass graft (CABG) surgery.

Keywords: extracellular matrix, biomaterials, epicardium, heart failure, cardiac surgery, bioscaffold, myocardial infarction

OPEN ACCESS

Edited by:
Sharan Ramaswamy, Florida International University, United States

Reviewed by:
Sveva Bollini, University of Genoa, Italy
Alexander Von Gise, Hannover Medical School, Germany

****Correspondence:***
Paul W. M. Fedak
paul.fedak@gmail.com

Specialty section:
This article was submitted to Cardiovascular Biologics and Regenerative Medicine, a section of the journal Frontiers in Cardiovascular Medicine

Received: *17 June 2019*
Accepted: *06 August 2019*
Published: *20 August 2019*

Citation:
Pattar SS, Fatehi Hassanabad A and Fedak PWM (2019) Application of Bioengineered Materials in the Surgical Management of Heart Failure. Front. Cardiovasc. Med. 6:123. doi: 10.3389/fcvm.2019.00123

INTRODUCTION TO HEART FAILURE

Heart failure is a chronic and progressive condition characterized by maladaptive structural cardiac remodeling and poor cardiac pump function. The most common cause of heart failure is damage to the cardiac muscle caused by ischemic injury, otherwise known as myocardial infarction (MI) (1). There are an increasing number of individuals living with heart failure, with 960,000 new cases reported each year in the US alone (2). As a result, an estimated >8 million individuals

will be living with heart failure in the US by 2030 (3). Surgical revascularization remains the primary treatment modality for patients who have suffered from an MI. However, nearly one in every five heart failure patients is readmitted for heart failure or other related causes within 30 days (1). Therefore, heart failure is often referred to as a "revolving door condition" due to high rates of readmission. Given its increasing prevalence and high rate of readmission, it is necessary to improve our understanding of the surgical management of heart failure. Extracellular matrix (ECM) bioscaffolds may be the key to unlocking the potential of the epicardial surface of the heart with the ultimate goal of driving endogenous mechanisms of repair and attenuating progressive heart failure following ischemic injury.

THE CURRENT SURGICAL MANAGEMENT OF HEART FAILURE

According to current guidelines, the primary objective in the surgical management of MI is to restore blood flow to the infarct region in order to preserve myocardial viability and alleviate symptoms (4, 5). Revascularization may be achieved by coronary artery bypass graft (CABG) surgery or percutaneous coronary intervention (PCI), and has been shown to improve survival in patients (4–8). A recent meta-analysis including twenty-one studies and 16,191 patients found revascularization by CABG or PCI was beneficial compared to medical treatment alone in patients suffering from ischemic heart disease and reduced left ventricular ejection fraction (LVEF) (9). The survival benefits of surgical revascularization are clear, and the completeness of revascularization is integral to preserving myocardial viability (4). Despite surgical intervention, studies have documented 12 and 22% readmission rates in patients who have undergone CABG or PCI, respectively, due to heart failure (6, 10).

For patients who progress to end-stage clinical heart failure, cardiac transplantation remains the gold standard treatment modality (11, 12). However, limited donor supply and an increasing number of eligible patients for cardiac transplants have driven the need for innovative alternative strategies. Mechanical circulatory support (MCS), specifically the left ventricular assist device (LVAD), has vastly improved since the seminal work of Dr. Michael E. DeBakey, Dr. Denton A. Cooley, and others (13–16). MCS may be utilized as a bridge to recovery, bridge to transplantation, or as a destination therapy in patients who are ineligible for cardiac transplantation (17, 18). INTERMACS (Interagency Registry for Mechanically Assisted Circulatory Support) includes >15,000 patients from 158 hospitals; it reports a 1-year survival rate of 80% and 2-year survival rate of 70% in patients receiving a continuous-flow device (17, 19). Importantly, despite the improvements made in MSC technology, a number of complications are still associated with its use (19–22). Adverse events reported at 2-year follow up of 133 patients treated using a continuous flow LVAD include, bleeding requiring blood transfusion (81%), cardiac arrhythmia (56%), right-sided heart failure (20%), LVAD-related infection (35%), stroke (18%), LVAD-thrombosis (4%), and pump replacement (9%) (23). Therefore, an opportunity exists to better understand and address the underlying cellular and molecular causes of heart failure in order to improve the prognosis of patients with heart failure.

TAKING A STEM CELL-BASED APPROACH

An array of stem cell-based approaches have emerged in the past two decades with the aim of restoring myocardial function and preventing the progression of heart failure. Despite the numerous clinical trials conducted and their important contribution to our current understanding of the treatment of heart failure following MI, an efficacious stem cell-based therapy with clinically relevant outcomes has yet to emerge (24–26). Clinical trial data regarding the use of a stem cell-based approach in patients suffering from acute myocardial infarction or ischemic cardiomyopathy remains variable and inconclusive (24, 25, 27).

In the case of acute myocardial infarction, earlier trials such as BOOST (BOne marrOw transfer to enhance ST-elevation infarct regeneration) and REPAIR-AMI (Reinfusion of Enriched Progenitor Cells and Infarct Remodeling in Acute Myocardial Infarction) showed improved LVEF in patients treated with bone marrow mononuclear cells (BM-MNCs) (28–30). However, these improvements were not replicated in future studies using BM-MNCs, including but not limited to, BOOST-2 (BOne marrOw transfer to enhance ST-elevation infarct regeneration-2), LATE-TIME (Late Timing in Myocardial Infarction Evaluation), and SWISS-AMI (SWiss multicenter Intracoronary Stem cells Study in Acute Myocardial Infarction) (24, 31–33).

Similarly, in the case of ischemic cardiomyopathy, patients with advanced heart failure who received BM-MNC therapy displayed a 9% improvement in LVEF at 4-months follow-up compared to baseline (34). However, the FOCUS-CCTRN (First Mononuclear Cells injected in the United States conducted by the CCTRN) trial showed a modest 2.7% LVEF improvement in patients treated with BM-MNC compared to placebo, alongside no significant improvement in infarct size (35). Furthermore, CHART-1 (Congestive Heart Failure Cardiopoietic Regenerative Therapy) found no significant difference amongst advanced heart failure patients ($n = 157$) receiving cardiopoietic cell therapy compared to sham control ($n = 158$) at 39-weeks follow-up (24, 36).

In addition to the variable clinical trial results discussed, poor stem cell engraftment at the site of delivery and the inherent conflict of introducing stem cells to an injured and hostile cardiac environment present significant hurdles to directing optimal cell function and tissue recovery (37, 38). The recent controversy surrounding c-kit$^+$ cardiac stem cells and interruption of the CONCERT-HF (Combination of Mesenchymal and C-kit+ Cardiac Stem Cells as Regenerative Therapy for Heart Failure) trial has significantly contributed to uncertainty regarding the clinical efficacy of this approach (39–45).

THE PARACRINE HYPOTHESIS

Despite the challenges associated with a stem cell-based approach, it has become clear that stem cells largely exert

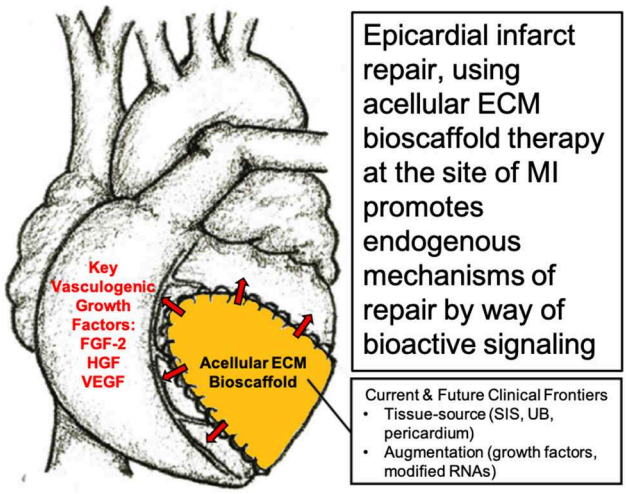

FIGURE 1 | Surgical implantation of acellular extracellular matrix (ECM) bioscaffold on the epicardial surface of the heart promotes endogenous mechanisms of repair by way of bioactive paracrine signaling. Image, in part, provided courtesy of Dr. Holly Mewhort, Section of Cardiac Surgery, Department of Cardiac Sciences, Cumming School of Medicine, Libin Cardiovascular Institute of Alberta, University of Calgary, Calgary, Alberta, Canada.

their effects in a paracrine fashion (41, 46–53). The ability of bone marrow-derived cells to produce a potent angiogenic growth factor response, enhance endothelial cell proliferation, and improve perfusion and function in models of ischemic injury has been described (49, 53–55). Specifically, autologous bone marrow cells are capable of producing a vascular endothelial growth factor (VEGF)-dependent response that drives angiogenesis and improves perfusion in a porcine model of MI (54). Moreover, human mesenchymal stem cell conditioned media (MSC-CM) has been shown to reduce MI size, enhance capillary density, and improve overall cardiac function compared to control media using a porcine model of MI (56, 57). Overall, it is the paracrine factors produced that play a fundamental role in mediating the effects of stem cell therapy.

The question, therefore, becomes *"is the delivery of cells necessary for a therapeutic effect?"* Given the challenges associated with a stem cell-based approach, our research group alongside many others have directed their attention toward modulating the local cardiac microenvironment and paracrine response, without the administration of stem cells, in order to direct endogenous mechanisms of cardiac repair (48, 51, 57–62). In particular, our research group has shown the benefits of using acellular bioactive extracellular matrix (ECM) scaffolds for epicardial infarct repair (63–66). By providing an optimal ECM microenvironment with the necessary paracrine growth factors, the aim is to limit infarct expansion by attenuating cardiac fibrosis and to promote vasculogenesis in order to improve blood flow to the infarcted myocardium (63, 65, 67) (**Figure 1**).

TARGETING THE EPICARDIUM IN CARDIAC SURGERY

A unique opportunity exists to enhance endogenous repair mechanisms of the heart at its epicardial surface. In the case of routine cardiac surgery, surgeons gain access to the heart by way of sternotomy followed by cardiotomy, at which point they are presented with the epicardial surface of the heart. The epicardium is a promising anatomic niche that is involved in early cardiac development, the production and regulation of ECM components, paracrine signaling, and response to ischemic injury (68).

This thin outermost mesothelial layer of the heart contributes to normal cardiac development as it gives rise to multipotent cardiac progenitor cells, called epicardium derived progenitor cells (EPDCs) (68, 69). EPDCs have been found to differentiate to coronary vascular smooth muscle cells and cardiac fibroblasts by way of epithelial to mesenchymal transition (EMT) (70–73) (**Figure 2**). Studies have also reported EPDC differentiation to endothelial cell and cardiomyocyte populations (74–77). However, the contribution of EPDCs to endothelial cell and cardiomyocyte populations remains highly debatable and further lineage tracing is warranted to ascertain the extent of this contribution (71, 73, 77–82) (**Figure 2**).

During early cardiac development, the epicardium dictates myocardial maturation and compaction, and the formation of the coronary vasculature and Purkinje fibers (68, 83–85). Beyond its contribution to various cell populations, the epicardium has been shown to be a key player involved in paracrine signaling and the modulation of ECM components (82, 86–90). This makes the epicardium an ideal candidate that may be targeted to manipulate ECM remodeling and promote endogenous repair and regeneration of the adult human heart.

ISCHEMIC INJURY LEADS TO ECM REMODELING

Normally, the epicardium is quiescent in the healthy adult human heart, yet it may hold great regenerative capacity (68, 83, 91, 92). Following an MI, EPDCs become activated and migrate to the site of injury, where they have been shown to largely differentiate into vascular smooth muscle cells or fibroblasts (70, 92, 93) (**Figure 2**). The expression of markers including, Wilms tumor protein (Wt1), T-box transcription factor 18 (Tbx18), and retinaldehyde dehydrogenase 2 (Raldh2), has been reported in activated EPDC populations (69, 82, 92). Recent findings have further highlighted the heterogeneity within EPDC populations following an MI based on the differential expression of stem-cell antigen 1 (Sca-1), CD44, and CD90; these subpopulations may present clinically relevant targets (94). Overall, activation of the epicardium has been shown to play an important role in supporting the development of new vasculature by way of a robust paracrine response (79, 92). EPDC derived conditioned media has been reported to induce functional recovery in a mouse model of MI by way of a robust fibroblast growth factor-2 (FGF-2) and VEGF mediated angiogenic response (92). Clearly,

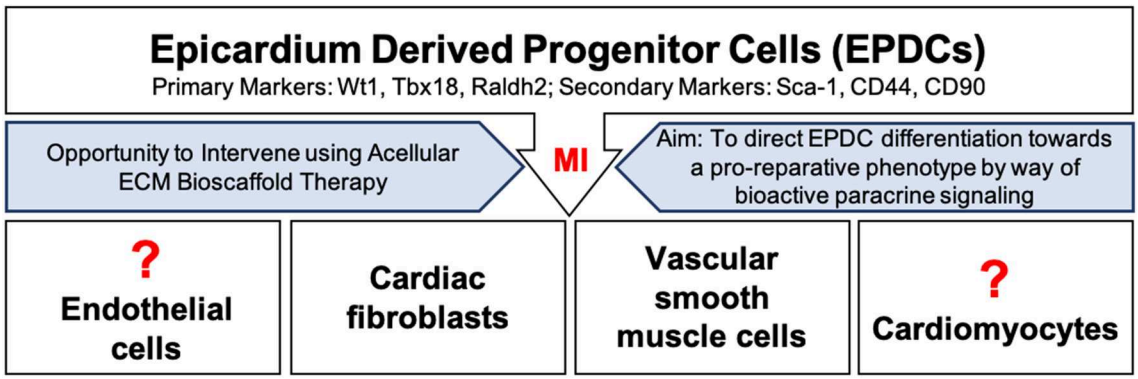

FIGURE 2 | Epicardium derived progenitor cell (EPDC) activation, mobilization, and differentiation following myocardial infarction. EPDCs may differentiate into cardiac fibroblasts, vascular smooth muscle cells, or possibly into endothelial cells or cardiomyocytes. Intervention using acellular ECM bioscaffold therapy may be used to direct EDPCs toward a pro-reparative, vasculogenic fate.

an opportunity exists to direct EPDCs toward a pro-reparative or pro-vasculogenic fate, and away from a pro-fibrotic fate. As mentioned above, the completeness of revascularization is critical to the preservation of myocardial viability following an MI (4). Therefore, the aim is to promote vasculogenesis in order to improve blood flow to the infarcted myocardium, and to limit infarct scar expansion by attenuating the activity of cardiac fibroblasts.

Cardiac fibroblasts play an essential role in normal heart function, not only structurally and mechanically, but with regards to the biochemical and electrical properties of the cardiac environment as well (95–99). In the event of an ischemic injury and the resulting disruption of the local microenvironment of the infarcted myocardium, these fibroblasts become activated. Activated fibroblasts, known as myofibroblasts, are the key mediators of ECM remodeling (96, 98, 100, 101). Fibrotic remodeling of the infarcted myocardium is exacerbated by the migration and activation of additional cardiac fibroblasts at the site of injury. Of note, the epicardium is a significant source of these migratory cardiac fibroblasts (79, 82, 92, 93, 102–104). Myofibroblast activity at the site of MI leads to dysregulation of ECM homoeostasis, resulting in the deposition of a collagenous scar (98, 104, 105). Initially, this response is crucial in preventing ventricular free wall rupture at the site of an MI. However, persistent myofibroblast activation when left unchecked leads to infarct scar expansion, diastolic, and systolic dysfunction due to structural cardiac remodeling, and eventually end-stage clinical heart failure (97, 98, 105–108).

Therefore, targeting the epicardium post-MI by providing the necessary bioinductive cues capable of promoting a pro-reparative phenotype rather than a pro-fibrotic phenotype is compelling. Our research group and others believes that acellular ECM bioscaffolds offer an ideal approach by which the post-MI cardiac environment may be directed toward a pro-reparative phenotype by way of bioactive signaling (**Figures 1**, **2**).

BIO-ENGINEERED MATERIALS FOR EPICARDIAL INFARCT REPAIR

Collagen is commonly studied for ECM bioscaffold-based infarct repair as it is the primary component of the cardiac ECM (109–111). Acellular type I collagen cardiac bioscaffold has been shown to preserve contractility, reduce cardiac fibrosis, and attenuate LV remodeling using a murine model of MI (112, 113). Additionally, acellular type I collagen cardiac bioscaffold therapy has been reported to promote a pro-vasculogenic response, which is accompanied by increased vessel density in the injured heart (112–115) Other natural bioscaffolds, such as fibrin, gelatin, Matrigel, alginate, and chitosan-based scaffolds, have also been investigated for infarct repair and regeneration (111, 116–119). Acellular fibrin-based scaffolds leverage the blood clotting cascade to polymerize *in situ*, and have been reported to preserve cardiac function and improve neovascularization in a rat model of MI (111, 120, 121). Despite the potential of these acellular strategies, there are challenges associated with the use of natural bioscaffolds, such as rapid degradation and poor mechanical performance (111, 122).

Promising results have also been found using synthetic scaffold solutions, which typically include the use of polylactic acid (PLA), polyglycolic acid (PGA), poly-ε-caprolactone (PCL), polyester urethane urea (PEUU), polytetrafluoroethylene (PTFE), or varying combinations of the aforementioned materials (110, 122, 123). For example, polyester urethane urea (PEUU) scaffold implantation in a rat model of MI is capable of improving overall contractile function and cardiac remodeling (124). While the mechanical properties of synthetic scaffold solutions are highly tunable, they lack the biological complexity required to target the epicardial surface of the heart by way of paracrine signaling and bioactive factors.

As such, the development of decellularized tissue-derived ECM bioscaffolds remains a focal point within the field. These acellular ECM bioscaffolds facilitate directing endogenous mechanisms of repair and regeneration at the site of ischemic

injury by way of bioactive paracrine signaling (63–65, 109, 125–128) (**Figure 1**). Acellular ECM bioscaffolds retain the native ECM architecture and composition, including a variety of embedded growth factors, of the tissue from which they were derived (125, 126, 129). These complex bioscaffolds may be exploited to provide an optimal microenvironment capable of enhancing blood flow and attenuating cardiac myofibroblast activity at the site of an MI. Of the tissue-derived ECM bioscaffolds, acellular porcine-derived small intestinal submucosa (SIS) ECM is best characterized in the literature with regards to epicardial infarct repair. We have previously described the collection of acellular ECM bioscaffolds available for a variety of indications in cardiac surgery (98).

The small intestine is a highly vascularized organ and therefore the composition and structure of SIS-derived ECM bioscaffold is proposed to be highly conducive to revascularization itself (109, 126). Specifically, 90% of SIS-ECM bioscaffold is type I collagen, fibronectin, laminin, and glycosaminoglycans (GAGs) ECM components (109, 130). The role of fibronectin and laminin in endothelial cell adhesion and the maintenance of vascular structures, respectively, has been characterized (109, 131–133). Additionally, GAGs play an important role in binding the growth factors and cytokines within the ECM and therefore present a possible target for modifying tissue-derived ECM bioscaffolds with signaling factors (109, 134). Finally, SIS-ECM itself has been shown to naturally contain essential growth factors, both bound by GAGs and embedded within the ECM itself, including fibroblast growth factor-2 (FGF-2), VEGF, and hepatocyte growth factor (HGF), which play key roles in vasculogenesis (109, 135).

In the context of epicardial infarct repair, our research group has highlighted the promise of acellular SIS-ECM bioscaffold, CorMatrix® ECM (CorMatrix Cardiovascular Inc., USA) (63–66). We have shown that the interaction of human cardiac fibroblasts with CorMatrix® ECM results in a robust fibroblast growth factor-2 (FGF-2) dependent cell-mediated paracrine response capable of stimulating new blood vessel assembly (65). This is recapitulated *in vivo*, using a rat MI model: animals treated via surgical implantation of CorMatrix® ECM post-MI compared to animals treated with sham or inactivated CorMatrix® ECM displayed an FGF-2-dependent increase in vascularity, reduced LV dilatation, improved ejection fraction, and improved contractility (65). Further studies using a large pre-clinical porcine ischemia-reperfusion model have similarly demonstrated that surgical implantation of CorMatrix® ECM improves vascularity and functional recovery of the infarct region (63, 64) (**Figure 3**). Other groups have assessed SIS-ECM bioscaffold in surgical reconstruction of septal defects, vascular or outflow tract augmentation, and valve reconstruction, and have yielded positive results (136). However, long-term patient follow up is required to truly understand the impact of this intervention. Notably, our research group is characterizing the clinical use of commercially-available CorMatrix® ECM in an on-going first-in-human phase I clinical trial (NCT02887768) for epicardial infarct repair at the time of surgical revascularization (CABG surgery).

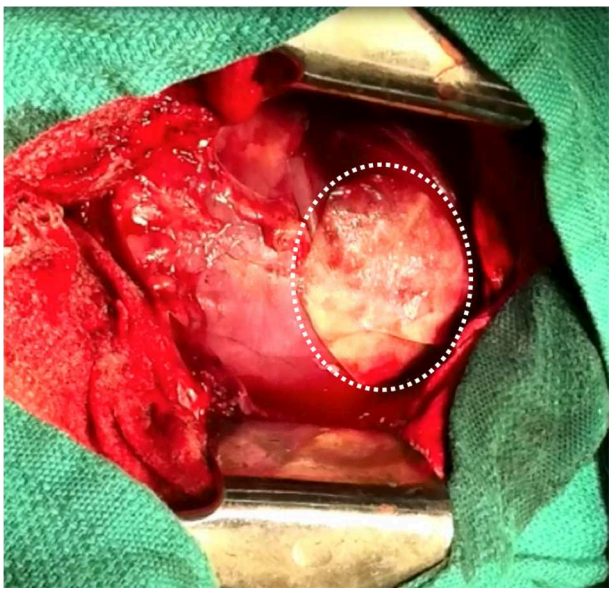

FIGURE 3 | Surgical implantation of porcine-derived acellular small intestine submucosa (SIS) extracellular matrix (ECM) bioscaffold (CorMatrix® ECM, CorMatrix Cardiovascular Inc., USA) over the site of ischemia-reperfusion injury on the anterior wall of the left ventricle, in a porcine model. Image provided courtesy of the Fedak Research Group (Dr. Holly Mewhort and Jeannine Turnbull) Campbell Family Cardiac Translational Laboratory, Libin Cardiovascular Institute of Alberta, University of Calgary, Calgary, Alberta, Canada.

Beyond SIS-ECM bioscaffold therapy for epicardial infarct repair, acellular ECM bioscaffolds derived from other tissue sources, such as the urinary bladder (UB), amniotic membrane (AM), and cardiac tissue have been investigated (137–140). Given the fact that ECM bioscaffolds are a function of the physiological requirements of the tissue from which they are derived, the tissue source will influence each bioscaffold's ability to direct cardiac repair. UB-ECM bioscaffold has been reported to outperform PTFE synthetic scaffold, and displays favorable tissue integration and replacement in a porcine MI model (139). More recently, an acellular pericardium-derived ECM bioscaffold was shown to support neovascularization and neoinnervation, alongside improved LVEF, cardiac output, and reduced infarct size in a porcine MI model at 30-day follow-up (137). Future work should continue to investigate acellular ECM bioscaffolds derived from various tissue sources in the context of epicardial infarct repair.

Additionally, augmentation of the aforementioned bioscaffolds with additional growth factors and/or modified RNAs, may also play an important role in modulating the local paracrine environment and enhancing their therapeutic effect. While the specific details and challenges are beyond the scope of this review, modified RNAs may be utilized to promote angiogenesis following an MI (141–143). Intramyocardial injection of VEGF-A modified RNA has been reported to enhance $Wt1^{+}$-EPDC to endothelial cell differentiation and to promote functional vessel formation in a mouse model of MI (143). Similarly, our research group has shown that

enhancement of SIS-ECM with additional FGF-2 further improves ECM homeostasis and cardiac function in a rat model of MI (63, 66). Overall, acellular tissue-derived ECM bioscaffolds are a promising therapeutic strategy for the modulation of cardiac repair at the site of an MI. The important role that bioactive paracrine signaling plays in directing endogenous mechanisms of repair at the site of an MI should remain a focal point moving forward.

CONCLUSION

A unique opportunity exists to augment surgical revascularization via CABG surgery using acellular ECM bioscaffold therapy. The epicardial surface is readily accessible in open heart surgery. As it is an anatomic niche responsible for normal cardiac development and paracrine signaling, which becomes activated in response to ischemic injury, we can leverage the epicardium to direct endogenous repair at the site of an MI. Acellular ECM bioscaffold therapy has been shown to improve vascularization and attenuate cardiac fibroblast-mediated ventricular remodeling following an MI by way of its bioactive signaling. By providing an optimal ECM bioscaffold signaling environment the goal is to shift the damaged cardiac tissue toward a pro-reparative phenotype, and away from a pro-fibrotic phenotype, and to improve overall revascularization of the tissue. Overall, by targeting the underlying cellular and molecular causes of heart failure using acellular ECM bioscaffold therapy, this innovative strategy may be able to significantly improve the prognosis of patients who have suffered from an MI.

AUTHOR CONTRIBUTIONS

SP, AF, and PF designed, drafted, and revised the manuscript.

FUNDING

This research was funded by the Heart and Stroke Foundation of Canada to PF.

REFERENCES

1. Heart and Stroke Foundation. *The Burden of Heart Failure: 2016 Report on the Health of Canadians.* (2016). Available online at: https://www.heartandstroke.ca/-/media/pdf-files/canada/2017-heart-month/heartandstroke-reportonhealth-2016.ashx?la=en (accessed November 25, 2017).
2. Benjamin EJ, Blaha MJ, Chiuve SE, Cushman M, Das SR, Deo R, et al. Heart disease and stroke statistics-−2017 update: a report from the American heart association. *Circulation.* (2017) 135:e146–603. doi: 10.1161/CIR.0000000000000485
3. Benjamin EJ, Muntner P, Alonso A, Bittencourt MS, Callaway CW, Carson AP, et al. Heart disease and stroke statistics-−2019 update: a report from the american heart association. *Circulation.* (2019) 139:e56–28. doi: 10.1161/CIR.0000000000000659
4. Neumann FJ, Sousa-Uva M, Ahlsson A, Alfonso F, Banning AP, Benedetto U, et al. 2018 ESC/EACTS Guidelines on myocardial revascularization. *Eur Heart J.* (2018) 76:1585–664. doi: 10.5603/KP.2018.0228
5. Yancy CW, Jessup M, Bozkurt B, Butler J, Casey DE, Drazner MH, et al. 2013 ACCF/AHA guideline for the management of heart failure. *Circulation.* (2013) 128:e240–327. doi: 10.1161/CIR.0b013e31829e8776
6. Marui A, Kimura T, Nishiwaki N, Komiya T, Hanyu M, Shiomi H, et al. Three-year outcomes after percutaneous coronary intervention and coronary artery bypass grafting in patients with heart failure: from the CREDO-Kyoto percutaneous coronary intervention/coronary artery bypass graft registry cohort-2 The CREDO-Kyoto PCI/CAB. *Eur J Cardio-thoracic Surg.* (2014) 47:316–21. doi: 10.1093/ejcts/ezu131
7. Velazquez EJ, Lee KL, Jones RH, Al-Khalidi HR, Hill JA, Panza JA, et al. Coronary-artery bypass surgery in patients with ischemic cardiomyopathy. *N Engl J Med.* (2016) 374:1511–20. doi: 10.1056/NEJMoa1602001
8. Yusuf S, Zucker D, Passamani E, Peduzzi P, Takaro T, Fisher L, et al. Effect of coronary artery bypass graft surgery on survival: overview of 10-year results from randomised trials by the Coronary Artery Bypass Graft Surgery Trialists Collaboration. *Lancet.* (1994) 344:563–70. doi: 10.1016/S0140-6736(94)91963-1
9. Wolff G, Dimitroulis D, Andreotti F, Kołodziejczak M, Jung C, Scicchitano P, et al. Survival benefits of invasive versus conservative strategies in heart failure in patients with reduced ejection fraction and coronary artery disease. *Circ Hear Fail.* (2017) 10:e003255. doi: 10.1161/CIRCHEARTFAILURE.116.003255
10. Hannan EL, Zhong Y, Lahey SJ, Culliford AT, Gold JP, Smith CR, et al. 30-day readmissions after coronary artery bypass graft surgery in New York State. *JACC Cardiovasc Interv.* (2011) 4:569–76. doi: 10.1016/j.jcin.2011.01.010
11. Kittleson MM, Kobashigawa JA. Cardiac transplantation. *JACC Hear Fail.* (2017) 5:857–68. doi: 10.1016/j.jchf.2017.08.021
12. Mehra MR, Canter CE, Hannan MM, Semigran MJ, Uber PA, Baran DA, et al. The 2016 international society for heart lung transplantation listing criteria for heart transplantation: a 10-year update. *J Hear Lung Transplant.* (2016) 35:1–23. doi: 10.1016/j.healun.2015.10.023
13. Cooley DA. The total artificial heart. *Nat Med.* (2003) 9:108–11. doi: 10.1038/nm0103-108
14. Cooley DA, Liotta D, Hallman GL, Bloodwell RD, Leachman RD, Milam JD. Orthotopic cardiac prosthesis for two-staged cardiac replacement. *Am J Cardiol.* (1969) 24:723–30. doi: 10.1016/0002-9149(69)90460-3
15. DeBakey ME. Development of mechanical heart devices. *Ann Thorac Surg.* (2005) 79:S2228–31. doi: 10.1016/j.athoracsur.2005.03.029
16. Liotta D, Hall CW, Henly WS, Cooley DA, Crawford ES, DeBakey ME. Prolonged assisted circulation during and after cardiac or aortic surgery: prolonged partial left ventricular bypass by means of intracorporeal circulation. *Am J Cardiol.* (1963) 12:399–405. doi: 10.1016/0002-9149(63)90235-2
17. Cook JL, Colvin M, Francis GS, Grady KL, Hoffman TM, Jessup M, et al. Recommendations for the use of mechanical circulatory support: ambulatory and community patient care: a scientific statement from the american heart association. *Circulation.* (2017) 135:e1145–58. doi: 10.1161/CIR.0000000000000507
18. Wilson SR, Givertz MM, Stewart GC, Mudge GH. Ventricular assist devices. *J Am Coll Cardiol.* (2009) 54:1647–59. doi: 10.1016/j.jacc.2009.06.035
19. Kirklin JK, Naftel DC, Pagani FD, Kormos RL, Stevenson LW, Blume ED, et al. Seventh INTERMACS annual report: 15,000 patients and counting. *J Hear Lung Transplant.* (2015) 34:1495–504. doi: 10.1016/j.healun.2015.10.003
20. Dang NC, Topkara VK, Mercando M, Kay J, Kruger KH, Aboodi MS, et al. Right heart failure after left ventricular assist device implantation in patients with chronic congestive heart failure. *J Hear Lung Transplant.* (2006) 25:1–6. doi: 10.1016/j.healun.2005.07.008
21. Lima B, Bansal A, Abraham J, Rich JD, Lee SS, Soleimani B, et al. Controversies and challenges of ventricular assist device therapy. *Am J Cardiol.* (2018) 121:1219–24. doi: 10.1016/j.amjcard.2018.01.034
22. Nguyen AB, Uriel N, Adatya S. New challenges in the treatment of patients with left ventricular support: LVAD thrombosis. *Curr Heart Fail Rep.* (2016) 13:302–9. doi: 10.1007/s11897-016-0310-z
23. Slaughter MS, Rogers JG, Milano CA, Russell SD, Conte JV, Feldman D, et al. Advanced heart failure treated with continuous-flow left ventricular assist device. *N Engl J Med.* (2009) 361:2241–51. doi: 10.1056/NEJMoa0909938

24. Banerjee MN, Bolli R, Hare JM. Clinical studies of cell therapy in cardiovascular medicine. *Circ Res.* (2018) 123:266–87. doi: 10.1161/CIRCRESAHA.118.311217
25. Fisher SA, Zhang H, Doree C, Mathur A, Martin-Rendon E. Stem cell treatment for acute myocardial infarction. *Cochrane Database Syst Rev.* (2015) 30:CD006536. doi: 10.1002/14651858.CD006536.pub4
26. Mathur A, Fernández-Avilés F, Dimmeler S, Hauskeller C, Janssens S, Menasche P, et al. The consensus of the Task Force of the European Society of Cardiology concerning the clinical investigation of the use of autologous adult stem cells for the treatment of acute myocardial infarction and heart failure: update 2016. *Eur Heart J.* (2017) 38:2930–5. doi: 10.1093/eurheartj/ehw640
27. Gyöngyösi M, Wojakowski W, Lemarchand P, Lunde K, Tendera M, Bartunek J, et al. Meta-analysis of cell-based cardiac studies (ACCRUE) in patients with acute myocardial infarction based on individual patient data. *Circ Res.* (2015) 116:1346–60. doi: 10.1161/CIRCRESAHA.116.304346
28. Schachinger V, Erbs S, Elsasser A, Haberbosch W, Hambrecht R, Holschermann H, et al. Improved clinical outcome after intracoronary administration of bone-marrow-derived progenitor cells in acute myocardial infarction: final 1-year results of the REPAIR-AMI trial. *Eur Heart J.* (2006) 27:2775–83. doi: 10.1093/eurheartj/ehl388
29. Schächinger V, Erbs S, Elsässer A, Haberbosch W, Hambrecht R, Hölschermann H, et al. Intracoronary bone marrow–derived progenitor cells in acute myocardial infarction. *N Engl J Med.* (2006) 355:1210–21. doi: 10.1056/NEJMoa060186
30. Wollert KC, Meyer GP, Lotz J, Ringes Lichtenberg S, Lippolt P, Breidenbach C, et al. Intracoronary autologous bone-marrow cell transfer after myocardial infarction: the BOOST randomised controlled clinical trial. *Lancet.* (2004) 364:141–8. doi: 10.1016/S0140-6736(04)16626-9
31. Sürder D, Manka R, Moccetti T, Lo Cicero V, Emmert MY, Klersy C, et al. Effect of bone marrow–derived mononuclear cell treatment, early or late after acute myocardial infarction. *Circ Res.* (2016) 119:481–90. doi: 10.1161/CIRCRESAHA.116.308639
32. Traverse JH, Henry TD, Ellis SG, Pepine CJ, Willerson JT, Zhao DXM, et al. Effect of intracoronary delivery of autologous bone marrow mononuclear cells 2 to 3 weeks following acute myocardial infarction on left ventricular function. *JAMA.* (2011) 306:2110. doi: 10.1001/jama.2011.1670
33. Wollert KC, Meyer GP, Müller-Ehmsen J, Tschöpe C, Bonarjee V, Larsen AI, et al. Intracoronary autologous bone marrow cell transfer after myocardial infarction: the BOOST-2 randomised placebo-controlled clinical trial. *Eur Heart J.* (2017) 38:2936–43. doi: 10.1093/eurheartj/ehx188
34. Perin EC, Dohmann HFR, Borojevic R, Silva SA, Sousa ALS, Mesquita CT, et al. Transendocardial, autologous bone marrow cell transplantation for severe, chronic ischemic heart failure. *Circulation.* (2003) 107:2294–302. doi: 10.1161/01.CIR.0000070596.30552.8B
35. Perin EC, Willerson JT, Pepine CJ, Henry TD, Ellis SG, Zhao DXM, et al. Effect of transendocardial delivery of autologous bone marrow mononuclear cells on functional capacity, left ventricular function, and perfusion in chronic heart failure. *JAMA.* (2012) 307:1717–26. doi: 10.1001/jama.2012.418
36. Bartunek J, Terzic A, Davison BA, Filippatos GS, Radovanovic S, Beleslin B, et al. Cardiopoietic cell therapy for advanced ischemic heart failure: results at 39 weeks of the prospective, randomized, double blind, sham-controlled CHART-1 clinical trial. *Eur Heart J.* (2016) 38:ehw543. doi: 10.1093/eurheartj/ehw543
37. Kanda P, Davis DR. Cellular mechanisms underlying cardiac engraftment of stem cells. *Expert Opin Biol Ther.* (2017) 17:1127–43. doi: 10.1080/14712598.2017.1346080
38. Li X, Tamama K, Xie X, Guan J. Improving cell engraftment in cardiac stem cell therapy. *Stem Cells Int.* (2016) 2016:1–11. doi: 10.1155/2016/2470351
39. Balsam LB, Wagers AJ, Christensen JL, Kofidis T, Weissman IL, Robbins RC. Haematopoietic stem cells adopt mature haematopoietic fates in ischaemic myocardium. *Nature.* (2004) 428:668–73. doi: 10.1038/nature02460
40. Bolli R, Hare JM, March KL, Pepine CJ, Willerson JT, Perin EC, et al. Rationale and design of the CONCERT-HF trial (Combination of mesenchymal and c-kit cardiac stem cells as regenerative therapy for heart failure). *Circ Res.* (2018) 122:1703–15. doi: 10.1161/CIRCRESAHA.118.312978
41. Chien KR, Frisén J, Fritsche-Danielson R, Melton DA, Murry CE, Weissman IL. Regenerating the field of cardiovascular cell therapy. *Nat Biotechnol.* (2019) 37:232–7. doi: 10.1038/s41587-019-0042-1
42. Curfman G. Stem Cell Therapy for Heart Failure. *JAMA.* (2019) 321:1186. doi: 10.1001/jama.2019.2617
43. Davis DR. Cardiac stem cells in the post-Anversa era. *Eur Heart J.* (2019) 40:1039–41. doi: 10.1093/eurheartj/ehz098
44. Murry CE, Soonpaa MH, Reinecke H, Nakajima H, Nakajima HO, Rubart M, et al. Haematopoietic stem cells do not transdifferentiate into cardiac myocytes in myocardial infarcts. *Nature.* (2004) 428:664–8. doi: 10.1038/nature02446
45. Sultana N, Zhang L, Yan J, Chen J, Cai W, Razzaque S, et al. Resident c-kit+ cells in the heart are not cardiac stem cells. *Nat Commun.* (2015) 6:8701. doi: 10.1038/ncomms9701
46. Braunwald E. Cell-based therapy in cardiac regeneration. *Circ Res.* (2018) 123:132–7. doi: 10.1161/CIRCRESAHA.118.313484
47. D'amore A, Yoshizumi T, Luketich SK, Wolf MT, Gu X, Cammarata M, et al. Bi-layered polyurethane e Extracellular matrix cardiac patch improves ischemic ventricular wall remodeling in a rat model. *Biomaterials.* (2016) 107:1–14. doi: 10.1016/j.biomaterials.2016.07.039
48. Fedak PWM. Paracrine effects of cell transplantation: modifying ventricular remodeling in the failing heart. *Semin Thorac Cardiovasc Surg.* (2008) 20:87–93. doi: 10.1053/j.semtcvs.2008.04.001
49. Gnecchi M, He H, Liang OD, Melo LG, Morello F, Mu H, et al. Paracrine action accounts for marked protection of ischemic heart by Akt-modified mesenchymal stem cells. *Nat Med.* (2005) 11:367–8. doi: 10.1038/nm0405-367
50. Gnecchi M, Zhang Z, Ni A, Dzau VJ. Paracrine mechanisms in adult stem cell signaling and therapy. *Circ Res.* (2008) 103:1204–19. doi: 10.1161/CIRCRESAHA.108.176826
51. Hodgkinson CP, Bareja A, Gomez JA, Dzau VJ. Emerging concepts in paracrine mechanisms in regenerative cardiovascular medicine and biology. *Circ Res.* (2016) 118:95–107. doi: 10.1161/CIRCRESAHA.115.305373
52. Malliaras K, Marban E. Cardiac cell therapy: where we've been, where we are, and where we should be headed. *Br Med Bull.* (2011) 98:161–85. doi: 10.1093/bmb/ldr018
53. Yoshioka T, Ageyama N, Shibata H, Yasu T, Misawa Y, Takeuchi K, et al. Repair of infarcted myocardium mediated by transplanted bone marrow-derived CD34+ stem cells in a nonhuman primate model. *Stem Cells.* (2005) 23:355–64. doi: 10.1634/stemcells.2004-0200
54. Fuchs S, Baffour R, Zhou YF, Shou M, Pierre A, Tio FO, et al. Transendocardial delivery of autologous bone marrow enhances collateral perfusion and regional function in pigs with chronic experimental myocardial ischemia. *J Am Coll Cardiol.* (2001) 37:1726–32. doi: 10.1016/S0735-1097(01)01200-1
55. Kinnaird T, Stabile E, Burnett MS, Shou M, Lee CW, Barr S, et al. Local delivery of marrow-derived stromal cells augments collateral perfusion through paracrine mechanisms. *Circulation.* (2004) 109:1543–9. doi: 10.1161/01.CIR.0000124062.31102.57
56. Timmers L, Lim SK, Arslan F, Armstrong JS, Hoefer IE, Doevendans PA, et al. Reduction of myocardial infarct size by human mesenchymal stem cell conditioned medium. *Stem Cell Res.* (2008) 1:129–37. doi: 10.1016/j.scr.2008.02.002
57. Timmers L, Lim SK, Hoefer IE, Arslan F, Lai RC, van Oorschot AAM, et al. Human mesenchymal stem cell-conditioned medium improves cardiac function following myocardial infarction. *Stem Cell Res.* (2011) 6:206–14. doi: 10.1016/j.scr.2011.01.001
58. Hynes B, Kumar AHS, O'Sullivan J, Klein Buneker C, Leblond A-L, Weiss S, et al. Potent endothelial progenitor cell-conditioned media-related anti-apoptotic, cardiotrophic, and pro-angiogenic effects post-myocardial infarction are mediated by insulin-like growth factor-1. *Eur Heart J.* (2013) 34:782–9. doi: 10.1093/eurheartj/ehr435
59. Kervadec A, Bellamy V, El Harane N, Arakélian L, Vanneaux V, Cacciapuoti I, et al. Cardiovascular progenitor–derived extracellular vesicles recapitulate the beneficial effects of their parent cells in the treatment of chronic heart failure. *J Hear Lung Transplant.* (2016) 35:795–807. doi: 10.1016/j.healun.2016.01.013

60. Menasché P. The future of stem cells: Should we keep the "stem" and skip the "cells"? *J Thorac Cardiovasc Surg.* (2016) 152:345–9. doi: 10.1016/j.jtcvs.2016.02.058
61. Tseliou E, Fouad J, Reich H, Slipczuk L, de Couto G, Aminzadeh M, et al. Fibroblasts rendered antifibrotic, antiapoptotic, and angiogenic by priming with cardiosphere-derived extracellular membrane vesicles. *J Am Coll Cardiol.* (2015) 66:599–611. doi: 10.1016/j.jacc.2015.05.068
62. Wei K, Serpooshan V, Hurtado C, Diez-Cuñado M, Zhao M, Maruyama S, et al. Epicardial FSTL1 reconstitution regenerates the adult mammalian heart. *Nature.* (2015) 525:479–85. doi: 10.1038/nature15372
63. Mewhort HEM, Turnbull JD, Meijndert HC, Ngu JMC, Fedak PWM. Epicardial infarct repair with basic fibroblast growth factor–enhanced CorMatrix-ECM biomaterial attenuates postischemic cardiac remodeling. *J Thorac Cardiovasc Surg.* (2014) 147:1650–9. doi: 10.1016/j.jtcvs.2013.08.005
64. Mewhort HEM, Turnbull JD, Satriano A, Chow K, Flewitt JA, Andrei AC, et al. Epicardial infarct repair with bioinductive extracellular matrix promotes vasculogenesis and myocardial recovery. *J Hear Lung Transplant.* (2016) 35:661–70. doi: 10.1016/j.healun.2016.01.012
65. Mewhort HEM, Svystonyuk DA, Turnbull JD, Teng G, Belke DD, Guzzardi DG, et al. Bioactive extracellular matrix scaffold promotes adaptive cardiac remodeling and repair. *JACC Basic Transl Sci.* (2017) 2:450–64. doi: 10.1016/j.jacbts.2017.05.005
66. Park D, Mewhort H, Teng G, Belke D, Turnbull J, Svystonyuk D, et al. Heparin augmentation enhances bioactive properties of acellular extracellular matrix scaffold. *Tissue Eng Part A.* (2017) 24:128–34. doi: 10.1089/ten.TEA.2017.0004
67. Mewhort HEM, Lipon BD, Svystonyuk DA, Teng G, Guzzardi DG, Silva C, et al. Monocytes increase human cardiac myofibroblast-mediated extracellular matrix remodeling through TGF-β_1. *Am J Physiol Hear Circ Physiol.* (2016) 310:H716–24. doi: 10.1152/ajpheart.00309.2015
68. Smart N, Riley PR. The epicardium as a candidate for heart regeneration. *Future Cardiol.* (2012). 8:53–69. doi: 10.2217/fca.11.87
69. Masters M, Riley PR. The epicardium signals the way towards heart regeneration. *Stem Cell Res.* (2014) 13:683–92. doi: 10.1016/j.scr.2014.04.007
70. Dettman RW, Denetclaw W, Ordahl CP, Bristow J. Common epicardial origin of coronary vascular smooth muscle, perivascular fibroblasts, and intermyocardial fibroblasts in the avian heart. *Dev Biol.* (1998) 193:169–81. doi: 10.1006/dbio.1997.8801
71. Gittenberger-de Groot AC, Vrancken Peeters MP, Mentink MM, Gourdie RG, Poelmann RE. Epicardium-derived cells contribute a novel population to the myocardial wall and the atrioventricular cushions. *Circ Res.* (1998) 82:1043–52. doi: 10.1161/01.RES.82.10.1043
72. Mikawa T, Gourdie RG. Pericardial mesoderm generates a population of coronary smooth muscle cells migrating into the heart along with ingrowth of the epicardial organ. *Dev Biol.* (1996) 174:221–32. doi: 10.1006/dbio.1996.0068
73. Wessels A, Pérez-Pomares JM. The epicardium and epicardially derived cells (EPDCs) as cardiac stem cells. *Anat Rec Part A Discov Mol Cell Evol Biol.* (2004) 276A:43–57. doi: 10.1002/ar.a.10129
74. Cai C-L, Martin JC, Sun Y, Cui L, Wang L, Ouyang K, et al. A myocardial lineage derives from Tbx18 epicardial cells. *Nature.* (2008) 454:104–8. doi: 10.1038/nature06969
75. Cano E, Carmona R, Ruiz-Villalba A, Rojas A, Chau YY, Wagner KD, et al. Extracardiac septum transversum/proepicardial endothelial cells pattern embryonic coronary arterio–venous connections. *Proc Natl Acad Sci USA.* (2016) 113:656–61. doi: 10.1073/pnas.1509834113
76. Smart N, Bollini S, Dubé KN, Vieira JM, Zhou B, Davidson S, et al. *De novo* cardiomyocytes from within the activated adult heart after injury. *Nature.* (2011) 474:640–4. doi: 10.1038/nature10188
77. Zhou B, Ma Q, Rajagopal S, Wu SM, Domian I, Rivera-Feliciano J, et al. Epicardial progenitors contribute to the cardiomyocyte lineage in the developing heart. *Nature.* (2008) 454:109–13. doi: 10.1038/nature07060
78. Christoffels VM, Grieskamp T, Norden J, Mommersteeg MTM, Rudat C, Kispert A. Tbx18 and the fate of epicardial progenitors. *Nature.* (2009) 458:E8–9. doi: 10.1038/nature07916
79. Dubé KN, Thomas TM, Munshaw S, Rohling M, Riley PR, Smart N. Recapitulation of developmental mechanisms to revascularize the ischemic heart. *JCI Insight.* (2017) 2:e96800. doi: 10.1172/jci.insight.96800
80. Manner J. Does the subepicardial mesenchyme contribute myocardioblasts to the myocardium of the chick embryo heart? A quail-chick chimera study tracing the fate of the epicardial primordium. *Anat Rec.* (1999) 255:212–26. doi: 10.1002/(SICI)1097-0185(19990601)255:2andlt;212::AID-AR11andgt;3.0.CO;2-X
81. Pérez-Pomares JM, Carmona R, González-Iriarte M, Atencia G, Wessels A, Muñoz-Chápuli R. Origin of coronary endothelial cells from epicardial mesothelium in avian embryos. *Int J Dev Biol.* (2002) 46:1005–13.
82. van Wijk B, Gunst QD, Moorman AFM, van den Hoff MJB. Cardiac regeneration from activated epicardium. *PLoS ONE.* (2012) 7:e44692. doi: 10.1371/journal.pone.0044692
83. Cao J, Poss KD. The epicardium as a hub for heart regeneration. *Nat Rev Cardiol.* (2018) 15:631–47. doi: 10.1038/s41569-018-0046-4
84. Olivey HE, Svensson EC. Epicardial–myocardial signaling directing coronary vasculogenesis. *Circ Res.* (2010) 106:818–32. doi: 10.1161/CIRCRESAHA.109.209197
85. Pérez-Pomares JM, de la Pompa JL. Signaling during epicardium and coronary vessel development. *Circ Res.* (2011) 109:1429–42. doi: 10.1161/CIRCRESAHA.111.245589
86. Chablais F, Jazwinska A. The regenerative capacity of the zebrafish heart is dependent on TGF signaling. *Development.* (2012) 139:1921–30. doi: 10.1242/dev.078543
87. Kikuchi K, Holdway JE, Major RJ, Blum N, Dahn RD, Begemann G, et al. Retinoic acid production by endocardium and epicardium is an injury response essential for zebrafish heart regeneration. *Dev Cell.* (2011) 20:397–404. doi: 10.1016/j.devcel.2011.01.010
88. Lavine KJ, Yu K, White AC, Zhang X, Smith C, Partanen J, et al. Endocardial and epicardial derived FGF signals regulate myocardial proliferation and differentiation *in vivo*. *Dev Cell.* (2005) 8:85–95. doi: 10.1016/j.devcel.2004.12.002
89. Wang J, Karra R, Dickson AL, Poss KD. Fibronectin is deposited by injury-activated epicardial cells and is necessary for zebrafish heart regeneration. *Dev Biol.* (2013) 382:427–35. doi: 10.1016/j.ydbio.2013.08.012
90. Lepilina A, Coon AN, Kikuchi K, Holdway JE, Roberts RW, Burns CG, et al. A dynamic epicardial injury response supports progenitor cell activity during zebrafish heart regeneration. *Cell.* (2006) 127:607–19. doi: 10.1016/j.cell.2006.08.052
91. Simões FC, Riley PR. The ontogeny, activation and function of the epicardium during heart development and regeneration. *Development.* (2018) 145:dev155994. doi: 10.1242/dev.155994
92. Zhou B, Honor LB, He H, Ma Q, Oh J-H, Butterfield C, et al. Adult mouse epicardium modulates myocardial injury by secreting paracrine factors. *J Clin Invest.* (2011) 121:1894–904. doi: 10.1172/JCI45529
93. Ruiz-Villalba A, Simón AM, Pogontke C, Castillo MI, Abizanda G, Pelacho B, et al. Interacting resident epicardium-derived fibroblasts and recruited bone marrow cells form myocardial infarction scar. *J Am Coll Cardiol.* (2015) 65:2057–66. doi: 10.1016/j.jacc.2015.03.520
94. Bollini S, Vieira JMN, Howard S, Dubè KN, Balmer GM, Smart N, et al. Re-activated adult epicardial progenitor cells are a heterogeneous population molecularly distinct from their embryonic counterparts. *Stem Cells Dev.* (2014) 23:1719–30. doi: 10.1089/scd.2014.0019
95. Baum J, Duffy HS. Fibroblasts and myofibroblasts: what are we talking about? *J Cardiovasc Pharmacol.* (2011) 57:376–9. doi: 10.1097/FJC.0b013e3182116e39
96. Dixon IMC, Wigle J. Cardiac fibrosis and heart failure : cause or effect? In: *Cardiac Fibrosis and Heart Failure: Cause or Effect?* Springer. (2015). Available online at: https://books.google.ca/books?id=0D0PCgAAQBAJanddq=ian$+$dixon$+$cardiac$+$fibroblast$+$sentinel$+$cellandsource=gbsnavlinkss (accessed February 14, 2019).
97. Fedak PWM, Verma S, Weisel RD, Li R-K. Cardiac remodeling and failure: from molecules to man (Part I). *Cardiovasc Pathol.* (2005) 14:1–11. doi: 10.1016/j.carpath.2004.12.002
98. Pattar SS, Fatehi Hassanabad A, Fedak PWM. Acellular extracellular matrix bioscaffolds for cardiac repair and regeneration. *Front Cell Dev Biol.* (2019) 7:63. doi: 10.3389/fcell.2019.00063
99. Souders CA, Bowers SLK, Baudino TA. Cardiac fibroblast: the renaissance cell. *Circ Res.* (2009) 105:1164–76. doi: 10.1161/CIRCRESAHA.109.209809

100. Fan D, Takawale A, Lee J, Kassiri Z. Cardiac fibroblasts, fibrosis and extracellular matrix remodeling in heart disease. *Fibrogenesis Tissue Repair.* (2012) 5:15. doi: 10.1186/1755-1536-5-15
101. Fang M, Xiang F-L, Braitsch CM, Yutzey KE. Epicardium-derived fibroblasts in heart development and disease. *J Mol Cell Cardiol.* (2016) 91:23–7. doi: 10.1016/j.yjmcc.2015.12.019
102. Braitsch CM, Kanisicak O, van Berlo JH, Molkentin JD, Yutzey KE. Differential expression of embryonic epicardial progenitor markers and localization of cardiac fibrosis in adult ischemic injury and hypertensive heart disease. *J Mol Cell Cardiol.* (2013) 65:108–19. doi: 10.1016/j.yjmcc.2013.10.005
103. Kennedy-Lydon T, Rosenthal N. Cardiac regeneration: epicardial mediated repair. *Proc R Soc B Biol Sci.* (2015) 282:20152147. doi: 10.1098/rspb.2015.2147
104. Travers JG, Kamal FA, Robbins J, Yutzey KE, Blaxall BC. Cardiac fibrosis: the fibroblast awakens. *Circ Res.* (2016) 118:1021–40. doi: 10.1161/CIRCRESAHA.115.306565
105. Brown RD, Ambler SK, Mitchell MD, Long CS. THE CARDIAC FIBROBLAST: therapeutic target in myocardial remodeling and failure. *Annu Rev Pharmacol Toxicol.* (2005) 45:657–87. doi: 10.1146/annurev.pharmtox.45.120403.095802
106. Beltrami CA, Finato N, Rocco M, Feruglio GA, Puricelli C, Cigola E, et al. Structural basis of end-stage failure in ischemic cardiomyopathy in humans. *Circulation.* (1994) 89:151–63. doi: 10.1161/01.CIR.89.1.151
107. Krenning G, Zeisberg EM, Kalluri R. The origin of fibroblasts and mechanism of cardiac fibrosis. *J Cell Physiol.* (2010) 225:631–7. doi: 10.1002/jcp.22322
108. Richardson WJ, Holmes JW. Why is infarct expansion such an elusive therapeutic target? *J Cardiovasc Transl Res.* (2015) 8:421–30. doi: 10.1007/s12265-015-9652-2
109. Badylak SF. The extracellular matrix as a scaffold for tissue reconstruction. *Semin Cell Dev Biol.* (2002) 13:377–83. doi: 10.1016/S1084952102000940
110. Cui Z, Yang B, Li RK. Application of biomaterials in cardiac repair and regeneration. *Engineering.* (2016) 2016:141–8. doi: 10.1016/J.ENG.2016.01.028
111. Domenech M, Polo-Corrales L, Ramirez-Vick JE, Freytes DO. Tissue engineering strategies for myocardial regeneration: acellular versus cellular scaffolds? *Tissue Eng Part B Rev.* (2016) 22:438–58. doi: 10.1089/ten.teb.2015.0523
112. Gaballa MA, Sunkomat JNE, Thai H, Morkin E, Ewy G, Goldman S. Grafting an acellular 3-dimensional collagen scaffold onto a non-transmural infarcted myocardium induces neo-angiogenesis and reduces cardiac remodeling. *J Hear Lung Transplant.* (2006) 25:946–54. doi: 10.1016/j.healun.2006.04.008
113. Serpooshan V, Zhao M, Metzler SA, Wei K, Shah PB, Wang A, et al. The effect of bioengineered acellular collagen patch on cardiac remodeling and ventricular function post myocardial infarction. *Biomaterials.* (2013) 34:9048–55. doi: 10.1016/j.biomaterials.2013.08.017
114. Callegari A, Bollini S, Iop L, Chiavegato A, Torregrossa G, Pozzobon M, et al. Neovascularization induced by porous collagen scaffold implanted on intact and cryoinjured rat hearts. *Biomaterials.* (2007) 28:5449–61. doi: 10.1016/j.biomaterials.2007.07.022
115. Xiang Z, Liao R, Kelly MS, Spector M. Collagen-GAG scaffolds grafted onto myocardial infarcts in a rat model: a delivery vehicle for mesenchymal stem cells. *Tissue Eng.* (2006) 12:2467–78. doi: 10.1089/ten.2006.12.2467
116. Christman KL, Lee RJ. Biomaterials for the treatment of myocardial infarction. *J Am Coll Cardiol.* (2006) 48:907–13. doi: 10.1016/j.jacc.2006.06.005
117. Esmaeili Pourfarhangi K, Mashayekhan S, Asl SG, Hajebrahimi Z. Construction of scaffolds composed of acellular cardiac extracellular matrix for myocardial tissue engineering. *Biologicals.* (2018) 53:10–8. doi: 10.1016/j.biologicals.2018.03.005
118. Rane AA, Christman KL, Jolla L. Biomaterials for the treatment of myocardial infarction A 5-year update. *J Am Coll Cardiol.* (2011) 58:2615–29. doi: 10.1016/j.jacc.2011.11.001
119. Venugopal JR, Prabhakaran MP, Mukherjee S, Ravichandran R, Dan K, Ramakrishna S. Biomaterial strategies for alleviation of myocardial infarction. *J R Soc Interface.* (2012) 9:1–19. doi: 10.1098/rsif.2011.0301
120. Christman KL, Fok HH, Sievers RE, Fang Q, Lee RJ. Fibrin glue alone and skeletal myoblasts in a fibrin scaffold preserve cardiac function after myocardial infarction. *Tissue Eng.* (2004) 10:403–9. doi: 10.1089/107632704323061762
121. Christman KL, Vardanian AJ, Fang Q, Sievers RE, Fok HH, Lee RJ. Injectable fibrin scaffold improves cell transplant survival, reduces infarct expansion, and induces neovasculature formation in ischemic myocardium. *J Am Coll Cardiol.* (2004) 44:654–60. doi: 10.1016/j.jacc.2004.04.040
122. Arnal-Pastor M, Chachques JC, Monleón Pradas M, Vallés-Lluch A. Biomaterials for cardiac tissue engineering. In: Andrades JA, editor. *Regenerative Medicine and Tissue Engineering.* IntechOpen (2013). Available online at: https://www.intechopen.com/books/regenerative-medicine-and-tissue-engineering/biomaterials-for-cardiac-tissue-engineering
123. Lister Z, Rayner KJ, Suuronen EJ. How biomaterials can influence various cell types in the repair and regeneration of the heart after myocardial infarction. *Front Bioeng Biotechnol.* (2016) 4:62. doi: 10.3389/fbioe.2016.00062
124. Fujimoto KL, Tobita K, Merryman WD, Guan J, Momoi N, Stolz DB, et al. An elastic, biodegradable cardiac patch induces contractile smooth muscle and improves cardiac remodeling and function in subacute myocardial infarction. *J Am Coll Cardiol.* (2007) 49:2292–300. doi: 10.1016/j.jacc.2007.02.050
125. Badylak SF. The extracellular matrix as a biologic scaffold material. *Biomaterials.* (2007) 28:3587–93. doi: 10.1016/j.biomaterials.2007.04.043
126. Badylak SF, Freytes DO, Gilbert TW. Reprint of: extracellular matrix as a biological scaffold material: structure and function. *Acta Biomater.* (2015) 23(Suppl):S17–26. doi: 10.1016/j.actbio.2015.07.016
127. Svystonyuk DA, Mewhort HEM, Fedak PWM. Using acellular bioactive extracellular matrix scaffolds to enhance endogenous cardiac repair. *Front Cardiovasc Med.* (2018) 5:35. doi: 10.3389/fcvm.2018.00035
128. Taylor DA, Chandler AM, Gobin AS, Sampaio LC. Maximizing cardiac repair. *Circ Res.* (2017) 120:30–2. doi: 10.1161/CIRCRESAHA.116.309959
129. Swinehart IT, Badylak SF. Extracellular matrix bioscaffolds in tissue remodeling and morphogenesis. *Dev Dyn.* (2016) 245:351–60. doi: 10.1002/dvdy.24379
130. Mosala Nezhad Z, Poncelet A, de Kerchove L, Gianello P, Fervaille C, El Khoury G. Small intestinal submucosa extracellular matrix (CorMatrix®) in cardiovascular surgery: a systematic review. *Interact Cardiovasc Thorac Surg.* (2016) 22:839–50. doi: 10.1093/icvts/ivw020
131. Hodde J, Record R, Tullius R, Badylak S. Fibronectin peptides mediate HMEC adhesion to porcine-derived extracellular matrix. *Biomaterials.* (2002) 23:1841–8. doi: 10.1016/S0142-9612(01)00310-6
132. McPherson TB, Badylak SF. Characterization of fibronectin derived from porcine small intestinal submucosa. *Tissue Eng.* (1998) 4:75–83. doi: 10.1089/ten.1998.4.75
133. Ponce ML, Nomizu M, Delgado MC, Kuratomi Y, Hoffman MP, Powell S, et al. Identification of endothelial cell binding sites on the laminin gamma 1 chain. *Circ Res.* (1999) 84:688–94. doi: 10.1161/01.RES.84.6.688
134. Hodde JP, Badylak SF, Brightman AO, Voytik-Harbin SL. Glycosaminoglycan content of small intestinal submucosa: a bioscaffold for tissue replacement. *Tissue Eng.* (1996) 2:209–17. doi: 10.1089/ten.1996.2.209
135. Seghezzi G, Patel S, Ren CJ, Gualandris A, Pintucci G, Robbins ES, et al. Fibroblast growth factor-2 (FGF-2) induces vascular endothelial growth factor (VEGF) expression in the endothelial cells of forming capillaries: an autocrine mechanism contributing to angiogenesis. *J Cell Biol.* (1998) 141:1659–73. doi: 10.1083/jcb.141.7.1659
136. Witt RG, Raff G, Van Gundy J, Rodgers-Ohlau M, Si M-S. Short-term experience of porcine small intestinal submucosa patches in paediatric cardiovascular surgery. *Eur J Cardio-Thoracic Surg.* (2013) 44:72–6. doi: 10.1093/ejcts/ezs638

137. Gálvez-Montón C, Fernandez-Figueras MT, Martí M, Soler-Botija C, Roura S, Perea-Gil I, et al. Neoinnervation and neovascularization of acellular pericardial-derived scaffolds in myocardial infarcts. *Stem Cell Res Ther.* (2015) 6:108. doi: 10.1186/s13287-015-0101-6
138. Khorramirouz R, Kameli SM, Fendereski K, Daryabari SS, Kajbafzadeh A-M. Evaluating the efficacy of tissue-engineered human amniotic membrane in the treatment of myocardial infarction. *Regen Med.* (2019) 14:113–26. doi: 10.2217/rme-2018-0024
139. Robinson KA, Li J, Mathison M, Redkar A, Cui J, Chronos NAF, et al. Extracellular matrix scaffold for cardiac repair. *Circulation.* (2005) 112(Suppl 9):I135–43. doi: 10.1161/CIRCULATIONAHA.104.525436
140. Sarig U, Sarig H, de-Berardinis E, Chaw SY, Nguyen EBV, Ramanujam VS, et al. Natural myocardial ECM patch drives cardiac progenitor based restoration even after scarring. *Acta Biomater.* (2016) 44:209–20. doi: 10.1016/j.actbio.2016.08.031
141. Hadas Y, Katz MG, Bridges CR, Zangi L. Modified mRNA as a therapeutic tool to induce cardiac regeneration in ischemic heart disease. *Wiley Interdiscip Rev Syst Biol Med.* (2017) 9:e1367. doi: 10.1002/wsbm.1367
142. Hulot JS, Ishikawa K, Hajjar RJ. Gene therapy for the treatment of heart failure: promise postponed. *Eur Heart J.* (2016) 37:1651–8. doi: 10.1093/eurheartj/ehw019
143. Zangi L, Lui KO, von Gise A, Ma Q, Ebina W, Ptaszek LM, et al. Modified mRNA directs the fate of heart progenitor cells and induces vascular regeneration after myocardial infarction. *Nat Biotechnol.* (2013) 31:898–907. doi: 10.1038/nbt.2682

Conflict of Interest Statement: The authors declare that the research was conducted in the absence of any commercial or financial relationships that could be construed as a potential conflict of interest.

frontiers in Cardiovascular Medicine

ORIGINAL RESEARCH
published: 19 May 2020
doi: 10.3389/fcvm.2020.00069

Physiologically Relevant Fluid-Induced Oscillatory Shear Stress Stimulation of Mesenchymal Stem Cells Enhances the Engineered Valve Matrix Phenotype

Brittany A. Gonzalez[1†], Manuel Perez-Nevarez[1†], Asad Mirza[1†], Marcos Gonzalez Perez[1], Yih-Mei Lin[1], Chia-Pei Denise Hsu[1], Allen Caobi[2], Andrea Raymond[2], Mario E. Gomez Hernandez[3,4], Francisco Fernandez-Lima[3,4], Florence George[5] and Sharan Ramaswamy[1]*

[1] Cardiovascular Therapeutics Laboratory (CV-PEUTICS Lab), Department of Biomedical Engineering, Florida International University, Miami, FL, United States, [2] Department of Immunology and Nano-Medicine, Florida International University, Miami, FL, United States, [3] Advanced Mass Spectrometry Facility, Florida International University, Miami, FL, United States, [4] Department of Chemistry and Biochemistry, Florida International University, Miami, FL, United States, [5] Department of Mathematics and Statistics, Florida International University, Miami, FL, United States

OPEN ACCESS

Edited by:
Maurizio Pesce,
Centro Cardiologico Monzino (IRCCS), Italy

Reviewed by:
Huseyin Cagatay Yalcin,
Qatar University, Qatar
Xuechong Hong,
Boston Children's Hospital and Harvard Medical School, United States

***Correspondence:**
Sharan Ramaswamy
sramaswa@fiu.edu

[†]These authors have contributed equally to this work

Specialty section:
This article was submitted to Cardiovascular Biologics and Regenerative Medicine, a section of the journal Frontiers in Cardiovascular Medicine

Received: 30 December 2019
Accepted: 07 April 2020
Published: 19 May 2020

Citation:
Gonzalez BA, Perez-Nevarez M, Mirza A, Perez MG, Lin Y-M, Hsu C-PD, Caobi A, Raymond A, Gomez Hernandez ME, Fernandez-Lima F, George F and Ramaswamy S (2020) Physiologically Relevant Fluid-Induced Oscillatory Shear Stress Stimulation of Mesenchymal Stem Cells Enhances the Engineered Valve Matrix Phenotype. Front. Cardiovasc. Med. 7:69. doi: 10.3389/fcvm.2020.00069

Support of somatic growth is a fundamental requirement of tissue-engineered valves. However, efforts thus far have been unable to maintain this support long term. A key event that will determine the valve's long-term success is the extent to which healthy host tissue remodeling can occur on the valve soon after implantation. The construct's phenotypic-status plays a critical role in accelerating tissue remodeling and engineered valve integration with the host via chemotaxis. In the current study, human bone-marrow-derived mesenchymal stem cells were utilized to seed synthetic, biodegradable scaffolds for a period of 8 days in rotisserie culture. Subsequently, cell-seeded scaffolds were exposed to physiologically relevant oscillatory shear stresses (overall mean, time-averaged shear stress, ~7.9 dynes/cm^2; overall mean, oscillatory shear index, ~0.18) for an additional 2 weeks. The constructs were found to exhibit relatively augmented endothelial cell expression (CD31; compared to static controls) but concomitantly served to restrict the level of the activated smooth muscle phenotype (α-SMA) and also produced very low stem cell secretion levels of fibronectin ($p < 0.05$ compared to static and rotisserie controls). These findings suggest that fluid-induced oscillatory shear stresses alone are important in regulating a healthy valve phenotype of the engineered tissue matrix. Moreover, as solid stresses could lead to increased α-SMA levels, they should be excluded from conditioning during the culture process owing to their associated potential risks with pathological tissue remodeling. In conclusion, engineered valve tissues derived from mesenchymal stem cells revealed both a relatively robust valvular phenotype after exposure to physiologically relevant scales of oscillatory shear stress and may thereby serve to accelerate healthy valve tissue remodeling in the host post-implantation.

Keywords: somatic growth, engineered valve, mechanical conditioning, physiologically relevant, mesenchymal stem cells, endothelial phenotype, smooth muscle phenotype, oscillatory flow

INTRODUCTION

Heart valve disease requires a largely singular treatment in the form of artificial valve replacement. Indeed, prosthetic valve replacement devices offer reasonable solutions; however, durability and risk factors are of concern. Mechanical heart valves are durable but carry increased risks of blood clotting and require life-long anticoagulation therapy, excluding them from patient subsets, such as children with critical congenital valve defects. Bioprosthetic valves are well-tolerated by the body but are not durable and exhibit accelerated calcification, particularly in younger patients (1). Hence, in the case of pediatric critical congenital valvular diseases, no ideal treatment options exist as somatic growth is required to avoid multiple reoperations as the child grows; in addition small, sizing options [<15 mm (2)] for artificial valves remain unavailable commercially.

Regenerative medicine using tissue-engineered valvular constructs (TEVCs) may provide long lasting solutions for the treatment of critical congenital heart valve diseases in the young. TEVCs are potentially ideal because they can provide somatic growth, biological repair, and remodeling. TEVCs offer the promise of fully replacing valvular tissue functionality and the long-term integration with host tissues, without the need of surgical reinterventions.

Evidence suggests that stem cells can facilitate the acceleration of tissue production and regeneration (3). A variety of stem cells are available and used in tissue repair and regeneration including mesenchymal stem cells (MSCs). MSCs are of particular interest in cardiovascular regeneration due to their potential for self-renewal and differentiation (3). Moreover, MSCs have an added benefit of immunomodulation and angiogenesis promotion, both factors that will enhance TEVCs (3).

To develop TEVCs, it is generally accepted that mechanical forces innate to the cardiovascular system, namely, flow, stretch, and flex, can optimize *in vitro de novo* tissue growth (4–6). To facilitate this mechanical conditioning, bioreactors are commonly used to dynamically culture engineered valve tissue constructs (5, 6). The general approach to dynamically culture tissue engineered valves begins with seeding of the cells on a scaffold of choice and placing them in a bioreactor that simulates the mechanical conditions to support valvular tissue formation and phenotype of interest. Our group, and others, have previously shown that human bone marrow mesenchymal stem cells (hBM-MSCs) can produce robust engineered tissues *in vitro* (5, 7). Moreover, these seeded hBM-MSCs were able to differentiate to both endothelial cells on the surface and activated interstitial cells deeper within the constructs, similar to the native valve, when exposed to a combination of physiologically relevant cyclic flexure (1 Hz) and steady fluid-induced shear stress (4–5 dynes/cm^2) states (5). The combination of cyclic flexure and steady flow (flex–flow) induces pulsatile and/or oscillatory flow patterns on the surfaces of TEVCs. Our work, as well as others, have shown the importance of oscillatory flow conditions on developing valve tissues (6, 8–10). However, a physiologically relevant pulsatile flow waveform may be able to induce oscillations similar to the conditions experienced in the native valve, which will mechanically condition these TEVCs. Indeed, we previously were able to show that hBM-MSCs have a significant upregulation of valve phenotypic gene expression, while valve disease-relevant genes, including osteogenic markers, were significantly downregulated after exposure to an aortic pulsatile flow profile (2D) for 48 h (11), in monolayer culture.

In the current study, we scaled our investigation to three dimensions utilizing hBM-MSC-seeded scaffolds that were mechanically conditioned using a physiologically relevant, aortic pulsatile flow waveform (11). In particular, we subsequently assessed the resulting phenotypic changes to the engineered tissue constructs after being subjected to oscillatory shear stresses resulting from the aortic flow profile, in comparison to our previous work in which oscillatory patterns in the culture media was induced under a combination of steady flow and cyclic flexure, i.e., flex–flow (cyclic flexure of 1 Hz and steady fluid-induced shear stress of 4–5 dynes/cm^2). Notably, in the current study, the oscillations were solely fluid induced, without any structural deformation (e.g., cyclic flexure or cyclic stretch) of the specimens. He and Ku (12) have previously shown that these fluid oscillations can be quantified using the oscillatory shear index (OSI; Equation 1). Similarly, wall shear stress (WSS) has been reported to affect differentiation of valve-specific phenotypes (13). The time-averaged WSS (TAWSS) was used as metric to quantify the physiological relevance of the shear stress magnitudes on the surface of the specimens (Equation 2).

$$\mathrm{OSI} = 0.5\left(1 - \frac{\left|\int_0^T \overrightarrow{\mathrm{WSS}}\,\mathrm{dt}\right|}{\int_0^T \left|\overrightarrow{\mathrm{WSS}}\right|\mathrm{dt}}\right) \quad (1)$$

$$\mathrm{TAWSS} = \frac{1}{T}\int_0^T \left|\overrightarrow{\mathrm{WSS}}\right|\mathrm{dt} \quad (2)$$

MATERIALS AND METHODS

Computational Model Setup

Computational fluid dynamic (CFD) simulations were performed using commercially available software (COMSOL, Burlington, MA). An adaptation of the flow–stretch–flex (FSF) bioreactor geometry (7) was used, which primarily consisted of a U-shaped housing with a constant internal diameter of 13 mm (**Figure 1A**). This computational geometry had been previously used by our laboratory in numerous studies (5, 6, 9). The meshed geometry consisted of 441,000 elements and 472,000 nodes, which was based off our previous, validated mesh of the same geometry (11). Each side of the cell-seeded scaffold specimens was identified as either the proximal or distal side relative to its physical distance to the centerline axis of the bioreactor (**Figure 1A**).

The inlet CFD velocity waveform (**Figure 1B**) was derived from the experimentally captured bioreactor inlet flow waveform (see *Bioreactor Setup*); a time step of 2 ms was applied. The outlet was set to a pressure condition (**Figure 1B**) using an acquired pressure waveform from our transducers (**Supplementary Figure A**). The walls of the bioreactor were prescribed a no-slip boundary condition. The fluid was assumed

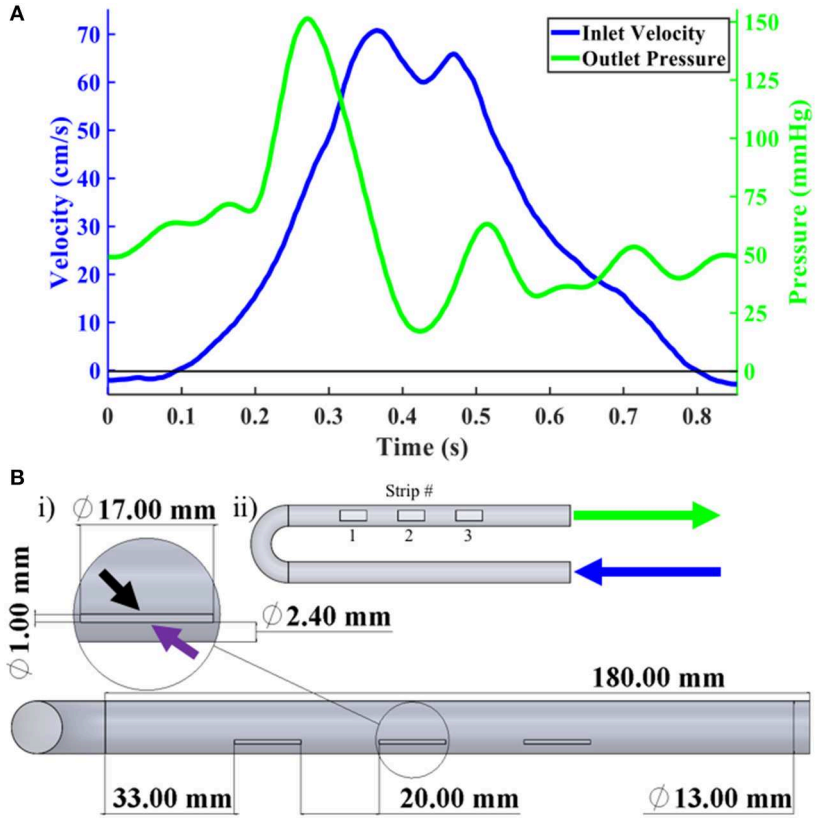

FIGURE 1 | Boundary conditions and FSF Bioreactor CAD. **(A)** i) Overall CAD geometry of FSF bioreactor primarily showing the three scaffold strip locations. Magnified inset showed one of the scaffold strips with the black and purple arrows pointing to the proximal and distal sides, respectively. ii) Scaffold strip numbering designation as well as arrow labels showing inlet (blue) and outlet (green), which correspond with the information from **(B)** regarding their respective velocity and pressure profiles. **(B)** Velocity (blue), in cm/s, and pressure (green), in mmHg, waveforms recorded by our flow probe and pressure transducers.

to be incompressible with a constant density of 1.01 g/cm^3, which matched that of basal cell culture media, and a dynamic viscosity of 1.27 cP (7). A convergence criterion of 1×10^{-9} was set for the residuals of the continuity and momentum equations. After ensuring cyclic independence between three cycles, the results from the second cycle were analyzed.

hBM-MSCs Culture and Expansion

A total of 2×10^6 hBM-MSCs (RoosterVial-hBM-1M, RoosterBio, Part No. MSC-003) were plated into six T75 flasks ($n = 3$ flasks/vial) with culture medium (h-MSC high-performance basal medium, RoosterBio, Part No. SU-005) and supplement (RoosterBooster-MSC Media Booster, RoosterBio, Part No. SU-003). The media was changed every 3 days until the hBM-MSCs were confluent, which were then harvested according to the manufacturer's protocol. In brief, the media was removed for each T75, and 3 ml of 0.25% trypsin was added and incubated in 37°C for 5 min. An equal amount of fresh media was added to the flasks and transferred to 50 ml conical tubes and centrifuged at 200 × *g* for 10 min. The supernatant was removed and resuspended in new media. The hBM-MSCs were grown to passage 6 with a total density of 18×10^6 cells.

Scaffold Preparation and Cell Seeding

An equal ratio of poly-glycolic acid (PGA) and poly-L-lactic acid (PLLA) non-woven polymer felt (PGA-PLLA; Biofelt, Biomedical Structures, Warwick, RI) (4, 14, 15), scaffolds were used for this experiment. Scaffolds were cut in rectangular-shaped strips (17 × 6 × 1 mm, $n = 9$) and gas sterilized with ethylene oxide (EtO; AN 306, Anprolene, Andersen Products Inc., HawRiver, NC) for 12 h and treated with 70% ethanol before seeding. The seeding of the hBM-MSCs on the scaffolds were similar to our previous studies (5); the supernatant was removed, and the cell pellet was resuspended with fresh Dulbecco's modified Eagle's medium (DMEM, Fisher Scientific), supplemented with 10% fetal bovine serum (Atlanta Biologics, GA, USA), 1% penicillin and streptomycin (Thermo Scientific™ HyClone™; Fisher Scientific), 2 ng/ml basic fibroblast growth factor (bFGF, Corning™; Fisher Scientific), and 82 µg/ml ascorbic acid 2 phosphate (AA2P, Sigma-Aldrich). Each scaffold was placed in a 50-ml vented conical tube (Product no. TP87050, TPP, TubeSpin Bioreactor, Zollstrasse 7, CH-8219 Trasadingen, Switzerland) and seeded with 2×10^6 hBM-MSCs in 20 ml of tissue culture media. These tubes were then placed in a rotisserie (Labquake™ Rotisserie Hybridization Rotators, Thermo Scientific, USA) at

8 rpm in the incubator with controlled cell culture conditions (37°C, 5% CO_2) for 8 days without media change.

Bioreactor Setup

A flow perfusion bioreactor system was used to subject the seeded scaffolds to physiologically relevant pulsatile aortic flow regimens. Specific components of the system included a separable and insertable cylindrical specimen holder (**Figure 2A**), *U*-shaped bioreactor chambers (**Figure 2B**) that housed the hBM-MSC-seeded scaffolds (7), and flow that was facilitated by a programmable pulsatile pump system (ViVitro Labs Inc., Victoria, BC, Canada). Three scaffolds were placed in each bioreactor chamber in a parallel configuration to the flow direction and were fully immersed in the media solution (**Figure 2C**). Note that this bioreactor system and its applicability for heart valve tissue engineering purposes has been previously validated (7).

The long axis of each scaffold specimen was oriented parallel to the direction of flow, with flow passing over their surfaces. The pump was connected via silicone tubing (Masterflex 96410-35, Cole-Parmer, Vernon Hills, IL) to two bioreactor chambers in a parallel configuration (**Figure 3**). The diameter of the tubing was 0.5 in, reflecting a spatial dimension closer to that of the descending aorta [normal diameter of the aorta ranges between 0.3″ and 0.6″ from infant to adolescent (16)]. Other components of the flow loop (**Figure 4**) included a glass media bottle, flow probes (Carolina Medical Electronics Inc., NC, USA), pressure sensors, and test software (Vivitest, ViVitro Systems), used to obtain the relevant hydrodynamic data during the flow and pressure testing phase.

To validate that the required flow waveform imparted by the pulsatile pump (S35-HR70-SV40) physiological waveform (Vivitest software, Vivtro Laboratories) was reproduced within the bioreactor chamber at the site of the hBM-MSC-seeded

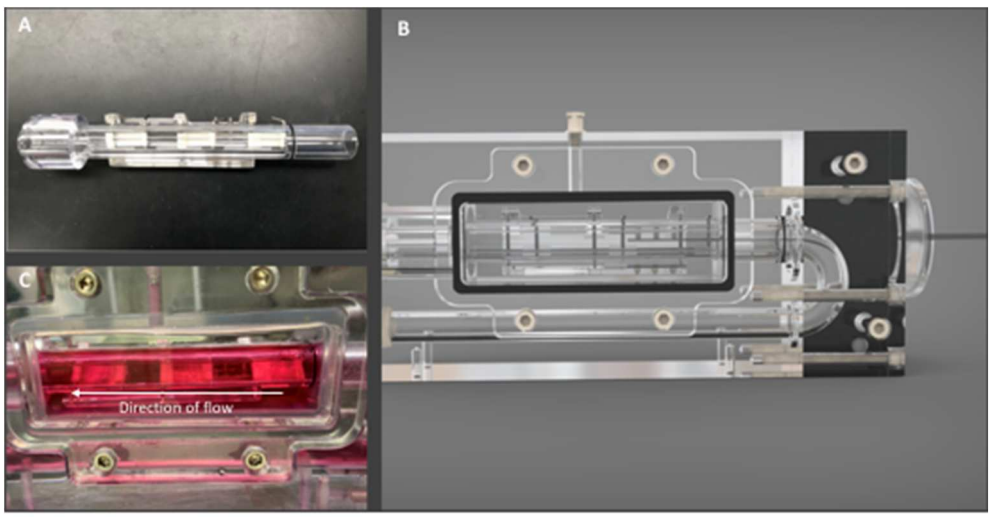

FIGURE 2 | Bioreactor components. **(A)** View of scaffold holder detailing the positioning of scaffolds with metal pins, **(B)** bioreactor chamber with imaging window for direct view of scaffold holder within the chamber, and **(C)** Bioreactor imaging window with scaffolds immersed in flow media. Arrow signifies the direction of flow.

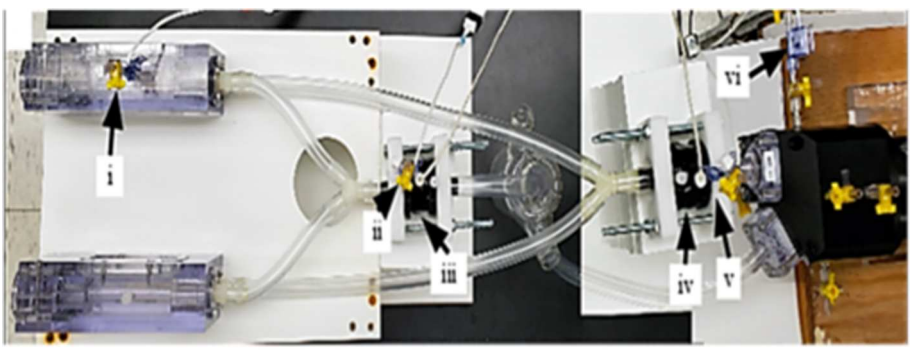

FIGURE 3 | Assembled bioreactor pulsatile flow loop. The major components of the bioreactor include: the **(i)** pressure sensor at bioreactor chamber, **(ii)** pressure sensor at bioreactor exit, **(iii)** flow probe at bioreactor exit, **(iv)** flow probe at pump exit, **(v)** pressure sensor at pump exit, and the **(vi)** pressure sensor inserted into pump-head interior.

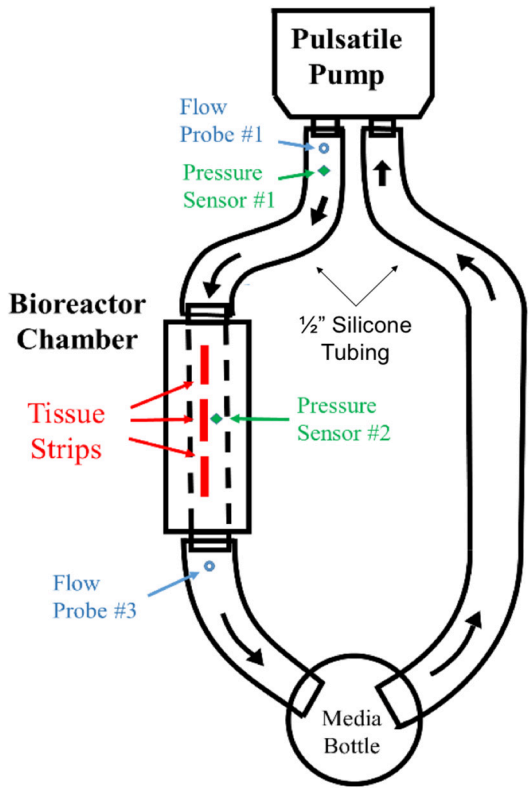

FIGURE 4 | Flow diagram for FSF bioreactor dynamic conditioning system. Pressure and flow sensors at pump outlet (V1, P1) and at a pressure sensor at bioreactor chamber (P2) were used to validate flow velocities within the bioreactor chamber.

scaffolds, flow and pressure sensors were placed at the pump exit location to record pump output flowrate (Q_1) and pressure (P_1) data (**Figures 3iv,v**). Note also that for the purposes of validation, only a single chamber (as opposed to two parallel chambers used in the tissue engineering experiments; **Figure 3**) was used. The flow velocity (V_1) at the pump output location was subsequently computed using conservation of mass principles as:

$$Q_1 = V_1 A_1 \tag{3}$$

A pressure sensor was inserted in the bioreactor housing at the mid-point directly overhead of the scaffold flow field (P_2 location; **Figure 3i**). With the application of the Bernoulli's equation (Equation 4), the velocity within the bioreactor chamber (V_2) was estimated (Equation 5) and its corresponding flow rate subsequently computed (Q_2; Equation 6). Additionally, a flow probe was placed at the exit of the bioreactor chamber (**Figure 3ii**) to further validate flow conditions (Q_3) within the chamber and scaffold specimens.

$$P_1 + \frac{\rho V_1^2}{2} + \rho g h_1 = P_2 + \frac{\rho V_2^2}{2} + \rho g h_2 \tag{4}$$

$$V_2 = \sqrt{V_1^2 + \frac{2}{\rho}(P_1 - P_2)} \tag{5}$$

$$Q_2 = V_2 A_2 \tag{6}$$

Flow and pressure data for 10 pulse cycles were collected and averaged to produce flowrate waveforms for pump exit (V_1 location; **Figure 3iv**), bioreactor chamber (V_2 location; **Figure 3i**) and bioreactor exit (V_3 location; **Figure 3iii**). These three flow profiles were then plotted to compare the pump output waveform to the corresponding pulsatile flow field that was presented at the site of the hBM-MSC-seeded scaffold specimens and at the exit location of the bioreactor chamber (**Figure 3**). A percentage error in maximum and mean flowrates between the pump output region and the two secondary locations were subsequently computed as:

$$\text{Max Flow Rate \% Error} : \quad \frac{\text{max flow @ pump exit} - \text{max flow @ specimen}}{\text{max flow @ pump exit}} \times 100\% \tag{7}$$

$$\text{Mean Flow Rate \% Error} : \quad \frac{\text{mean flow @ pump exit} - \text{mean flow @ specimen}}{\text{mean flow @ pump exit}} \times 100\% \tag{8}$$

Tissue Engineering Experiments

After the hBM-MSCs were seeded on the scaffolds, the specimens were subjected to 8 days of rotisserie culture; next, they were split into two groups: (1) no flow (static controls, $n = 3$) and (2) physiological oscillatory flow (bioreactor group, $n = 3$/chamber). The cell-seeded specimens in the no flow group (hereby referred to as the "static" group) were immersed in media within a 6-well plate and left within in a tissue culture incubator for an additional 14 days without media change. Meanwhile for the oscillatory flow group, the cell-seeded specimens were sutured on both ends to metallic springs and inserted onto stationary rods within a *U*-shaped bioreactor device (drawings and details in (7)). The bioreactors were then connected to a pneumatic piston pulsatile flow pump, with a pump head module (ViVitro Labs Inc., Victoria, BC, Canada) that housed the tubing to transport media to the specimens housed within the bioreactors (one bioreactor chamber contained another scaffold material that was conditioned identically, but not connected to the present study). Physiologically relevant fluid-induced wall shear stresses (WSS) of 3–9 dynes/cm^2 have been shown to be conducive to proper cell conditioning (17). Similarly, fluid oscillations, measured with oscillatory shear index (OSI), between 0.18 and 0.23 have been reported to assist in promoting genes that support the valve phenotype (11). Hence, an aortic flow waveform (11), which could elicit valve relevant of TAWSS and OSI (as determined from the CFD simulations; *Computational Model Setup*) was applied to the bioreactor for an additional 14 days, beyond the initial 8-days rotisserie culture period. Total culture time of the engineered tissue constructs in both the static and bioreactor time was therefore 22 days (using the same media formulation as in *Scaffold Preparation and Cell Seeding*), which consisted of 8 days rotisserie culture followed by either an additional 14 days static or 14 days pulsatile flow culture. Viability of cells after bioreactor culture was verified independently via observation of cell proliferation prior and after a 14-days oscillatory flow conditioning experiment with stem cells (unpublished observation).

Immunofluorescence

Once the experiment was complete, the scaffolds were prepared for immunofluorescence assessment similar to our previous work (18). In brief, the scaffolds were fixed in formalin (10% *v*/*v*) for 24 h followed by embedding in a slow freeze process in optimal cutting temperature (OCT). The embedded samples were then placed in −80°C overnight and then sliced (16 μm of thickness) and placed on glass slides (TruBond 380, Newcomer Supply, Middleton, "Wisconsin") and left to dry at room temperature to allow for immunofluorescence staining. The slides were stained with primary antibodies for valvular components, including endothelial and interstitial cells; CD31 was used as an endothelial

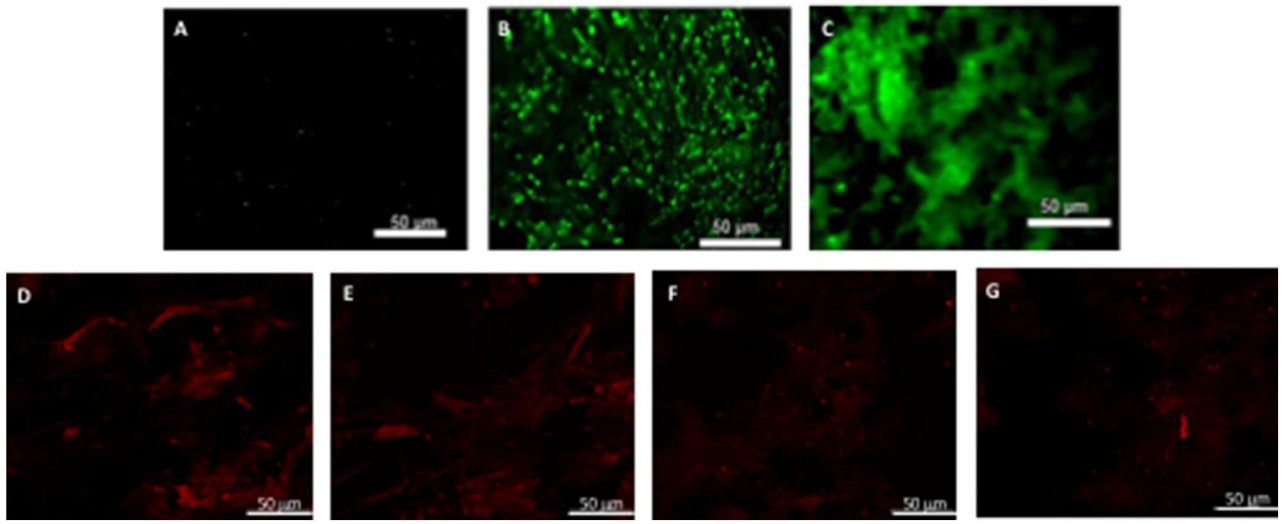

FIGURE 5 | hBM-MSCs differentiation toward α-SMA phenotype. PGA-PLLA scaffolds seeded with hBM-MSCs (5) demonstrated the presence of α-SMA phenotype in **(A)** static, **(B)** flex-flow and **(C)** PHV groups; the same cell-seeded scaffolds from our experiments focusing on **(D,E)** static, and **(F,G)** physiologically-relevant oscillatory flow groups demonstrate the presence of α-SMA phenotype. Image magnification of 72X.

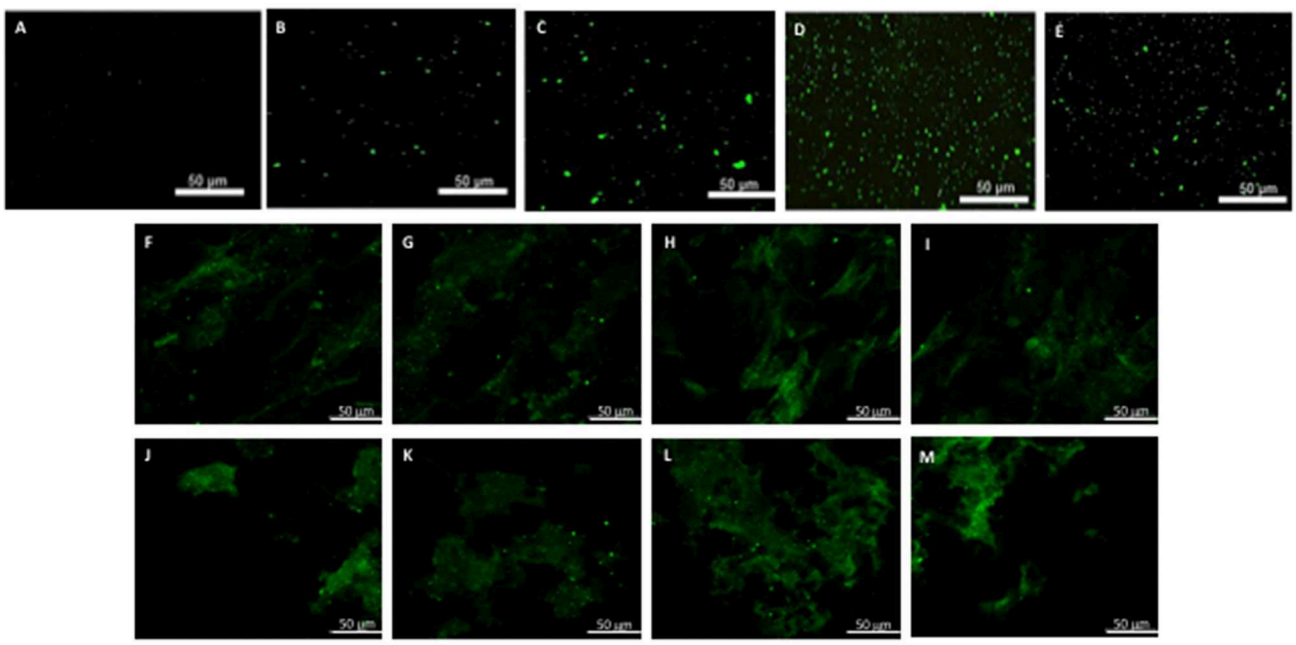

FIGURE 6 | hBM-MSCs differentiation toward CD31 phenotype. PGA-PLLA scaffolds seeded with hBM-MSCs (5) demonstrated the presence of CD31 phenotype in **(A)** static, **(B,C)** flex-flow, and **(D,E)** PHV groups; the same cell-seeded scaffolds from our experiments focusing on **(F–I)** static and **(J–M)** physiologically-relevant oscillatory flow groups demonstrate the presence of CD31 phenotype. Image magnification of 72X.

cell marker (Invitrogen, REF: PA5-14372), and alpha smooth muscle actin (α-SMA) was used as an interstitial cell marker (Invitrogen, REF: 14-9760-82), separately. Donkey antirabbit (Abcam, ab150073) and donkey antimouse (Abcam, ab150108) were used as secondary antibodies, respectively, for CD31 and α-SMA. Immunofluorescence images were captured with confocal microscopy (Nikon Eclipse T*i*, Minato, Tokyo, Japan).

All samples from the static control and oscillatory flow groups were stained for CD 31 and α-SMA immunostaining at the same time. On the other hand, in order to make observations with previously reported (5) samples from flex–flow experiments and positive porcine valve (PHV) controls, the signal intensities in all groups were normalized relative to the average intensity of the static samples across the previous and the present investigations.

Image Analysis

Images from previous work in our laboratory were gathered for comparison purposes (static, flex–flow, and porcine native heart valve) [**Figures 5A–C**, **6A–E**, (5)], while confocal images of α-SMA and CD31 were taken on our experimental groups of static (no flow) and bioreactor (oscillatory flow) groups (**Figures 5D–G**, **6F–M**). All images were sized to a resolution of 1,024 × 690 pixels to be able to make these comparisons. The static images, from both our experiments and from our previous work, were merged together into and averaged static image (MATLAB, Mathworks, Natick, MA). The mean intensity of this image was determined and was used to normalize the average static image. This image was used, with its mean intensity, to normalize all the other groups of interest (i.e., oscillatory flow, flex–flow, and PHV). Heat maps were computed (MATLAB) to demonstrate the intensity differences in the pixels of each image, maintaining the same scale throughout. This procedure was used for α-SMA and CD31 images independently.

Protein Quantification

Conditioned media was collected from static, 8-days rotisserie, and oscillatory flow groups and centrifuged at 3,000 × *g* for 15 min to remove cell debris. An appropriate volume of ExoQuick-TC solution (System Biosciences, Palo Alto, CA) was added to each group to precipitate the exosomes that were secreted by hBM-MSCs. The media/ExoQuick-TC mixture was refrigerated overnight (∼16 h) at 4°C and then centrifuged at 1,500 × *g* for 30 min. The supernatant was removed, and the residual of ExoQuick-TC precipitation solution was aspirated after the centrifugation at 1,500 × *g* for 5 min. Exosome pellets were resuspended in 250 μl phosphate-buffered saline (PBS) and filtered with 0.2-μm syringe filters (Thermo Scientific™ Nalgene™, Fisher Scientific, Hampton, NH) (**Figure 7**). To extract proteins from the membrane of exosomes, radioimmunoprecipitation assay (RIPA) buffer (Fisher Scientific) was added at the ratio 1:1. The mixture was gently shaken on ice for 15 min and centrifuged at 14,000 × *g* for 15 min. DC Protein Assay (Bio-Rad, Hercules, CA, USA) was used to determine protein concentration. The absorbance of the samples was read at 800 nm wavelength by a spectrophotometer (Synergy HT, BioTek Instruments Inc., Winooski, VT).

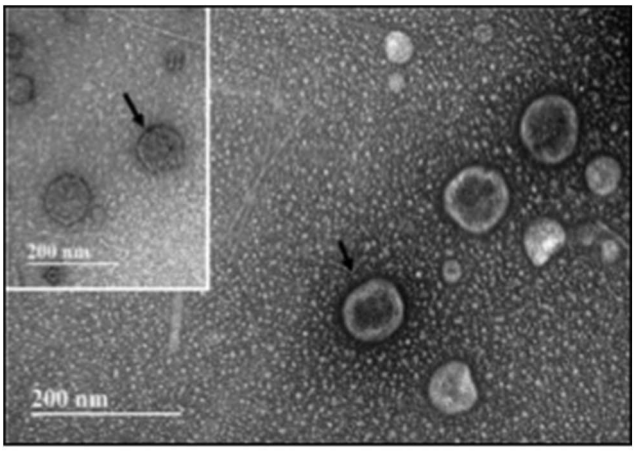

FIGURE 7 | Transmission electron microscopy (TEM) of exosomes isolated from hBM-MSCs after an initial 8 days of rotisserie culture and followed by oscillatory flow conditioning in our bioreactor for 2 weeks. Insert: Immunogold labeling with CD 9 antibody. Arrow indicates site of CD9-Immunogold labeling. Scale bar = 200 nm.

Liquid Chromatography–Tandem Mass Spectrometry Analysis

Samples were digested according to the protocol of In-Solution Tryptic Digestion and Guanidination Kit (Thermo Scientific™, Fisher Scientific). In brief, samples were first reduced and denatured with 15 μl digestion buffer and 1.5 μl reducing buffer and incubated at 95°C for 5 min. Afterwards, 3 μl alkylation buffer was added to the samples to perform the process of alkylation in the dark at room temperature for 20 min. Second, 1 μl activated trypsin was added for digestion and incubated at 37°C for 3 min. Additional 1 μl activated trypsin was added, and the samples were incubated overnight (∼18 h) at 30°C. Lastly, 3 μl formic acid (Thermo Scientific™ Pierce™ LC-MS Grade, Fisher Scientific) was added to stop the reaction. Liquid chromatography–tandem mass spectrometry (LC-MSMS) analysis was conducted on a Bruker tims-TOF UHR MS (Bruker Scientific. Billerica, MA) instrument operated in positive (+) ion mode in the mass range from 300 to 2,400. Chromatography separation was conducted utilizing a 46-min-long LC method with optima grade water (0.1% formic acid) as the aqueous phase and optima grade acetonitrile with (0.1% formic) as the organic phase on a Shimadzu Prominence HPLC (Tokyo, Japan) equipped with a Waters XBridge C18 Proteomics Column (Milford, MA). Moreover, the in-solution digested extracts were diluted 1:10 in 50:50 MeOH/water [0.1% formic acid (FA)] and stored in silanized glass inserts placed inside a sampling vial, which were then loaded onto a high-performance liquid chromatography (HPLC) autosampler (Shimadzu Prominence, Nakagyo-ku, Japan). Thereafter, a 20-μl aliquot was injected into the HPLC for separation prior to mass spectrometry (MS) analysis. The MS was calibrated with a tuning mix solution (Agilent, Santa Clara, CA) with a reported standard deviation <1 ppm. Tandem MS/MS peptide

fragmentation was conducted with collision-induced dissociation of the 25 most abundant precursors. After data acquisition, the obtained raw mass spectrometry data were processed using Peaks Studio 8.5 (Bioinformatics Solution Inc., Waterloo, ON, Canada) for protein identification, peptide sequencing, and label-free quantification.

Statistical Analysis

All results were reported as means ± standard error of mean. The average intensities of the images (averages static, oscillatory flow) were statistically analyzed via a *t*-test whenever normality was held; otherwise, a non-parametric test was used (Minitab, Inc., State College, PA). For fibronectin protein intensity from the collected media a log-transformed dataset was used to perform a parametric ANOVA and Tukey's honestly significant difference (HSD). Statistical significance between any two given groups was found to have occurred when $p < 0.05$). Note that comparisons to our previously published work on analogous flex–flow experiments (5) was done observationally (rather than statistically) due to a limited ability to increase sample size from a work that was published 5 years ago.

RESULTS

Velocity

Velocity contours with streamlines are presented in **Figure 8** during two time points of the flow waveform (maximum and minimum flow; **Figure 1B**). Two views are shown—a longitudinal (**Figure 8**) and transverse view (**Figure 8**). Overall, the flow streamlines exhibited uniformity in their pattern around the specimen surfaces. At the instance of maximum flow, in both the distal and proximal sides, there were areas of local flow reversal at the initial plane of fluid contact with each sample. On

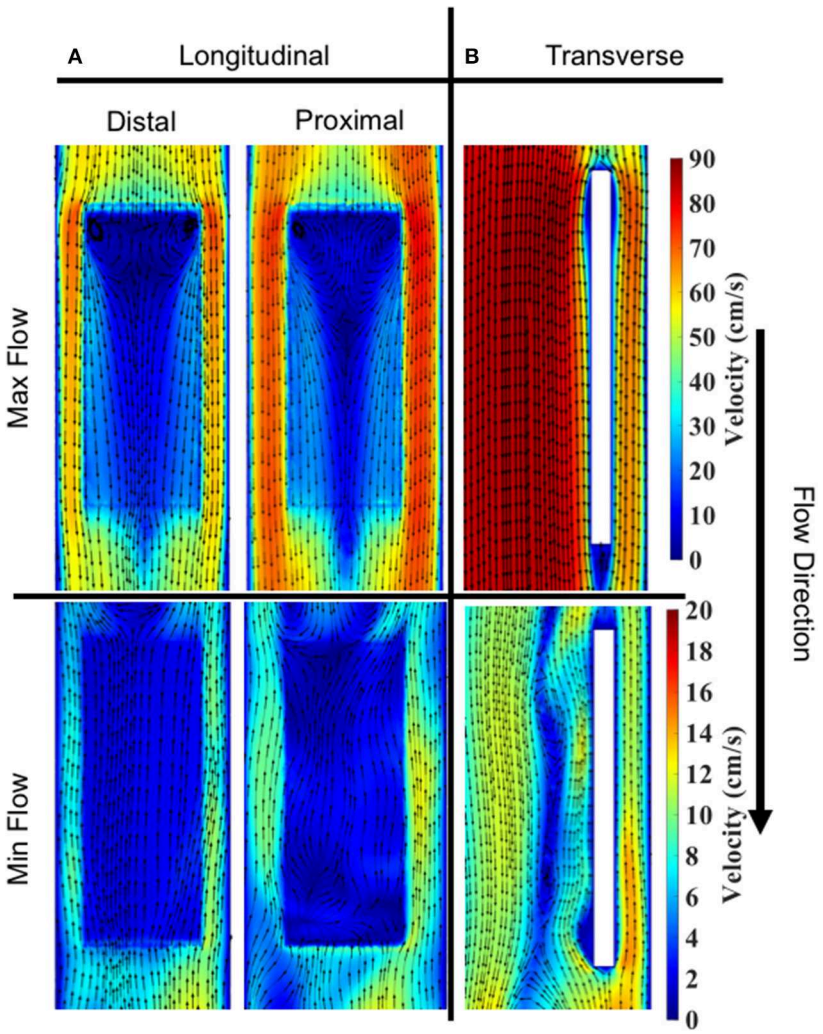

FIGURE 8 | Velocity contours and streamlines on specimen #2. Max and min flow corresponded to ∼0.368 and ∼0.83 s, respectively, in the enforced velocity waveform. **(A)** Longitudinal slice showing a comparison of streamlines on distal vs. proximal surfaces. Cut planes were taken 200 μm above and below the specimen to extract velocity contours. **(B)** Transverse slice showing a comparison of streamlines during Max vs. Min flow. Cut planes were taken through the center of specimen.

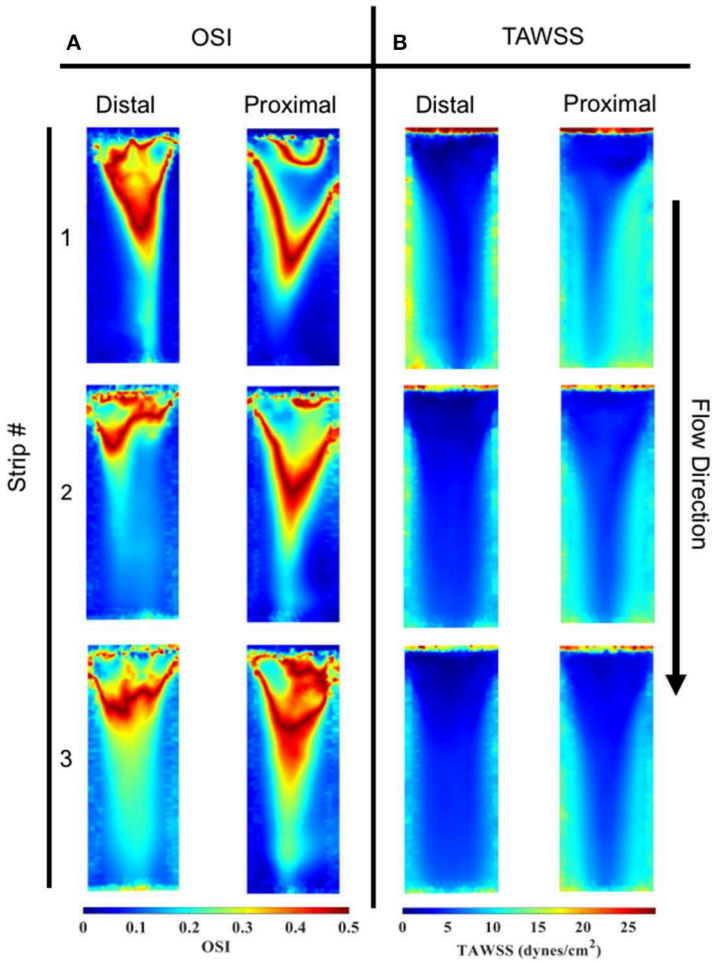

FIGURE 9 | OSI and TAWSS contours across all three specimens for both the distal and proximal sides. **(A)** In order of specimen number OSI averages were; Distal: 0.145, 0.170, and 0.211, Proximal: 0.148, 0.163, and 0.189. **(B)** In order of specimen number TAWSS (dynes/cm^2) averages were: Distal: 8.985, 7.703, and 6.122, Proximal: 9.057, 7.944, and 7.549.

the other hand, at the instance of minimum flow, the flow was largely reversed on the surface of the specimens.

Specimen Shear Stress

Spatial distributions of TAWSS for both the distal and proximal walls of the bioreactor scaffolds are shown (**Figure 9B**). Overall, the proximal side had a slightly larger TAWSS (mean ± SEM) than the distal side, 8.18 ± 0.26 vs. 7.60 ± 0.48 dynes/cm^2 ($n = 3$). However, the first specimen on both the distal and proximal sides had a larger TAWSS than the proceeding two cell-seeded scaffolds.

Oscillatory Shear Index

OSI distributions are shown (**Figure 9A**) for both the distal and proximal walls of the bioreactor scaffold strips. Overall, the proximal and distal side showed comparable OSI (mean ± SEM), 0.17 ± 0.007 vs. 0.18 ± 0.01. Upstream regions of all three specimens had a higher OSI compared to its corresponding downstream location. There was also the presence of a "V"-shaped OSI contour present on both distal and proximal sides of the specimens; a similar "V" shape was exhibited when looking at the same location's TAWSS (**Figure 9B**).

Bioreactor Setup

Waveform prediction (at the vicinity of the housed bioreactor samples; **Figures 3**, **4**) and measurements (at the pump and bioreactor exits; **Figure 3**) for the cardiac cycle showed close agreement with one another (**Figure 10**, **Supplementary Figure A**). Quantitative analysis of this flow data showed a 0.06% error in maximum flowrate and a 2.67% error in mean flowrates between the pump output and the temporal flowrates at the specimen locations, indicating that the cell-seeded constructs would receive the intended aortic pulsatile flow profile during the bioreactor experiments. Thus, overall, the pulsatile bioreactor system was able to recreate the flow profiles imparted by the pump within the bioreactor chamber with a high degree of fidelity.

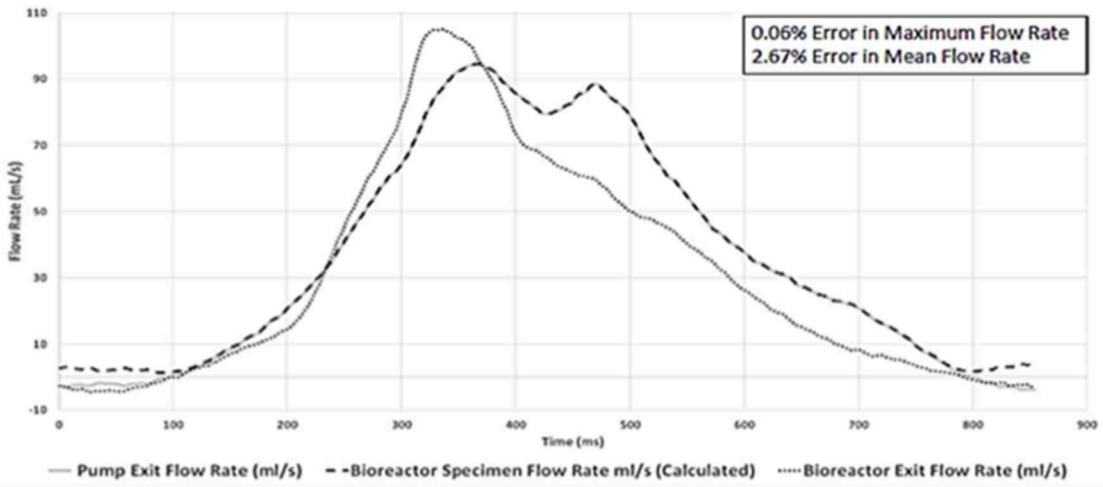

FIGURE 10 | Physiologically-relevant pulsatile flow profile comparison at three flow-loop locations. Close agreements between the pump exit and the bioreactor specimen location flow rates (peak flow error 0.06%; mean flow error 2.67%) were found. This demonstrated that the bioreactor chamber-housed, cell-seeded scaffold specimens would receive the intended aortic pulsatile flow waveform utilized in the tissue engineering experiments.

Immunofluorescence and Image Analysis

After analyzing the static, flex–flow, and PHV images captured from the previous studies (**Figures 5, 6**) conducted in our laboratory (5), the average intensities were calculated for α-SMA and CD31 (for our groups, i.e., static and oscillatory flow) (**Figure 11A**), and heat maps based off of the florescence signal intensities were computed (MATLAB) for all groups (i.e., static, PHV, flex–flow, and oscillatory flow) (**Figures 12, 13**). Observationally, the flex–flow group (from previous studies) had a larger α-SMA intensity than our oscillatory flow group (**Figure 12**). For statistical comparisons, only our static and oscillatory flow groups were assessed due to sample size limitations (static, $n = 12$; oscillatory flow, $n = 10$ or 16; flex–flow, $n = 1$; PHV, $n = 1$). For α-SMA, the average intensities were found to be 1.0 ± 0.15 and 1.4 ± 0.11 for static and oscillatory flow, respectively (**Figure 11A**). Similarly, the average intensities were only computed for static and oscillatory flow groups since both the flex–flow and PHV groups had small samples ($n = 2$). It was found that the average intensities were 1.0 ± 0.18 and 1.8 ± 0.26 for static ($n = 12$) and oscillatory flow ($n = 10$), respectively (**Figure 11A**). The p-values are given in **Supplementary Figures B, C**. The corresponding heat maps for both α-SMA and CD31 are shown in **Figures 12**, **13**.

Protein Quantification

Once the media was collected form all three groups, i.e., static, 8-days rotisserie, and oscillatory flow, the protein intensity was analyzed through mass spectrometry. One protein of interest was fibronectin, which demonstrated a significantly lower ($p < 0.05$) intensity of fibronectin in the oscillatory flow group compared to the static and 8-days rotisserie groups (**Figure 11B**). There was no significance ($p > 0.05$) between the static and 8-days rotisserie group (**Figure 11B**). The p-values and further details on the statistical analysis are given in **Supplementary Figure D**.

DISCUSSION

Congenital heart valve defects in the young have no viable treatment options currently available mainly due to limitations in current artificial valve sizing options and their inability to support somatic growth. Regenerative medicine using TEVCs may provide long-lasting solutions since TEVCs can facilitate provisions for somatic growth, biological repair, and remodeling. MSCs are one of the most promising and suitable cell types for regeneration since they can differentiate into endothelial and interstitial-line cell subtypes, which reside in heart valves. The microenvironment of these cells includes both biochemical factors and hemodynamic forces that influence differentiation. On the other hand, a standard reproducible protocol to develop a valvular construct to be used *in vivo* for longitudinal purpose is lacking (19). The objective of the current study was to determine whether using a physiologically relevant pulsatile flow profile that would elicit oscillatory shear stresses on MSC-seeded scaffold constructs could advance a tissue-engineered valve construct's phenotype within the *in vitro* domain prior to implantation. Phenotypic matching of the implant with host tissues is an important attribute in subsequent *de novo* tissue remodeling *in vivo*, due to chemotactic events that are initiated by the implanted engineered extracellular matrix and cells, which may accelerate host tissue regeneration due to its niche (20). Such an outcome is especially critical in situations such as heart valve replacement in children, where support of somatic growth by the engineered valve construct is critically needed.

Our immunofluorescence intensity assessment demonstrated that the α-SMA quantification between the groups (i.e., average static and oscillatory flow) were significantly different ($p < 0.05$) (**Figure 11A** and **Supplementary Figure B**); similarly, the CD31 levels were found to be significantly different ($p < 0.05$) (**Figure 11A** and **Supplementary Figure C**). These findings can

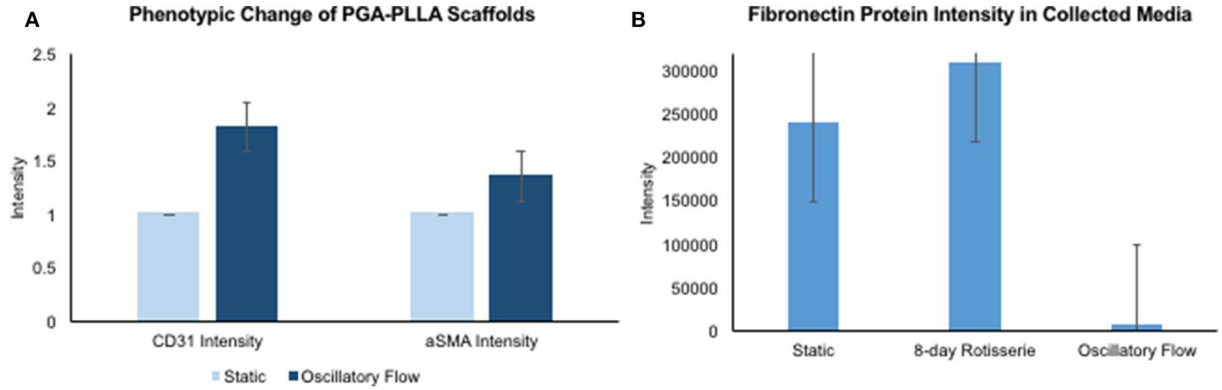

FIGURE 11 | hBM-MSCs differentiation toward α-SMA and CD31 valvular phenotypes and fibronectin protein intensity in collected media. PGA-PLLA scaffolds seeded with hBM-MSCs demonstrating **(A)** average intensity values of α-SMA and CD31 in static and oscillatory flow groups. There was a significant difference ($p < 0.05$) in both α-SMA and CD31 phenotypes intensities between the groups. In the oscillatory flow group there was an increase in both α-SMA and CD31 compared to the static group (significant, $p < 0.05$). **(B)** Media was collected and fibronectin intensities were assessed for static, 8-day rotisserie and oscillatory flow groups. The oscillatory flow group was significantly lower ($p < 0.05$) than both the static and 8-day rotisserie groups. *P*-values and boxplots for specific statistical analysis can be seen in **Supplementary Figures B–D**.

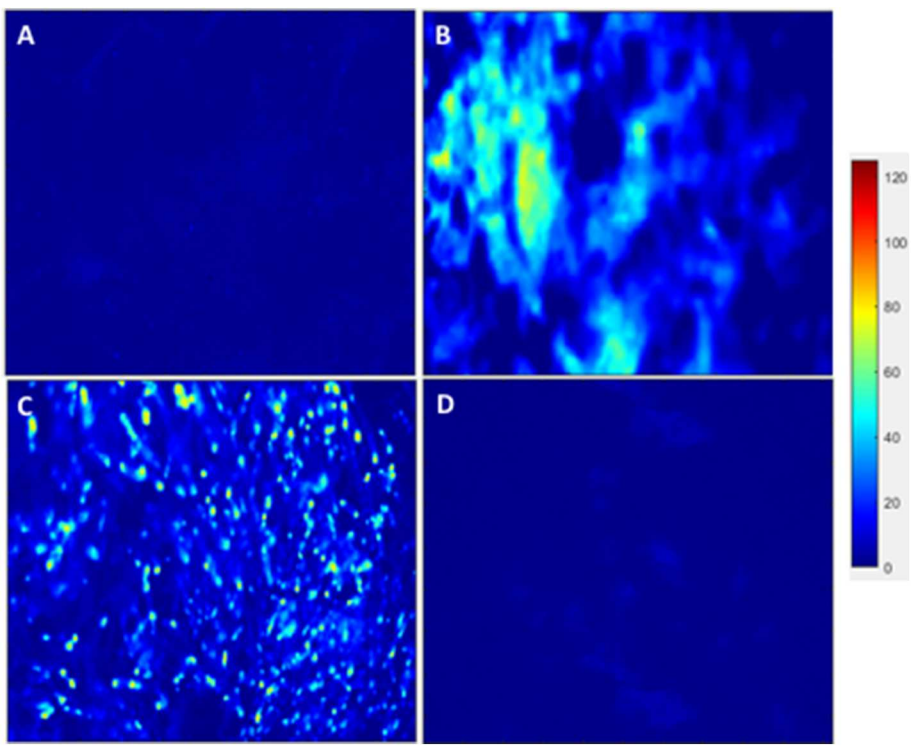

FIGURE 12 | hBM-MSCs differentiation toward α-SMA heat map. PGA-PLLA scaffolds seeded with hBM-MSCs from previous experiments (5) compared to our experiments demonstrating heat maps of α-SMA in averaged **(A)** static, **(B)** PHV, **(C)** flex-flow, and **(D)** oscillatory flow groups. Resolution of 1,024 × 690 pixels.

be attributed to the microenvironment that the hBM-MSCs were exposed to. The physiological nature of the aortic oscillatory flow waveform that was used during our experiment was intended to mimic hemodynamic shearing forces, which occur physiologically *in vivo*. Shear stresses that the hBM-MSCs are exposed to play a critical role in differentiating the cells toward the endothelial phenotype (19, 21–23). This supports our finding that the oscillatory flow group had a higher CD31 expression (endothelial phenotype). Studies in valve tissue engineering have suggested that valvular endothelial cells (VECs; CD31 marker) are the critical factor needed when compared to the valvular interstitial cells (VICs; α-SMA marker)

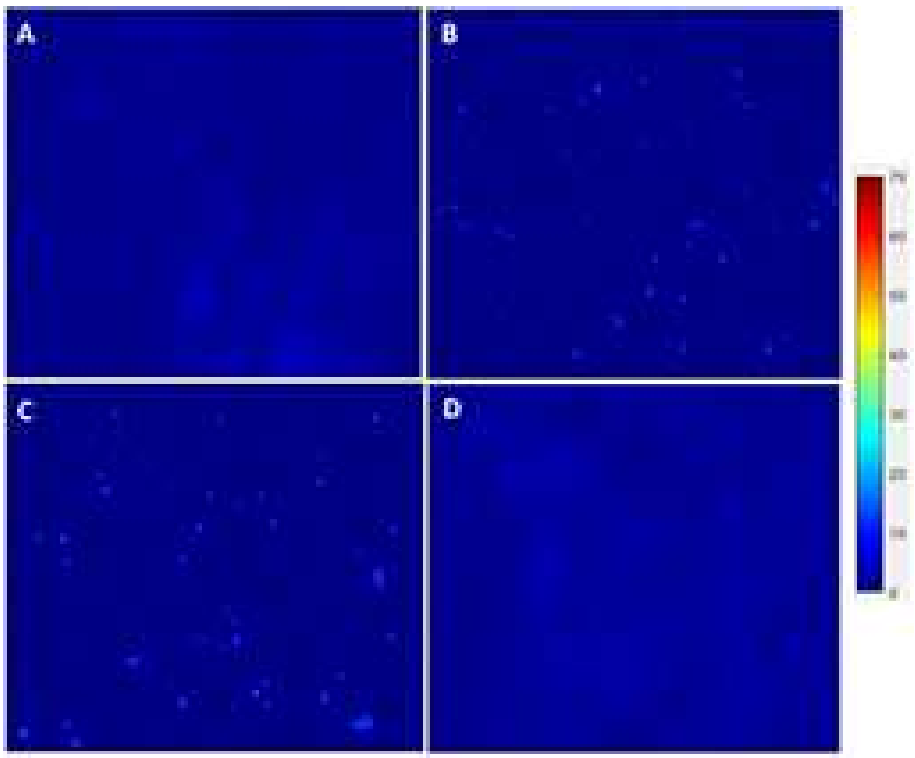

FIGURE 13 | hBM-MSCs differentiation toward CD31 heat map. PGA-PLLA scaffolds seeded with hBM-MSCs from previous experiments (5) compared to our experiments demonstrating heat maps of CD31 in averaged **(A)** static, **(B)** PHV, **(C)** flex-flow, and **(D)** oscillatory flow groups. Resolution of 1,024 × 690 pixels.

for *in vivo* implantation (24–27). In one study, autologous, ovine endothelial cell-seeded scaffolds were exposed to pulsatile flow conditioning for a week and demonstrated a complete endothelial layer on the leaflet surface but no presence of interstitial cells (25, 27). The conditioned valves were implanted in the descending aorta of a sheep for 3 months, functioning normally, with an observed endothelial layer but minimal leaflet interstitial recellularization (25, 27). Yet, another study investigated mechanically conditioned (rotisserie culture for 24 h followed by continuous flow at 15 ml/min with the circulation maintained for 21 days) tissue-engineered valves in two pediatric patients using a decellularized human pulmonary valve scaffold seeded with autologous mononuclear cells isolated from peripheral blood (24, 27). These scaffolds were monolayer with its surface positive for EC phenotypes, yet exhibited a complete absence of interstitial cells (24, 27). After a 3.5-years follow-up, both patients had normal valve function without any complications (24, 27). Both these studies suggest that with solely the presence of the endothelial phenotype, a valve construct can be implanted and function normally; nevertheless, the efficacy of these valves longer term still remains unclear. In the context of our study, we have demonstrated for the first time that physiologically relevant oscillatory shear stresses alone (overall mean, time-averaged shear stress, ∼7.9 dynes/cm^2; overall mean, oscillatory shear index, ∼0.18), with the absence of solid stresses in the mechanical conditioning protocol can augment the endothelial phenotype while restricting the activated smooth muscle phenotype (α-SMA) to relatively low levels. Note that oscillatory flow is distinct from pulsatile flow in that the latter may not necessarily induce oscillations in the fluid.

Furthermore, it has been reported that while shear stress promotes endothelial differentiation (CD31), it downregulates the differentiation toward smooth muscle cell phenotype (α-SMA) (**Figures 12**, **13**) (19, 28, 29). While the flex–flow group had greater α-SMA expression compared to our oscillatory flow group (**Figure 12**), this may not necessarily be desirable since α-SMA is both an indicator of healthy tissue remodeling as well as disease (27). Moreover, the extent of α-SMA necessary during engineered valve tissue construct to promote healthy (as opposed to pathological) remodeling after implantation is at present unknown. Finally, we also found that our oscillatory flow group had a significantly lower ($p < 0.05$) fibronectin expression intensity compared to our static and 8-days rotisserie groups (**Figure 11B**), which may be a sign of a healthy tissue remodeling, since fibronectin has been linked to transforming growth factor-β1 (TGF-β1) binding interactions (30); in turn, mechanically stimulated TGF-β1 signaling is associated with valve calcification (31).

Our study had the following limitations: The culture media used in our bioreactor system was void of two ingredients (AA2P

and bFGF) compared to our previous work (5). However, these biochemical agents are primarily to augment collagen content, which was not the focus of the current study (14). Moreover, immunostaining intensities of engineered valve constructs in the present investigation were compared to corresponding intensities in our previous work on flex–flow and PHV groups (5) observationally (as opposed to statistically), as we were limited by the number of images (and hence sample size) available in the latter.

In conclusion, in our previous work, we found that the samples from the flex–flow group exhibited a valve-like distribution of cells that expressed endothelial (CD31) and myofibroblast (α-SMA) phenotypes within the surface and interstitial layers, respectively (5). We interpret that this was likely due to the presence of oscillatory shear stresses (overall mean, OSI ∼0.11) on the sample, induced during the time-varying flow on the sample surface, which was created via the cyclic flexure of the immersed samples in the steady flow environment (5). In the current study, we similarly found that physiologically relevant, flow oscillations (overall, mean OSI ∼0.18) that were directly created via the aortic flow waveform augmented the CD31 phenotype. In contrast to flex–flow conditions, however, oscillatory flow without the presence of concomitant flexural stresses served to substantially reduce the α-SMA phenotype. Therefore, physiologically relevant oscillatory flow alone may serve as a means to promote controlled *in vitro* valve tissue regeneration, by enhancing the endothelial phenotype while restricting myofibroblast phenotypic expression. Since α-SMA is indicative of both normal as well as pathological tissue remodeling activity, it would therefore be more prudent to minimize α-SMA expression while augmenting other valvular parameters that can be achieved via mechanical conditioning. However, since solid stresses may serve to also considerably increase α-SMA, a compromise can be achieved via the sole application of physiologically relevant oscillatory fluid-induced stresses, without structural deformation of the specimens. Lastly, a very low level (relative to controls) of fibronectin expression found within the conditioned media of the oscillatory flow-stimulated, hBM-MSC-seeded scaffolds is suggestive of the potential for physiologically relevant oscillatory shear stresses to minimize the risk of provoking TGF-β-mediated, pathological valve remodeling activity following *in vivo* translation.

DATA AVAILABILITY STATEMENT

The datasets in this study are available by request to the corresponding author.

AUTHOR CONTRIBUTIONS

BG carried out the static and bioreactor experiments, immunostaining, performed confocal microscopy, wrote parts of the manuscript, including the primary preparation of references, and figures as well as manuscript organization. MP-N set-up the bioreactor system to conduct flow and pressure measurements, performed the subsequent data analyses to verify the accuracy of the flow field within the bioreactor system, and wrote parts of the manuscript. AM performed all the CFD-related set-up, simulations and post-processing, assisted in flow and pressure testing, and wrote parts of the manuscript. MP was responsible for generating the heat maps from the florescence signal intensities derived from the α-SMA and CD31 images. Y-ML performed protein quantification and mass spectrometry on collected media samples and wrote parts of the manuscript. C-PH assisted in the bioreactor experiments, operation of the pulsatile flow pump as well as in the acquisition of raw data during flow, and pressure testing. AR and AC assisted in isolation of exosomes from the conditioned media and with the process of protein quantification, as well as sample preparation for mass spectrometry. MG and FF-L performed mass spectrometry analysis and wrote parts of the manuscript. FG identified the appropriate statistical methods and conducted the statistical analyses for the study. SR conceived the study, wrote parts of the manuscript, reviewed all procedures, and verified the writing for factual accuracy.

FUNDING

This work was funded by the American Heart Association (Award ID: 16GRNT31090009). Funding from the Miami Heart Research Institute is also gratefully acknowledged.

SUPPLEMENTARY MATERIAL

The Supplementary Material for this article can be found online at: https://www.frontiersin.org/articles/10.3389/fcvm.2020.00069/full#supplementary-material

REFERENCES

1. Saleeb SF, Newburger JW, Geva T, Baird CW, Gauvreau K, Padera RF, et al. Accelerated degeneration of a bovine pericardial bioprosthetic aortic valve in children and young adults. *Circulation*. (2014) 130:51–60. doi: 10.1161/CIRCULATIONAHA.114.009835
2. Alsoufi B. Aortic valve replacement in children: options and outcomes. *J Saudi Heart Assoc*. (2014) 26:33–41. doi: 10.1016/j.jsha.2013.11.003
3. Kwon SG, Kwon YW, Lee TW, Park GT, Kim JH. Recent advances in stem cell therapeutics and tissue engineering strategies. *Biomater Res*. (2018) 22:1–8. doi: 10.1186/s40824-018-0148-4
4. Engelmayr GC Jr, Sales VL, Mayer JE Jr, Sacks MS. Cyclic flexure and laminar flow synergistically accelerate mesenchymal stem cell-mediated engineered tissue formation: implications for engineered heart valve tissues. *Biomaterials*. (2006) 27:6083–95. doi: 10.1016/j.biomaterials.2006.07.045
5. Rath S, Salinas M, Villegas AG, Ramaswamy S. Differentiation and distribution of marrow stem cells in flex-flow environments demonstrate support of the valvular phenotype. *PLoS ONE*. (2015) 10:e0141802. doi: 10.1371/journal.pone.0141802
6. Salinas M, Rath S, Villegas A, Unnikrishnan V, Ramaswamy S. Relative effects of fluid oscillations and nutrient transport in the *in vitro* growth of valvular tissues. *Cardiovasc Eng Technol*. (2016) 7:170–81. doi: 10.1007/s13239-016-0258-x

7. Ramaswamy S, Boronyak SM, Le T, Holmes A, Sotiropoulos F, Sacks MS. A novel bioreactor for mechanobiological studies of engineered heart valve tissue formation under pulmonary arterial physiological flow conditions. *J Biomech Eng*. (2014) 136:121009. doi: 10.1115/1.4028815
8. Vermot J, Forouhar AS, Liebling M, Wu D, Plummer D, Gharib M, et al. Reversing blood flows act through klf2a to ensure normal valvulogenesis in the developing heart. *PLoS Biol*. (2009) 7:e1000246. doi: 10.1371/journal.pbio.1000246
9. Salinas M, Ramaswamy S. Computational simulations predict a key role for oscillatory fluid shear stress in *de novo* valvular tissue formation. *J Biomech*. (2014) 47:3517–23. doi: 10.1016/j.jbiomech.2014.08.028
10. Castellanos G, Nasim S, Almora DM, Rath S, Ramaswamy S. Stem cell cytoskeletal responses to pulsatile flow in heart valve tissue engineering studies. *Front Cardiovas Med*. (2018) 5:58. doi: 10.3389/fcvm.2018.00058
11. Williams A, Nasim S, Salinas M, Moshkforoush A, Tsoukias N, Ramaswamy S. A "sweet-spot" for fluid-induced oscillations in the conditioning of stem cell-based engineered heart valve tissues. *J Biomech*. (2017) 65:40–8. doi: 10.1016/j.jbiomech.2017.09.035
12. He X, Ku DN. Pulsatile flow in the human left coronary artery bifurcation: average conditions. *J Biomech Eng*. (1996) 118:74–82. doi: 10.1115/1.2795948
13. Holliday CJ, Ankeny RF, Jo H, Nerem RM. Discovery of shear- and side-specific mRNAs and miRNAs in human aortic valvular endothelial cells. *Am J Physiol Heart Circ Physiol*. (2011) 301:H856–7. doi: 10.1152/ajpheart.00117.2011
14. Ramaswamy S, Gottlieb D, Engelmayr GC Jr, Aikawa E, Schmidt DE, Gaitan-Leon DM, et al. The role of organ level conditioning on the promotion of engineered heart valve tissue development *in-vitro* using mesenchymal stem cells. *Biomaterials*. (2010) 31:1114–25. doi: 10.1016/j.biomaterials.2009.10.019
15. Alfonso AR, Rath S, Rafiee P, Hernandez-Espino M, Din M, George F, et al. Glycosaminoglycan entrapment by fibrin in engineered heart valve tissues. *Acta Biomater*. (2013) 9:8149–57. doi: 10.1016/j.actbio.2013.06.009
16. Akturk Y, Ozbal Gunes S. Normal abdominal aorta diameter in infants, children and adolescents. *Pediatr Int*. (2018) 60:455–60. doi: 10.1111/ped.13542
17. Sacks MS, Yoganathan AP. Heart valve function: a biomechanical perspective. *Philos Trans R Soc B*. (2007) 362:1369–91. doi: 10.1098/rstb.2007.2122
18. Gonzalez BA, Pour Issa E, Mankame OV, Bustillos J, Cuellar A, Rodriguez AJ, et al. Porcine small intestinal submucosa mitral valve material responses support acute somatic growth. *Tissue Eng*. Part A (2020). doi: 10.1089/ten.tea.2019.0220. [Epub ahead of print].
19. Dan P, Velot É, Decot V, Menu P. The role of mechanical stimuli in the vascular differentiation of mesenchymal stem cells. *J Cell Sci*. (2015) 128:2415–22. doi: 10.1242/jcs.167783
20. Hoshiba T, Chen G, Endo C, Maruyama H, Wakui M, Nemoto E, et al. Decellularized extracellular matrix as an *in vitro* model to study the comprehensive roles of the ECM in stem cell differentiation. *Stem Cells Int*. (2016) 2016:6397820. doi: 10.1155/2016/6397820
21. Yamamoto K, Sokabe T, Watabe T, Miyazono K, Yamashita JK, Obi S, et al. Fluid shear stress induces differentiation of Flk-1-positive embryonic stem cells into vascular endothelial cells *in vitro*. *Am J Physiol Heart Circ Physiol*. (2005) 288:H1915–24. doi: 10.1152/ajpheart.00956.2004
22. Ahsan T, Nerem RM. Fluid shear stress promotes an endothelial-like phenotype during the early differentiation of embryonic stem cells. *Tissue Eng A*. (2010) 16:3547–53. doi: 10.1089/ten.tea.2010.0014
23. Cheng M, Guan X, Li H, Cui X, Zhang X, Li X, et al. Shear stress regulates late EPC differentiation via mechanosensitive molecule-mediated cytoskeletal rearrangement. *PLoS ONE*. (2013) 8:e67675. doi: 10.1371/journal.pone.0067675
24. Cebotari S, Lichtenberg A, Tudorache I, Hilfiker A, Mertsching H, Leyh R, et al. Clinical application of tissue engineered human heart valves using autologous progenitor cells. *Circulation*. (2006) 114(1 Supp.l):I-132–7. doi: 10.1161/CIRCULATIONAHA.105.001065
25. Tudorache I, Calistru A, Baraki H, Meyer T, Höffler K, Sarikouch S, et al. Orthotopic replacement of aortic heart valves with tissue-engineered grafts. *Tissue Eng A*. (2013) 19:1686–94. doi: 10.1089/ten.tea.2012.0074
26. Kajbafzadeh AM, Tafti SHA, Mokhber-Dezfooli MR, Khorramirouz R, Sabetkish S, Sabetkish N, et al. Aortic valve conduit implantation in the descending thoracic aorta in a sheep model: the outcomes of pre-seeded scaffold. *Int J Surg*. (2016) 28:97–105. doi: 10.1016/j.ijsu.2016.02.061
27. VeDepo MC, Detamore MS, Hopkins RA, Converse GL. Recellularization of decellularized heart valves: progress toward the tissue-engineered heart valve. *J Tissue Eng*. (2017) 8:2041731417726327. doi: 10.1177/2041731417726327
28. Wang H, Li M, Lin PH, Yao Q, Chen C. Fluid shear stress regulates the expression of TGF-β1 and its signaling molecules in mouse embryo mesenchymal progenitor cells. *J Surg Res*. (2008) 150:266–70. doi: 10.1016/j.jss.2007.12.801
29. Gu YQ, Li CM, Wang CR, Feng ZG, Qiu RX, Chen B, et al. Response of mesenchymal stem cells to shear stress in tissue-engineered vascular grafts. *Acta Pharmacol Sin*. (2009) 30:530. doi: 10.1038/aps.2009.40
30. Cushing MC, Liao JT, Anseth KS. Activation of valvular interstitial cells is mediated by transforming growth factor-β1 interactions with matrix molecules. *Matrix Biol*. (2005) 24:428–37. doi: 10.1016/j.matbio.2005.06.007
31. Hu XJ, Dong NG, Shi JW, Liu JW, Chen S, Deng C, et al. Role of TGF-β1 signaling in heart valve calcification induced by abnormal mechanical stimulation in a tissue engineering model. *Curr Med Sci*. (2018) 38:765–75. doi: 10.1007/s11596-018-1943-9

Conflict of Interest: The authors declare that the research was conducted in the absence of any commercial or financial relationships that could be construed as a potential conflict of interest.

frontiers in Cardiovascular Medicine

CASE REPORT
published: 30 October 2020
doi: 10.3389/fcvm.2020.562136

Reconstruction of the Neopulmonary Root After Coronary Button Harvest for Arterial Switch Operation Using 2-ply Extracellular Matrix (Tyke): A Post-Implant Histology

Steve Bibevski[1]*, *Mark Ruzmetov*[1], *Elena Ladich*[1,2], *Laura E. Mendoza*[1] and *Frank G. Scholl*[1]

[1] Division of Pediatric Cardiothoracic Surgery, The Heart Institute, Joe DiMaggio Children's Hospital, Hollywood, FL, United States, [2] Section of Pathology, The Heart Institute, Joe DiMaggio Children's Hospital, Hollywood, FL, United States

In children with Transposition of the Great Arteries (TGA), the pulmonary artery, and aorta are connected to the heart abnormally resulting in blue blood (deoxygenated) recirculating to the body and red blood (oxygenated) recirculating to the lungs. The arterial switch operation (ASO) is the standard of care for transposition of the great arteries (TGA), and given the low risk of early mortality and satisfactory long-term outcomes, focus is now on managing longer term complications such as neo-aortic root dilatation, and pulmonary artery stenosis. Since May 2016, we have used 2-ply extracellular matrix (ECM; Tyke) for reconstruction of the coronary button defects using a pantaloon patch. We present histology of implanted 2-ply ECM (Tyke) from a patient who went back to surgery for development of subaortic stenosis ∼12 months after ASO.

Keywords: extra cellular matrix, ECM, heart repair, histology, pulmonary artery, arterial switch operation, CorMatrix

OPEN ACCESS

Edited by:
Maurizio Pesce, Centro Cardiologico Monzino (IRCCS), Italy

Reviewed by:
Giovanni Biglino, University of Bristol, United Kingdom
James Todd Pearson, National Cerebral and Cardiovascular Center, Japan

***Correspondence:**
Steve Bibevski
SBibevski@mhs.net

Specialty section:
This article was submitted to Cardiovascular Biologics and Regenerative Medicine, a section of the journal Frontiers in Cardiovascular Medicine

Received: *05 June 2020*
Accepted: *06 October 2020*
Published: *30 October 2020*

Citation:
Bibevski S, Ruzmetov M, Ladich E, Mendoza LE and Scholl FG (2020) Reconstruction of the Neopulmonary Root After Coronary Button Harvest for Arterial Switch Operation Using 2-ply Extracellular Matrix (Tyke): A Post-Implant Histology. Front. Cardiovasc. Med. 7:562136. doi: 10.3389/fcvm.2020.562136

In a normal heart, there are two large arteries that carry blood out of the heart, the pulmonary artery which carries blood to the lungs, and the aorta which carries blood to the body. In children with Transposition of the Great Arteries (TGA), these arteries are connected to the heart abnormally resulting in blue blood (deoxygenated) recirculating to the body and red blood (oxygenated) recirculating to the lungs. This happens because the aorta is attached to the right-sided pumping chamber instead of the left, and the pulmonary artery is attached to the left-sided pumping chamber instead of the right.

The arterial switch operation (ASO) is the standard of care for transposition of the great arteries (TGA). The arterial switch operation involves cutting off the aorta and pulmonary arteries just above the point where they leave the heart, and reconnecting them to the proper ventricle. The valve stays attached to the ventricle, so what was once the pulmonary valve is now the aortic valve and vice versa. Since the coronary arteries must stay with the aorta, they must be taken off the area above the valve and reimplanted separately above the new aortic valve. This leaves a defect in the vessel from where they were removed, and this requires patching the defect with some type of material (**Figure 1**).

Given the low risk of early mortality and satisfactory long-term outcomes, focus is now on managing longer term complications such as neo-aortic root dilatation, and pulmonary artery stenosis (1). The incidence of pulmonary artery stenosis following ASO is surprisingly relatively high (2). Although relief with intervention is generally effective, technique used for reconstruction

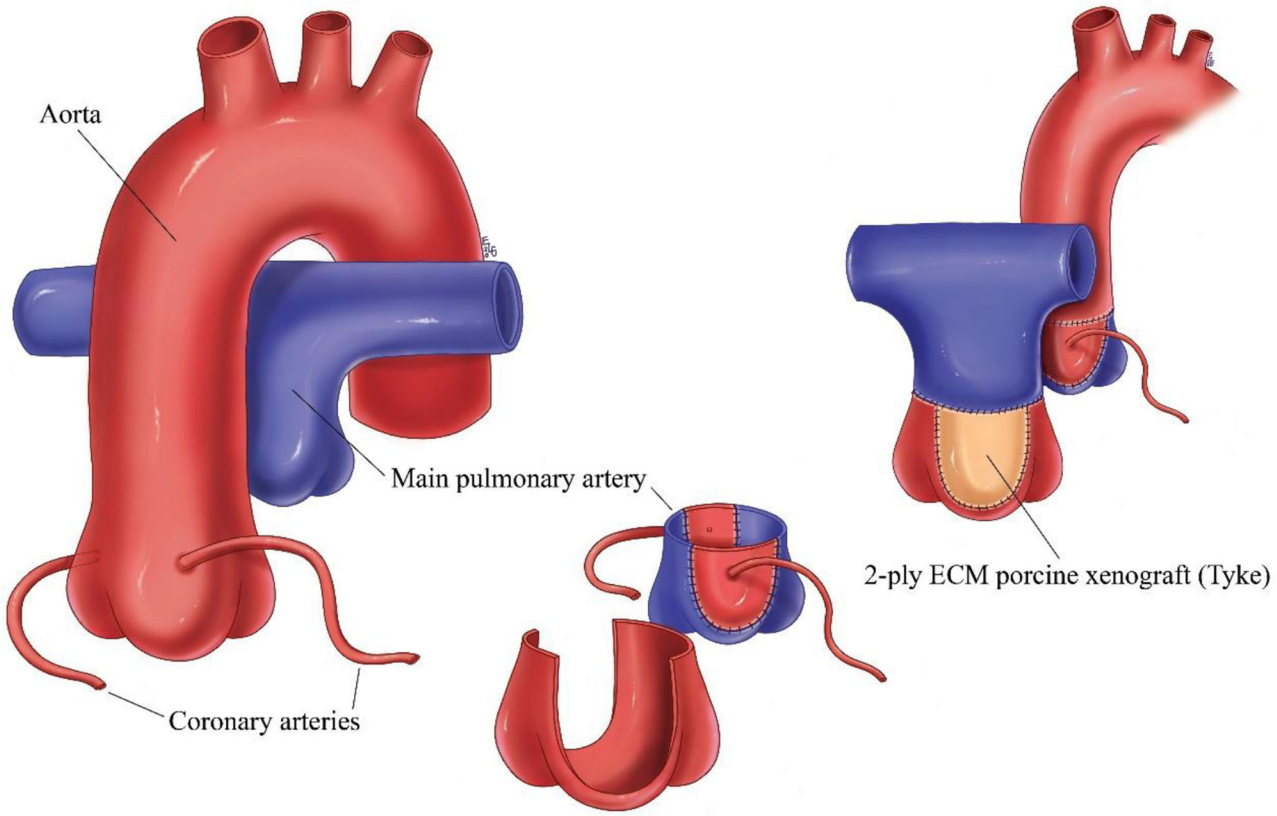

FIGURE 1 | Schematic of arterial switch operation demonstrating the translocation of the great vessels, removal of the coronary arteries and patching of the defect left behind from removal of the coronary arteries with ECM.

of the coronary buttons and material used may impact on the incidence. Since May 2016, we have used 2-ply extracellular matrix (ECM; Tyke) for reconstruction of the coronary button defects using a pantaloon patch. We present histology of implanted 2-ply ECM (Tyke) from a patient who went back to surgery for development of subaortic stenosis ∼12 months after ASO.

CLINICAL SUMMARY

The original surgery was performed in a patient with prenatal diagnosis born at 37 weeks with no intrapartum complications. Postnatal echocardiographic diagnosis of double outlet right ventricle with TGA (aorta from right ventricle, anterior and right of pulmonary artery), sub pulmonic ventricular septal defect (VSD) with overriding pulmonary artery was made. Patient underwent repair at 11 days old where an arterial switch procedure and closure of VSD was performed. A LeCompte maneuver was performed and the posterior neo-pulmonary artery root where the coronary buttons were harvested was reconstructed using a pantaloon shaped patch of 2-ply ECM core porcine xenograft (Tyke) with running 7-0 Prolene suture. The patient did well and was discharged at 18 days postoperatively.

Post-operatively the patient was evaluated by the genetics service and a diagnosis of Sotos syndrome (chromosome disorder 5q35.2q35.3 duplication that interrupts NSD1 gene) was made which is associated with congenital cardiac defects. At 11 months of age, a follow up echocardiogram revealed significant sub-aortic stenosis. The patient was referred for cardiac catheterization which revealed significant outflow tract gradient of 92 mmHg and the patient was referred for surgical repair.

During this procedure, the aorta and pulmonary arteries were separated easily. The pulmonary artery was transected allowing access to the aorta which was also transected. This allowed for inspection of the left ventricular outflow tract through the aortic valve which revealed an exceedingly tight opening in the left ventricular outflow tract measuring ∼3 mm in diameter. A longitudinal incision was carefully made down into the left ventricle and connected with a transverse incision excising a large chunk of septal left ventricular outflow tract muscle, now allowing a 10 mm dilator to pass easily. Before re-anastomosing the pulmonary artery, the pantaloon patch was examined from the inside and could not be distinguished from the native tissue except for the suture line. The tissue looked and felt like normal pulmonary artery. A small 1 mm sample of the pulmonary artery anastomosis was therefore taken from the rim of pantaloon patch for histology to evaluate the destiny of the inserted ECM patch.

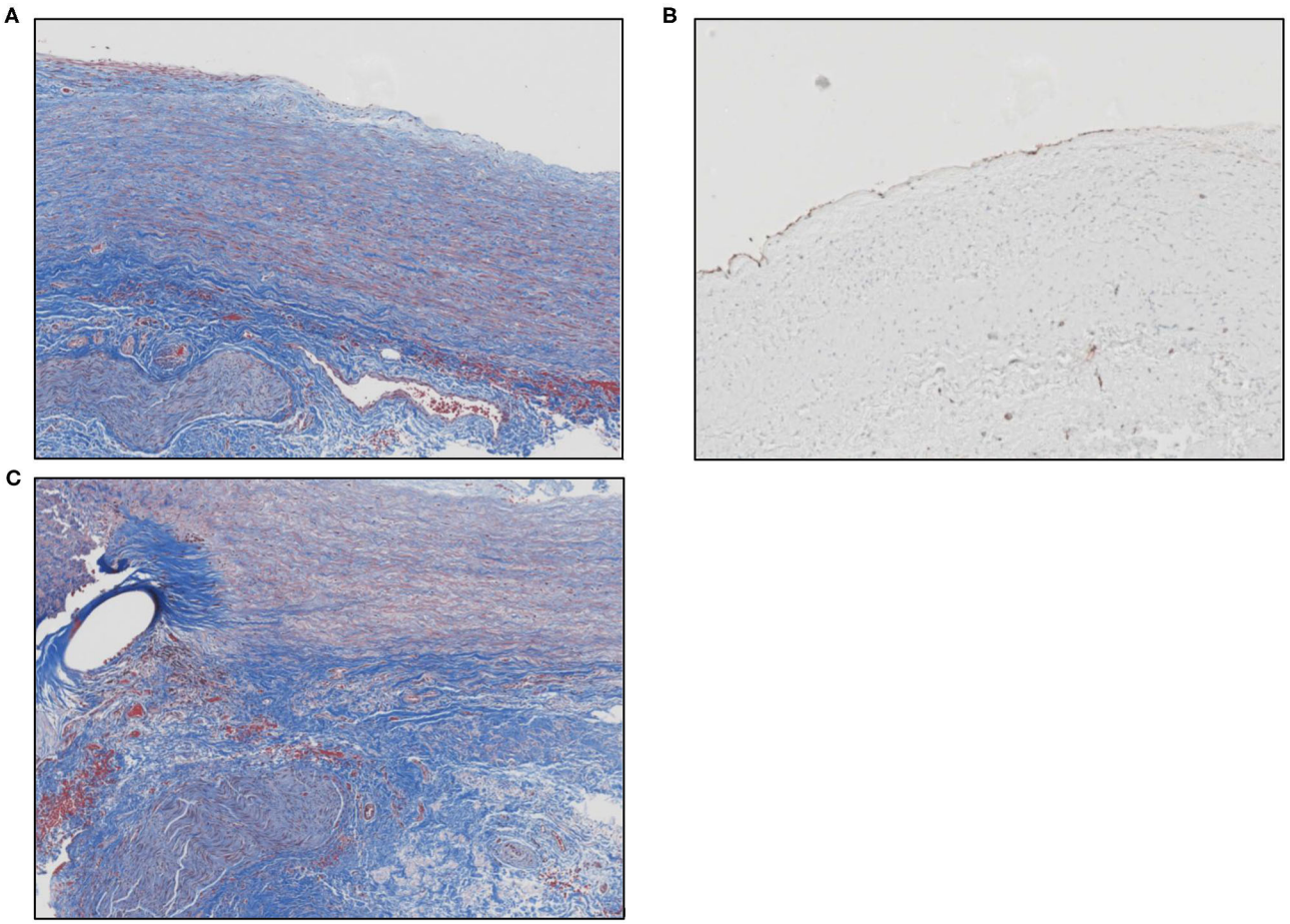

FIGURE 2 | (A) Masson's trichrome stain shows the remodeled ECM scaffold material. The neo-tissue is characterized by a highly aligned and organized accumulation of spindle cells and collagen fibers oriented along the length of the pulmonary artery. The luminal surface (top) is lined by endothelial cells and there is a vascular adventitia on the abluminal surface. Sections of a nerve fiber can also be seen at the lower left corner of the image. **(B)** Image showing positive immunolabeling for CD31+ endothelial cells along the luminal surface of the remodeled graft material. **(C)** Masson's trichrome stain shows the anastomotic site between the native pulmonary artery and the graft material. The oval unstained space at the left represents the site of suture placement. The graft material (to the right of the suture) is characterized by an organized, aligned accumulation of collagen fibers and spindle-shaped cells. The bottom portion of the picture shows the vascular adventitia with a section of nerve fiber.

The patient recovered well, without any complications, and was discharged uneventfully.

The specimen was dehydrated in a graded series of ethanol and infiltrated with paraffin. The block was sectioned at 4–6 microns, mounted on a glass slide, and stained with hematoxylin and eosin and Masson's trichrome stains. In addition, immunohistochemistry for CD31 was performed on the paraffin block.

Microscopic evaluation of the graft at the pulmonary anastomosis showed a small region of acellular laminated Cormatrix collagen with surrounding spindle cells and collagen deposition with re-endothelialization of the surface demonstrated by CD31 staining. Overall, inflammation was mild and consisted predominantly of lymphohistiocytic inflammation around suture material, nerve fiber, and at the interface with the ECM patch material. **Figure 2** shows the histology of remodeled ECM scaffold material.

Postoperative echocardiography performed more than year and half after initial switch operation demonstrated nicely functioning pulmonary valve with trivial pulmonary insufficiency and 18 mmHg peak pulmonary gradient (**Figure 3**).

DISCUSSION

Decellularized matrices are biological grafts capable of stimulating *in vivo* migration and proliferation of endothelial cells, recruitment and differentiation of mural cells, culminating in the formation of a bio integrated tissue (3). CorMatrix ECM, is an extracellular matrix (ECM) derived from porcine small intestinal submucosa. It offers potential for natural in growth and development of native arterial cells and structure (3, 4). Cormatrix ECM has been used for repair of a variety of cardiac structures including valvular, arterial, and pericardial sites. In several studies, use of CorMatrix for valve repair has

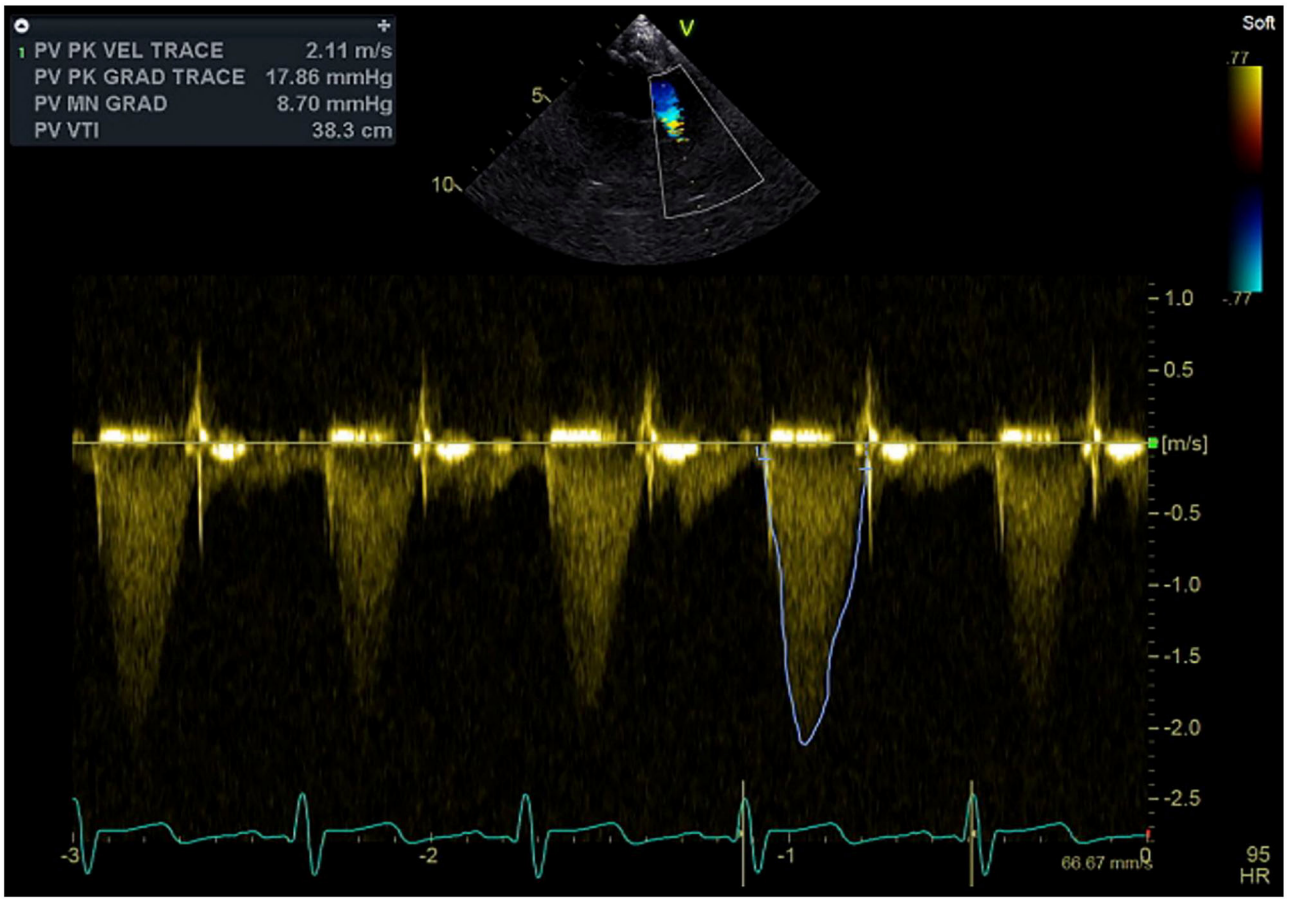

FIGURE 3 | Continuous wave Doppler signal with the sample volume at the level of the pulmonary outflow tract, neo-pulmonary valve, and pulmonary trunk demonstrating well-functioning valve and absence of obstruction.

been associated with an intense inflammatory response in the surrounding native tissue, the typical response included macrophages and giant cells in contact with the material, surrounded by lymphocytes, macrophages, plasma cells, and eosinophils; and little or no remodeling to form tissue resembling a 3-layered native valve was seen at ≤9 months after implantation (4, 5). However, in another preliminary experience with cardiac reconstruction using decellularized porcine ECM scaffold, the explanted tissue showed resorption of the SIS-ECM, replacement with organized collagen, and re-endothelialization (6). Longer-term follow-up was suggested to assess the potential for growth. A recent pathology study evaluating Cormatrix tissues in a variety of cardiovascular surgical sites demonstrated that the Cormatrix tissue itself remained acellular up to 2 years post-implantation but appeared to serve as a scaffold onto which new tissue formed, akin to neointimal proliferation (7). Neointimal thickness increased over time and a limited amount of elastic fiber deposition was observed at timepoints beyond 2 years. Interestingly, severe chronic inflammation was an uncommon finding in arterial repairs, including anastomotic sites. The authors postulated that the degree of inflammatory response observed in explanted Cormatrix tissue may be dependent on anatomic site with great vessel grafts less prone to inflammation as compared to valvular grafts (7). In our patient's arterial scaffold, mild chronic inflammation was observed, in keeping with these observations. A variety of other factors may explain the variation in inflammation severity observed between studies including variable immunologic responses to the porcine tissues, patient age, and clinical setting, e.g., graft failures removed as surgical specimens or at autopsy.

Bioscaffolds such as Cormatrix become incorporated by host tissue cells with eventual collagen deposition characteristic of wound healing (8). There have been no reports to date proving *de novo* growth of true histologic three layered arteries or valves resembling native cardiac structures in human explants. At ∼1 year post-implantation in a pediatric patient, we report incorporation of the Cormatrix scaffold by collagen deposition, re-endothelialization, and mild chronic inflammation, reflecting a typical healing response for implant duration similar to other reports. Additional studies evaluating longer term explants may further elucidate the mechanisms of tissue incorporation and potential for reconstitution of native structures.

This research did not receive any specific grant from funding agencies in the public, commercial, or not-for-profit sectors.

DATA AVAILABILITY STATEMENT

The raw data supporting the conclusions of this article will be made available by the authors, without undue reservation.

ETHICS STATEMENT

The studies involving human participants were reviewed and approved by Memorial Healthcare System Office of Human Research. Written informed consent to participate in this study was provided by the participants' legal guardian/next of kin.

AUTHOR CONTRIBUTIONS

All authors listed have made a substantial, direct and intellectual contribution to the work, and approved it for publication.

ACKNOWLEDGMENTS

Thank you to Ms. Emily L. Geisler for her excellent medical illustration.

REFERENCES

1. Xiao Y, Zhang P, Su W, Dong N. Early and mid-term follow-up of patients receiving arterial switch operation: a single-center experience. *J Thorac Dis*. (2018) 10:732–9. doi: 10.21037/jtd.2017.12.103
2. Bokenkamp R, Aguilar E, van der Palen RLF, Sojak V, Bruggemans EF, Hruda J, et al. Reoperation for right ventricular outflow tract obstruction after arterial switch operation for transposition of the great arteries and aortic arch obstruction. *Eur J Cardio-Thorac Surg*. (2016) 49:e91–e6. doi: 10.1093/ejcts/ezw026
3. Moroni F, Mirabella T. Decellularized matrices for cardiovascular tissue engineering. *Am J Stem Cells*. (2014) 3:1–20. Available online at: www.AJSC.us/
4. Zaidi AH, Nathan M, Emani S, Baird C, del Nido PJ, Gauvreau K, et al. Preliminary experience with porcine intestinal submucosa (CorMatrix) for valve reconstruction in congenital heart disease: histologic evaluation of explanted valves. *J Thorac Cardiovasc Surg*. (2014) 148:2216–25. doi: 10.1016/j.jtcvs.2014.02.081
5. Woo JS, Fishbein MC, Reemsten B. Histologic examination of decellularized porcine intestinal submucosa extracellular matrix (CorMatrix) in pediatric congenital heart surgery. *Cardiovasc Pathol*. (2016). 25:12–7. doi: 10.1016/j.carpath.2015.08.007
6. Scholl FG, Boucek MM, Chan KC, Valdes-Cruz L, Perryman R. Preliminary experience with cardiac reconstruction using decellularized porcine extracellular matrix scaffold: human applications in congenital heart disease. *World J Pediatr Congenit Heart Surg*. (2010) 1:132–6. doi: 10.1177/2150135110362092
7. Cox JL, Hammel JM, Radio SJ. Evaluation of cellular ingrowth within porcine extracellular matrix scaffolding in congenital heart disease surgery. *Cardiovasc Pathol*. (2019) 39:54–60. doi: 10.1016/j.carpath.2018.12.003
8. Fallon A, Goodchild T, Wang R, Matheny RG. Remodeling of extracellular matrix patch used for carotid artery repair. *J Surg Res*. (2012) 175:25–34. doi: 10.1016/j.jss.2011.11.001

Conflict of Interest: The authors declare that the research was conducted in the absence of any commercial or financial relationships that could be construed as a potential conflict of interest.

frontiers in Cardiovascular Medicine

ORIGINAL RESEARCH
published: 11 February 2021
doi: 10.3389/fcvm.2021.631750

Extracellular Matrix Patches for Endarterectomy Repair

Keith B. Allen[1], Joshua D. Adams[2], Stephen F. Badylak[3], H. Edward Garrett[4], Nicolas J. Mouawad[5], Steven W. Oweida[6], Manesh Parikshak[7] and Parvez K. Sultan[8]*

[1] St. Luke's Hospital of Kansas City, St. Luke's Mid America Heart Institute, Kansas City, MO, United States, [2] Carilion Clinic Aortic and Endovascular Surgery, Roanoke, VA, United States, [3] Department of Bioengineering, Department of Surgery, McGowan Institute for Regenerative Medicine, University of Pittsburgh, Pittsburgh, PA, United States, [4] Cardiovascular Surgery Clinic, University of Tennessee, Memphis, Memphis, TN, United States, [5] McLaren Bay Heart and Vascular, Bay City, MI, United States, [6] Vascular Surgical Associates, Marietta, GA, United States, [7] Cardiac Surgery Associates, Indianapolis, IN, United States, [8] Cardio-Thoracic Surgeons, Birmingham, AL, United States

Patch repair is the preferred method for arteriotomy closure following femoral or carotid endarterectomy. Choosing among available patch options remains a clinical challenge, as current evidence suggests roughly comparable outcomes between autologous grafts and synthetic and biologic materials. Biologic patches have potential advantages over other materials, including reduced risk for infection, mitigation of an excessive foreign body response, and the potential to remodel into healthy, vascularized tissue. Here we review the use of decellularized extracellular matrix (ECM) for cardiovascular applications, particularly endarterectomy repair, and the capacity of these materials to remodel into native, site-appropriate tissues. Also presented are data from two post-market observational studies of patients undergoing iliofemoral and carotid endarterectomy patch repair as well as one histologic case report in a challenging iliofemoral endarterectomy repair, all with the use of small intestine submucosa (SIS)-ECM. In alignment with previously reported studies, high patency was maintained, and adverse event rates were comparable to previously reported rates of patch angioplasty. Histologic analysis from one case identified constructive remodeling of the SIS-ECM, consistent with the histologic characteristics of the endarterectomized vessel. These clinical and histologic results align with the biologic potential described in the academic ECM literature. To our knowledge, this is the first histologic demonstration of SIS-ECM remodeling into site-appropriate vascular tissues following endarterectomy. Together, these findings support the safety and efficacy of SIS-ECM for patch repair of femoral and carotid arteriotomy.

Keywords: endarterectomy, extracellular matrix, biologic patch, tissue regeneration, tissue integration, cerebrovascular disease, peripheral arterial disease, atherosclerosis

OPEN ACCESS

Edited by:
Sharan Ramaswamy, Florida International University, United States

Reviewed by:
Udi Sarig, Technion Israel Institute of Technology, Israel
Matthew Wolf, National Cancer Institute at Frederick, United States

****Correspondence:***
Keith B. Allen
kallen2340@aol.com

Specialty section:
This article was submitted to Cardiovascular Biologics and Regenerative Medicine, a section of the journal Frontiers in Cardiovascular Medicine

Received: *20 November 2020*
Accepted: *25 January 2021*
Published: *11 February 2021*

Citation:
Allen KB, Adams JD, Badylak SF, Garrett HE, Mouawad NJ, Oweida SW, Parikshak M and Sultan PK (2021) Extracellular Matrix Patches for Endarterectomy Repair. Front. Cardiovasc. Med. 8:631750. doi: 10.3389/fcvm.2021.631750

INTRODUCTION

Arteries consist of an intimal lining surrounded by a thick, muscular media layer enveloped within the connective tissue of the adventitia (1). Together, these layers allow the artery to withstand high pressures from the heart (1,600–8,250 mmHg) (2). During the process of atherosclerosis, progressive accumulation of cholesterol, fatty acid salts, and tissue debris in the intima of the

vessel wall leads to bulky atheroma formation and intimal tissue necrosis (3). Endarterectomy is a recommended approach to the management of significant atherosclerotic stenosis of the femoral or carotid arteries. In a surgical endarterectomy, an arteriotomy is performed and a cleavage plane is developed within the arterial wall between the intima and the media to remove the pathologic intima and to increase the luminal area of the artery (4). In some cases, the media may also be partially or completely removed during stripping of the atheroma, leaving the treated vessel without the smooth intimal lining and, possibly, portions of the muscular media (4–6).

Following endarterectomy, the arteriotomy can be closed by primary repair or with a vascular patch. Based on expanding evidence of superior outcomes with patch angioplasty compared to primary repair, patch closure is currently the preferred method (7–10). An ideal arterial patch must be able to withstand systemic arterial pressures over the long term, while maintaining low risk for restenosis, compliance similar to native artery, and resistance to thrombosis and/or infection (11, 12). ECM has also been investigated as a potential solution for replacement of small-caliber vessels. Some success has been reported using decellularized carotid artery ECM and human-engineered vessels as replacement small vessel grafts, and has been discussed in detail elsewhere (13, 14).

Vascular patches currently used for arterial reconstruction include autologous tissues and synthetic or biologic materials. Despite available evidence, choosing among these options remains a clinical challenge. Clinical studies have reported roughly comparable outcomes between autologous and non-autologous grafts, and between synthetic and biologic patches (7, 15, 16). The cost of synthetic patches are generally less than comparably-sized biologic patches, yet there are important differences between patch materials that may affect short- and long-term clinical outcomes. Autologous tissues have been widely used for endarterectomy repair, are readily accessed in most patients, and do not induce a foreign body response, but often require additional operative time, anesthesia, and result in increased patient morbidity due to the need for vein harvest (e.g., saphenous vein), and may affect future cardiovascular procedures (e.g., vein harvest for coronary artery bypass). Furthermore, vein grafts for arterial repair have demonstrated reduced compliance compared to native artery or even ECM-based biomaterials (17). Synthetic materials, such as polyethylene terephthalate (Dacron®) or polytetrafluoroethylene (PTFE), are ready to use and have a long shelf-life, have high biomechanical strength, but do not mimic the native vasculature, and stimulate a foreign body response on implantation which can lead to post-operative complications due to chronic inflammation, lack of remodeling, limited compliance, and poor resistance to infection.

Compared to autologous vein grafts, biologic materials [such as those derived from the extracellular matrix (ECM) of small intestine submucosa (SIS) and pericardium] have the advantage of off-the-shelf availability, obviating the need for a separate harvest procedure and its associated morbidity. Biological patches also have demonstrated advantages over synthetic materials, including a biologically natural three-dimensional (3D) structure, reduced risk for infection, good biocompatibility, an inflammatory profile that promotes healing, the presence of bioactive compounds (such as growth factors), and a natural capacity for conducting tissue turnover at the cellular level, through which these materials can be remodeled into native vascular tissues (17–20). The innate 3D structure of ECM includes natural cross-linking of collagen fibrils to adjacent fibrils to keep tissues strong and intact, yet allows for the ECM's natural degradation process to take place. Exogenous crosslinking of collagen fibers in ECM scaffolds can be performed during manufacturer processing with physical, biological, or chemical agents such as glutaraldehyde to enhance mechanical stability and minimize degradation of the ECM. However, exogenous crosslinking of ECM scaffolds may impede the natural remodeling process, resulting in calcification and potential scaffold failure (18, 21–23). Overall, the mechanical strength of synthetic materials exceeds that of non-chemically crosslinked biologic materials, in particular during the early stages of remodeling of the ECM into native tissues (24–26). However, non-chemically crosslinked biomaterials have demonstrated sufficient strength for vascular applications, including arterial repair (11, 17, 27). Importantly, biologic arterial patches made from SIS have demonstrated similar compliance to native arteries, and substantially greater compliance than autologous vein grafts or synthetic materials (17). It has been proposed that a biodegradable implant would be an ideal patch option if it supported the creation of organized, functional vascular tissues over time (1). Although biologic materials come with the disadvantage of lot-to-lot variability and potential uncontrolled bioactivity, thrombosis, and neointimal hyperplasia upon contact with blood, evidence from clinical and preclinical studies demonstrates that certain biologic patch materials display clinically-beneficial characteristics (15, 17, 18, 28–30).

Biologic patches composed of ECM are natural biomaterials that retain the properties and bioactive constituents of native tissue ECM. The decellularized ECM of non-chemically crosslinked biomaterials acts both as a scaffold and a stimulus for the ingrowth of new vascular tissue (17). These characteristics have led to the successful use of such biomaterials, including SIS-ECM, in a wide range of cardiovascular procedures, from repairs of congenital heart and vascular defects to vascular reconstructions following trauma, hemodialysis (arteriovenous fistulas), and surgical interventions (31–38).

This article discusses the regenerative characteristics of ECM and relates these properties to the benefits of ECM-based materials in endarterectomy patch repair. We present a discussion of observational data on the use of a SIS-ECM scaffold for iliofemoral and carotid endarterectomy reconstruction (previously presented in part) (39) and a histological analysis of SIS-ECM explanted from a previous endarterectomy repair, which demonstrates the regenerative potential of this biologic material. Finally, we compare these findings to previously published endarterectomy patch experiences with SIS-ECM scaffold used for the same application (31, 32, 40–42).

BENEFITS OF ECM-BASED BIOMATERIALS: BIOACTIVITY, INFECTION RESISTANCE, AND CONSTRUCTIVE REMODELING

Based on current evidence, ECM-based materials may be preferred to other options for endarterectomy patch repair. As noted, clinical outcomes with biologic, synthetic, and autologous grafts appear to be roughly comparable. However, ECM-based materials have numerous potential advantages as outlined below.

ECM Materials Are Bioactive

The structure of ECM transmits biomechanical forces and serves as a substrate for cell migration and differentiation. Because it is biologically derived, this structure can adapt following implantation, providing not only structural support, but also a range of bioactive compounds. Components of ECM are highly conserved across species and include collagens, glycoproteins, proteoglycans, mucins, elastin fibers, and growth factors, each of which may influence the function of the ECM, host response, and remodeling (20). In addition to containing a range of structural and functional proteins, non-chemically crosslinked ECM materials are naturally degraded by proteases, a process that releases additional bioactive peptides and degradation products. ECM degradation is a natural activity present in all living tissues and is paramount to tissue remodeling.

The rate of ECM scaffold degradation varies across material types. For example, degradation of ECM is inhibited by chemical crosslinking, whereas certain methods of terminal sterilization may increase degradation rate (43–45). Non-chemically crosslinked ECM materials are typically degraded steadily after implantation. Approximately 60% of ECM mass is degraded and resorbed within 4 weeks of implantation, with full degradation by ∼3 months (46, 47). The rate of ECM scaffold degradation appears to be similar to the rate of new tissue deposition, although there can be a loss of mechanical strength before the degraded ECM is fully replaced by host tissues (45). Peripheral blood-derived macrophages are central to the early and rapid degradation of ECM scaffolds (45).

In addition to releasing naturally occurring anti-microbial peptides (AMPs), this degradation process exposes molecular sites and signaling molecules that influence cell behaviors such as chemotaxis, adhesion, differentiation, and angiogenesis (20, 48–54) [For an extensive review on matricellular proteins, see Ramaswamy et al. (55)] In other words, degradation of ECM-based materials by the host appears to be central to the successful regeneration of native tissues. This bidirectional interaction between cells and the ECM has been termed dynamic reciprocity (20).

ECM Materials Are Resistant to Infection

The *in-vivo* antimicrobial effects of ECM-based bioscaffolds are not the direct result of inherent ECM molecular structure or composition. When intact SIS is exposed to bacteria *in vitro*, microbial growth is not inhibited, which contrasts with findings in preclinical animal models (56). However, when ECM materials are digested/degraded *in vitro*, the resulting degradation products show robust antibacterial activity (49, 57). In fact, the degradation of ECM materials *in vivo* is critical to their demonstrated ability to resist infection and remodel into native tissues. This *in vivo* degradation process explains the discrepancy between animal and *in vitro* studies, in which the ECM is not digested by acids or proteases *in vitro* and therefore does not release cryptic antimicrobial peptides (AMPs) and other bioactive factors.

Synthetic materials can harbor bacteria and generally must be removed when infected (28, 29). In a porcine model comparing SIS-ECM to expanded PTFE (ePTFE), vascular grafts were implanted and deliberately contaminated with *Staphylococcus aureus* or *S. epidermidis* (30). During the 6-week study period, inoculated SIS-ECM grafts demonstrated less neointimal hyperplasia, extensive remodeling into native arterial tissue, and importantly, no bacterial growth compared to ePTFE grafts, which had high bacterial counts. Another porcine study comparing SIS-ECM to PTFE for vascular reconstruction in the setting of gastrointestinal contamination reported a 73% rate of infection in the PTFE group, compared to 8% in the SIS-ECM group [$P < 0.03$; (58)]. The rate of pseudoaneurysm was also lower with SIS-ECM (25% PTFE vs. 0% SIS-ECM). Studies in other animal models have reported similar findings: that is, resistance to bacterial infection with biological materials, such as SIS-ECM, compared to inflammation and bacterial growth with ePTFE or Dacron (59, 60).

ECM Materials Are Immunomodulatory and Support Constructive Remodeling

The host response to ECM-based materials, especially those of xenogeneic (usually porcine) origin has been extensively investigated (18, 61–64). The processing of ECM-based materials removes not only cells but also cell-associated xenogeneic epitopes [e.g., Galα1,3Galβ1,4GlcNAc-R (α-Gal)] responsible for antigenicity, thereby minimizing the risk for immune rejection. Decellularized, non-chemically crosslinked ECM-based materials have been shown to modulate the native immune response to favor constructive remodeling, while mitigating chronic inflammation (64). Part of the complex cellular response to an implanted prosthesis such as ECM is the attraction and polarization of macrophages. Two broad phenotypes of macrophages, often called M1 and M2, promote differing responses to the prosthesis. Macrophages with a dominantly M1 phenotype promote inflammation and the killing of pathogens, whereas macrophages with a dominantly M2 anti-inflammatory phenotype promote immunoregulation and constructive remodeling of tissues (18, 21). Studies have demonstrated that ECM-based materials that are not extensively crosslinked stimulate a response characterized by the presence of M2 macrophages, which are associated with incorporation into native tissue, whereas extensively crosslinked ECM and synthetic materials encourage an M1 phenotype, which is associated with chronic inflammation, resistance to degradation, and a foreign body response (18, 21–23, 26, 64).

The early transition from M1 proinflammatory to M2 pro-remodeling macrophage response is a necessary step toward

constructive remodeling of ECM-based materials and a favorable clinical outcome (45). In fact, the early macrophage phenotypic response to ECM implants can predict subsequent remodeling outcomes (65). The specific mechanisms by which ECM-based materials modulate this phenotypic response are not fully understood, but studies report that it is linked to the release of bioactive peptides, proteins, and matrix bound nanovesicles (MBV) from the degrading ECM (45, 66–68). The ability to recruit and control differentiation of stem and progenitor cells through the release of these bioactive peptides is what drives ECM-mediated tissue remodeling (69). Other factors that contribute to constructive remodeling include the application of site-appropriate mechanical loading, as is generated following implantation of ECM-based materials into living tissues, such as arteries (70, 71). The remodeling of SIS-ECM has been demonstrated clinically as early as 3 months post-implantation and, in animal studies, as early as 2 weeks, with complete remodeling within 6 months (27, 30, 72–75).

When considering biologic grafts, the manufacturing processes used to create specific materials must also be considered. The importance of patch manufacturing processes is demonstrated by the impact of chemical crosslinking on macrophage phenotype, as discussed above. Extensive chemical crosslinking and certain methods of decellularization, sterilization, and other manufacturing processes can alter the native ECM architecture, physiochemical properties, and growth factor content, potentially attenuating constructive remodeling of the patch and instead promoting inflammation, foreign body response, and encapsulation (17, 20, 44, 45, 65). Unlike SIS-ECM, other currently available vascular patch products, which are either synthetic or made from chemically crosslinked animal tissues (such as bovine pericardium), have been shown to elicit a sustained M1 macrophage phenotype and a foreign body response characterized by scarring, calcification, and fibrosis (17, 22, 26, 76, 77).

CLINICAL EXPERIENCE WITH ECM AS AN ENDARTERECTOMY PATCH

SIS-ECM in Iliofemoral and Carotid Endarterectomy: Observational Data

Despite growing evidence of the utility of biologic patches in vascular surgery, the clinical performance of individual materials remains incompletely described. An ECM patch derived from porcine SIS (SIS-ECM) is commercially available, constructed of multi-laminate (six-ply), decellularized, non-chemically crosslinked, lyophilized, and specifically indicated for use as a patch material in vascular reconstruction (VasCure®, Aziyo Biologics, Silver Spring, MD, USA). All investigators for the data reported herein prepared the patch according to manufacturer instructions for use (hydration in sterile isotonic solution for 1–2 min prior to implantation).

The safety and efficacy of this SIS-ECM for vascular repair following endarterectomy was evaluated in two manufacturer-sponsored, prospective, observational, post-market studies of 259 patients undergoing iliofemoral repair (the PERFORM Study) and carotid patch repair (the Carotid Registry). These studies were conducted with the approval of each site's IRB or through a centralized IRB. All enrolled subjects were consented with their site's approved Informed Consent Form. Across datasets, the repairs achieved high procedural success rates (∼100%) and high patency up to 12–24 months of follow up, with very low rates of restenosis (<3%), and adverse event rates comparable to those reported by other studies of patch angioplasty. Of the reported adverse events, <0.8% were reported as definitely related to the SIS-ECM patch. These results support the safety and efficacy of this SIS-ECM material for the repair of iliofemoral and carotid endarterectomies.

Also presented is a histologic analysis of explanted SIS-ECM from one patient after a healed femoral endarterectomy repair and obtaining informed patient consent. We believe this is the first histologic report of site-appropriate vascular tissue remodeling of SIS-ECM following endarterectomy.

SIS-ECM in Iliofemoral Artery Reconstruction—PERFORM Study

Data from 38 symptomatic patients (45 femoral arterial reconstructions) with peripheral arterial disease (PAD) undergoing iliofemoral endarterectomy and arteriotomy closure with SIS-ECM patch repair were collected at three centers. Patient demographics, comorbidities, indications for endarterectomy, procedures performed, and follow up time are listed in **Table 1**.

The procedural success rate was 100%. Patency was measured by duplex ultrasound and patient-reported complications, and was maintained in 42 out of 43 arteries (97.7%) of procedures through a mean follow-up of 252 ± 166 days (range 29–448). The only patient with a non-patent limb had Fontaine Class III PAD and underwent above-the-knee left leg amputation due to failed repeat revascularization procedures. Over 12 months, there were zero (0%) adverse events reported that were considered related to the SIS-ECM patch. Importantly, there were no (0%) patch ruptures, explants, patch-related pseudoaneurysms, or patch infections.

Five patients (13.2%) experienced a total of seven procedure-related adverse events (**Table 2**), which is consistent with previously reported rates in the literature (78–80). One pseudoaneurysm was reported 3 days after the index procedure due to a broken anastomosis suture; the ECM patch and femoral artery remained intact in this patient. A superficial wound infection was reported for one patient, and seroma was reported for two patients, one of which was infected; both were successfully treated without explantation of the SIS-ECM patch. The incidence of adverse events did not differ between patients with or without previous groin surgery ($P > 0.05$).

These efficacy findings align with published studies of femoral endarterectomy with patch angioplasty, which have reported 1-year and long-term patency rates of 90–100% and 85–96%, respectively (78–82). However, limited prospective evidence has been published comparing outcomes of SIS-ECM with different types of patches for femoral endarterectomy.

TABLE 1 | Patient demographics, comorbidities, indications, and procedures—PERFORM study.

Characteristic	Value
Number of patients (*n*)	38
Mean age, years ± SD	63.7 ± 11.0
Sex, male, *n* (%)	27 (71.1)
Race, *n* (%)	
White	29 (76.3)
Black or African American	9 (23.7)
Comorbidities, *n* (%)	
Hypertension	35 (92.1)
Hyperlipidemia	26 (68.4)
Diabetes	18 (47.4)
Obesity	3 (7.9)
Active tobacco use	15 (39.5)
Sedentary lifestyle	12 (31.6)
Family history of vascular disease	12 (31.6)
Previous vascular surgery	20 (52.6)
Previous groin surgery	13 (34.2)
Previous myocardial infarction	9 (23.7)
History of coronary artery bypass grafting	10 (26.3)
Chronic renal insufficiency	7 (18.4)
Indications for endarterectomy, *n* (%)	
Claudication	34 (79.1)
Acute critical limb ischemia	7 (16.3)
Rest and night pain	4 (9.3)
Gangrene	2 (4.7)
Other	2 (4.7)
Procedure performed, *n* (%)	
Iliofemoral endarterectomy	30 (66.7)
Femoral endarterectomy	11 (24.4)
Iliofemoral endarterectomy with profundaplasty	3 (6.7)
Other	1 (2.2)
Patient follow up	
Days of hospital stay ± SD (range)	5.5 ± 4.6 (1–18)
Days of follow up ± SD (range)	252 ± 166 (29–448)
Patients completing 12-month follow-up, *n* (%)	21 (55.3)
Procedures completing 12-month follow-up, *n* (%)	24 (53.3)

TABLE 2 | Procedure-related adverse events—PERFORM study.

Adverse event	*n* (%)
Pseudoaneurysm (suture break)	1 (2.3)
Superficial site seroma	2 (4.7)
Superficial wound infection	1 (2.3)
Pain and/or numbness of extremity	3 (7.0)

SIS-ECM for Carotid Artery Reconstruction—Carotid Registry

Data from 221 patients undergoing standard interventional carotid endarterectomy and SIS-ECM patch repair were collected at six centers. The demographic characteristics, comorbidities, and procedures performed are listed in **Table 3**. Follow-up evaluations, including carotid duplex imaging, were performed at 1–3, 6, 12, and 24 months after the index procedure. A follow-up evaluation was considered completed only if duplex imaging was available for the subject/visit.

TABLE 3 | Patient demographics, comorbidities, and procedures—Carotid Registry.

Characteristic	Value
Number of patients (*n*)	221
Number of patients with preoperative stenosis >50% (%) (per duplex ultrasound or CT)	219 (99.1)
Mean age, years ± SD	69.9 ± 10.0
Sex, male, *n* (%)	118 (53.4)
Race, *n* (%)	
White	203 (91.9)
Black or African American	16 (7.2)
Asian	2 (0.9)
Comorbidities, *n* (%)	
Hypertension	182 (82.4)
Diabetes	84 (38.0)
Obesity	47 (21.3)
Active tobacco use	75 (33.9)
COPD	32 (14.5)
Previous neck surgery	34 (15.4)
Previous neck radiation	2 (0.9)
Previous transient ischemic attack	51 (23.1)
Previous transient ischemic attack (symptomatic)	22 (10.0)
Previous stroke	43 (19.5)
Previous stroke (symptomatic)	20 (9.0)
Valve disease	9 (4.1)
Previous atrial fibrillation	22 (10.0)
Previous myocardial infarction	45 (20.4)
Congestive heart failure	19 (8.6)
Chronic renal insufficiency	19 (8.6)
Procedure performed, *n* (%)	
Internal carotid endarterectomy	220 (99.5)
Common carotid endarterectomy	1 (0.5)

The results show reductions in stenosis following carotid endarterectomy (**Table 4**), with mean change from baseline in maximum carotid stenosis of at least 50% across all time points with patency maintained in 89% of patients through 24 months. Restenosis occurred in six (2.7%) subjects. These findings align with previous studies, which reported long-term patency rates of 79–100% with synthetic patches and 87–100% with biologic materials following carotid endarterectomy (7, 11, 83). There was a low rate of adverse events reported: 10 (4.5%) were reported as possibly related to the device, 1 (0.45%) was reported as probably related to the device, and 2 (0.9%) (occurring in the same patient) were reported as definitely related to the device (**Table 5**).

Histology Reveals Transformation of SIS-ECM at Femoral Artery Endarterectomy Site

The regenerative potential of SIS-ECM when used in patch angioplasty is demonstrated through histology from a

TABLE 4 | Follow-up of stenosis in subjects who underwent carotid repair.

Time point (months)	Completed follow-up *n* (%)	Restenosis <50% *n* (%)	Maximum mean carotid stenosis, %	Mean change from baseline in carotid stenosis	
				Maximum, %	Minimum, %
Baseline	NA	NA	85.5	NA	NA
1–3	198 (89.6)	26 (13.1)	32.2	−52.5	−64.5
6	167 (75.6)	26 (15.6)	32.6	−52.6	−63.9
12	166 (75.1)	24 (14.5)	33.6	−51.8	−63.4
24	155 (70.1)	17 (11.0)	33.8	−51.1	−64.2

TABLE 5 | Adverse events possibly, probably, or definitely related to the SIS-ECM patch—Carotid Registry.

Adverse event	*n* (%)
Possibly related	
Restenosis	6 (2.7)
Irregular area of left bifurcation/distal common carotid artery patch	1 (0.45)
Occlusion	1 (0.45)
Thrombus on wall of carotid artery opposite ECM patch	1 (0.45)
Hematoma	1 (0.45)
Probably related	
Bleeding status post-left carotid endarterectomy	1 (0.45)
Definitely related	
Patch dehiscence/patch rupture	1 (0.45)
Pseudoaneurysm	1 (0.45)

complicated case showing successful integration of the SIS-ECM patch into site-appropriate endarterectomized vessel tissue. A 55-year-old Caucasian male underwent right CFA endarterectomy with patch angioplasty using a SIS-ECM patch (**Figures 1**, **2**) with no subsequent adverse events. Sixteen months later, due to disease progression at a distal adjacent site, an additional operation was performed. The previously placed SIS-ECM patch in the right CFA was found to be grossly indistinguishable from the surrounding endarterectomy site arterial tissue. At this surgery, the patch could be identified only by the presence of the polypropylene sutures used for the initial repair (**Figures 1**, **3**). An additional endarterectomy and vascular reconstruction were performed with another SIS-ECM patch, extending the previous patch. On follow-up, the patient did well, with unremarkable non-invasive testing.

Nineteen months after the initial procedure, the patient again developed disabling symptoms and presented with further progression of distal disease. A month later, a right femoral-to-above-knee popliteal artery bypass was performed using a prosthetic conduit. At the time of this surgery, both previously placed SIS-ECM patches were indistinguishable from the surrounding vascular tissue and could only be identified by the perimeter polypropylene sutures used to implant the patches (**Figures 1**, **4**). Similar to the fate of the first patch used, the second patch was also visually indistinguishable from the rest of the vessel walls. Since this procedure required a longitudinal arteriotomy in the CFA at the level of the initial SIS-ECM patch, a tissue specimen including the anastomosis between the first patch and the previous endarterectomized vessel was removed and sent for evaluation by an independent laboratory. Analysis of the specimen showed the area of the patch to be histologically identical to the adjacent endarterectomized vascular tissue, with no evidence of inflammation or degeneration in any areas of the patch (**Figure 5**). Post-operatively, the patient had normal non-invasive testing and complete resolution of their lower extremity discomfort.

DISCUSSION

Efficacy of SIS-ECM Patch Following Endarterectomy

Overall, studies comparing synthetic and biologic patch materials for endarterectomy repair have reported similar outcomes (e.g., patency rates, durability, risk for adverse events such as pseudoaneurysm, and survivability) across patch types (16, 83). The majority of current evidence for biologic patches relates to the use of bovine pericardium in carotid endarterectomy. For example, a 2018 meta-analysis of 18 randomized trials comparing bovine pericardium to synthetic patch materials (Dacron or PTFE) or vein grafts for repair of carotid endarterectomy found no significant differences between groups across a range of outcomes (15). When comparing bovine pericardium to synthetic patch materials, no significant differences were found in the incidence of 30-day stroke, transient ischemic attack, local neck hematoma, or death.

More recently, an analysis of primary carotid endarterectomy cases recorded in the Vascular Quality Initiative (VQI) registry compared outcomes between bovine pericardium, autogenous vein, Dacron, and PTFE patches (7). At 1-year post-procedure, bovine pericardium had the lowest incidence of restenosis and was also associated with a lower incidence of return to the operating room. Bovine pericardium and Dacron had lower incidence of stroke or transient ischemic attack compared to PTFE, vein patch, or primary repair. The authors concluded that this large dataset enabled identification of superior outcomes with bovine pericardium post-operatively and at 1 year compared to synthetic and autologous patch materials.

With regard to SIS-ECM specifically, a published case study of a patient undergoing repeat carotid endarterectomy used

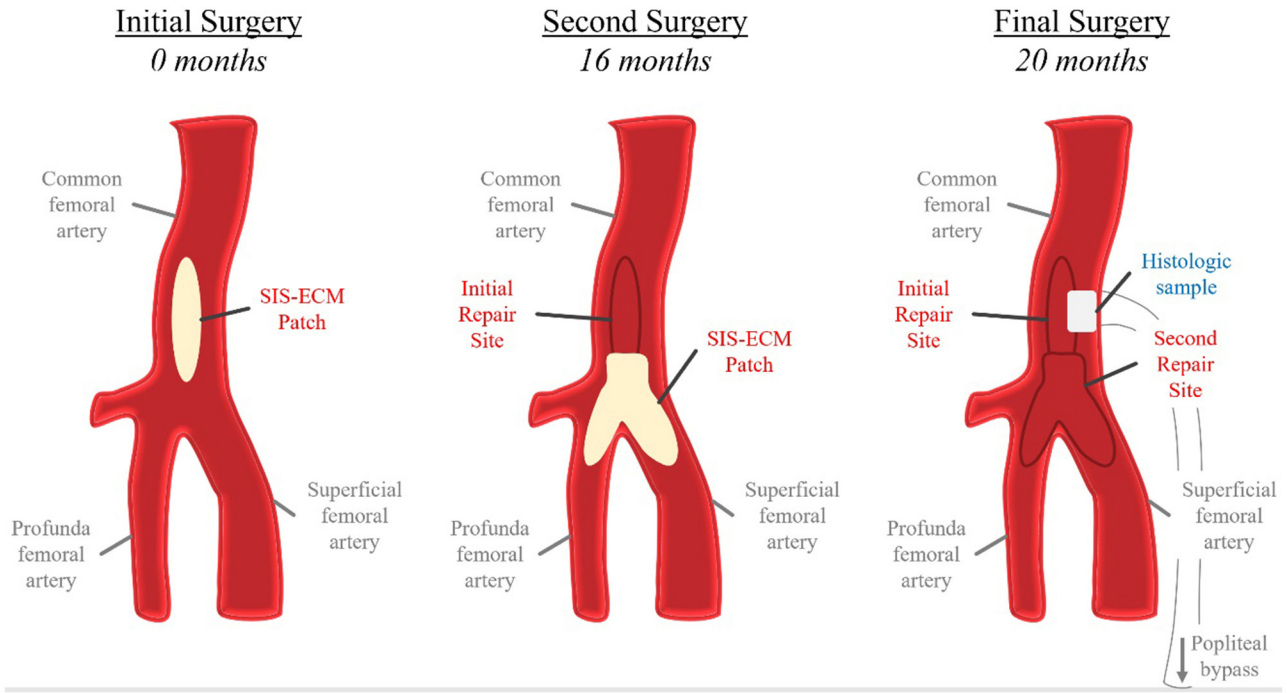

FIGURE 1 | Schematic representation of repeated iliofemoral endarterectomies in the histologic case study. At the initial surgery, a SIS-ECM patch was placed in the common femoral artery (CFA) following removal of the atheroma. The second surgery was conducted 16 months later due to progression of disease distal to the previous SIS-ECM repair. Following endarterectomy, a Y-shaped SIS-ECM patch was placed at the branching of the CFA, profunda femoral artery, and superficial femoral artery. The previous SIS-ECM patch remained widely patent. The final surgery, a femoral-to-above-knee popliteal artery bypass, was conducted at 20 months after the index procedure due to progression of distal disease. Both previously placed SIS-ECM patches remained widely patent. At this time, a biopsy of the original SIS-ECM patch, including the area of anastomosis between the patch and the native artery, was obtained for histologic analysis.

the same SIS-ECM patch used in the present studies (31). The authors reported procedural success with the SIS-ECM material and high patency of the patched internal carotid during follow up. However, no histologic analysis was reported evaluating the tissue characteristics of this successful use.

A recent case series of four patients undergoing femoral endarterectomy reported experience with the same SIS-ECM material used in this study (32). One patient died of cardiac arrest 2 days after the procedure; the other three showed widely patent common femoral arteries at the area of the patch repair 1 year post-procedure. Although the authors reported overall clinical success when using the ECM patch for this application, no histologic analysis was reported to characterize the tissue.

The results reported here not only add to a growing evidence base supporting the efficacy of SIS-ECM for vascular reconstruction, but the incorporation of the SIS-ECM into endarterectomized vascular tissue is illustrated by the histology described above and provides a specific example of the fate of SIS-ECM when used in this application. To our knowledge, this is the first histologic example showing that SIS-ECM functionally adopts the anatomy of adjacent endarterectomized vascular tissue. In this complex patient, histologic analysis of the patch sample obtained upon reoperation demonstrated moderately dense, well-organized collagen, and occasional capillaries (**Figure 5**). While small areas of remnant patch material could be identified at 20 months post-implantation, even these scattered regions were characterized by remodeling and replacement with organized collagen. Importantly, no evidence of inflammation was detected.

Safety of SIS-ECM Patch Following Endarterectomy

Although generally safe, endarterectomy with patch angioplasty has been associated with rare but serious complications, such as patch rupture, patch infection, and pseudoaneurysm formation. No (0%) adverse events were reported in the histologic case study related to the SIS-ECM patch. In the PERFORM dataset, there were also no (0%) device-related adverse events, which compares favorably to rates reported in other studies evaluating venous, bovine, and prosthetic graft materials following endarterectomy (84–86). Only one patient (2.3%) developed a pseudoaneurysm, and investigation determined the cause to be a broken suture along the line of the anastomosis, with the ECM patch remaining intact.

The Carotid Registry experience identified one case of pseudoaneurysm related to the patch, one case of patch dehiscence/rupture, and no cases of patch infection. This low rate of pseudoaneurysm (0.45%) compares favorably with rates

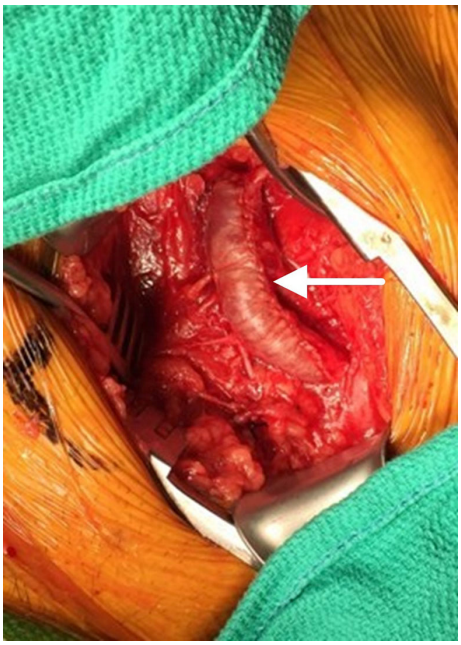

FIGURE 2 | Initial patch angioplasty of the common femoral artery using an SIS-ECM patch (arrow) following endarterectomy.

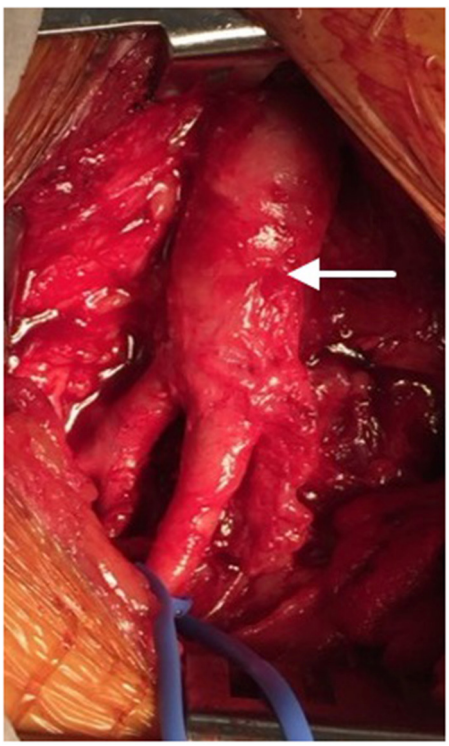

FIGURE 3 | After 16 months, the SIS-ECM patch previously placed in the right common femoral artery (CFA) (arrow) was found to be completely incorporated into native vascular tissue.

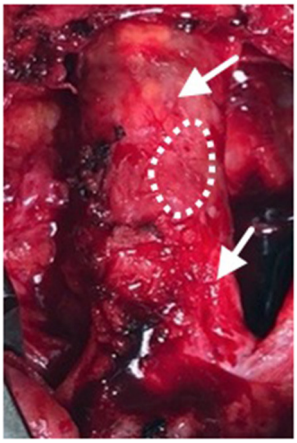

FIGURE 4 | Following progression of distal disease 20 months after the index procedure, a third operation was performed with creation of a right femoral to above-knee popliteal artery bypass. At this time, the two previous SIS-ECM patches in the common femoral artery appeared to be completely incorporated into the native femoral system (arrows). A specimen, including the anastomosis between the patch and the endarterectomized artery, was removed for histologic evaluation (dashed outline).

of 0.2–3.6% reported in studies of other patch materials (10, 16). Resistance of SIS-ECM to rupture and pseudoaneurysm demonstrated by these data may relate to the greater thickness of the six-ply SIS-ECM compared to other patches and the ability of SIS-ECM to conform to the repaired vessel and remodel into native tissue.

Few previous case series have reported higher rates of pseudoaneurysm with SIS-ECM (40–42). One study of a four-ply SIS-ECM material (Cook Biotech Inc., West Lafayette, IN) for patch closure of carotid endarterectomy reported no adverse events with the first 69 of 76 patients implanted with the patch (40). Subsequently, seven patients (9.2%) developed asymptomatic pseudoaneurysms, six of which required surgical intervention. Mechanical testing of patches from the same material lots associated with pseudoaneurysm identified thinner and more variable physical characteristics compared to a control lot. Of important note, the SIS-ECM patch used in the endarterectomy studies reported here consists of six layers (VasCure®, Aziyo Biologics, Silver Spring, MD, USA), and is therefore thicker and stronger than the SIS-ECM that was used in the referenced study.

A case series using this same six-ply SIS-ECM reported three cases (8.1%) of pseudoaneurysm out of 37 patients, occurring 4–6 months after repair of carotid endarterectomy (41). These events occurred at different hospitals over a 14-week period and were not caused by suture failure or infection. Histologic analysis demonstrated neovascularization and remodeling of the patches. As the authors suggested, it is possible that SIS-ECM patch strength is reduced during the remodeling process, which may increase risk for pseudoaneurysm in some cases.

Finally, SIS-ECM was used for patch angioplasty for femoral artery repair following endarterectomy in a case series of six patients (seven procedures) (42). Significant, early vascular

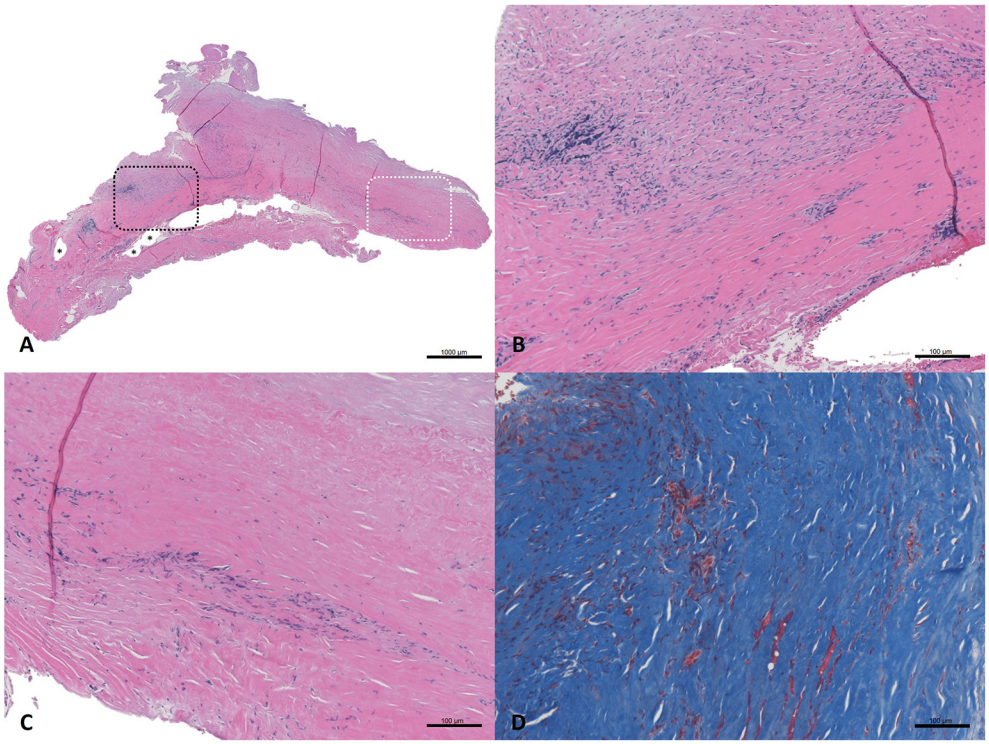

FIGURE 5 | Haematoxylin and eosin-stained sections **(A–C)** and Masson's trichrome stained section **(D)** from SIS-ECM graft explanted from the common femoral artery. **(A)** Full field of view; a black dashed box marks an area of remnant graft material, and asterisks (*) denote intact suture holes. An area of interest is highlighted with a white dashed box which represents remodeled graft. **(B)** Detailed view of a full thickness section of remnant graft material undergoing active remodeling (top of the image), surrounded by organized collagen (bottom of the image). **(C)** Detailed view of the area of interest; a full thickness section of the remodeled graft, with no evidence of the originally implanted ECM material remaining. The more luminal side of the graft (top of the image) shows well organized and aligned collagen, minimal cellularity, and no evidence of inflammation. The more abluminal surface (bottom of the image) shows slightly less organized collagenous connective tissue, moderate, and localized cellularity consistent with residual remodeling, and no evidence of active inflammation or necrosis. The collagenous tissue shows a population of morphologically normal spindle cells, which are most likely fibroblasts. **(D)** Detailed view of trichrome stained tissue representing a remodeled ECM area showing well organized, dense accumulation of collagen. The tissue was aligned in a circumferential fashion, as would be expected for a normal blood vessel. Small areas of red staining represent islets of smooth muscle.

complications occurred in three of the procedures (43%); patch rupture occurred in two procedures (29%), requiring immediate reoperation; and asymptomatic pseudoaneurysm occurred in one procedure, which was identified on routine follow up. No late complications were identified. Again, this case series used a four-ply SIS-ECM unlike the stronger six-ply SIS-ECM used in the present study.

Further, the lack of true pseudoaneurysm in the present report, including up to 24 months of follow up, suggest that this is a rare event. Additional long-term studies are required to better characterize this risk.

Infection of vascular patches is a potentially serious complication that may require removal of the patch and vein bypass to establish revascularization. Although patch infection may be underreported, studies have identified low rates of patch infection following endarterectomy repair (0–3%), with roughly similar rates across patch types (10, 15, 16, 29, 83, 84). In the histologic and observational data reported herein, no (0%) patch infections were identified. Resistance to infection may relate to the inherent antimicrobial properties of non-chemically crosslinked ECM (17, 49). In fact, SIS-ECM products have been successfully used in sites with active infection, whereas synthetic materials are generally avoided in the setting of infection (30, 58–60, 87–89).

In summary, non-chemically crosslinked ECM-based materials provide comparable clinical outcomes to other options for endarterectomy repair, but with several potential advantages (7, 16, 90). These materials, including SIS-ECM, release bioactive factors during early degradation following implantation, foster an immune response associated with constructive remodeling, provide sufficient mechanical strength and compliance similar to native arteries, resist infection, and, as demonstrated by the histology described above, remodel into site-appropriate vascular tissues. One advantage of the analyses presented above is that the data reflect real-world clinical practice and the performance of a 6-ply SIS-ECM patch in a heterogeneous, unselected patient population. Indeed, the outcomes were excellent, with high long-term patency rates, low incidence of adverse events,

and compare favorably to outcomes of patch endarterectomy repair reported in the literature. It is possible that improved patient selection could further enhance the performance of this material in endarterectomy repair; future studies should seek to identify risk factors for adverse outcomes (e.g., restenosis) with SIS-ECM.

LIMITATIONS

There are several limitations to the data presented above. First, the studies reported were not randomized or controlled trials; these data consist of real-world observational experiences that included only patients managed with SIS-ECM, thereby precluding the possibility of direct comparisons with other vascular patches. Second, follow up was limited, with some patients lost to follow up and a varying range of follow-up times. Longer and more complete follow-up will be required to confirm and extend the long-term safety and efficacy findings of SIS-ECM in iliofemoral and carotid endarterectomy. A more robust mechanism for ensuring follow-up may improve tracking of patients through long-term time points. Third, in the patients undergoing iliofemoral repair, the diagnosis of PAD was based on a comprehensive physical examination, and abnormal findings were confirmed by non-invasive diagnostic testing. However, results from these diagnostic tests were not collected as part of this dataset. There was a high incidence of patients with procedures performed for claudication in the iliofemoral group, yet documentation of the severity or progression of this symptom was not captured. Finally, the histologic analysis included a sample from only one patient.

The safety and efficacy findings reported in this manuscript conflict somewhat with previously published data that used SIS-ECM patch material for carotid or femoral endarterectomy patch repair. As outlined in the discussion, some authors reported similar success to that presented here but others have reported patch failures, early pseudoaneurysms, and/or restenosis. Because those data were generated from experiences at single centers, small patient populations, or four-ply versions of the SIS-ECM used in this report, this broader set of multi-center, multi-physician, six-ply ECM data can be expected to deviate from previous accounts. However, more robust studies are still needed to confirm the results observed herein, and larger randomized studies are needed to understand the full potential of SIS-ECM patches for vascular repair.

CONCLUSION

Vascular patches play an essential role in the repair of arteriotomies following carotid and iliofemoral endarterectomy. The optimal choice of patch material remains unclear. Based on the perceived benefits of biologic materials, bovine pericardium has been widely used for this application, and recent clinical data support its efficacy and safety. In the present report, the clinical use of a biologic vascular patch material, which consists of six-ply SIS-ECM is reported. Observational data and histology from a complex case describe the reliable efficacy and strong safety of SIS-ECM for the repair of carotid and iliofemoral endarterectomies. The findings also demonstrate full tissue integration of the patch into endarterectomized vascular tissue, with low rates of restenosis, pseudoaneurysm, or other adverse vascular outcomes. Future research is needed to expand the understanding of the efficacy, safety, and host response to ECM-based materials in arterial reconstruction procedures.

DATA AVAILABILITY STATEMENT

The original contributions presented in the study are included in the article, further inquiries can be directed to the corresponding author.

ETHICS STATEMENT

The studies involving human participants were reviewed and approved by either a Local IRB or Centralized IRB. The patients/participants provided their written informed consent to participate in this study.

AUTHOR CONTRIBUTIONS

KA, JA, HG, NM, SO, MP, and PS contributed substantially to the conception, design, data collection, and analysis of the work. SB contributed their expertise to the conception, design, analysis, and interpretation of data. All authors accept accountability for the accuracy of this work, and drafted, revised, and approved the final version of the manuscript to be published within this journal.

ACKNOWLEDGMENTS

We thank Joshua Kilbridge (Kilbridge Associates) for his medical writing and editorial expertise.

REFERENCES

1. Abalymov A, Parakhonskiy B, Skirtach AG. Polymer- and hybrid-based biomaterials for interstitial, connective, vascular, nerve, visceral and musculoskeletal tissue engineering. *Polymers.* (2020) 12:620. doi: 10.3390/polym12030620
2. van Hinsbergh VWM. Physiology of blood vessels. In: Krams R, Bäck M, editors. *The ESC Textbook of Vascular Biology* Oxford: Oxford University Press (2017). p. 17–30. doi: 10.1093/med/9780198755777.003.0002
3. Tabas I. Consequences of cellular cholesterol accumulation: basic concepts and physiological implications. *J Clin Invest.* (2002) 110:905–11. doi: 10.1172/JCI0216452
4. Niizuma K, Shimizu H, Inoue T, Watanabe M, Tominaga T. Maximum preservation of the media in carotid endarterectomy. *Neurol Med Chir.* (2014) 54:812–8. doi: 10.2176/nmc.tn.2014-0202
5. van der Heijden FH, Borst C, van Reedt Dortland RW, Steijling JJ, Eikelboom BC. The cleavage plane in semi-closed endarterectomy of the

superficial femoral artery: a histologic study. *J Vasc Surg.* (1994) 20:607–12. doi: 10.1016/0741-5214(94)90285-2
6. Roberts CS, Roberts WC. The layer where the coronary arterial "endarterectomy" specimen separates from the underlying artery. *Am J Cardiol.* (2020) 125:999–1000. doi: 10.1016/j.amjcard.2019.12.013
7. Edenfield L, Blazick E, Eldrup-Jorgensen J, Healey C, Bloch P, Hawkins R, et al. Outcomes of carotid endarterectomy in the Vascular Quality Initiative based on patch type. *J Vasc Surg.* (2020) 71:1260–7. doi: 10.1016/j.jvs.2019.05.063
8. Huizing E, Vos CG, van den Akker PJ, Schreve MA, de Borst GJ, Unlu C. A systematic review of patch angioplasty versus primary closure for carotid endarterectomy. *J Vasc Surg.* (2019) 69:1962–74 e4. doi: 10.1016/j.jvs.2018.10.096
9. Rerkasem K, Rothwell PM. Patch angioplasty versus primary closure for carotid endarterectomy. *Cochrane Database Syst Rev.* (2009) 2009:CD000160. doi: 10.1002/14651858.CD000160.pub3
10. Rerkasem K, Rothwell PM. Systematic review of randomized controlled trials of patch angioplasty versus primary closure and different types of patch materials during carotid endarterectomy. *Asian J Surg.* (2011) 34:32–40. doi: 10.1016/S1015-9584(11)60016-X
11. Muto A, Nishibe T, Dardik H, Dardik A. Patches for carotid artery endarterectomy: current materials and prospects. *J Vasc Surg.* (2009) 50:206–13. doi: 10.1016/j.jvs.2009.01.062
12. Roeder R, Wolfe J, Lianakis N, Hinson T, Geddes LA, Obermiller J. Compliance, elastic modulus, and burst pressure of small-intestine submucosa (SIS), small-diameter vascular grafts. *J Biomed Mater Res.* (1999) 47:65–70. doi: 10.1002/(SICI)1097-4636(199910)47:1<65::AID-JBM9>3.0.CO;2-F
13. Dahan N, Sarig U, Bronshtein T, Baruch L, Karram T, Hoffman A, et al. Dynamic autologous reendothelialization of small-caliber arterial extracellular matrix: a preclinical large animal study. *Tissue Eng Part A.* (2017) 23:69–79. doi: 10.1089/ten.tea.2016.0126
14. Gutowski P, Gage SM, Guziewicz M, Ilzecki M, Kazimierczak A, Kirkton RD, et al. Arterial reconstruction with human bioengineered acellular blood vessels in patients with peripheral arterial disease. *J Vasc Surg.* (2020) 72:1247–58. doi: 10.1016/j.jvs.2019.11.056
15. Texakalidis P, Giannopoulos S, Charisis N, Giannopoulos S, Karasavvidis T, Koullias G, et al. A meta-analysis of randomized trials comparing bovine pericardium and other patch materials for carotid endarterectomy. *J Vasc Surg.* (2018) 68:1241–56. doi: 10.1016/j.jvs.2018.07.023
16. Ho KJ, Nguyen LL, Menard MT. Intermediate-term outcome of carotid endarterectomy with bovine pericardial patch closure compared with Dacron patch and primary closure. *J Vasc Surg.* (2012) 55:708–14. doi: 10.1016/j.jvs.2011.10.007
17. Piterina AV, Cloonan AJ, Meaney CL, Davis LM, Callanan A, Walsh MT, et al. ECM-based materials in cardiovascular applications: inherent healing potential and augmentation of native regenerative processes. *Int J Mol Sci.* (2009) 10:4375–417. doi: 10.3390/ijms10104375
18. Badylak SF, Gilbert TW. Immune response to biologic scaffold materials. *Semin Immunol.* (2008) 20:109–16. doi: 10.1016/j.smim.2007.11.003
19. Badylak SF, Freytes DO, Gilbert TW. Extracellular matrix as a biological scaffold material: structure and function. *Acta Biomater.* (2009) 5:1–13. doi: 10.1016/j.actbio.2008.09.013
20. Brown BN, Badylak SF. Extracellular matrix as an inductive scaffold for functional tissue reconstruction. *Transl Res.* (2014) 163:268–85. doi: 10.1016/j.trsl.2013.11.003
21. Sheikh Z, Brooks PJ, Barzilay O, Fine N, Glogauer M. Macrophages, foreign body giant cells and their response to implantable biomaterials. *Materials.* (2015) 8:5671–701. doi: 10.3390/ma8095269
22. Mosala Nezhad Z, Poncelet A, Fervaille C, Gianello P. Comparing the host reaction to CorMatrix and different cardiac patch materials implanted subcutaneously in growing pigs. *Thorac Cardiovasc Surg.* (2019) 67:44–9. doi: 10.1055/s-0037-1607332
23. Dziki JL, Wang DS, Pineda C, Sicari BM, Rausch T, Badylak SF. Solubilized extracellular matrix bioscaffolds derived from diverse source tissues differentially influence macrophage phenotype. *J Biomed Mater Res A.* (2017) 105:138–47. doi: 10.1002/jbm.a.35894
24. Costa A, Naranjo JD, Turner NJ, Swinehart IT, Kolich BD, Shaffiey SA, et al. Mechanical strength vs. degradation of a biologically-derived surgical mesh over time in a rodent full thickness abdominal wall defect. *Biomaterials.* (2016) 108:81–90. doi: 10.1016/j.biomaterials.2016.08.053
25. Costa A, Adamo S, Gossetti F, D'Amore L, Ceci F, Negro P, et al. Biological scaffolds for abdominal wall repair: future in clinical application? *Materials.* (2019) 12:2375. doi: 10.3390/ma12152375
26. Delgado LM, Bayon Y, Pandit A, Zeugolis DI. To cross-link or not to cross-link? Cross-linking associated foreign body response of collagen-based devices. *Tissue Eng Part B Rev.* (2015) 21:298–313. doi: 10.1089/ten.teb.2014.0290
27. Fallon A, Goodchild T, Wang R, Matheny RG. Remodeling of extracellular matrix patch used for carotid artery repair. *J Surg Res.* (2012) 175:e25–34. doi: 10.1016/j.jss.2011.11.001
28. Schmitt DD, Bandyk DF, Pequet AJ, Towne JB. Bacterial adherence to vascular prostheses. A determinant of graft infectivity. *J Vasc Surg.* (1986) 3:732–40. doi: 10.1016/0741-5214(86)90037-6
29. Sapienza P, Napoli F, Tartaglia E, Venturini L, Sterpetti AV, Brachini G, et al. Infection of prosthetic patches after femoral endarterectomy: an unreported complication. *Ann Vasc Surg.* (2019) 56:11–6. doi: 10.1016/j.avsg.2018.07.069
30. Shell DHt, Croce MA, Cagiannos C, Jernigan TW, Edwards N, Fabian TC. Comparison of small-intestinal submucosa and expanded polytetrafluoroethylene as a vascular conduit in the presence of gram-positive contamination. *Ann Surg.* (2005) 241:995–1001. doi: 10.1097/01.sla.0000165186.79097.6c
31. Madden NJ, Troutman DA, DeMarsico AJ. Use of a small intestine submucosa extracellular matrix patch in repeated carotid endarterectomy. *J Am Osteopath Assoc.* (2014) 114:732–4. doi: 10.7556/jaoa.2014.143
32. Penovic S, Stula I, Boric T, Pgorelic Z. The effect of extracellular matrix on femoral artery after endarterectomy. *J Vascular Med Surg.* (2018) 6:1000371. doi: 10.4172/2329-6925.1000371
33. Quarti A, Nardone S, Colaneri M, Santoro G, Pozzi M. Preliminary experience in the use of an extracellular matrix to repair congenital heart diseases. *Interact Cardiovasc Thorac Surg.* (2011) 13:569–72. doi: 10.1510/icvts.2011.280016
34. Eckhauser AW, Hannon D, Molitor M, Scaife E, Gruber PJ. Repair of traumatic aortoinnominate disruption using CorMatrix. *Ann Thorac Surg.* (2013) 95:e99–101. doi: 10.1016/j.athoracsur.2012.09.060
35. Deorsola L, Pace Napoleone C, Abbruzzese PA. Repair of an unusual aortic coarctation using an extracellular matrix patch. *Ann Thorac Surg.* (2014) 97:1059–61. doi: 10.1016/j.athoracsur.2013.06.109
36. Khan MS, Yeager MR, Bryant R, 3rd, Lorts A, Morales DL. Coronary artery reconstruction using a bioengineered patch and epicardial tunnel. *Ann Thorac Surg.* (2016) 101:363–5. doi: 10.1016/j.athoracsur.2015.03.072
37. Leskovar B, Furlan T, Poznic S, Hrastelj M, Adamlje A. Using CorMatrix for partial and complete (re)construction of arteriovenous fistulas in haemodialysis patients: (Re)construction of arteriovenous fistulas with CorMatrix. *J Vasc Access.* (2019) 20:597–603. doi: 10.1177/1129729819826032
38. Mosala Nezhad Z, Poncelet A, de Kerchove L, Gianello P, Fervaille C, El Khoury G. Small intestinal submucosa extracellular matrix (CorMatrix(R)) in cardiovascular surgery: a systematic review. *Interact Cardiovasc Thorac Surg.* (2016) 22:839–50. doi: 10.1093/icvts/ivw020
39. Adams JD, Robinson WP, Lumsden AB. Preliminary results of a prospective, multi-center study of extracellular matrix scaffold for femoral arterial reconstruction. *Presented at: VEITH symposium/ISVS Associate Faculty Global Podium Presentations: VEITH symposium Associate Faculty Global Podium Presentations*. Vol. 25. New York, NY. Vascular (2017). p. 11–80. doi: 10.1177/1708538117729061
40. McCready RA, Hodde J, Irwin RJ, Coffey AC, Divelbiss JL, Bryant MA, et al. Pseudoaneurysm formation in a subset of patients with small intestinal submucosa biologic patches after carotid endarterectomy. *J Vasc Surg.* (2005) 41:782–8. doi: 10.1016/j.jvs.2005.02.035
41. Weber SS, Annenberg AJ, Wright CB, Braverman TS, Mesh CL. Early pseudoaneurysm degeneration in biologic extracellular matrix patch for carotid repair. *J Vasc Surg.* (2014) 59:1116–8. doi: 10.1016/j.jvs.2013.05.012
42. Dobrilovic N, Soukas P, Sadiq I, Goldstein L, Raman J. Early complications of biologic extracellular matrix patch after use for femoral artery repair. *J Vasc Surg.* (2017) 65:705–10. doi: 10.1016/j.jvs.2016.07.131
43. Badylak SF. Decellularized allogeneic and xenogeneic tissue as a bioscaffold for regenerative medicine: factors that influence the host response. *Ann Biomed Eng.* (2014) 42:1517–27. doi: 10.1007/s10439-013-0963-7

44. Dearth CL, Keane TJ, Carruthers CA, Reing JE, Huleihel L, Ranallo CA, et al. The effect of terminal sterilization on the material properties and *in vivo* remodeling of a porcine dermal biologic scaffold. *Acta Biomater.* (2016) 33:78–87. doi: 10.1016/j.actbio.2016.01.038
45. Valentin JE, Stewart-Akers AM, Gilbert TW, Badylak SF. Macrophage participation in the degradation and remodeling of extracellular matrix scaffolds. *Tissue Eng Part A.* (2009) 15:1687–94. doi: 10.1089/ten.tea.2008.0419
46. Gilbert TW, Stewart-Akers AM, Simmons-Byrd A, Badylak SF. Degradation and remodeling of small intestinal submucosa in canine Achilles tendon repair. *J Bone Joint Surg Am.* (2007) 89:621–30. doi: 10.2106/JBJS.E.00742
47. Record RD, Hillegonds D, Simmons C, Tullius R, Rickey FA, Elmore D, et al. *In vivo* degradation of 14C-labeled small intestinal submucosa (SIS) when used for urinary bladder repair. *Biomaterials.* (2001) 22:2653–9. doi: 10.1016/S0142-9612(01)00007-2
48. Li F, Li W, Johnson S, Ingram D, Yoder M, Badylak S. Low-molecular-weight peptides derived from extracellular matrix as chemoattractants for primary endothelial cells. *Endothelium.* (2004) 11:199–206. doi: 10.1080/10623320490512390
49. Brennan EP, Reing J, Chew D, Myers-Irvin JM, Young EJ, Badylak SF. Antibacterial activity within degradation products of biological scaffolds composed of extracellular matrix. *Tissue Eng.* (2006) 12:2949–55. doi: 10.1089/ten.2006.12.2949
50. Davis GE. Matricryptic sites control tissue injury responses in the cardiovascular system: relationships to pattern recognition receptor regulated events. *J Mol Cell Cardiol.* (2010) 48:454–60. doi: 10.1016/j.yjmcc.2009.09.002
51. Davis GE, Bayless KJ, Davis MJ, Meininger GA. Regulation of tissue injury responses by the exposure of matricryptic sites within extracellular matrix molecules. *Am J Pathol.* (2000) 156:1489–98. doi: 10.1016/S0002-9440(10)65020-1
52. Maquart FX, Bellon G, Pasco S, Monboisse JC. Matrikines in the regulation of extracellular matrix degradation. *Biochimie.* (2005) 87:353–60. doi: 10.1016/j.biochi.2004.10.006
53. Brennan EP, Tang XH, Stewart-Akers AM, Gudas LJ, Badylak SF. Chemoattractant activity of degradation products of fetal and adult skin extracellular matrix for keratinocyte progenitor cells. *J Tissue Eng Regen Med.* (2008) 2:491–8. doi: 10.1002/term.123
54. Haviv F, Bradley MF, Kalvin DM, Schneider AJ, Davidson DJ, Majest SM, et al. Thrombospondin-1 mimetic peptide inhibitors of angiogenesis and tumor growth: design, synthesis, and optimization of pharmacokinetics and biological activities. *J Med Chem.* (2005) 48:2838–46. doi: 10.1021/jm0401560
55. Ramaswamy AK, Vorp DA, Weinbaum JS. Functional vascular tissue engineering inspired by matricellular proteins. *Front Cardiovasc Med.* (2019) 6:74. doi: 10.3389/fcvm.2019.00074
56. Holtom PD, Shinar Z, Benna J, Patzakis MJ. Porcine small intestine submucosa does not show antimicrobial properties. *Clin Orthop Relat Res.* (2004) 427:18–21. doi: 10.1097/01.blo.0000143573.03645.b4
57. Sarikaya A, Record R, Wu CC, Tullius B, Badylak S, Ladisch M. Antimicrobial activity associated with extracellular matrices. *Tissue Eng.* (2002) 8:63–71. doi: 10.1089/107632702753503063
58. Jernigan TW, Croce MA, Cagiannos C, Shell DH, Handorf CR, Fabian TC. Small intestinal submucosa for vascular reconstruction in the presence of gastrointestinal contamination. *Ann Surg.* (2004) 239:733–8. doi: 10.1097/01.sla.0000124447.30808.c7
59. Badylak SF, Coffey AC, Lantz GC, Tacker WA, Geddes LA. Comparison of the resistance to infection of intestinal submucosa arterial autografts versus polytetrafluoroethylene arterial prostheses in a dog model. *J Vasc Surg.* (1994) 19:465–72. doi: 10.1016/S0741-5214(94)70073-7
60. Badylak SF, Wu CC, Bible M, McPherson E. Host protection against deliberate bacterial contamination of an extracellular matrix bioscaffold versus Dacron mesh in a dog model of orthopedic soft tissue repair. *J Biomed Mater Res B Appl Biomater.* (2003) 67:648–54. doi: 10.1002/jbm.b.10062
61. Valentin JE, Badylak JS, McCabe GP, Badylak SF. Extracellular matrix bioscaffolds for orthopaedic applications. A comparative histologic study. *J Bone Joint Surg Am.* (2006) 88:2673–86. doi: 10.2106/00004623-200612000-00015
62. Allman AJ, McPherson TB, Badylak SF, Merrill LC, Kallakury B, Sheehan C, et al. Xenogeneic extracellular matrix grafts elicit a TH2-restricted immune response. *Transplantation.* (2001) 71:1631–40. doi: 10.1097/00007890-200106150-00024
63. Allman AJ, McPherson TB, Merrill LC, Badylak SF, Metzger DW. The Th2-restricted immune response to xenogeneic small intestinal submucosa does not influence systemic protective immunity to viral and bacterial pathogens. *Tissue Eng.* (2002) 8:53–62. doi: 10.1089/107632702753503054
64. Badylak SF, Valentin JE, Ravindra AK, McCabe GP, Stewart-Akers AM. Macrophage phenotype as a determinant of biologic scaffold remodeling. *Tissue Eng Part A.* (2008) 14:1835–42. doi: 10.1089/ten.tea.2007.0264
65. Brown BN, Londono R, Tottey S, Zhang L, Kukla KA, Wolf MT, et al. Macrophage phenotype as a predictor of constructive remodeling following the implantation of biologically derived surgical mesh materials. *Acta Biomater.* (2012) 8:978–87. doi: 10.1016/j.actbio.2011.11.031
66. Huleihel L, Bartolacci JG, Dziki JL, Vorobyov T, Arnold B, Scarritt ME, et al. Matrix-bound nanovesicles recapitulate extracellular matrix effects on macrophage phenotype. *Tissue Eng Part A.* (2017) 23:1283–94. doi: 10.1089/ten.tea.2017.0102
67. Huleihel L, Hussey GS, Naranjo JD, Zhang L, Dziki JL, Turner NJ, et al. Matrix-bound nanovesicles within ECM bioscaffolds. *Sci Adv.* (2016) 2:e1600502. doi: 10.1126/sciadv.1600502
68. Huleihel L, Dziki JL, Bartolacci JG, Rausch T, Scarritt ME, Cramer MC, et al. Macrophage phenotype in response to ECM bioscaffolds. *Semin Immunol.* (2017) 29:2–13. doi: 10.1016/j.smim.2017.04.004
69. Sarig U, Sarig H, de-Berardinis E, Chaw SY, Nguyen EB, Ramanujam VS, et al. Natural myocardial ECM patch drives cardiac progenitor based restoration even after scarring. *Acta Biomater.* (2016) 44:209–20. doi: 10.1016/j.actbio.2016.08.031
70. Boruch AV, Nieponice A, Qureshi IR, Gilbert TW, Badylak SF. Constructive remodeling of biologic scaffolds is dependent on early exposure to physiologic bladder filling in a canine partial cystectomy model. *J Surg Res.* (2010) 161:217–25. doi: 10.1016/j.jss.2009.02.014
71. Hodde JP, Badylak SF, Shelbourne KD. The effect of range of motion on remodeling of small intestinal submucosa (SIS) when used as an Achilles tendon repair material in the rabbit. *Tissue Eng.* (1997) 3:27–37. doi: 10.1089/ten.1997.3.27
72. Ferng A, Connell A, Nunez M, Johnson K, Braunhut B, Lick S, et al. Cardiac regeneration in the human left ventricle after CorMatrix implantation. *Ann Thorac Surg.* (2017) 104:e239–41. doi: 10.1016/j.athoracsur.2017.03.044
73. Slachman FN. Constructive remodeling of CorMatrix extracellular matrix after aortic root repair in a 90-year-old woman. *Ann Thorac Surg.* (2014) 97:e129–31. doi: 10.1016/j.athoracsur.2013.10.103
74. Padalino MA, Castellani C, Dedja A, Fedrigo M, Vida VL, Thiene G, et al. Extracellular matrix graft for vascular reconstructive surgery: evidence of autologous regeneration of the neoaorta in a murine model. *Eur J Cardiothorac Surg.* (2012) 42:e128–35. doi: 10.1093/ejcts/ezs462
75. Sandusky GE Jr., Badylak SF, Morff RJ, Johnson WD, Lantz G. Histologic findings after *in vivo* placement of small intestine submucosal vascular grafts and saphenous vein grafts in the carotid artery in dogs. *Am J Pathol.* (1992) 140:317–24.
76. van den Heever JJ, Neethling WM, Smit FE, Litthauer D, Joubert G. The effect of different treatment modalities on the calcification potential and cross-linking stability of bovine pericardium. *Cell Tissue Bank.* (2013) 14:53–63. doi: 10.1007/s10561-012-9299-z
77. Li X, Jadlowiec C, Guo Y, Protack CD, Ziegler KR, Lv W, et al. Pericardial patch angioplasty heals via an Ephrin-B2 and CD34 positive cell mediated mechanism. *PLoS ONE.* (2012) 7:e38844. doi: 10.1371/journal.pone.0038844
78. Wieker CM, Schonefeld E, Osada N, Luhrs C, Beneking R, Torsello G, et al. Results of common femoral artery thromboendarterectomy evaluation of a traditional surgical management in the endovascular era. *J Vasc Surg.* (2016) 64:995–1001. doi: 10.1016/j.jvs.2016.04.036
79. Kuma S, Tanaka K, Ohmine T, Morisaki K, Kodama A, Guntani A, et al. Clinical outcome of surgical endarterectomy for common femoral artery occlusive disease. *Circ J.* (2016) 80:964–9. doi: 10.1253/circj.CJ-15-1177
80. Al-Khoury G, Marone L, Chaer R, Rhee R, Cho J, Leers S, et al. Isolated femoral endarterectomy: impact of SFA TASC classification on recurrence of

symptoms and need for additional intervention. *J Vasc Surg.* (2009) 50:784–9. doi: 10.1016/j.jvs.2009.05.053
81. Ballotta E, Gruppo M, Mazzalai F, Da Giau G. Common femoral artery endarterectomy for occlusive disease: an 8-year single-center prospective study. *Surgery.* (2010) 147:268–74. doi: 10.1016/j.surg.2009.08.004
82. Elsherif M, Tawfick W, Elsharkawi M, Campell R, Hynes N, Sultan S. Common femoral artery endarterectomy in the age of endovascular therapy. *Vascular.* (2018) 26:581–90. doi: 10.1177/1708538118772682
83. Stone PA, AbuRahma AF, Mousa AY, Phang D, Hass SM, Modak A, et al. Prospective randomized trial of ACUSEAL versus Vascu-Guard patching in carotid endarterectomy. *Ann Vasc Surg.* (2014) 28:1530–8. doi: 10.1016/j.avsg.2014.02.017
84. Derksen WJ, Verhoeven BA, van de Mortel RH, Moll FL, de Vries JP. Risk factors for surgical-site infection following common femoral artery endarterectomy. *Vasc Endovascular Surg.* (2009) 43:69–75. doi: 10.1177/1538574408323502
85. Kechagias A, Ylonen K, Biancari F. Long-term outcome after isolated endarterectomy of the femoral bifurcation. *World J Surg.* (2008) 32:51–4. doi: 10.1007/s00268-007-9309-7
86. Kang JL, Patel VI, Conrad MF, Lamuraglia GM, Chung TK, Cambria RP. Common femoral artery occlusive disease: contemporary results following surgical endarterectomy. *J Vasc Surg.* (2008) 48:872–7. doi: 10.1016/j.jvs.2008.05.025
87. Czub PS, Arendarczyk A, Kopala M, Budnik M, Hendzel P. Usefulness of CorMatrix-based tricuspid valve repair in the treatment of infective endocarditis. *Kardiol Pol.* (2018) 76:476. doi: 10.5603/KP.2018.0047
88. Wallen J, Rao V. Extensive tricuspid valve repair after endocarditis using CorMatrix extracellular matrix. *Ann Thorac Surg.* (2014) 97:1048–50. doi: 10.1016/j.athoracsur.2013.05.117
89. Gerdisch MW, Boyd WD, Harlan JL, Richardson JB, Jr., Flack JE, et al. Early experience treating tricuspid valve endocarditis with a novel extracellular matrix cylinder reconstruction. *J Thorac Cardiovasc Surg.* (2014) 148:3042–8. doi: 10.1016/j.jtcvs.2014.06.092
90. Leonore FT, Elsa F, David PC, Ludovic C, Pascal B, Charles Henri MA, et al. Short- and long-term outcomes following biological pericardium patches versus prosthetic patches for carotid endarterectomy: a retrospective Bicentric study. *Ann Vasc Surg*. (2020). doi: 10.1016/j.avsg.2020.04.010. [Epub ahead of print].

Conflict of Interest: The authors declare that this study received funding from Aziyo Biologics, Inc. The funder had the following involvement with the study: study design, data collection and analysis, and supported preparation of the manuscript.

Advantages of publishing in Frontiers

OPEN ACCESS
Articles are free to read for greatest visibility and readership

FAST PUBLICATION
Around 90 days from submission to decision

HIGH QUALITY PEER-REVIEW
Rigorous, collaborative, and constructive peer-review

TRANSPARENT PEER-REVIEW
Editors and reviewers acknowledged by name on published articles

Frontiers
Avenue du Tribunal-Fédéral 34
1005 Lausanne | Switzerland

Visit us: www.frontiersin.org
Contact us: frontiersin.org/about/contact

REPRODUCIBILITY OF RESEARCH
Support open data and methods to enhance research reproducibility

DIGITAL PUBLISHING
Articles designed for optimal readership across devices

FOLLOW US
@frontiersin

IMPACT METRICS
Advanced article metrics track visibility across digital media

EXTENSIVE PROMOTION
Marketing and promotion of impactful research

LOOP RESEARCH NETWORK
Our network increases your article's readership